

**The relationship between histone acetylation
and the transcriptional activity of genes**

Giorgia Siriaco

PhD

The University of Edinburgh

1997



DECLARATION

I declare that:

- a) this thesis has been composed by myself
- b) the work is my own, except where otherwise stated

Giorgia Siriaco

May 1997

ACKNOWLEDGEMENTS

There are many people who have helped me over my last four years as a PhD student.

Firstly, I would like to thank Peter for having devised the project, and for having patiently proof-read my thesis several times. Thanks also to Wendy for her enthusiasm and encouragement, particularly at moments in which my belief in the project was low, and for her comments on the thesis.

I am indebted to many members of the Chromosome Biology Section for their technical support, in particular Brenda and Nio, who showed me how to make a decent blot, and Linda for her company in the lab and for having shown me the basics of cytochemistry.

Thanks also to Paul Perry who helped me through innumerable hitches with the image-processing.

I am enormously grateful to Adrian for having given me a second chance. Thanks also to everyone in the Bird Lab, who have put up with me especially over the last few hectic months. Thanks in particular to Heather for talking through the results with me, and Martin for taking the time to help me juggle between computer programs and printers.

Most importantly, my final thanks goes to family and friends. To Elena for her warmth and affection, and for improving my Italian, to Brenda for her encouragement and faith in me, and to Rebecca and Donald for having put up with me in the flat for so long, and for their friendship and support. And to Matteo, who has had more faith in my abilities than I've had at times, for his untiring patience and for always being there for me. And lastly, to my family, without whom these four years would not have been possible, for their unrelenting support and presence at my side.

ABSTRACT

Acetylation of histone H4 has been shown to be associated with transcribed chromatin. This research project has employed a cytological approach to gain further insight into the relationship between histone H4 acetylation and the transcriptional activity of genes, using two different systems.

The inducible HMG-R gene was studied in the Chinese hamster UT-1 cell line, where it has been amplified by growing the cells in presence of a competitive inhibitor of the gene product. The amplified gene locus, visible at a cytological level, allowed histone acetylation to be monitored for a single gene, and related to differential expression of the gene. The chromosomal location of HMG-R was identified by FISH, and the histone H4 acetylation profile by immunofluorescence. The gene mapped to an acetylated domain, adjacent to a large region of underacetylation. Cytological analysis showed no detectable variation in H4 acetylation when comparing cells grown under conditions reported to fully induce or repress the gene. The corresponding levels of HMG-R expression were studied by Northern analysis and quantitative RT-PCR analysis. Contrary to expectation, significant levels of HMG-R transcription were found in the uninduced state, accounting for the level of H4 acetylation, and induction of the gene did not result in a large increase in transcription.

The chicken genome is organised into 39 chromosome pairs, of which 29 are microchromosomes. The difficulty in distinguishing between microchromosomes has resulted in a bias of genes being assigned to the macrochromosomes. However, CpG islands have been shown to concentrate on the microchromosomes, indicating they do not contain genetically inert DNA. The H4 acetylation profile of chicken chromosomes was determined by immunofluorescence. Acetylated histone H4 was shown to be distributed throughout both macro- and microchromosomes. Whereas microchromosomes exhibited a uniform level of acetylation, suggesting they contain mainly active DNA, macrochromosomes contained multiple underacetylated domains indicative of heterochromatin. The sex-determining W chromosome, previously shown to be largely heterochromatic, was also underacetylated. Microchromosomes were shown to replicate early in S phase, whereas regions of the macrochromosomes (and the W chromosome) replicated later. These results are consistent with the microchromosomes containing predominantly transcriptionally active, CpG island-rich DNA.

These results are discussed in context of the growing awareness of the role that histones and their biochemical modifications play in regulating the activity of genes.

ABBREVIATIONS USED

μ	micro
A	adenine
AMCA	7-amino-4-methylcoumarin-3-acetic acid
AMP	ampicillin
bio	biotin
bp	base pairs
BSA	bovine serum albumin
cDNA	complementary deoxyribnucleic acid
C	cytosine
CGI	CpG island
CHO	Chinese hamster ovary
Ci	Curies
CREST	calcsinosis, Raynauds phenomenon, esophageal dismobility, sclerodactyly, telangiectasia
CsCl	ceasium chloride
dATP	deoxyadenosine triphosphate
dCTP	deoxycytosine triphosphate
dGTP	deoxyguanine triphosphate
dNTP	deoxynucleotide triphosphate
dTTP	deoxythymidine triphosphate
dUTP	deoxyuridine triphosphate
dH ₂ O	distilled water
Da	Daltons
DAPI	4,6-diamino-2-phenylindole
DEPC	diethylpyrocarbonate
DMEM	Dulbecco's modified eagle's medium
DMSO	dimethylsulfoxide
DNA	deoxyribonucleic acid
DNase	deoxyribonuclease
DTT	dithiothreitol
EDTA	ethylenediaminetetra-acetic acid
EtBr	ethidium bromide
EtOH	ethanol
FCS	foetal calf serum
FISH	fluorescence <i>in situ</i> hybridisation
FITC	fluorescein isothiocyanate
g	grams
G	guanine

HCl	hydrochloric acid
hr	hours
k	kilo
K	1000 revolutions per minute
KCl	potassium chloride
KCM	potassium chromosome medium
l	litre
LMP	low melting point
m	milli
M	molar
mRNA	messenger RNA
Mb	megabases
min	minutes
n	nano
°C	degrees Celsius
OD	optical density
oligo	oligonucleotide
o/n	overnight
p	pico
PBS	phosphate-buffered saline
PCR	polymerase chain reaction
PFGE	pulse field gel electrophoresis
RNA	ribonucleic acid
RNase	ribonuclease
rpm	revolutions per minute
RT	room temperature
RT-PCR	reverse-transcriptase polymerase chain reaction
s	seconds
SDS	sodium dodecyl sulphate
T	thymine
TRITC	tetramethylrhodamine isothiocyanate
UTR	untranslated region
UV	ultraviolet
V	volts
vol	volume

LIST OF FIGURES

Figure 1.1	Chromatin maturation and compaction	3
Figure 1.2	The nucleosome	6
Figure 1.3	Core histone tail modifications	10
Figure 1.4	Involvement of histone acetylation in chromatin assembly and maturation	17
Figure 1.5	Reversible acetylation-deacetylation reaction	25
Figure 1.6	Inhibition of transcription by deacetylation	26
Figure 1.7	Deposition- and transcription-related acetylation sites are distinct and nonoverlapping	29
Figure 1.8	Model of molecular functions of p300/CBP and P/CAF	31
Figure 1.9	Inhibitors of histone deacetylase	34
Figure 1.10	Derepression of transcription by acetylation	37
Figure 1.11	A model for transcription through a nucleosome core	46
Figure 1.12	A model for the formation of heterochromatin and transcriptional repression at yeast telomeres	49
Figure 1.13	A model for the establishment of silencing by SIR1 at the HMR locus	50
Figure 1.14	Expression levels of β^p and β^A at the chicken β globin locus in 5- and 15-day old chicken erythrocytes	54
Figure 2.1	Timing of the DT40 cell cycle	96
Figure 3.1a	Biochemical pathway for cholesterol synthesis	102
Figure 3.1b	Feedback mechanism of HMG-R regulation	103
Figure 3.2	Restriction map of HMG-R genomic sequence	105
Figure 3.3	Exon-intron organisation of the HMG-R gene	106
Figure 3.4	cDNA sequence of the HMG-R gene	107
Figure 3.5	Restriction map of HMG-R cDNA sequence	108
Figure 3.6	pRED227 plasmid	109
Figure 3.7	Resistance of CHO-K1 and UT-1 cells to simvastatin	114
Figure 3.8	Localisation of HMG-R by FISH	118

Figure 3.9	Southern analysis of HMG-R amplification in UT-1 cells	121
Figure 3.10	Experimental approach for pulse field gel analysis of HMG-R amplicon size	123
Figure 3.11	Acetylation profile of metaphase chromosomes determined by immunofluorescence	125
Figure 3.12	Localisation of HMG-R on metaphase chromosomes relative to their acetylation profile	127
Figure 3.13	Acetylation profile at the HMG-R locus - HMG-R induced	130
Figure 3.14	Quantification of fluorescence	131
Figure 3.15	Acetylation profile at the HMG-R locus - HMG-R repressed	132
Figure 3.16	Quantification of fluorescence	133
Figure 3.17	Acetylation profile at the HMG-R locus in early-passage UT-1 cells	136
Figure 3.18	Quantification of fluorescence - HMG-R induced	137
Figure 3.19	Quantification of fluorescence - HMG-R repressed	138
Figure 3.20	Northern analysis of HMG-R expression in CHO-K1 and UT-1 cells RT-PCR experiment	140
Figure 3.21	Theoretical kinetics of the amplification reaction	143
Figure 3.22	RT-PCR experiment	144
Figure 3.23	Quantitative RT-PCR experiment	146
Figure 3.24	Kinetics of RT-PCR amplification shown in Figure 3.23	147
Figure 4.1	Construction of a CpG island library	156
Figure 4.2	DT40 metaphase chromosomes counterstained with DAPI	158
Figure 4.3	Karyotype of DT40 chromosomes	159
Figure 4.4	CpG island (CGI) distribution on DT40 chromosomes	160
Figure 4.5	DT40 metaphase chromosomes labelled by immunofluorescence with anti-acetylated H4.	162
Figure 4.6	Schematic representation of progression of S phase monitored by BrdU incorporation	165
Figure 4.7	Incorporation of BrdU in replicating DNA of DT40 chromosomes	166
Figure 4.8	Schematic representation of BrdU incorporation in	168

	late or early replicating DNA	
Figure 4.9	DNA replication following methotrexate block	169
Figure 4.10	DNA replication prior to methotrexate block	170
Figure 4.11	FACS scan analysis of DT40 cells grown in presence of methotrexate	173
Figure 4.12	Schematic representation of BrdU incorporation in early replicating DNA	174
Figure 4.13	Alignment of chromosome 1	175
Figure 4.14	A selection of cosmids mapping to DT40 metaphase macrochromosomes by FISH	177
Figure 4.15	A selection of cosmids mapped to chicken metaphase microchromosomes by FISH	178

LIST OF TABLES

Table 1.1	Acetylation sites in mammalian histones	15
Table 1.2	$t_{1/2}$ for monoacetylated histone H4	22
Table 1.3	Summary of histone acetyltransferases and deacetylases isolated to date	33
Table 2.1	Fragment sizes of DNA markers used in gel electrophoresis	77
Table 3.1	Growth conditions for UT-1 cells expressing/repressing HMG-R	115
Table 4.1	Cosmid chromosomal location and CGI content	179

TABLE OF CONTENTS

Declaration	i
Acknowledgements	ii
Abstract	iii
Abbreviations used	iv
List of Figures	ix
List of Tables	ix
Table of Contents	x
Chapter One - Introduction	1
1.1 Organization of the eukaryotic genome	2
1.1.1 Introduction	2
1.1.2 Organization of DNA within the nucleus	2
1.1.3 The nuclear matrix	4
1.1.4 The nucleosome	4
1.1.5 The core histones	5
1.1.6 Linker histone	5
1.2 Post-translational modifications of histones	9
1.2.1 Introduction	9
1.2.2 Core histone ADP-ribosylation	9
1.2.3 Core histone phosphorylation	11
1.2.4 Modification of histone H1	11
1.2.5 Core histone methylation	12
1.2.6 Core histone ubiquitination	13
1.3 Core histone acetylation	14
1.3.1 Introduction	14
1.3.2 Core histone acetylation	14
1.3.3 Deposition-related histone acetylation	15
1.3.4 Non-random usage of acetylation sites	18
1.3.5 Specific pattern of histone acetylation	20
1.3.6 Kinetics of histone acetylation and deacetylation	21

1.3.7 Enzymes catalysing reversible histone acetylation	24
1.3.8 Inhibitors of histone deacetylase	33
1.4 Structural consequences of histone acetylation - direct and indirect	36
1.4.1 Introduction	36
1.4.2 Biophysical and biochemical analyses of the structural consequences of histone acetylation	36
1.4.3 Effects of histone acetylation on nucleosome linking number	38
1.4.4 Histone acetylation as a regulatory signal	41
1.4.5 Core acetylation effects on linker histone binding	43
1.4.6 Genetic analysis of histone tail function	45
1.5 Histone acetylation and transcriptional activity	51
1.5.1 Introduction	51
1.5.2 Immunoprecipitation of acetylated histones	52
1.5.3 Detection of histone acetylation by immunofluorescence	56
1.5.4 Histone acetylation and heterochromatin	58
Chapter Two - Materials and Methods	60
2.1 Cell Culture	61
2.1.1 Media and Solutions	61
2.1.2 Cell lines	61
2.1.3 Thawing of cells stored in liquid nitrogen	61
2.1.4 Maintenance of cell lines in culture	62
2.1.5 Selection conditions	62
2.1.6 Delipidisation of FCS	62
2.2 Bacterial cell culture	63
2.2.1 Media and solutions	63
2.2.2 Bacterial strains	63
2.2.3 Preparation of competent cells for electroporation	63
2.2.4 Transformation of competent cells by electroporation	64
2.5 Plasmid DNA preparation	65
2.3.1 Solutions	65
2.3.2 Small scale plasmid DNA preparation - rapid boiling method	65
2.3.3 Large scale plasmid DNA preparation	65

2.4 Preparation of genomic DNA	67
2.4.1 Solutions	67
2.4.2 Rapid isolation of DNA from mammalian cells	67
2.4.3 Making plugs from mammalian tissue culture cells	68
2.5 Purification and concentration of DNA	69
2.5.1 Phenol:chloroform extraction	69
2.5.2 Ethanol precipitation	69
2.6 Enzymatic manipulation of DNA	70
2.6.1 Restriction enzyme digestion of plasmid DNA	70
2.6.2 Restriction enzyme digestion of genomic DNA	70
2.6.3 Restriction enzyme digestion of agarose plugs	70
2.7 Amplification of DNA by polymerase chain reaction (PCR)	71
2.7.1 Preparation of oligonucleotides	71
2.7.2 PCR materials	71
2.7.3 PCR conditions	71
2.7.4 Primers and conditions for PCR	72
2.8 Isolation of RNA and preparation of cDNA	73
2.8.1 Solutions	73
2.8.2 Isolation of RNA by acid guanidinium thiocyanate extraction	73
2.8.3 RNA isolation for RT-PCR	74
2.8.4 cDNA synthesis	74
2.9 Electrophoresis	76
2.9.1 Electrophoresis solutions	76
2.9.2 Size markers	76
2.9.3 DNA agarose gel electrophoresis	76
2.9.4 Purification of DNA from agarose	78
2.9.5 Pulsed field gel electrophoresis	78
2.9.6 Electrophoresis of RNA	79
2.10 Transfer of DNA and RNA onto membranes	80
2.10.1 Solutions	80
2.10.2 Southern transfer	80
2.10.3 Northern transfer	81

2.11 Radiolabelling of DNA	82
2.11.1 Random priming of DNA probes	82
2.11.2 End-labelling of DNA oligonucleotides	82
2.12 Hybridisation of membranes	84
2.12.1 Solutions	84
2.12.2 Pre-hybridisation	84
2.12.3 Hybridisation	84
2.12.4 Hybridisation washes	84
2.12.5 Detection of hybridisation signal	85
2.12.6 Re-using filters	85
2.13 Immunofluorescence	86
2.13.1 Media and solutions	86
2.13.2 Antibodies and sera	86
2.13.3 Cell culture	87
2.13.4 Preparation of metaphase spreads	88
2.13.5 Antibody reactions	88
2.13.6 Fluorescence microscopy	89
2.13.7 Treatment of slides following immunofluorescence	89
2.14 Fluorescence <i>in situ</i> hybridisation (FISH)	90
2.14.1 Materials for FISH	90
2.14.2 Materials for labelling probes by nick translation	91
2.14.3 Probes	92
2.14.4 Labelling of probes with biotin or digoxigenin by nick translation	92
2.14.5 Detection of biotin or digoxigenin	93
2.14.6 Cell culture	93
2.14.7 Preparation of metaphase spreads	93
2.14.8 <i>In situ</i> hybridisation with biotin labelled probes	94
2.14.9 <i>In situ</i> hybridisation with digoxigenin labelled probes	95
2.14.10 Fluorescence microscopy	95
2.15 Replication timing	96
2.15.1 Materials for replication timing	96
2.15.2 Replication timing experiments	96

2.15.3 BrdU detection	97
2.15.4 Fluorescence microscopy	98
Chapter Three - Results and Discussion	99
Histone H4 acetylation at the HMG-R locus	
3.1 Introduction	100
3.1.1 Aim of the project	100
3.1.2 3-hydroxy-3-methylglutaryl coenzyme A reductase (HMG-R)	101
3.1.3 UT-1 cell line	110
3.1.4 Experimental approach	112
3.2 Characterisation of the UT-1 cell line	113
3.2.1 Drug titration test	113
3.2.2 Regulation of HMG-R expression with cholesterol	115
3.3 Localisation of HMG-R by fluorescence <i>in situ</i> hybridisation	117
3.3.1 Localisation of HMG-R	117
3.4 Amplification of HMG-R in the UT-1 cell line	120
3.4.1 Southern analysis	120
3.4.2 PFG analysis	122
3.5 Acetylation profile of UT-1 chromosomes	124
3.5.1 Histone H4 acetylation profile	124
3.5.2 HMG-R locus relative to acetylation profile of UT-1 chromosomes	126
3.6 H4 acetylation at the HMG-R locus	129
3.6.1 H4 acetylation profile - HMG-R induced	129
3.6.2 H4 acetylation profile - HMG-R repressed	129
3.6.3 Quantification of fluorescence	134
3.6.4 Initial conclusions	134
3.7 Regulation of HMG-R expression	139
3.7.1 Northern analysis	139
3.7.2 RT-PCR analysis	141
3.7.3 Quantitative RT-PCR analysis	142
3.8 Discussion	148
3.8.1 Analysis of results	148

3.8.2 A role for histone acetylation?	150
Chapter Four - Results and Discussion	153
Gene distribution in chicken chromosomes	
4.1 Introduction	154
4.1.1 CpG islands	154
4.1.2 Purification of CpG islands	155
4.1.3 Bias of CpG islands for microchromosomes in chicken	157
4.2 Aim of the project	161
4.3 Histone H4 acetylation of chicken chromosomes	161
4.4 Replication timing of chicken chromosomes	163
4.4.1 Continuous labelling with BrdU	164
4.4.2 Pulse labelling with BrdU	171
4.5 Cosmid mapping	176
4.6 Discussion	179
Concluding remarks	182
List of References	183

CHAPTER ONE - INTRODUCTION

1.1 Organization of the eukaryotic genome

1.1.1 Introduction

In eukaryotic cells, two opposing requirements for the organization of the genome are met. 2m of nuclear DNA must be compacted so as to fit into a nucleus with a diameter of 10 μ m. This stringent organization must however allow the DNA to be accessible to a variety of enzymatic machineries necessary for carrying out replication, transcription, and repair of the genetic material required at each cell cycle.

These requirements are met by winding DNA into a higher order structure where controlled accessibility to the DNA can be mediated by modification of the structural proteins. Understanding the organization of nuclear DNA therefore allows us an insight into the functional aspects of regulation of gene expression.

1.1.2 Organization of DNA within the nucleus

The basic structural organization of DNA within the nucleus is a repeating unit, consisting of the nucleosome core particle and linker DNA (Van Holde 1988). When chromatin is viewed with an electron microscope, this repeating unit appears as a 10nm fiber, often referred to as 'beads-on-a-string': the 'beads' corresponding to the nucleosomes and the 'string' to linker DNA (Figure 1.1). This 10nm fiber, generally thought to represent actively transcribed chromatin, occurs rarely in the nucleus, and is normally found compacted further to form a 30nm fiber, which is in turn folded into loops of varying sizes (Jackson *et al* 1990). The loops are thought to be anchored by proteins located at their base to a supporting nuclear structure known as the nuclear matrix (Pienta *et al* 1991). This anchorage is believed by some to be mediated by specific DNA sequences that are evolutionarily conserved, known as the matrix (or scaffold) attachment regions (MARs or SARs).

An alternative model has been proposed by Cook and colleagues, whereby the structure of chromatin loops is managed by RNA polymerases such that

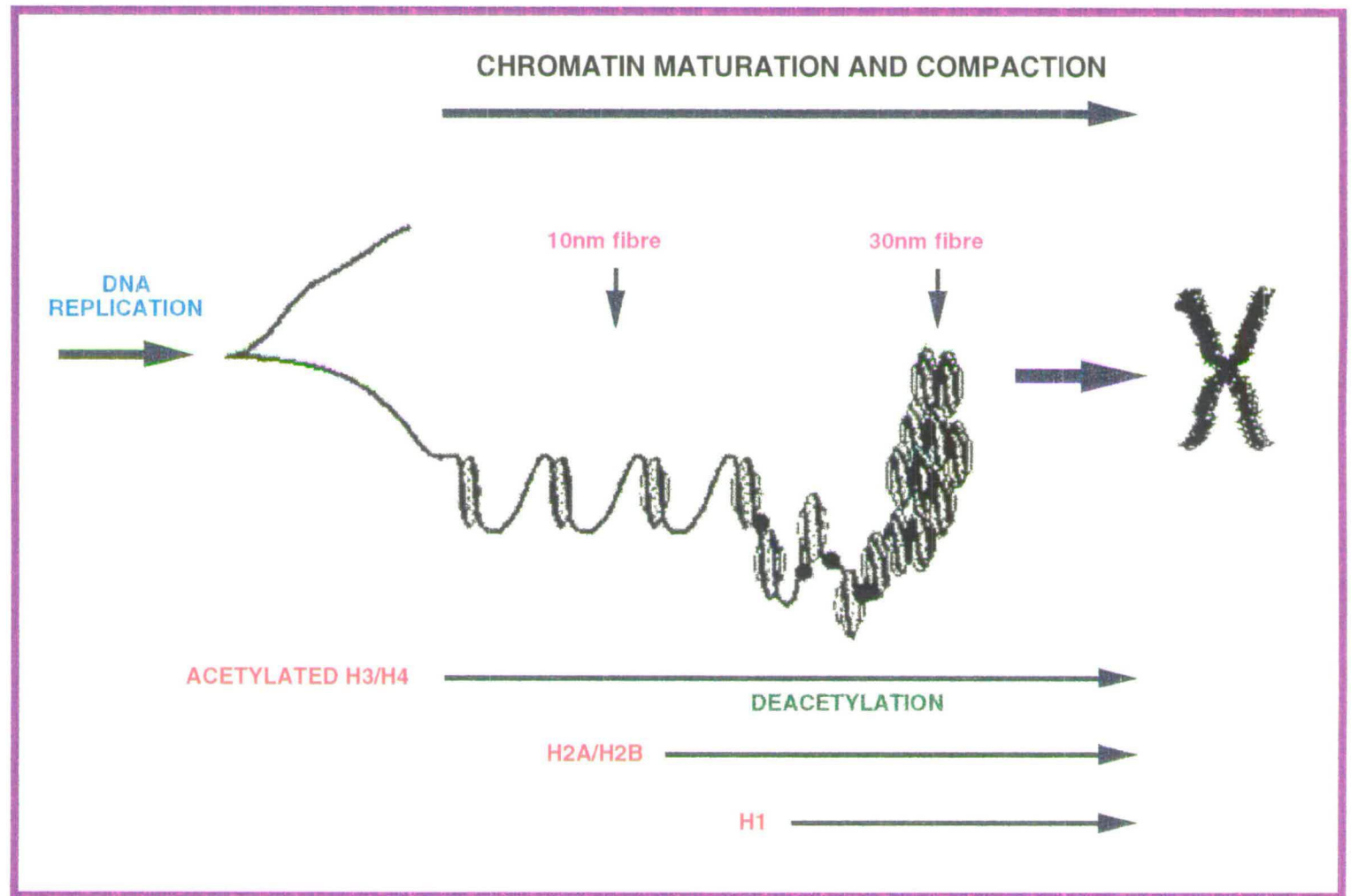


Figure 1.1

Chromatin maturation and compaction.

The structural organization of DNA within the nucleus consists of a repeating unit - the nucleosome. Chromatin compaction is accompanied by deacetylation of the nucleosomal core histones.

"factories" of polymerases organize clusters of loops. In contrast with the traditional view where the polymerase tracks along the template and is therefore mobile, Cook suggests that the active polymerase is found attached to the nucleus and RNA is synthesized as the template slides past the immobile enzyme (Cook 1994). The RNA polymerases thus provide the framework for chromatin organization within the nucleus.

1.1.3 The nuclear matrix

The nuclear matrix is defined as the structure that remains after nuclease-treated nuclei are extracted with salt. It is composed of residual nucleoli, the nuclear pore-lamina complex, and the internal nuclear matrix (Berezney 1991). The nuclear matrix defines the shape of the nucleus, and provides a structural support from which a variety of nuclear processes can take place, including DNA replication, transcription, and DNA repair (Pienta *et al* 1991).

The internal nuclear matrix has a fibrogranular appearance (He *et al* 1990) which may be due to an underlying network of core filaments whose composition is not known. The proteins composing the internal nuclear matrix are known as nuclear matrins (Nakasayu & Berezney 1991), some are common to all nuclear matrices while others vary in response to hormones, or differentiation and transformation of the cell. The major proteins of the nuclear pore-lamina are known as nuclear lamins (Kaufmann *et al* 1983). DNA loop attachment sites are thought to be located in the internal nuclear matrix, while the remainder of the loop is bound to the nuclear pore-lamina (Zini *et al* 1989).

1.1.4 The nucleosome

The nucleosome core particle has the appearance of a wedge-shaped disk, 5.7nm in height and 11nm in diameter. It consists of an octamer of core histones with two copies each of histones H2A (14.5kDa), H2B (13.7kDa), H3 (15.3kDa), and H4 (11.3kDa). The histone core is arranged as a central tetramer composed of two molecules each of histones H3 and H4, flanked on either side by a dimer composed of one molecule each of histones H2A

and H2B. Around this core structure are wrapped 1.75 left-handed turns (146bp) of DNA (Richmond *et al* 1984). The DNA joining nucleosomes is known as linker DNA. Figure 1.2 illustrates structure of a nucleosome schematically. This structure appears to be invariant, and occurs in all species and classes of chromatin studied to date (Felsenfeld 1978).

1.1.5 The core histones

The core histones H2A, H2B, H3, and H4 have a similar structure that has been evolutionarily conserved (Van Holde 1988). Each histone has a globular domain and a positively-charged lysine-rich N-terminal tail, about 30-35 amino acids in length. The globular portion of the molecule is responsible for the histone-histone and histone-DNA interactions that result in the formation of a core around which DNA is wrapped. The N-terminal tails do not appear to be contained within the nucleosome core, as enzymatic removal of the tails does not affect the structure of the nucleosome or its interaction with DNA. They are thought, however, to play an important role in protein-protein interactions outside of the nucleosome, as removal of the tails prevents the chromatin 10nm fiber from establishing a stable, higher order 30nm fiber (Allan *et al* 1982, Garcia-Ramirez *et al* 1992).

1.1.6 Linker histone

Histone H1, often referred to as the linker histone, is thought to be critical in maintaining the structure of the 30nm fiber. It is believed to bind to the exit and entry points of nucleosomal DNA, thus stabilizing two turns of DNA around the nucleosome core (van Holde & Zlatanova 1994). *In vitro* experiments have shown that the interchange between the 10nm and 30nm fibers depends on the addition and removal of linker histones. The presence of histone H1 *in vitro* results in the assembly of nucleosomes, at high ionic strength, into the 30nm solenoid, consisting of 6-7 nucleosomes per turn (Boulikas *et al* 1980). Similar sized fragments are seen *in vivo*, although it is believed that only transcriptionally inactive regions exist in this form.

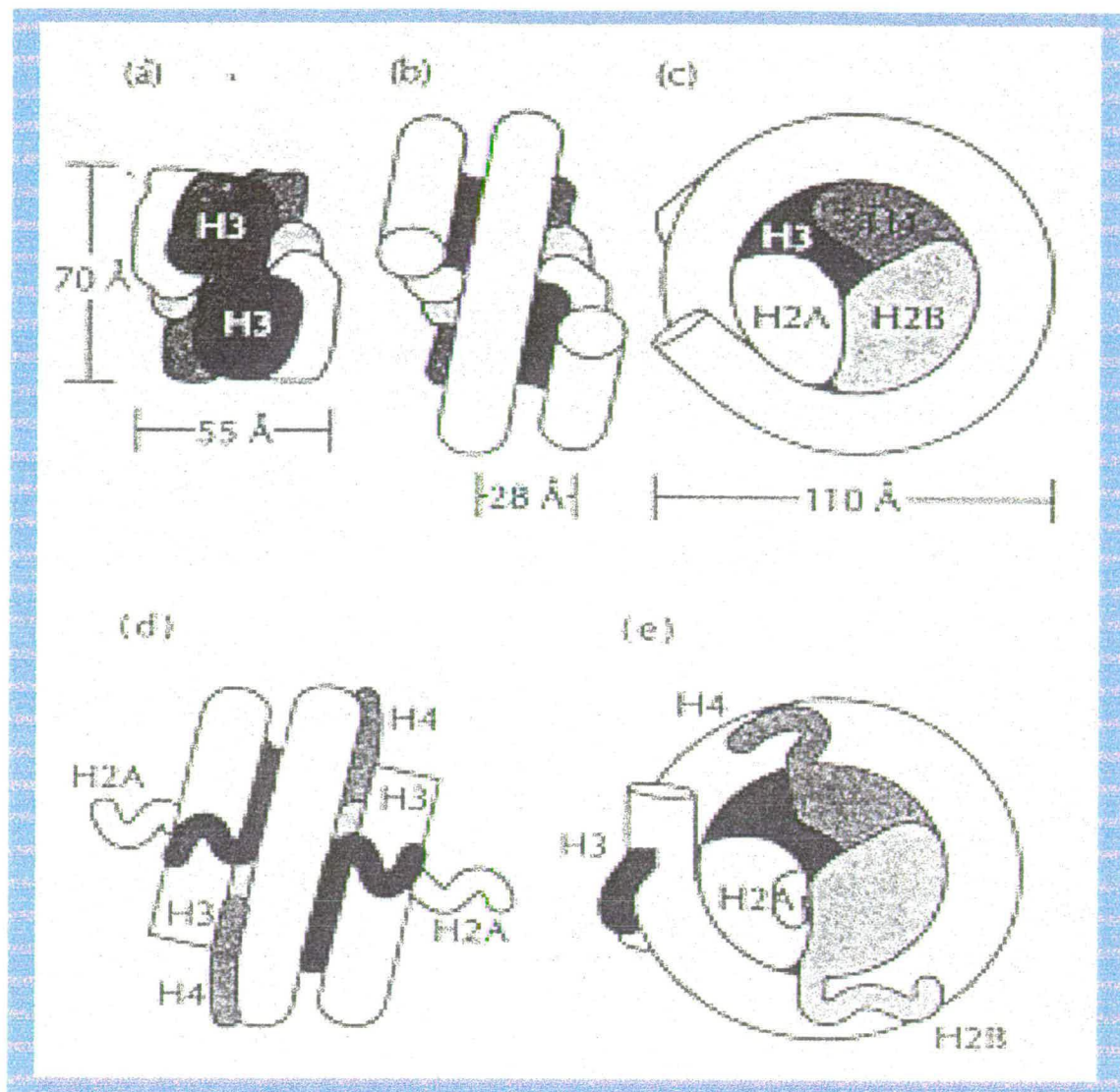


Figure 1.2

The nucleosome.

The nucleosome consists of an octamer of core histones. The core is arranged in a central tetramer of two molecules each of histones H3 and H4, flanked on either side by a dimer composed of one molecule each of histone H2A and H2B. Around this core are wrapped 1.75 turns of DNA.

This figure was taken from Turner *et al* 1992.

The histone H1 protein has three structural domains that are much less conserved than those of the core histones: a short N-terminal tail, a globular domain, and a long, highly basic C-terminal tail (Hartman *et al* 1977). It is currently believed that the N-terminal and C-terminal tails bind to the linker DNA, neutralizing its charge and facilitating chromatin condensation.

The role of histone H1 in controlling gene expression has been controversial. Tazi and Bird (Tazi & Bird 1990) examined the structure of transcriptionally active chromatin by isolating oligonucleosomes from unmethylated CpG islands, a fraction of chromatin associated with active transcription and the promoters of genes. They concluded that histone H1 was present in very low amounts in CpG island chromatin. Recent work (McArthur & Thomas 1996) has shown that histone H1 binds preferentially to DNA rich in methylated CpGs, irrespective of DNA sequence. The repressive effect of methylation on transcription may therefore be a direct result of its being packaged into a higher order chromatin conformation. In contrast, chromatin condensation of mitotic chromosomes in *Xenopus* was shown to occur in the absence of histone H1 (Ohsumi *et al* 1993). Ohsumi and colleagues immuno-depleted histone H1 from cell-free egg extracts, and then looked at the ability of the condensed sperm nuclei to form into metaphase chromosomes. Both H1-depleted and normal extracts were able to condense sperm nuclei into metaphase chromosomes, although the structure of the former was more fragile. H1 may thus be responsible for stabilizing the 30nm fiber of the metaphase chromosome, but is not essential for its condensation. The group suggests that condensation of chromatin into metaphase chromosomes may be triggered by other chromatin components, such as DNA topoisomerase type II.

Contrary to expectation, data obtained by Gorovsky and colleagues suggests that linker histones are dispensable for nuclear assembly and cell viability. In *Tetrahymena*, they disrupted the gene encoding histone H1 in the transcriptionally active macronucleus, in addition to the gene encoding the linker histone MicLH in the transcriptionally inactive micronucleus. The deletion strains grew at normal rates, demonstrating that linker histones are

not required for cell survival. However, nuclear size was increased relative to that of normal cells, indicative of decondensed chromatin structure (Shen *et al* 1995). In contrast with the transcriptional repression thought to be a consequence of histone H1-dependent chromatin condensation, histone H1 was also shown to be required for both positive and negative regulation of gene expression (Shen & Gorovsky 1996). Basal transcription of a repressed gene was increased in the H1-deleted strain, suggesting that H1 acts as a repressor of that gene, while the transcriptional activity of another gene was reduced, suggesting that H1 may play a role in promoting its expression. Indeed, loss of histone H1 did not appear to affect global transcription, as the total number of mature RNA remained unchanged in the deletion strains. It is thus likely that histone H1 does not function as a general repressor of transcription, as its ablation has limited phenotypic consequences, but rather that its architectural role lies in the specific assembly of a functional nucleoprotein complex (see section 1.4.5). The mechanism by which histone H1 may achieve this is as yet unclear, although given that linker histones represent a family of proteins that are much less conserved than the core histones, they are also open to a wider range of post-translational modifications, particularly phosphorylation (see section 1.2.4).

1.2 Post-translational modifications of histones

1.2.1 Introduction

Histone H1 and the core histones undergo a variety of post-translational modifications at their N-terminal tails (Figure 1.3), including ADP-ribosylation, phosphorylation, methylation, ubiquitination, and acetylation. I shall discuss the first 4 briefly in this section and cover the last in detail in section 1.3.

1.2.2 Core histone ADP-ribosylation

All four core histones are modified by adenosine-diphospho(ADP)-ribosylation, which involves the transfer of the ADP-ribose group to a histone receptor. One or more ADP-ribose groups may be transferred, resulting in histones carrying anything between mono-ADP-ribose and highly branched poly-ADP-ribose residues. Less than 5% of core histones are ADP-ribosylated, and the rate of turnover is high for the molecule. The acetylated forms of core histones are preferentially ADP-ribosylated (Boulikas *et al* 1988).

The enzyme responsible for catalysing the addition of ADP-ribose molecules onto histones is known as poly-ADP-ribose polymerase (or synthetase). It is a nuclear, DNA-dependent enzyme that is stimulated by DNA strand breaks, thus targeting its action to sites involved in replication, repair, and recombination (de Murcia *et al* 1988). Removal of ADP-ribose is catalysed by poly ADP-ribose glycohydrolase.

ADP-ribosylation appears to alter nucleosome structure. It has been proposed that poly-ADP-ribose polymerase is directed to sites of DNA double-stranded breaks, generating ADP-ribose polymers (Realini & Althaus 1992). These lead to the dissociation of histones from DNA onto the polymers (known as histone shuttling), thus allowing the DNA to be free for processing. The action of poly-ADP-ribose glycohydrolase then degrades the ADP-ribose polymers, leading to release of the histones, which then rebind to the DNA. Both poly-ADP-ribose and poly-ADP-ribose polymerase

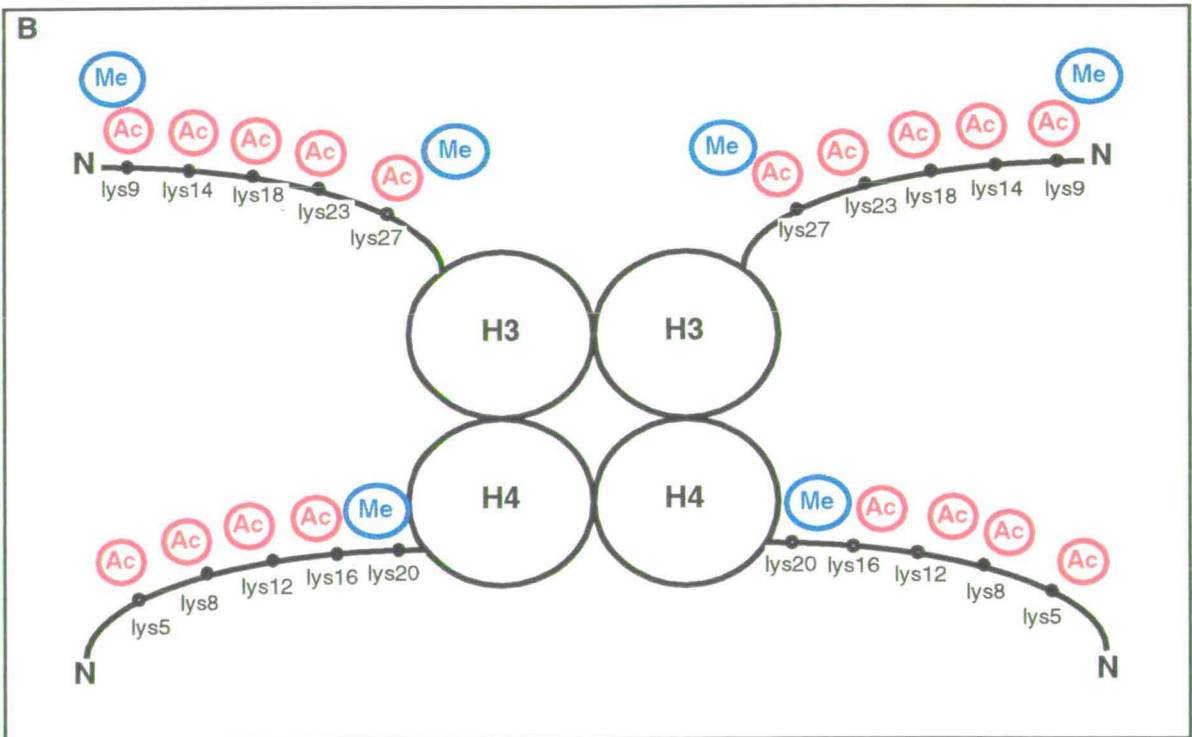
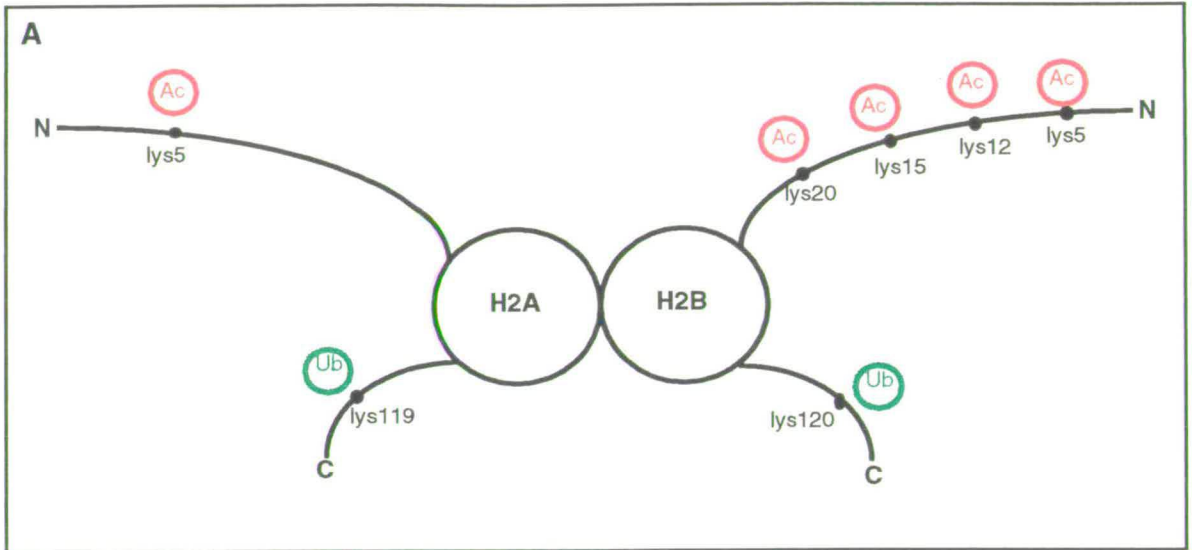


Figure 1.3

Core histone tail modifications.

Post-translational modifications at lysine residues of the N-terminal tails of core histones H2A and H2B, shown in panel A, and histones H3 and H4, shown in panel B.

Me - methylation, Ac - acetylation, Ub - ubiquitination.

are found associated with the nuclear matrix, and it is therefore possible that histone shuttling may also be transiently associated with the nuclear matrix.

1.2.3 Core histone phosphorylation

All four core histones are phosphorylated, usually at the N-terminal part of the histone. Histone H3 is phosphorylated to different extents throughout the cell cycle, increasing dramatically in mitosis (Shibata *et al* 1990), while histones H2A and H4 are phosphorylated at uniform rates. Phosphorylation has been implicated in both transcription and chromosome condensation.

Phosphorylation of histone H2A occurs in the transcriptionally active macronucleus of *Tetrahymena thermophila*, but not in the transcriptionally inactive micronucleus (Allis *et al* 1989). Treatment of quiescent mouse fibroblasts with growth factors or protein synthesis inhibitors leads to the transcriptional activation of immediate early genes, and rapid phosphorylation of histone H3 (Mahadevan *et al* 1991). Phosphorylation of histone H3 has been linked to premature condensation of chromosomes (Ajiro & Nishimoto 1985). All histone H3 molecules are phosphorylated at a single site prior to metaphase.

1.2.4 Modifications of histone H1

Histone H1 molecules can undergo both ADP-ribosylation and phosphorylation.

Histone H1 is poly-ADP-ribosylated at glutamic acid residues and the C-terminal lysine residue (Parseghian *et al* 1994). Highly ADP-ribosylated histone H1 is thought to be associated with decondensation of chromatin, possibly a prerequisite for presenting damaged DNA to enzymes involved in DNA repair, or to polymerases involved in DNA replication, as discussed earlier. Treatment with poly-ADP-ribose glycohydrolase reverses chromatin decondensation (de Murcia *et al* 1988).

Phosphorylation of histone H1 occurs at serine and threonine residues located in the amino- and carboxy-terminal domains of the protein (van Holde 1988). Phosphorylation can be catalysed by both cAMP- and cGMP-

dependent kinases. Phosphorylation that occurs during cell growth and division is catalysed by a chromatin-bound enzyme, p34^{cdc2} kinase, whose activity is regulated by both negative feedback and interaction with cyclins (Roth *et al* 1991). Histone H1 phosphorylation increases dramatically as cells progress through the cell cycle, reaching a maximum during mitosis. At this stage, most histone H1 molecules are phosphorylated at several sites in the C-terminal domain (van Holde 1988).

A role has been proposed for histone H1 phosphorylation in both chromatin condensation and decondensation. While reconstitution studies of chromatin with rat thymus histone H1 phosphorylated *in vitro* by p34^{cdc2} kinase have shown that phosphorylation of histone H1 does not induce a large alteration in chromatin structure, it has also been shown that at low ionic strength phosphorylation of histone H1 destabilises chromatin (Kaplan *et al* 1984). An antibody recognising highly phosphorylated histone H1 in HeLa cells has shown that in G₁ cells phosphorylated histone H1 is non-uniformly distributed, perhaps associating with transcriptionally active genes (Lu *et al* 1994). In the *Tetrahymena* macronucleus, both phosphorylated and dephosphorylated H1 localise non-randomly in distinct subdomains of the macronuclear chromatin (Lu *et al* 1995). The latter form of H1 appears to be associated with condensed transcriptionally silent chromatin, whereas phosphorylated H1 appears to be enriched in euchromatin. This supports the view that dephosphorylation of histone H1 facilitates or stabilises condensed chromatin.

1.2.5 Core histone methylation

The core histones H2B, H3 and H4 are modified by methylation, a relatively stable modification with a slow turnover rate (Wu *et al* 1986). The reaction is catalysed by histone-lysine methyltransferase, a chromatin-bound enzyme which adds methyl groups onto the ϵ -amino group of lysine residues of chromatin-bound histones H3 and H4 (Hendzel & Davie 1989).

While the role methylation of histones plays in altering chromatin structure is as yet unknown, it appears that methylation is associated with both

acetylation of histones and transcriptionally active DNA. In chicken immature erythrocytes, dynamically acetylated histones are selectively methylated (Hendzel & Davie 1991). The two processes are not directly coupled, however, as neither modification predisposes histones H3 and H4 to the other (Hendzel & Davie 1992).

1.2.6 Core histone ubiquitination

The core histones H2A and H2B are ubiquitinated in all eukaryotes (Wu *et al* 1986), with the exception of *Saccharomyces cerevisiae* which lacks ubiquitinated histone H2B (Swerdlow *et al* 1990). Histone ubiquitination is a reversible reaction, in which the C-terminal end of ubiquitin is attached to the ϵ -amino group of lysine residues. In higher eukaryotes, histone H2A is generally more frequently ubiquitinated than histone H2B, such that poly-ubiquitinated histone H2A is found in the form of a chain of ubiquitin molecules joined to each other and to the lysine residue by isopeptide bonds (Nickel & Davie 1989).

The enzymes responsible for catalysing the addition of ubiquitin to the histone molecules consist of a ubiquitin-activating enzyme (E1) and several ubiquitin-conjugating enzymes (E2s) (Hershko 1988). E1 catalyses the first step in the conjugation reaction, and is found in the nucleus (Schwartz *et al* 1992). Several E2s have been shown to catalyse the remaining steps in the reaction, although it is not yet known which particular enzymes are responsible for this reaction in the nucleus (Jentsch *et al* 1990).

Ubiquitinated histone H2B, and to a lesser extent histone H2A, appear to be associated with transcriptionally active DNA (Nickel & Davie 1989). It may be possible that introduction of ubiquitin results in the alteration of nucleosome structure (van Holde *et al* 1992). Ubiquitination of histone H2B is thought to be dependent on transcription (Davie & Murphy 1990, Davie & Murphy 1994), as the carboxy terminal of histone H2B is embedded within the nucleosome core. Transcription may therefore transiently alter the structure of the nucleosome, allowing the C-terminal end of histone H2B to become accessible to the enzymes catalysing the addition of ubiquitin.

1.3 Core histone acetylation

1.3.1 Introduction

The post-translational acetylation of core histones was first recognised by Allfrey and colleagues in 1963 (Allfrey *et al* 1964). It is a modification that occurs on all core histones, in all eukaryotes, and is both frequent and ubiquitous (Csordas 1990) - it is thus potentially of major influence in events such as transcription, replication, repair and packaging of DNA during the cell cycle.

While acetylation of core histones has been widely studied as a result of its conceptual appeal, particularly in the control of gene expression, definitive evidence as to the role it might be playing is lacking. Over recent years, however, genetic, biochemical and immunological approaches have yielded valuable insight into the significance of histone acetylation. These will be discussed in this and later sections.

1.3.2 Core histone acetylation

Histones are modified by two kinds of acetylation. The N-terminal nitrogen of histones H1, H2A and H4 is irreversibly acetylated. This modification takes place simultaneously with protein synthesis, and is not believed to influence the structure and function of the nucleosome core particle. The second kind of acetylation is reversible, and occurs at the ϵ -amino group of internal lysine residues located at the basic N-terminal tail of histone molecules. This type of acetylation is found in all events that require an alteration in chromatin structure, including transcription, replication, and repair of DNA (Vidali *et al* 1988, Turner 1991). All four core histones are reversibly acetylated, while histone H1 is not (Nelson 1982). Histone H2A is modified at one or two sites, while histones H2B, H3, and H4 are acetylated at four or five sites, giving rise to mono-, di-, tri-, and tetra-acetylated isoforms (Csordas 1990). Each acetate group added to a histone reduces its net positive charge by 1, and permits the resolution of the acetylated isoforms by acid/urea/Triton polyacrylamide electrophoresis (Alfageme *et al* 1974). The sites of

acetylation for each histone are summarised in Table 1.1 below, and are also shown diagrammatically in Figure 1.3, along with other modifications of the core histones.

Table 1.1
Acetylation sites in mammalian histones.

HISTONE	ACETYLATION SITES (preferred order of use in mammals)
H2A	lys5 - lys9
H2B	*lys12 / lys15 - lys20 - lys5
H3	lys14 - lys23 - lys18 - lys9
H4	lys16 - *lys8 / lys12 - lys5

- * In H2B sites 12 and 15 are both frequently acetylated in the mono-acetylated form. In H4 site 8 or 12 can be acetylated following site 16. This table has been adapted from Turner 1991.

1.3.3 Deposition-related histone acetylation

While the majority of current research has focused on the involvement of histone acetylation in regulation of gene expression, little is known about deposition-related acetylation, a modification of histones during their synthesis and deposition onto replicating chromatin. Biochemical analysis of deposition-related acetylation is hampered by the fact that only a small fraction of histones is affected, and this modification is altered once the newly-synthesized histone is deposited onto chromatin.

New DNA is packaged into chromatin in one of two ways: segregation of pre-existing (parental) histones onto nascent DNA (Cusick *et al* 1984, Seale 1978), or *de novo* nucleosome assembly, requiring the synthesis of new histones H3 and H4 for deposition onto newly replicated DNA. Histone synthesis appears to take place at high levels as DNA replication begins. The new histones are subsequently acetylated at specific lysine residues (Sobel *et al* 1995), and are deposited onto newly replicated DNA to ensure

both sister chromatids are assembled into chromatin. Histones H3 and H4 are deposited first, as a tetramer, followed by the addition of two H2A-H2B dimers, thus forming a nucleosome. A chromatin assembly factor (CAF-1) has been implicated in the assembly of nucleosomes following DNA replication (Verreault *et al* 1996). It is a three-subunit protein complex which mediates the assembly of new histones H3 and H4 specifically onto newly replicated DNA. Two of the subunits colocalise at sites of DNA synthesis, while the third (referred to as p48) is also a subunit of the histone deacetylase HD1 (the significance of this will be discussed in section 1.3.7). CAF-1 selectively uses cytoplasmic histones for chromatin assembly, and does not use nuclear parental histones. A model has been proposed by Roth and Allis (Roth 1996) whereby newly synthesised histones H3 and H4 are acetylated by histone acetyltransferases (HAT-B) and become closely associated with CAF-1 (Figure 1.4). This chromatin assembly complex (CAC) is thought to facilitate the assembly of H3-H4 tetramers onto replicating DNA. Removal of deposition-related acetyl groups is then catalysed by histone deacetylase. The high degree of similarity between these different complexes suggests they are connected in their role in coordinating the assembly of chromatin.

The acetylation status of segregated parental nucleosomes has been analysed by Perry and colleagues (Perry *et al* 1993) by performing replication reactions in intact cells *in vivo*, in the presence of cycloheximide (an inhibitor of translation), or using isolated HeLa cell nuclei *in vitro*, thus allowing endogenous enzymes to synthesize new DNA while pre-existing histones are segregated onto the new chromatin. Using antibodies specific for acetylated histone H4, they found nascent nucleosomes containing parental histones to be underacetylated relative to those assembled *de novo*. Parallel experiments by Perry and coworkers (Perry *et al* 1993) used these antibodies to immunoprecipitate newly-replicated nucleosomes containing newly-synthesised histones, *in vivo*, in an acetylation-dependent manner. In all eukaryotes studied so far, newly-synthesised histone H4 is reversibly

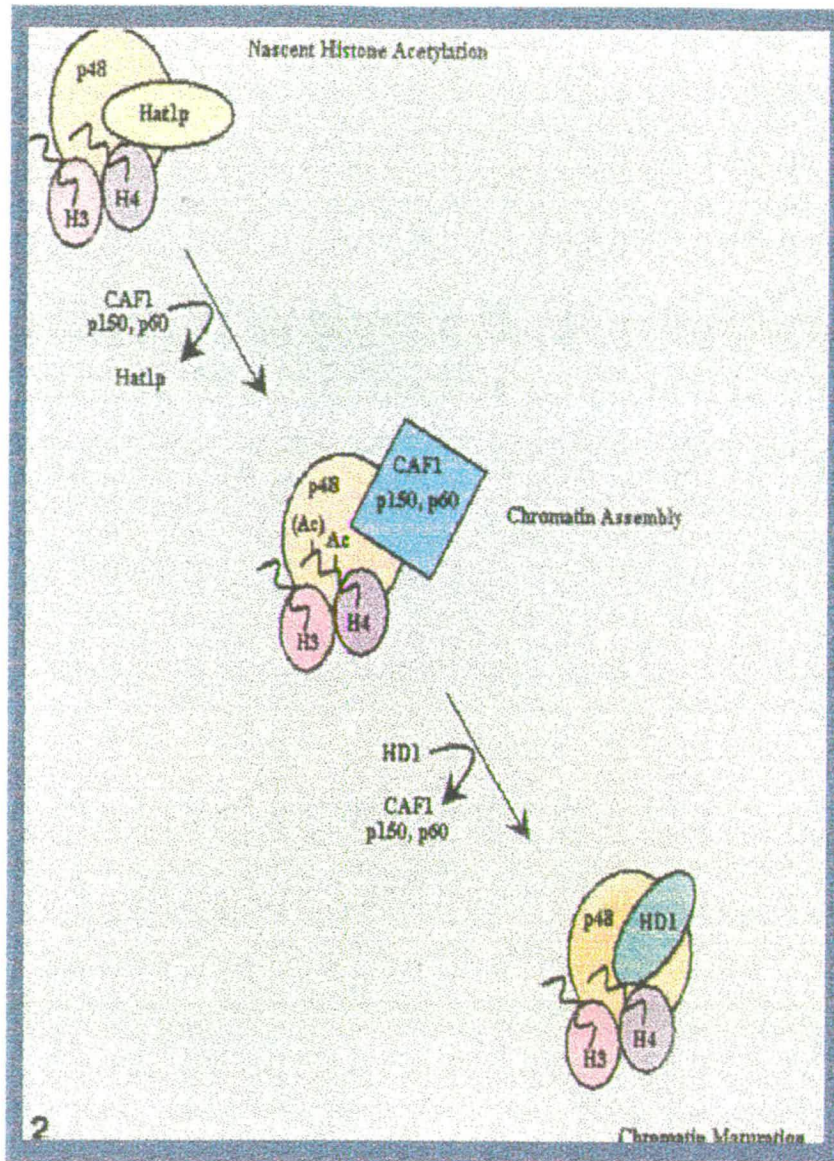


Figure 1.4

Involvement of histone acetylation in chromatin assembly and maturation.

Newly synthesised histones H3 and H4 associate in the cytoplasm. H4 is acetylated by HAT-B activities. Acetylated H3 and H4 subsequently associate with the chromatin assembly factor CAF1. This chromatin assembly complex (CAC) facilitates the formation of new H3-H4 tetramers onto replicating DNA. Removal of the deposition-related acetyl groups by the histone deacetylase HD1 may be required for the maturation of chromatin into a more compact, stable structure. HAT-B, CAF1, and HD1 closely resemble each other, suggesting they are coordinately involved in regulating chromatin assembly.

This figure has been taken from Roth & Allis 1996.

acetylated during chromatin assembly, and is typically deacetylated within minutes of its deposition (Jackson *et al* 1976). The results indicate that 60% of newly synthesised H2A and H2B were also contained in the acetylated fraction, and that newly-synthesised histones H3 and H4 co-precipitated and may thus form a preassembly histone complex.

Interestingly, it appears that deacetylation of histones, following their deposition onto new chromatin, is not required for proper nucleosome assembly. Chromatin replicated and assembled in the presence of sodium butyrate (an inhibitor of histone deacetylation) retains normal nucleosome structure, although it is sensitive to DNase I, suggesting that acetylation may inhibit complete folding of the nascent chromatin fiber perhaps by altering the binding affinity between the newly replicated chromatin and histone H1 (Perry & Annunziato 1991). Nascent histone deacetylation coincides with histone H1 deposition, suggesting that the two processes may complement each other in guiding chromatin higher order structure during nucleosome assembly.

Recently, data has been obtained by Sobel and colleagues (Sobel *et al* 1995) that proposes strong evolutionary conservation for deposition-related acetylation sites in histone H4. In *Tetrahymena*, residues 4 and 11 have been shown to be acetylated in newly synthesised histone H4, whereas in *Drosophila* the analogous residues, lys5 and lys12, are modified. In *Tetrahymena*, deposition-related acetylation is particularly distinct, due to the separation between germline and somatic nuclei. In both *Tetrahymena* and *Drosophila*, newly synthesised histone H3 is deposited in the acetylated form, and specific residues are modified (lys9, lys14, and lys14, lys23, respectively). In contrast, there appears to be no evidence for deposition-related acetylation of histone H3 in HeLa cells.

1.3.4 Non-random usage of acetylation sites

Two approaches have been used to establish whether the acetylation sites in different species are used in a controlled or random fashion, in particular those of histone H4. The mono-, di-, tri-, and tetra-acetylated isoforms of

histone H4 have been isolated and sequenced at the amino-terminal region in a variety of species (Chicoine & Allis 1986, Thorne *et al* 1990). Alternatively, Turner and colleagues have developed site-specific antibodies (Turner 1989, Turner & Fellows 1989, Turner *et al* 1989), which permit analysis of smaller amounts of starting material. In either case, the data represents the steady-state level of acetylation at each site, but does not take into consideration that each isoform will be the net result of the activity of acetylating and deacetylating enzymes, which may work at different rates, and perhaps in different parts of the genome.

In each of the species tested so far, site-usage has been shown to occur in a non-random manner. Given that the pattern of histone H4 acetylation varies between species but is specific to each species, with a more or less defined order of site-usage, and that the sequence of the amino-terminal region of histone H4 is identical between species, it seems likely that the differences in site-usage lie in the specificities and relative activities of the acetylating and deacetylating enzymes.

The pattern of acetylation site usage of histone H4 is essentially the same in all mammalian cells, but varies over greater evolutionary distances. In human or bovine cells, lys16 is predominantly modified in mono-acetylated histone H4. Either lys12 or lys8 is found acetylated in di- and tri-acetylated isoforms, and lys5 is generally found acetylated in tetra-acetylated isoforms (Turner *et al* 1989). In *Tetrahymena* and cuttlefish, the order of site usage is different (7, 5, 11, 15 and 12, 5, 16, 8, respectively) and is almost invariant. In contrast to this, the first acetate group to be added to histone H4 in *Drosophila* polytene chromosomes can be at lys 5, 8, 12, or 16. Interestingly, Turner and coworkers have shown in *Drosophila* that histone H4 molecules acetylated at particular lysine residues, are associated with specific, functionally distinct regions of the genome (Turner *et al* 1992). Histone H4 molecules acetylated at lys5 or lys8 are found in similar regions throughout the genome, but not in heterochromatin. Histone H4 acetylated at lys12 is present in heterochromatin and elsewhere in the genome, and histone H4 acetylated at lys16 is found almost exclusively in the transcriptionally

hyperactive male X chromosome (as discussed in section 1.3.5 below). The order in which lysine residues are acetylated in histone H4 molecules of *Xenopus* lampbrush chromosomes is very similar to that of mammalian cells. Lys16 is the most frequently acetylated residue in monoacetylated histone H4, lys16 and lys12 or lys8 are most frequently found acetylated in di-acetylated isoforms, and lys 5 is only found acetylated in tri- or tetra-acetylated isoforms (Sommerville *et al* 1993).

In the yeast *Saccharomyces cerevisiae*, the lys16-lys12/lys8-lys5 order of acetylation, as found in mammalian cells, applies (Clarke *et al* 1993). Genetic experiments by Grunstein and colleagues (discussed in detail in section 1.4.6), amongst others, have shown that mutant strains, in which lys16 has been substituted by a neutral residue, grow well in culture but fail to silence the HML α mating type locus (Johnson *et al* 1990, Megee *et al* 1990) and genes found near telomeres (Thompson *et al* 1994).

The sequencing approach has recently been used by Crane-Robinson and colleagues (Thorne *et al* 1990) to define the order of site usage of lysine residues of histones H2B and H3, in human and bovine cells. Again, site usage is both flexible and non-random, and the results are summarised in Table 1.1.

1.3.5 Specific pattern of histone acetylation

It has recently become possible to study the distribution of acetylated histones in chromatin by immunofluorescence, with the development of antisera specific for acetylated histone H4. This approach has been used by Lin and colleagues (Lin *et al* 1989) to demonstrate, both by immunofluorescence and immunoblotting, that hyperacetylated histone H4 is confined to the transcriptionally active macronucleus in *Tetrahymena*. Pfeffer and colleagues (Pfeffer *et al* 1988) have also shown a striking increase in histone H4 acetylation in erythrocyte nuclei activated by the fusion of transcriptionally active culture cells.

The antibodies have proved particularly useful in studying the distribution of acetylated histone H4 in metaphase and polytene chromosomes.

Immunolabelling of human metaphase chromosomes generates a distinctive pattern with several significant characteristics. Blocks of centric heterochromatin are weakly labelled, even when decondensed by growth of cells in 5'-azacytidine (Jeppesen *et al* 1992). There is a banding pattern on the chromosome arms, such that bright bands (corresponding to acetylated histone H4) have a similar distribution to R-bands, where the majority of genes are thought to be located (Jeppesen & Turner 1993, Craig & Bickmore 1994). A single weakly labelled chromosome is seen in female, but not male, cells, which has been shown to correspond to the inactive X chromosome (Jeppesen & Turner 1993). This is the X chromosome that, in mammalian females, becomes transcriptionally inactive and late-replicating in early development, thus equalising the dose of X-linked gene products in male and female cells (Riggs 1992). Interestingly, in *Drosophila* this dosage compensation is achieved by doubling the amount of male X-linked gene products. When labelling *Drosophila* polytene chromosomes with an antibody against histone H4 acetylated at lys16, male autosomes and all female chromosomes labelled weakly, whereas the male X chromosome gave a strong labelling pattern. This correlates with the increased rate of transcription found on the male X chromosome (Turner *et al* 1992, Bone *et al* 1994).

1.3.6 Kinetics of histone acetylation and deacetylation

Histone acetylation is a dynamic process, occurring at different rates. Covault and Chalkley (Covault & Chalkley 1980) studied the rates of histone acetylation in hepatoma tissue culture cells by selectively radiolabelling acetylated histone fractions on the basis of their different acetate exchange rates. In this manner, two distinct populations of acetylated histones were identified. One population of histones is rapidly acetylated and deacetylated (believed to represent about 15% of histones in hepatoma tissue culture cells), while a second is acetylated and deacetylated at a much slower rate, as shown in Table 1.2.

Table 1.2
 $t_{1/2}$ for monoacetylated histone H4.

	RAPID POPULATION	SLOW POPULATION
ACETYLATION	7min	200-300min
DEACETYLATION	3-7min	30min

This table has been adapted from Davie & Henzel 1994.

The population of rapidly acetylated histones can be further divided into two classes (Henzel *et al* 1991) - Class I histones become hyperacetylated (tetra-acetylated) in the presence of an inhibitor of deacetylase. Upon removal of the inhibitor, the hyperacetylated histone is rapidly deacetylated. Class II histones only achieve a low level of acetylation (mono- or di-acetylated) in the presence of the inhibitor, and are slowly deacetylated following its removal. It has been shown by Henzel and colleagues that Class I histones are primarily bound to transcriptionally active, gene-enriched chromatin in chicken erythrocytes, whereas Class II histones are not. Furthermore, chromatin fragments contained within the nuclear matrix were particularly enriched in Class I histones, an observation whose implications will be discussed later in this section.

The level of histone acetylation changes throughout the cell cycle (Bradbury 1992). The core histones are deacetylated during mitosis, in accordance with the condensation of chromatin to form metaphase chromosomes, although acetylation has been seen to persist during metaphase in regions corresponding to R bands (see section 1.3.5). The level of histone H4 acetylation subsequently increases in G1, where transcribable genes are reactivated. d'Anna and colleagues have looked at histone H4 acetylation during the cell cycle, in the presence of sodium butyrate, an inhibitor of deacetylation (d'Anna *et al* 1983). They have shown that levels of H4 acetylation in metaphase are reduced relative to those of interphase cells. In addition, 80% of H4 molecules were acetylated in butyrate-treated cells, whereas only 30% of H4 molecules were acetylated in untreated cells. The

fact that butyrate alters acetylation in metaphase chromosomes, indicates that the acetylation-deacetylation cycle is maintained during metaphase, and thus that the acetylating-deacetylating enzymes are part of the chromosome. Thus H4 acetylation is kept at a minimum during mitosis, perhaps in order to maintain the compact structure of mitotic chromosomes. Butyrate-treated chromosomes do however appear normal under the light microscope. Turner has similarly shown by immunodetection of acetylated histones (Turner 1989) that there is an overall reduction in H4 acetylation in metaphase cells, and that the cycle of acetylation and deacetylation continues through metaphase, given that treatment with butyrate results in a sharp increase in the level of acetylation. In addition, Turner showed that there is preferential loss of the more acetylated isoforms in metaphase, as well as a change in the order of site usage. It is unclear, however, whether the deacetylation which results in the reduction of acetylation at metaphase occurs randomly or site-specifically. The larger the number of acetylated sites on a given H4 molecule, the larger the probability that one of its sites will be acetylated ie. it is more likely that there is a decrease in tri- and tetra-acetylated forms of H4, than in mono- or di- acetylated H4.

While acetylation appears to be reduced in metaphase chromosomes, it is maintained nonetheless. It is possible that acetylation of metaphase chromosomes is merely a relic from the previous G2 phase, but this is unlikely to be the case, as acetylation must be actively maintained by acetylating enzymes for a distinct pattern to be seen. In the absence of re-acetylation during cell division, it would be eroded away by deacetylation. It is thus puzzling to find that acetylation of nucleosomes is maintained in metaphase, where chromatin is highly condensed and transcriptionally inactive. One explanation for this has been proposed by Jeppesen (Jeppesen 1997) whereby histone acetylation is thought to be a mechanism for promoting cell memory. Given that acetylation is generally thought to be a characteristic of transcriptionally active chromatin, one can also hold that the level of histone acetylation on metaphase chromosomes is a measure of potential gene activity. The role for histone acetylation that is generally

proposed - that it loosens chromatin structure or that it is part of the transcriptional process - does not seem to be relevant when considering condensed inactive metaphase chromosomes. Hence, why should acetylation be maintained? It may act as a way of marking the transcriptional status of different chromatin domains through successive cell divisions, so that each cell knows which genes should be expressed and which repressed at a particular point in its developmental pathway. In other words, to enable potentially transcribable chromatin to be reactivated after mitosis, at the start of G₁. In this way, histone acetylation propagates cell memory, much in the same manner as DNA methylation acts to maintain gene repression.

1.3.7 Enzymes catalysing reversible histone acetylation

Reversible histone acetylation is regulated by two types of enzyme (Figure 1.5) - histone acetyltransferase (HAT) and histone deacetylase (HD). The level of acetylation is established by the net activities of these two enzymes. A mammalian histone deacetylase was recently isolated by Taunton and colleagues (Taunton *et al* 1996), using a trapoxin affinity matrix. Trapoxin (discussed in more detail later in this section) is an irreversible inhibitor of deacetylation that acts by mimicking N-acetyl lysine. The deacetylating activity that co-purifies with trapoxin, in human Jurkat T cells, was identified as being a 55kD protein, referred to as HD1. Significantly, HD1 shares 60% identity with the yeast transcriptional regulator Rpd3p. The function of Rpd3p is not yet known, although it was isolated independently in four different mutant suppressor screens designed to identify transcriptional repressors (Nasmyth *et al* 1987, Vidal *et al* 1991, Bowdish & Mitchell 1993, McKenzie *et al* 1993, Stillman *et al* 1994). It is thought not to bind to DNA, and is not known to interact with any other proteins, although it has been shown to be functionally linked to another transcriptional regulator, Sin3p. A model has been proposed by Wolffe (Wolffe 1996) whereby Sin3p interacts with DNA binding proteins to direct transcriptional repression (Figure 1.6). Rpd3p subsequently enhances the activity of Sin3p by influencing the chromatin structure of the gene repressed by Sin3p. Rpd3p's action shifts the

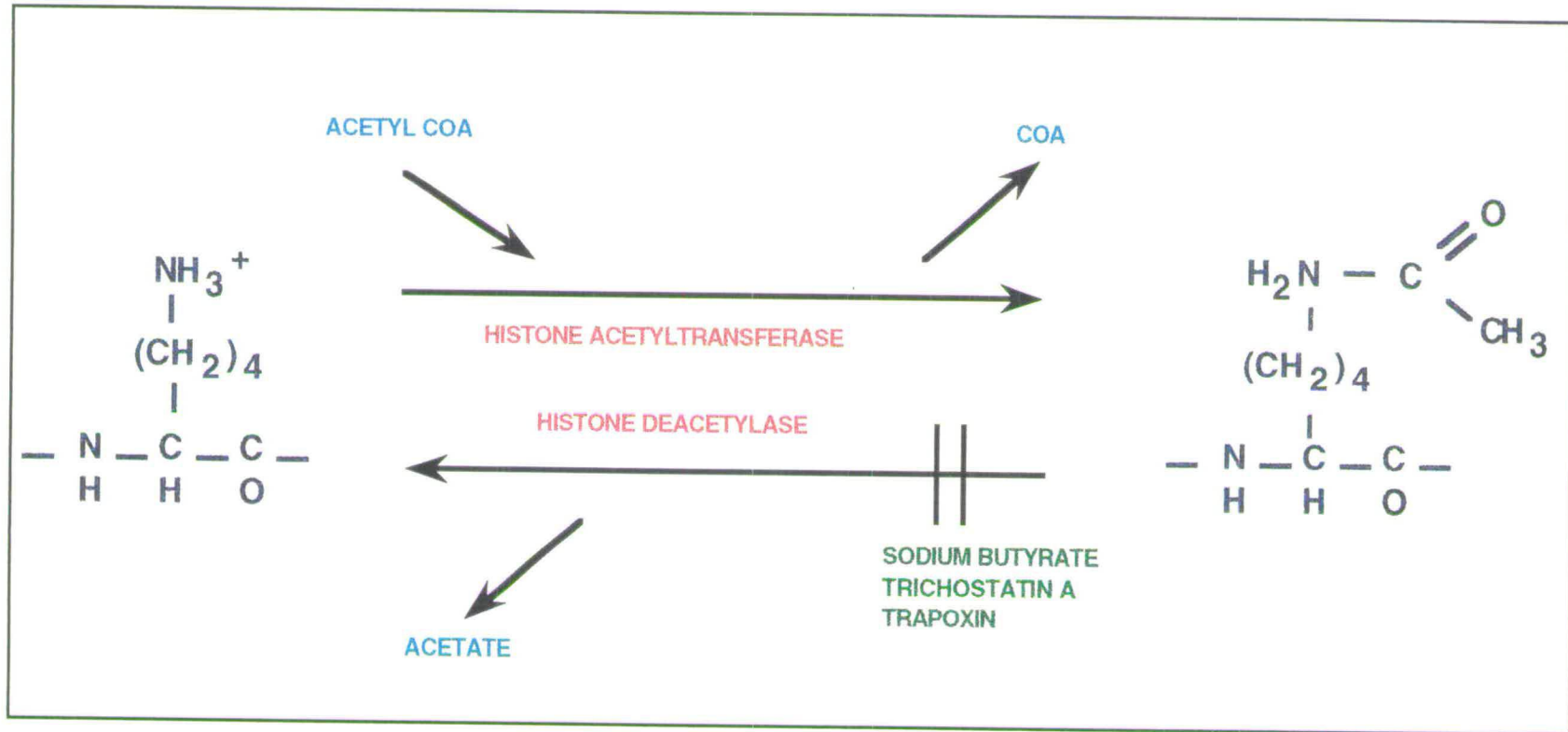


Figure 1.5

Reversible acetylation-deacetylation reaction.

Acetylation of the lysine residues of histone tails is catalysed by histone acetyltransferases(HATs). Deacetylation is catalysed by histone deacetylases (HDs). Sodium butyrate, trichostatin A and trapoxin inhibit the action of histone deacetylases.

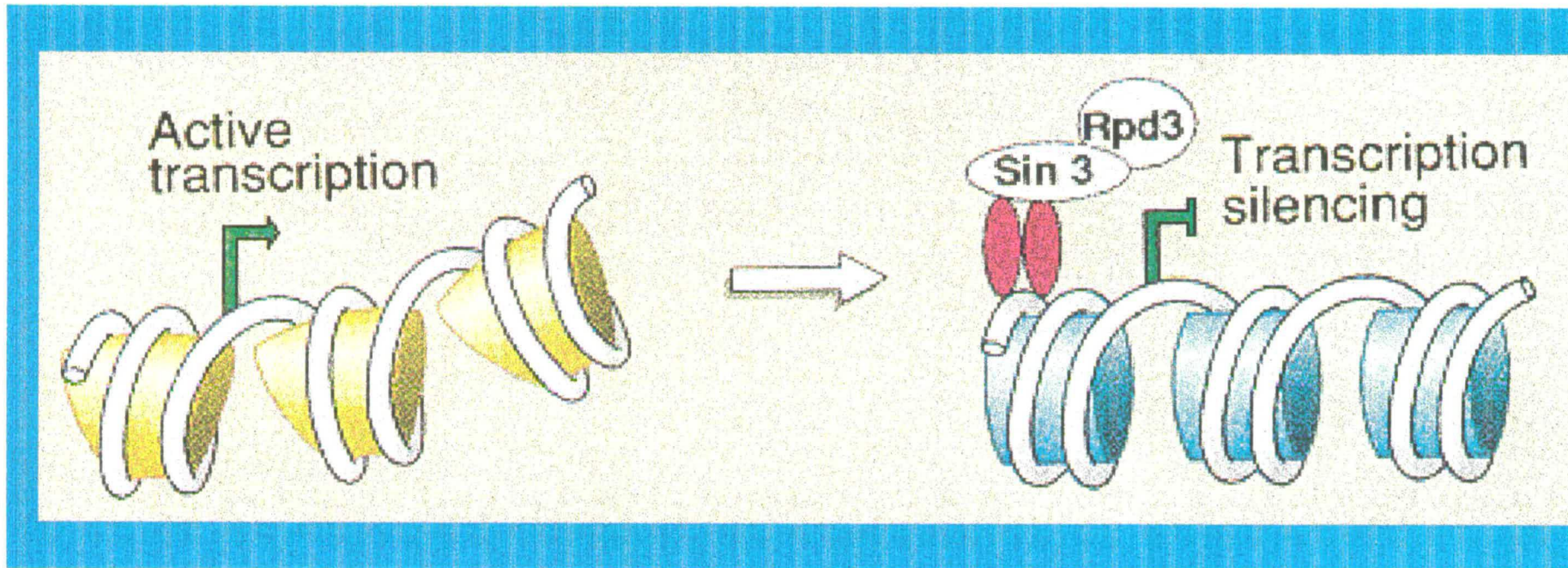


Figure 1.6

Inhibition of transcription by deacetylation.

Transcriptionally active chromatin contains hyperacetylated histones at the transcription start site (hooked arrow). Transcriptional silencing is achieved by targeting histone deacetylation to the start site. DNA-binding proteins (red) recruit Sin3p, which in turn interacts with Rpd3p, to modify the histones of the promoter region. Deacetylation generates stable and compact nucleosomes that inhibit transcription initiation.

This figure has been taken from Wolffe 1996.

acetylation equilibrium towards the deacetylated state, resulting in accompanying condensation of the chromatin environment. Thus the deacetylase activity may play a crucial role in amplifying repression mechanisms.

Several histone acetyltransferases have been identified. HAT-B is an enzyme that acetylates free histone H4 in the cytoplasm (Mingarro *et al* 1993), whereas HATs -A and -DB (DNA-binding) are nuclear and found bound to chromatin, and acetylate all four core histones when free or contained within a nucleosome (Attisano & Lewis 1990). Whereas the former are thought to acetylate newly synthesised histones during the deposition process, the latter are believed to be responsible for transcription-associated acetylation.

Recently, an SDS-PAGE-based activity assay was used by Allis and coworkers (Brownell & Allis 1995, Brownell *et al* 1996) to detect a single, catalytically active HAT-A subunit from *Tetrahymena* macronuclei. The assay used transcriptionally active macronuclei as an enriched source of hyperacetylated histones, while also ensuring that the enzyme preparation would be relatively free of contaminating cytoplasmic HAT-B activity. The acetyltransferase activity was identified as a single polypeptide of 55kDa, thought to constitute the native 220kDa enzyme by forming a complex containing four identical copies of the polypeptide. The 55kDa polypeptide was found to be a homologue of Gcn5p, a yeast adaptor protein required for the activity of a subset of transcriptional activators. Both proteins contain a highly conserved bromodomain motif found in a wide range of chromatin-associated proteins involved in transcriptional activation (Haynes *et al* 1992). The bromodomain, present in HAT-A and absent in HAT-B, may be important in targeting the enzyme to the transcriptional apparatus at specific chromatin sites. Its hydrophobic α helices may serve as sites for interaction with other transcription factors, thus recruiting the acetyltransferase to specific genes. Recombinant Gcn5p also has HAT activity, and exists in yeast in a heterotrimeric complex with two other polypeptides, Ada2p and Ada3p. Based on the high degree of conservation between yeast, ciliate,

Drosophila, and human components of the complex, this suggests that it functions as a HAT in all eukaryotes. While p55 appears to preferentially acetylate histone H3 in *Tetrahymena*, it is known that the native enzyme acetylates all four core histones, suggesting perhaps that the role of Ada2p and/or Ada3p may be to determine the substrate specificity. In addition, it has been reported that Gcn5p acetylates histone H3 and H4 in a non-random manner. Lys14 of H3, and lys8 and lys16 of H4 are preferentially acetylated. This is significant when considering that lys5 and lys 12 of H4 are the predominant sites used in deposition-associated acetylation, thus indicating that Gcn5p is involved in transcription-associated acetylation. Thus A- (transcription) and B- (deposition) type acetyltransferases function at distinct non-overlapping lysine residues (Figure 1.7). Recent data suggests there exists a functional interaction between Gcn5p and components of the SWI/SNF complex in yeast (Brownell *et al* 1996). The SWI/SNF complex is thought to create an open chromatin conformation by weakening histone/DNA interactions, thus facilitating transcription factor access to the DNA (Peterson & Herskowitz 1992, Cote *et al* 1994). It is thus possible that the SWI/SNF complex directs Gcn5p - the HAT activity - to specific sites in chromatin, encouraging chromatin modifications as a result of acetylation.

A cytoplasmic HAT-B type activity has been identified in the yeast *Saccharomyces cerevisiae* by Gottschling and colleagues (Parthun *et al* 1996). The two main components of the activity are Hat1p, encoding the catalytic subunit, and Hat2p, responsible for high affinity binding of the enzyme to histone H4. While Hat1p has the ability to specifically acetylate lys5 and lys12 of histone H4, its activity appears to be limited to acetylating only lys12 *in vivo*. This specificity may be a consequence of a modification of the subunit, and an alternative form of Hat1p may exist in the cytoplasm that acetylates H4 at lys5. Hat2p shows a high degree of similarity with both the human protein Rbap48, a component of the chromatin assembly factor CAF-1, and the human histone deacetylase HD1 (Parthun *et al* 1996, see section 1.3.3). The authors propose that the link between Hat2p, HD1, and Rbap48

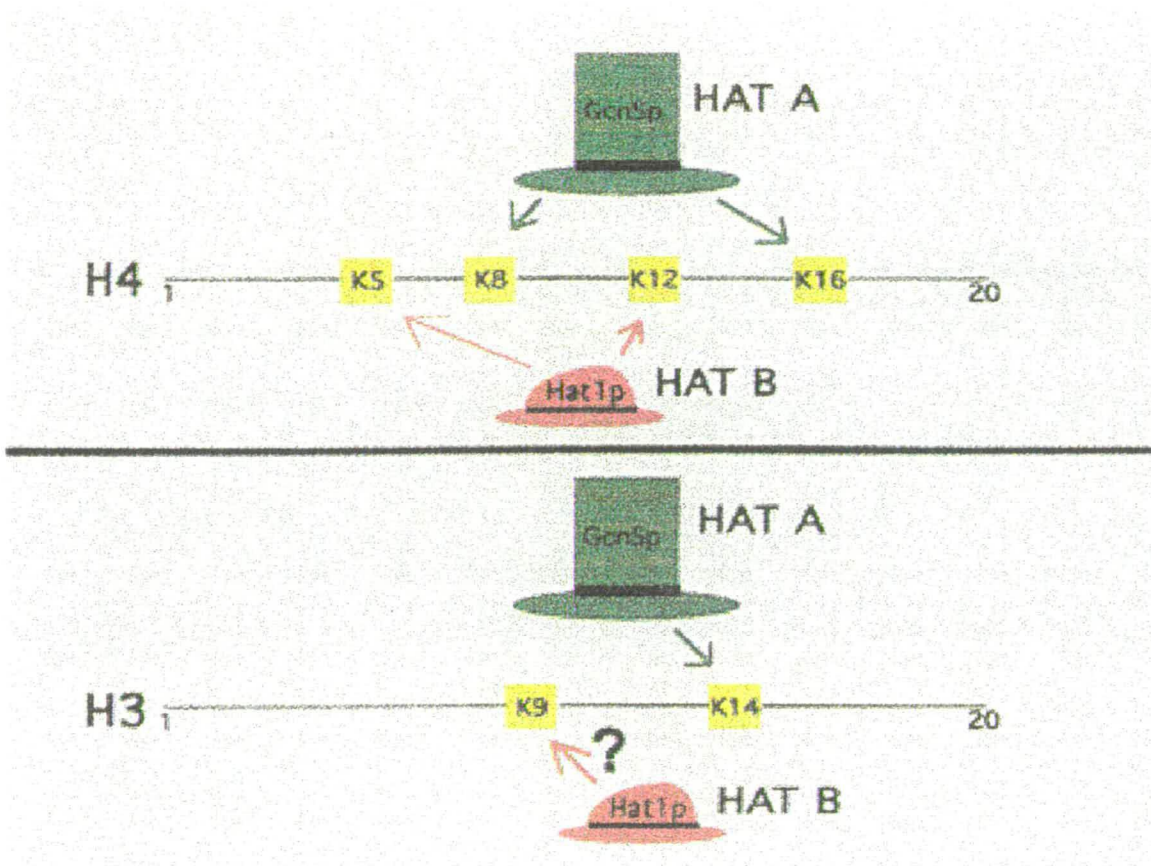


Figure 1.7

Deposition- and transcription-related acetylation sites are distinct and nonoverlapping.

Sites of acetylation in H3 and H4 are nonrandom. Cytosolic HAT-Bs preferentially acetylate H4 at lys12 and lys5. In contrast, transcriptionally-related acetylation sites lys8 and lys16 (and lys14 in H3) are preferentially acetylated by HAT-As. It is unclear whether a distinct HAT-B enzyme acetylates nascent H3.

This figure has been taken from Roth & Allis (1996).

is their interaction with histone H4 ie. that Hat2p and Rbap48 act as “escorts” for the acetylating and deacetylating activities, guiding them to histone H4.

Alone, Hat2p is unable to bind to the histone, requiring Hat1p for its highly specific interaction with H4. Both acetylated H4 and the Hat2p/Rbap48 protein are components of the chromatin assembly complex and, once assembled, the histone becomes rapidly deacetylated. This requires the action of HD1, which has been sequestered to the site by Rbap48.

One problem with this explanation is that deletion of *HAT1* and/or *HAT2* has no phenotypic effect. This may be due to a redundancy of HAT activity in yeast, given that there are putative homologues of *HAT* which may substitute. Alternatively, acetylation of histone H3 may compensate for the loss of H4 acetylation.

Two further human HAT activities have been identified by homology (Ogryzko *et al* 1996). CBP and p300 are transcriptional coactivators that are responsible for the regulation of a variety of DNA-binding transcription factors. The proteins show strong functional and sequence similarity to each other (they are often referred to as p300/CBP), and both share a region of homology with Ada2p (part of the Gcn5p-HAT activity in yeast, mentioned earlier) - the bromodomain. A further protein, the p300/CBP-associated factor (P/CAF) was recently isolated by homology (Yang *et al* 1996), as it shares an extended region of sequence homology to Gcn5p. It is also known to interact directly with p300/CBP. All of these proteins have been shown to copurify with HAT activity (Ogryzko *et al* 1996, Yang *et al* 1996). It is unclear why there are two putative HATs which appear to function cooperatively. One explanation is that one recruits the other to specific sites, via interaction with various DNA-binding transcription factors, resulting in targeted acetylation that ensures promoter activation (Figure 1.8). Alternatively, they may act synergistically by acetylating a specific histone from different angles, or different histones within the nucleosome. Whereas p300/CBP appears to be able to acetylate all four core histones, P/CAF's activity seems to be restricted to histones H3 and H4 *in vitro*, histone H3 being preferentially acetylated. Interestingly, both P/CAF and p300 interfere with cell cycle

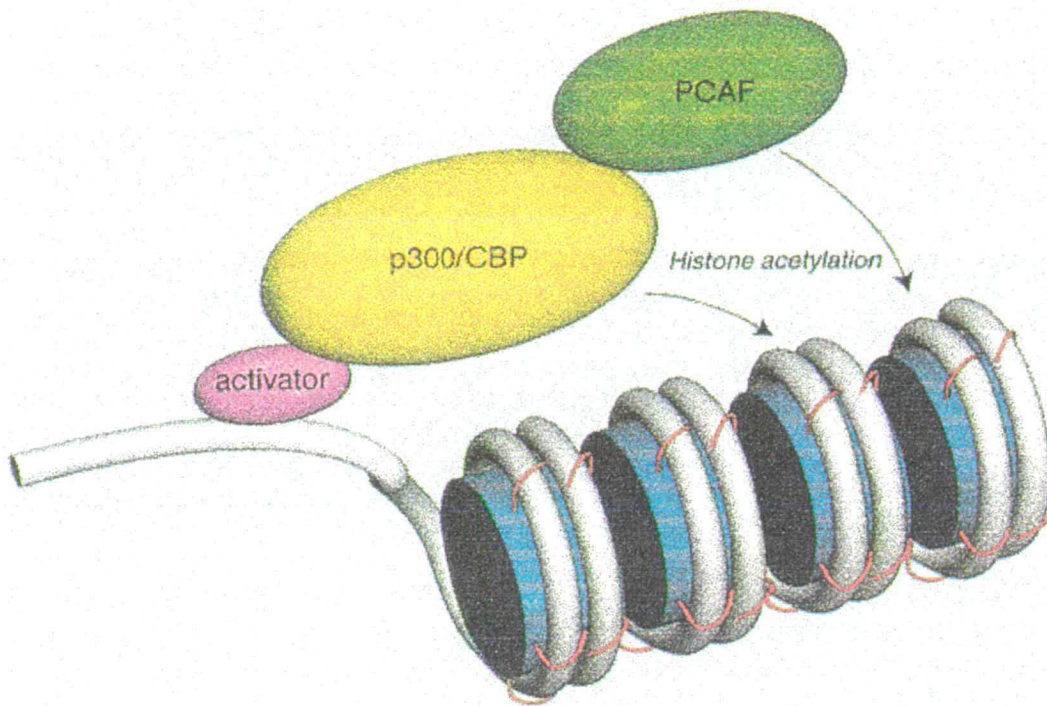


Figure 1.8

Model of molecular functions of p300/CBP and P/CAF.

p300/CBP and p/CAF form a complex at specific promoters via interaction with DNA-binding activators, and then acetylate histone tails (in red) in a promoter-specific manner. p300/CBP and P/CAF may act synergistically by targeting distinct histones from different angles on the same nucleosome.

This figure has been taken from Ogryzko *et al* 1996.

progression, suggesting that these factors may act as tumour suppressors. A new role for acetylation in tumorigenesis may well be uncovered by future research.

TFIID is a multimeric protein complex composed of a TATA box-binding protein (TBP) and several TBP-associated factors (TAF_{II}s). The TAF_{II}s mediate transcriptional activity by providing interaction sites for distinct activators and transcription initiators. CD Allis and colleagues showed that the human TAF_{II}250 and its homologues in *Drosophila* and yeast have HAT activity *in vitro* (Mizzen *et al* 1996). Both TAF_{II}250 and Gcn5p show a strong preference for H3 as an *in vitro* substrate, and the homology between these two proteins is found in their bromodomain. Deletion of the bromodomains of TAF_{II}250 did not alter the H3/H4 specificity of the HAT activity, indicating that it is unlikely that the bromodomain is involved in histone recognition.

Data obtained by Hendzel and colleagues have allowed them to propose a model for the presence of HAT and HD in transcription foci. Both HAT and HD were found to be present in the active/poised gene-enriched 0.15M NaCl-soluble chicken erythrocyte chromatin fractions (Hendzel *et al* 1991). This represents, however, only a minor portion of total nuclear HD activity, as most of the enzyme remains insoluble. Upon fractionating nuclei using a variety of different nuclear matrix isolation protocols, HD was consistently found to be associated with the nuclear matrix. In preparations of the nuclear pore-lamina complex, HD was solubilised, thus indicating that it is a component of the internal nuclear matrix. The same observation was made for HAT. Davie and Hendzel (Davie & Hendzel 1994) thus propose that both HAT and HD are attached to the internal nuclear matrix at sites of transcription, so that they are in contact with transcriptionally active nucleosomes, resulting in a site of rapid Class I acetylation that is observed in active chromatin. They speculate further that the close contact between nuclear matrix-bound enzymes, transcriptionally active chromatin, and the necessary transcription factors may contribute to the insoluble nature of active chromatin. It has been proposed recently that RNA polymerase II transcription localises to discrete nuclear compartments, known as

transcription foci. It may therefore be possible that both HAT and HD are also located at these foci, so that the enzymes are found organised in a spatial manner in order to facilitate their interaction with active chromatin. How non-coding DNA, that does not see transcription foci, is acetylated is not addressed.

A summary of the histone acetyltransferases and deacetylases isolated to date, and their interactions, are summarised in Table 1.3 shown below.

Table 1.3

Summary of histone acetyltransferases and deacetylases isolated to date.

HAT A - NUCLEAR	ORGANISM	FORMS COMPLEX WITH	HISTONES MODIFIED
p55 Gcn5p	<i>Tetrahymena</i> Yeast	Ada2p Ada3p SWI/SNF complex	H3 - H4
p300/CBP	human	transcriptional activators	H2A - H2B - H3 - H4
P/CAF	human	p300/CBP	H3 - H4
HAT B- CYTOPLASMIC	ORGANISM	FORMS COMPLEX WITH	HISTONES MODIFIED
Hat1p - Hat2p	yeast	Rbap48 (CAF1) HD1	H4
HD	ORGANISM	FORMS COMPLEX WITH	HISTONES MODIFIED
HD1	Human	?	?
Rpd3p?	Yeast	Sin3p?	?

This table has been adapted from Pennisi 1997.

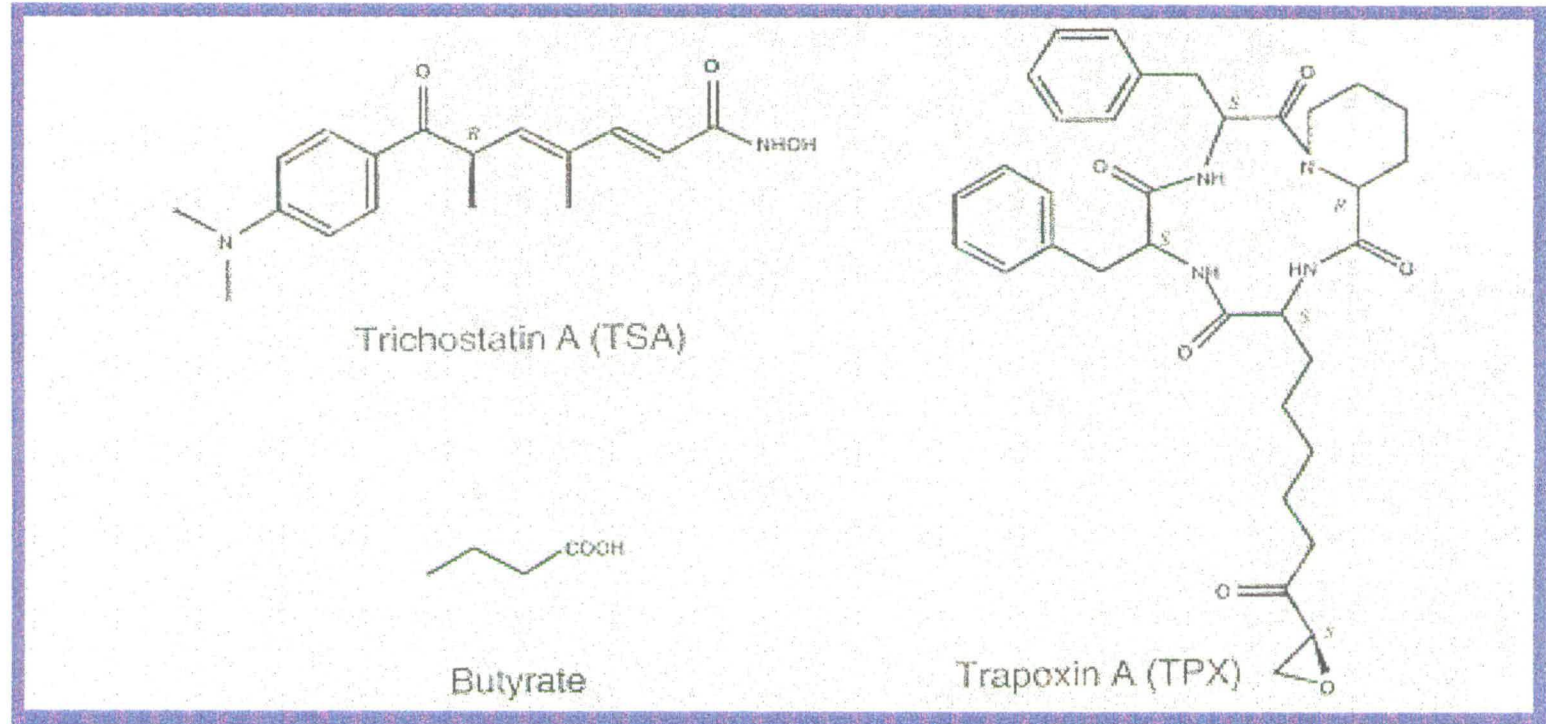


Figure 1.9

Inhibitors of histone deacetylase.

Chemical structures of trapoxin A, trichistatin A, and butyrate. These molecules inhibit the enzymatic deacetylation of lysine residues at the N-terminal tail of histones.

This figure has been taken from Yoshida *et al* 1995.

1.3.8 Inhibitors of histone deacetylase

The recent isolation of new inhibitors of HD (Figure 1.9) have provided additional information to the role played by the enzyme in acetylation of histones.

Sodium butyrate (NaB) has been the most widely used reversible inhibitor of HD (Kruh 1982). The inhibitor lacks specificity, however, and has multiple effects on nuclear function, as well as inducing expression of the histone H1⁰ gene (Khochbin & Wolffe 1993).

Specific inhibitors of HD, trapoxin and trichostatin A (TSA), have recently been isolated by Yoshida and colleagues (Yoshida *et al* 1990, Kijima *et al* 1993). These inhibitors work at nanomolar concentrations and are therefore far more potent than NaB. Trapoxin is an irreversible inhibitor of HD. It is an antitumour cyclic peptide, and contains an aliphatic epoxyketone side chain that is isosteric with N-acetyl lysine, thus enabling it to act as a substrate mimic (Kijima *et al* 1993). TSA is a reversible inhibitor of HD. It has been shown to block development of *Xenopus* (Almouzni *et al* 1994) and starfish (Ikegami *et al* 1993) embryos at specific stages, to induce differentiation in certain mammalian cell lines, to arrest cells in G1 and G2 phases (Yoshida *et al* 1990), and to induce expression of endogenous genes (Hoshikawa 1994). It is interesting to note that both NaB and TSA induce expression of the histone H1⁰ gene in cultured cells and embryos (Kress *et al* 1986, Khochbin *et al* 1993), and that patterns of histone acetylation in *Xenopus* are developmentally regulated (Dimitrov *et al* 1993).

While data obtained with HD inhibitors has provided intriguing correlations rather than clear evidence for the role of histone acetylation, it has shown that histone acetylation is involved in controlling both the cell cycle and gene expression.

1.4 Structural consequences of histone acetylation - direct and indirect

1.4.1 Introduction

Levels of histone acetylation are generally higher in transcriptionally active chromatin than in quiescent chromatin - this correlation has inspired a large amount of research to be devoted to the structural consequences of post-translational histone acetylation on nucleosome and higher order chromatin structure. The high affinity of histones for DNA creates a tightly bound environment for DNA to be transcribed in, where one side of the double helix is occluded as it faces the core histones. Histones were thus originally considered to be repressors of transcription. Acetylation was thought to be a mechanism of derepression, such that the resulting neutralisation of positive charges would decrease the binding affinity of histones to DNA, relaxing the nucleosomal environment, and allowing transcription to take place (Figure 1.10). While this proposal provides a simple solution, recent data implies the role of acetylation is not straightforward. Histone acetylation may otherwise affect the transcription process at several stages, and by one or more mechanisms. It might directly induce structural changes in chromatin, or facilitate histone displacement and repositioning during polymerase elongation. Or it may instigate interactions with other non-histone proteins such as transcription factors, presumably by means of the exposed N-terminal tails, which in turn allow transcription to take place.

Recent data obtained in an attempt to clarify the functional consequences of acetylation in the transcription process are summarised below, although only the most recent experiments are discussed in detail.

1.4.2 Biophysical and biochemical analyses of the structural consequences of histone acetylation

The first decade of research on histone acetylation was dedicated to the analysis of direct structural consequences of this modification on nucleosome structure. Several approaches were used - cells were incubated with sodium butyrate to analyse the structural alterations of hyperacetylated

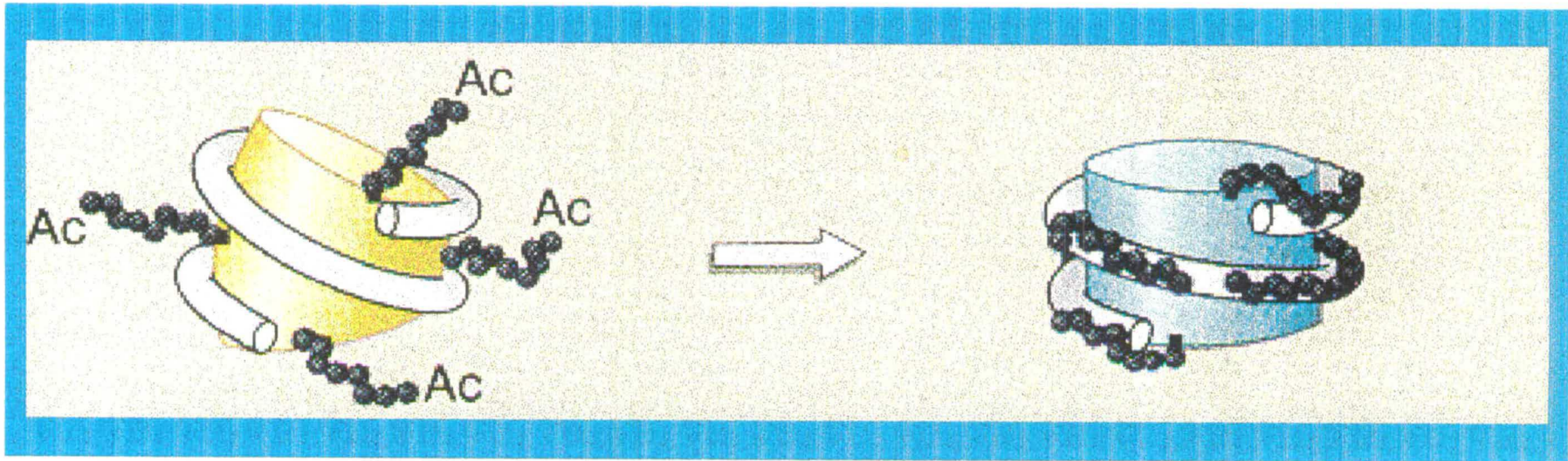


Figure 1.10

Derepression of transcription by acetylation.

Acetylation of histone N-terminal tails (black) loosens the nucleosome configuration by releasing contact between histones (yellow) and DNA (white), allowing access to transcription factors. Deacetylation stabilises contacts between the N-terminal tails and DNA, thus compacting the nucleosome structure (blue) and inhibiting access to transcription factors.

This figure has been taken from Wolffe 1996.

nucleosome core particles, nucleosomes were reconstituted *in vitro* and acetylated by treatment with sodium butyrate, and the contribution of the acetylable N-terminal tails was investigated by means of their deletion, both by proteolytic cleavage and by genetic mutation in yeast (Grunstein 1990).

Treatment of cells with sodium butyrate and the subsequent analysis by biophysical and biochemical means of the structural effects of acetylation, led to the conclusion that histone acetylation does not cause drastic changes in the conformation of a nucleosome core particle. Hyperacetylated histones were shown to have slightly decreased mobilities in non-denaturing nucleoprotein gel electrophoresis (Bode *et al* 1983), and altered accessibility of the histone H3 cysteine side-chain (Bode *et al* 1980). As a result of hyperacetylation, a site located 60bp from the ends of DNA in the nucleosome core particle, showed increased DNaseI sensitivity, suggesting the occurrence of a subtle conformational change within the 80-100bp of the nucleosome core particle in greatest contact with histones H3 and H4 (Ausio & Van Holde 1986, Richmond *et al* 1984). Acetylated cores were shown to be slightly more soluble than control cores (Perry & Chalkley 1982). Unchanged salt sensitivity as a result of hyperacetylation does not, however, support the idea that acetylated histones are more likely to be displaced as a result of their modification. And, using the technique of neutron scatter, no sign of unfolding could be detected in hyperacetylated nucleosomes (Imai *et al* 1986).

1.4.3 Effects of histone acetylation on nucleosome linking number

In prokaryotes, DNA is negatively supercoiled, and these supercoils are unconstrained. Topoisomerases, and the enzyme DNA gyrase, determine the extent of supercoiling, and this in turn regulates transcription of certain genes.

The situation in eukaryotes is less clear-cut. Eukaryotic DNA is supercoiled, but these supercoils are constrained by nucleosomes for most of the DNA. Transcriptionally active chromatin has been shown to contain constrained

supercoiling to the level found in typical nucleosomal organisation. However, initiation of transcription, both *in vivo* and *in vitro*, is found to be repressed from promoters contained within nucleosomal organisation, presumably due to a lack of accessibility of regulatory sequences for trans-acting factors. As only a small fraction of the genome is transcriptionally active at any one time, it is possible that the DNA of this transcriptionally active fraction exists in a less constrained state, perhaps as a result of nucleosome displacement. This would have the effect of allowing accessibility to DNA regulatory elements and would thus provide the appropriate environment for transcription to occur.

Recent work has addressed the hypothesis that histone hyperacetylation may be responsible for releasing constrained nucleosomal supercoils, thus allowing transcription to occur. The data obtained by several groups, discussed below in chronological order, has been conflicting, and it remains elusive whether histone acetylation affects nucleosomal structure.

Bradbury and colleagues (Norton *et al* 1989) used an *in vitro* system, developed by Simpson and coworkers (Simpson *et al* 1985), to determine whether hyperacetylation of nucleosome core particles would have an effect on the linking number per nucleosome particle. They used a closed DNA circle of tandemly repeated nucleosome-locating 5S RNA gene sequences, on which they reconstituted nucleosome core particles that differed in their acetylation levels (induced by treatment with sodium butyrate). Using this system they found that whereas the linking number change per control core particle (no treatment with sodium butyrate) was -1.04 ± 0.08 , the linking number change per hyperacetylated nucleosome core particle was -0.82 ± 0.05 . In other words, with increasing acetylation, the nucleosome DNA linking number decreased, indicative of relaxation in the supercoiled structure. The authors interpreted histone acetylation as having the property of a prokaryotic gyrase, in that it has the ability to release negative supercoils previously constrained by nucleosomes. While DNA gyrase can introduce unconstrained supercoiling into prokaryotic DNA, a eukaryotic version of the enzyme has not been identified.

In addition to this, the same group went on to show (Norton *et al* 1990), that nucleosome linking number change was controlled exclusively by acetylation of histones H3 and H4. Using the system described above, they determined the linking number change in minichromosomes reconstituted with fully acetylated histones H3 and H4 and very low levels of acetylation in H2A and H2B. The linking number change obtained was in close agreement with the linking number change for the hyperacetylated core particles found previously, in which all four core histones were highly acetylated. This result is interesting in view of evidence suggesting that acetylation of H3 and H4 has a different function to that of H2A and H2B (discussed in section 1.4.6). Thomsen and colleagues tested whether this hypothesis would hold *in vivo* (Thomsen *et al* 1991) by transfecting cells with an expression vector, and subsequently exposing the cells to differing concentrations of sodium butyrate. This would result in the newly transfected plasmid DNA being assembled into a minichromosome containing acetylated nucleosomes. Sodium butyrate, however, is known to inhibit DNA synthesis. This problem was overcome by treating the cells with sodium butyrate for an initial 16hr period, removing it for 24hrs to allow DNA replication to take place, and then adding it for a further 3hrs prior to harvesting the minichromosome. The results obtained indicated that a fraction (15%) of the total plasmid population was shifted to a lower level of superhelical density in response to sodium butyrate treatment. This was shown not to be an effect of nucleosome depletion, and was not affected by changes in rates of transcription. They suggested that perhaps only a subpopulation of minichromosomes contained fully acetylated chromosomes, and these were able to generate a detectable shift in linking number.

Lutter and colleagues (Lutter *et al* 1992) further tested this model, using a similar *in vivo* system. They tested the effect of histone hyperacetylation on minichromosomes of both SV40 and transfected plasmids, by adding sodium butyrate to cells prior to harvesting of the minichromosomes. In this study, however, they were unable to show a significant change in level of supercoiling. This discrepancy between the *in vitro* results obtained by

Bradbury and coworkers, and the *in vivo* results obtained by Thomsen and coworkers, was shown not to be due to specific properties of SV40, additional proteins being present on the *in vivo* assembled nucleosomes, or the assembly of a larger number of nucleosomes per minichromosome as a result of the sodium butyrate treatment. The authors suggest the *in vitro* results do not reflect the situation *in vivo*. The reduced linking number *in vitro* may be a consequence of acetylating the histones prior to assembly, or perhaps a result of the discrepancy between sequences used to bind nucleosomes. In addition, the data obtained by Bradbury and coworkers is derived from levels of nucleosome assembly which were 60% of those found in cellular chromatin. The response of nucleosomes at this under-saturated level may be different to that of nucleosomes found in cellular conditions.

Thus, while the simple concept that acetylation induces relaxation of the nucleosome structure by weakening of histone-DNA interactions, and thereby provides the necessary requirements for transcription, is attractive, it appears that acetylation by itself does not cause major changes in the structural conformation of chromatin. It remains to be seen to what extent these minor conformational changes, as a consequence of acetylation, are functionally relevant.

1.4.4 Histone acetylation as a regulatory signal

In vitro experiments have shown that while the presence of a nucleosome at a promoter sequence inhibits initiation of transcription, it does not inhibit elongation, as the elongation rate of transcription was found to be identical for a DNA sequence bound to a nucleosome or in a naked state (Lorch *et al* 1987). In addition, CpG island chromatin was shown to contain highly acetylated histones H3 and H4, and low amounts of histone H1 (Tazi & Bird 1990). Histone acetylation may thus be viewed as a mechanism for destabilising those nucleosomes which are located at a promoter sequence, in order to enable the binding of transcription factors and allow initiation of transcription. In this light, recent experiments investigating the role of histone acetylation in transcription factor binding are relevant.

Wolffe and colleagues (Lee *et al* 1993) have demonstrated a positive role for histone acetylation in TFIIIA binding to nucleosomal templates *in vitro*. Chromatin of the *Xenopus* 5S RNA gene was assembled *in vitro* with hyperacetylated core histones from sodium butyrate treated cells. Acetylation was found to relieve the inhibition of TFIIIA binding seen when the 5S RNA gene is found associated with unmodified histones, present as a tetramer (H3/H4)₂ or the octameric nucleosome core. The authors concluded that acetylation may alter the organisation of the nucleosome by releasing the inhibitory interaction of the N-terminal tails with DNA, such that the electrostatic interactions between the positive lysine residues in the tails and the phosphodiester backbone are reduced. Tryptic removal of the tails, including those lysine residues which may potentially be acetylated, facilitated TFIIIA binding, thus supporting this proposal. Furthermore, access of the transcription factor may be inhibited by the globular domains of the histones or the adjacent superhelix of DNA, both of which could be altered by acetylation of the tails. Alternatively, acetylation may promote direct interaction of the N-terminal tails with the transcription factor, although given that removal of the tails also allows TFIIIA binding, it is unlikely.

Vettese-Dadey and colleagues (Vettese-Dadey *et al* 1996) were further able to demonstrate, by coupling novel immunoblotting techniques to a gel retardation assay, that nucleosome cores with the highest affinity for the USF and GAL4-AH transcription factors, contained highly acetylated histone H4. In addition, nucleosome-transcription factor complexes appeared to be preferentially enriched in acetylated H4, relative to H3, indicating that acetylation of histone H4 in particular appears to play a primary role in enhancing transcription factor binding to DNA.

In contrast, Roberge and colleagues (Roberge *et al* 1991) showed that reconstituted nucleosomal cores containing either weakly or highly acetylated histones were equally inhibitory to the transcription of 5S RNA genes. The authors argue that while their results are likely to represent inhibition of transcription due to decreased binding of transcription factors, it may be that the *in vitro* system lacks factors present *in vivo*.

Other reports in the literature argue against a positive role for acetylation in transcription factor binding. Activation of the long terminal repeat fusion genes of the mouse mammary tumour virus was shown to be strongly inhibited by sodium butyrate (Bresnick *et al* 1990), and activation of the MyoD and myogenin genes in proliferating myoblasts and differentiating myotubes was shown to be inhibited by both sodium butyrate and trichostatin A (Johnson *et al* 1992), excluding possible side effects caused by sodium butyrate. Other *in vivo* experiments showed decreased prolactin receptor expression and binding in human breast cancer cells, in response to sodium butyrate treatment (Ormandy *et al* 1992). In these cases, inhibition of deacetylation appeared to repress transcriptional activation.

The discrepancy between the above results may partly be due to differences between *in vivo* and *in vitro* experiments.

1.4.5 Core acetylation effects on linker histone binding

Linker histone H1 (or H5 in chicken) is necessary for the condensed higher order packaging of DNA, and has been proposed to act as a transcriptional repressor. It was originally assumed that active genes were consequently devoid of linker histones, and that addition of H1 to the chromatin structure inhibited both transcriptional initiation and elongation. While this has been shown to be the case (O'Neill *et al* 1995), it has also been shown that H1 is present in active chromatin fractions, albeit in reduced amounts or with weakened affinity (Nacheva *et al* 1989) and, in *Tetrahymena*, strains where H1 has been deleted show little phenotypic differences relative to wild type strains (Shen *et al* 1995, Shen & Gorovsky 1996 - see section 1.1.6).

Wolffe and colleagues (Ura *et al* 1994) asked whether acetylation of core histone tails might impair the ability of linker histones to bind to transcriptionally active DNA. Using an *in vitro* assay for detecting binding of linker histones, they found that acetylation had no effect on association of the linker histone to the mononucleosome core. A single acetylated nucleosome core, derived from cells pre-treated with sodium butyrate, was assembled onto DNA containing the 5S RNA gene. The linker histone had

previously been shown to bind preferentially to nucleosome core particles relative to naked DNA (Hayes & Wolffe 1993). Hyperacetylation of the core histones did not significantly alter this preferential binding. Given that acetylation has been shown not to have a substantial effect on the overall shape of the core, or on the helical periodicity of DNA on the surface of the nucleosome, this result is not surprising.

Ausio and colleagues (Garcia-Ramirez *et al* 1992, Garcia-Ramirez *et al* 1995) propose a “multistate model of chromatin folding” which seeks to place the role of acetylation in folding of the chromatin fiber. According to this model, removal of histone H1 under physiological conditions results in the partial unfolding of the chromatin fiber, rather than a complete unfolding as is generally speculated to be the case. This gives rise to an intermediate rather than a lower order structure. Complete unfolding of the intermediate order structure to a lower order structure, which allows access of the activating factors required for transcription, replication and so forth, is only achieved by decreasing ionic strength (*in vitro*) or by removal of histone tails by trypsinization, thus lowering the concentration of ions. This event may be modulated *in vivo* by acetylation of the histone tails. Thus, acetylated chromatin in a lower order conformation becomes available to activating factors. The authors argue that chromatin depleted of H1 does not exhibit an extended conformation unless the histone tails are acetylated. Studies on the effect of acetylation on the compact higher order structure of chromatin showed the effect to be negligible. The authors therefore argue that acetylation may only act upon removal, or displacement, of histone H1, hence modifying the transcriptionally poised chromatin (in an intermediate order structure) into a transitionally unfolded conformation (lower order structure) allowing transcription to occur.

In order to account for the presumed barrier nucleosomes pose to transcription, a variety of models have been proposed. Nucleosome cores containing the full histone octamer have been shown to exhibit short-range mobility over 10bp DNA intervals. The location of a nucleosome can shift between various possible nucleosome positioning sites, providing the same

rotational setting of the DNA on the histone octamer is maintained (Pennings *et al* 1991, Meersseman *et al* 1992). This characteristic of nucleosomes may thus facilitate transcription factor access to active DNA. Linker histones have been shown to restrict nucleosome mobility (Pennings *et al* 1994, Ura *et al* 1995), locking the nucleosome into a unique position and possibly over an essential promoter, hence acting as transcriptional repressors. Felsenfeld and colleagues (Studitsky *et al* 1994, Studitsky *et al* 1995) have elaborated on this theme *in vitro*, claiming that a nucleosome can “step around” a transcribing polymerase without leaving the template. The idea is that transcription induces translocation of the histone octamer by up to 100bp, by the mechanism shown in Figure 1.11. RNA polymerase initiates transcription at the promoter. As the promoter approaches the nucleosome it induces dissociation of proximal DNA from the nucleosome. The DNA behind the polymerase associates with the exposed surface of the octamer to form a loop, while the DNA ahead of the polymerase continues to uncoil from the octamer. The nucleosome is thus reformed behind the polymerase, blocking the promoter, and the polymerase completes transcription. The kinetics of transcription gives support to this model, as the polymerase molecule appears to transcribe the first 25bp rapidly, then hits a barrier and pauses, and subsequently speeds up again, completing transcription as if the barrier had been removed. The barrier may be read as being the nucleosome, which the polymerase reaches and then side-steps via the intermediate DNA loop. Whether this idea holds *in vivo* is as yet unclear.

1.4.6 Genetic analysis of histone tail function

Mutational analysis in *Saccharomyces cerevisiae* has allowed the function of histone tails, in particular those of histones H3 and H4, to be studied. While it is unclear what role, if any, acetylation may play in the following experiments, it is important to outline the work carried out in this field over the last few years.

The sequence of H4 has remained almost invariant over evolution. While deletions in the hydrophobic core of H4 are lethal, deletions in the hydrophilic

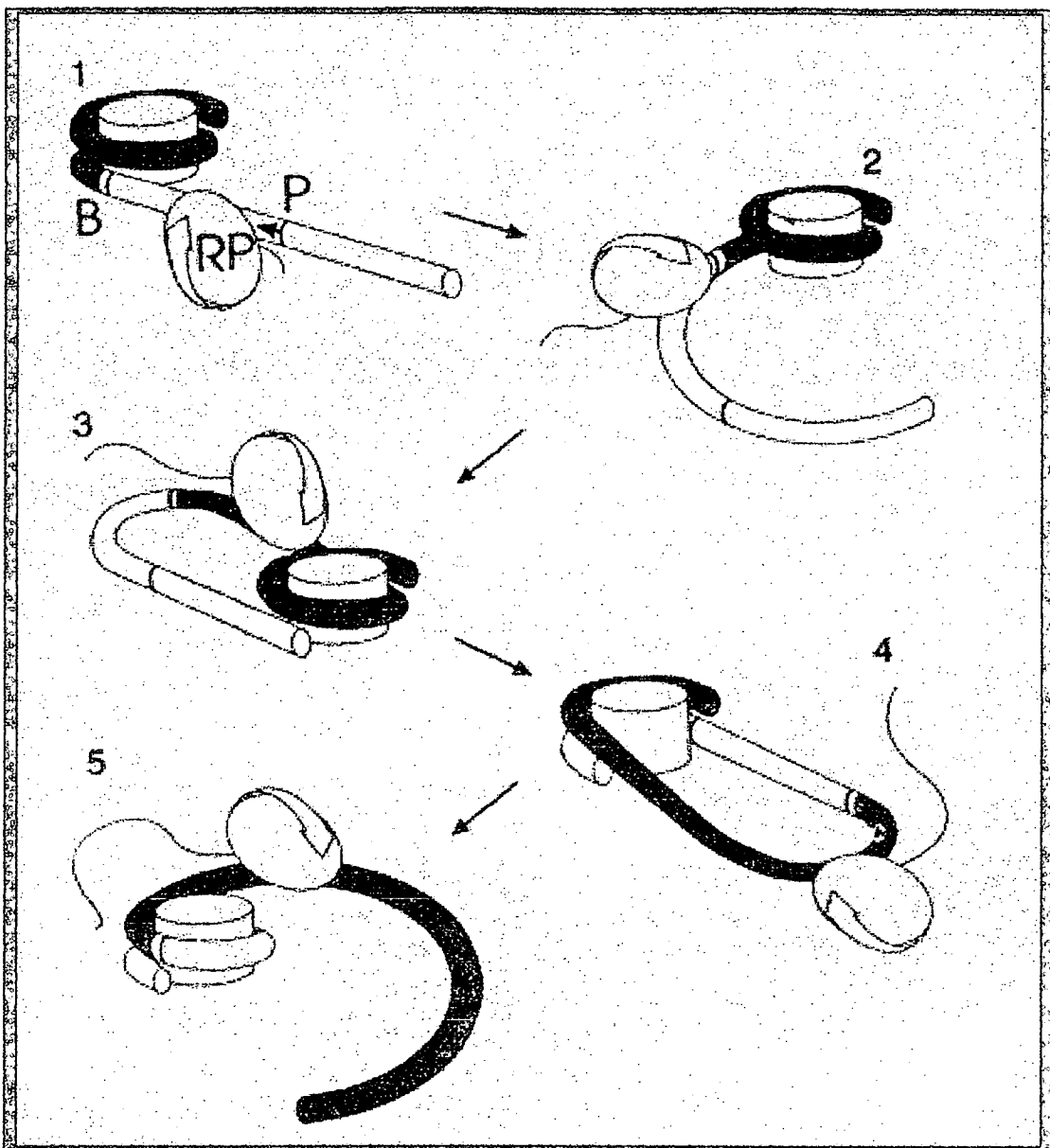


Figure 1.11

A model for transcription through a nucleosome core.

RNA polymerase (RP) initiates transcription at the promoter (P). As the polymerase approaches the core it induces the dissociation of proximal DNA from the core, exposing part of the octamer surface. The DNA behind the polymerase binds to the exposed octamer surface to form a loop. Ahead of the transcribing polymerase, the DNA continues to uncoil from the octamer, while behind the polymerase, DNA coils around the octamer. The nucleosome is reformed around the polymerase, and it completes the transcript.

This figure has been taken from Studitsky *et al*/1994.

N-terminus are viable, albeit with altered chromatin structure and lengthened cell cycle (Kayne *et al* 1988). In addition, deletions in the N-terminal tail of histone H4 derepress the silent mating type loci, HML α and HML α , suggesting there is an interaction between the histone tail and the SIR (silent information regulator) proteins, negative regulators of the silent loci. Additional studies have shown that the histone H3 tail is not required for repression of the silent loci, although it is important for repression at the telomeres and at partially disabled silent mating type loci (Thompson *et al* 1994). Specific histone domains are thus required for silencing at the mating type loci and at the telomeres, and have been narrowed down to amino acids 4-20 of histone H3 and 16-29 of histone H4, thus inclusive of acetylatable lysine residues (Johnson *et al* 1992, Thompson *et al* 1994). It has also been shown by Grunstein and colleagues (Ling *et al* 1996) that the tails of histones H3 and H4 are functionally redundant with respect to nucleosome assembly, as the presence of either tail restores viability and allows assembly in cell extracts. The tails need not be attached to the respective nucleosome cores for restored viability. Their exchange, however, does disrupt silencing of the mating type loci and gene regulation.

Significantly, an interaction between SIR3 and SIR4 proteins with specific silencing domains of the H3 and H4 tails was discovered by Grunstein and coworkers. Initially, mutations in the SIR3 gene were shown to suppress H4 substitution mutants, but not deletion mutants, suggesting that the SIR3 protein binds to the amino-terminal of H4 and forms part of a complex required for silencing (Johnson *et al* 1990). This was confirmed *in vitro*, using a protein-binding assay, and by immunofluorescence with both SIR3 and SIR4 (Hecht *et al* 1995), demonstrating that the silencing domains of H3 and H4 tails directly interact with SIR3 and SIR4. The authors propose a model for the formation of heterochromatin in yeast, where RAP1 (which binds to telomeric C₁₋₃A repeats) binds to the telomere, and interacts with SIR3 and SIR4 proteins, thereby recruiting SIR proteins to the telomeres and initiating the assembly of a multi-protein heterochromatic complex. This complex can

subsequently spread along the chromosome by interaction of the SIR proteins with the histone tails (Figure 1.12).

Silencing at the mating type loci is thought to function in a similar manner. The silent mating type loci, HML and HMR, each have flanking sequences required in *cis* for repression of gene expression. These silencers, known as E and I elements, contain binding sequences for RAP1 and ABF-1 (another transcriptional activator which binds to ARS (autonomously replicating sequence) elements). *Trans*-acting factors are also required for repression, namely the SIR proteins. While SIRs 2,3, and 4 appear to be required for maintaining the repressed state, by means of interactions with the histone tails, SIR1 is thought to be responsible for initially establishing silencing. One of the subunits of the multi-protein origin recognition complex (ORC1) has been shown to bind to SIR1 (Triolo & Sternglanz 1996). In addition, ORC is known to bind to the ARS consensus sequence contained within the silencer elements. These multiple interactions can thus be brought together into the following model for silencing of the mating type loci, as shown in Figure 1.13. The HML and HMR silencer elements contain binding sites for ORC1, RAP1, and ABF1. ORC is thought to recruit SIR1 via the ORC1 subunit, and RAP1 is thought to recruit SIR3. SIR4 is brought into proximity with SIR3 by interaction with SIR1, and the interaction between SIR3 and SIR4, known to form heterodimers with each other, creates a protein array that spreads to silence nearby genes. Establishment of this repressed state will occur by interaction of the SIR3/SIR4 complex with histone tails.

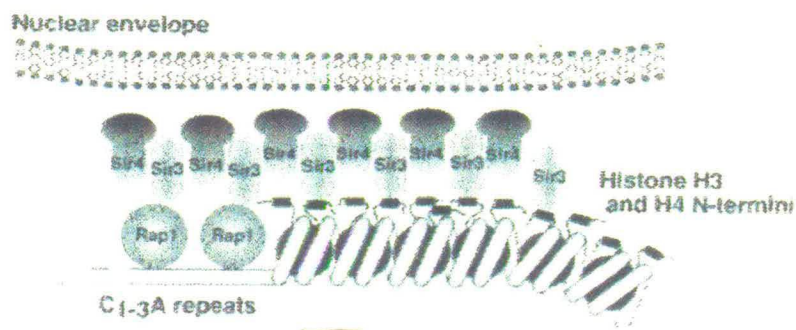


Figure 1.12

A model for the formation of heterochromatin and transcriptional repression at yeast telomeres.

RAP1 binds to telomeric C₁₋₃A repeats and is able to interact with SIR3 and SIR4. RAP1 may recruit SIR proteins to the telomeres and initiate the assembly of a multi-protein complex. SIR3 and SIR4 may interact with the histone H3 and H4 N-terminal tails, thus producing the heterochromatic complex that can spread along the chromosome.

This figure has been taken from Hecht *et al* 1995.

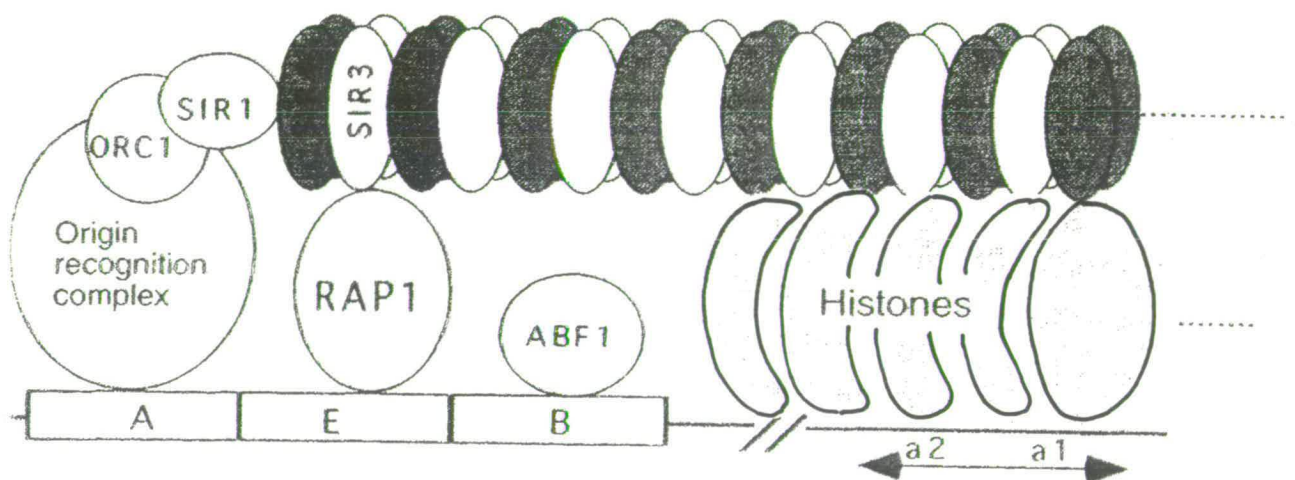


Figure 1.13

A model for the establishment of silencing by SIR1 at the HMR locus.

RAP1 and ABF1 bind to the silencer elements of the HMR locus. SIR3 interacts with RAP1, and with SIR4 to form an array. The SIR3/SIR4 array begins at the silencer and spreads to silence nearby genes. The role of ABF1 is not known.

This figure has been taken from Triolo & Stenglanz 1996.

1.5 Histone acetylation and transcriptional activity

1.5.1 Introduction

A wide range of data exists in support of Allfrey's original proposal (Allfrey *et al* 1964) that the major role of core histone acetylation is to facilitate transcription of genes packaged within the modified nucleosomes. In *Tetrahymena*, for example, the transcriptionally active macronucleus contains hyperacetylated core histones, whereas the inactive micronucleus does not (Vavra *et al* 1982, Chicoine & Allis 1986).

Biochemical fractionation procedures for selecting active gene sequences have often found histone acetylation to be associated with the transcriptionally active fractions. Ridsdale and Davie (Ridsdale & Davie 1987) showed that the transcriptionally competent β -globin gene sequence is soluble at physiological ionic strength, and is also associated with hyperacetylated histones H2A, H2B and H4. Ip and colleagues (Ip *et al* 1988) separated transcriptionally active genes on the basis of their low density, claimed to be a result of association of the active gene with additional proteins involved in the transcription process. The bulk of chromatin, isolated as a higher density material, contains both inactive genes and potentially active genes. The low density fraction was found to be highly enriched in rapidly acetylated histones. Nucleosomes found at the coding regions of ribosomal genes in *Physarum* can unfold to uncover the sulfhydryl groups of histone H3, making them accessible to sulfhydryl reagents. This characteristic of transcriptionally active chromatin allowed Allfrey and colleagues (Allegra *et al* 1987) to selectively retain active genes by binding of the sulfhydryl groups to organo-mercurial/agarose columns, thus taking advantage of the altered topology of the nucleosome during transcription. The retained fraction was shown to contain hyperacetylated histones, in particular histones H3 and H4. A further experiment was recently carried out by Bradbury and colleagues (Breneman *et al* 1996), where untreated and NaB-treated nucleosomes were fractionated according to their acetylation level. The resulting fractions were subsequently 'painted' back onto



metaphase chromosomes by FISH, and the pattern showed that regions of DNA are differentially packaged along chromosomes, in much the same way as was shown by Jeppesen and Turner using anti-acetylation antibodies (Jeppesen & Turner 1993 - see section 1.3.5). Following NaB treatment, weakly acetylated chromatin hybridised to centromeric regions, whereas hybridisation with highly acetylated chromatin resulted in a pattern similar to R banding. This pattern was also seen in control cells, although weakly acetylated chromatin labelled all of the chromosome at a moderate level. While chromatin selected by these fractionation procedures represents both transcriptionally active genes and acetylated histones, these components may be claimed to represent distinct subsets rather than being characteristics of the same stretch of chromatin. A direct link between the two has been established mainly by the use of antibodies against acetylated histones and immunoprecipitation techniques.

1.5.2 Immunoprecipitation of acetylated histones

A direct link between active genes and core histone acetylation has been established by the work of Crane-Robinson and colleagues, using an affinity-purified antibody to fractionate chromatin, that recognises the epitope ϵ -acetyl lysine. The group initially demonstrated the enrichment of acetylated histones in α^D globin sequences (Hebbes *et al* 1988) by taking chromatin from the erythrocytes of 15-day old chicken embryos. Chromatin fragments were then incubated with the affinity-purified antibody in a sodium butyrate-containing medium, thus separating the chromatin into antibody-bound and antibody-unbound fractions. Histones were subsequently extracted to assess core acetylation levels, and the bound fraction was shown to contain high levels of acetylation, particularly of histones H3 and H4. Probes were then used to screen for the presence of transcribed gene sequences. α^D globin, known to be transcribed in 15-day old chicken embryos, was found to be 15-30 fold enriched in the antibody-bound chromatin, relative to the input chromatin, whereas no enrichment of ovalbumin sequences, inactive in chicken erythrocytes, was found in the antibody-bound fraction.

This work was taken further (Hebbes *et al* 1992) to address whether acetylation is linked to developmentally regulated transcription, and whether it is a feature of “poised” genes - genes that, although they may not be undergoing the actual process of transcription, are capable of being transcribed in a particular tissue. This category does include those genes which have previously been transcribed but are no longer engaged in active transcription. The experimental approach was similar to that described above, selecting chromatin containing acetylated histones from both 5-day and 15-day old chicken erythrocytes (Figure 1.14). The acetylated chromatin fraction was then probed with DNA sequences of both the embryonic β^P gene (active at 5 days, inactive at 15 days) and the adult β^A gene (inactive at 5 days, active at 15 days). The data showed both active (β^P gene at 5 days, β^A gene at 15 days) and “poised” (β^P gene at 15 days, β^A gene at 5 days) genes were enriched in acetylated histones to a similar extent. The authors conclude that the level of acetylation at the β^P and β^A gene loci is similar, and is present at 5 days and has not changed by 15 days. The developmental switch in transcription from β^P to β^A is therefore not a consequence of acetylation.

This same technique of immunoprecipitation of acetylated chromatin followed by detection of sequences present in the selected fraction was used to analyse the distribution of acetylation throughout the chicken β -globin locus - to determine whether high levels of acetylation were restricted to the coding sequences (Hebbes *et al* 1994). Probes spanning several regions within the locus were used to map DNase I sensitivity throughout the locus, and to define the levels of acetylation at those regions. The results showed that core histone acetylation spanned the entire DNase I sensitive domain, covering both genes and intergenic DNA. The DNase I resistant chromatin found on either side of the β -globin locus correlated with reduced levels of acetylation, enforcing the previously observed correlation between DNase I sensitivity and hyperacetylation, perhaps as a result of an open conformation of the chromatin.

CHICKEN β GLOBIN LOCUS

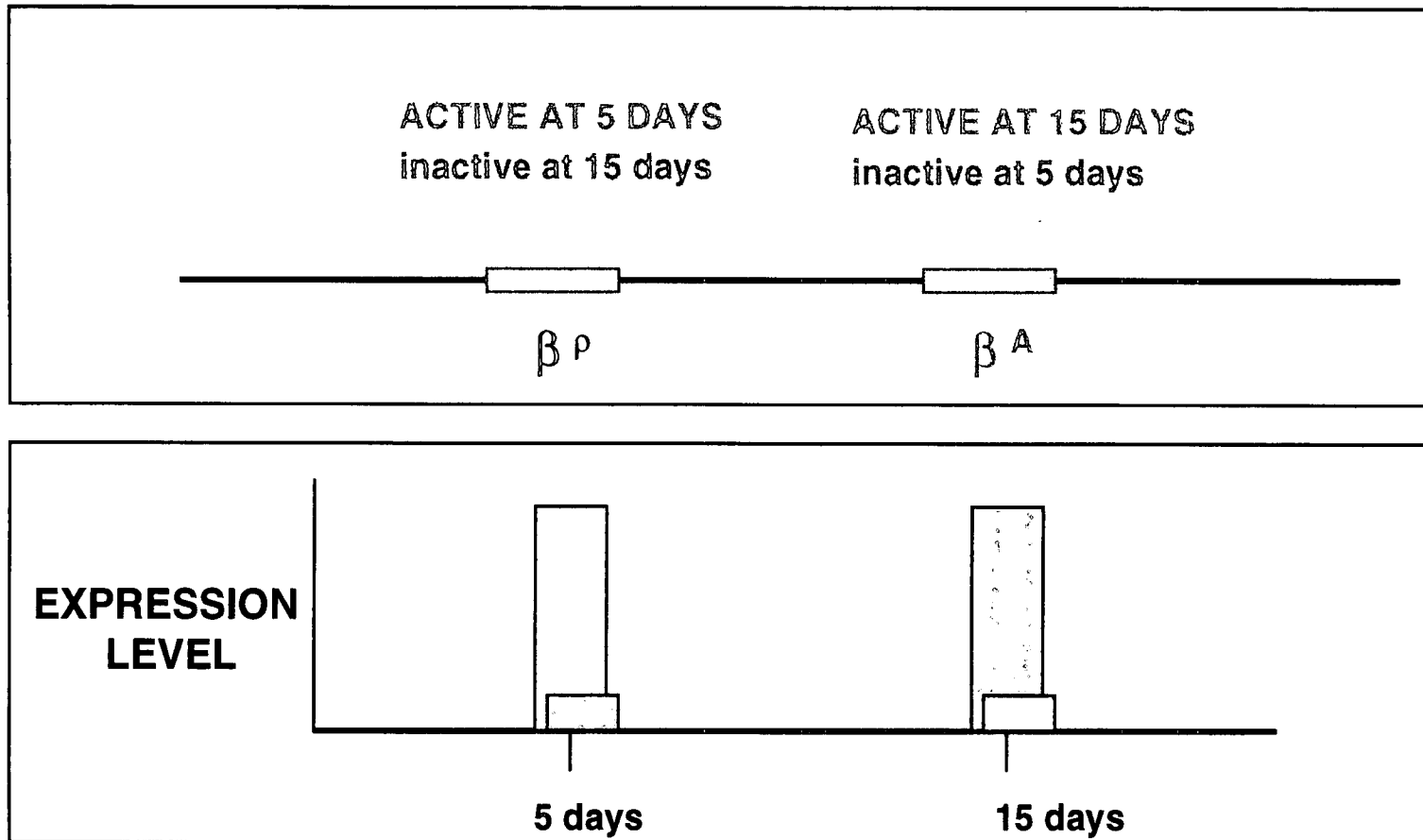


Figure 1.14

Expression levels of β^P and β^A at the chicken β globin locus in 5- and 15-day old chicken erythrocytes.

To test whether hyperacetylation might be induced on activation of a single gene in a cell line, Crane-Robinson and colleagues used their immunoprecipitation technique to look at the acetylation status of the platelet derived growth factor B chain (PDGF-B) gene, a gene which is induced to strong expression upon differentiation of the cell line (Clayton *et al* 1993). They observed the acetylation status of three genes - an actively transcribing gene (α -globin), a silent gene (human growth hormone (HGH)), and the inducible gene (PDGF-B). Prior to differentiation of the cell line, by treatment with the phorbol ester TPA, there was enrichment of α -globin in the antibody-bound fraction, and no enrichment of HGH. The inducible PDGF-B gene, although meant to be non-transcribing in undifferentiated cells, was found to be enriched in the antibody-bound chromatin, paralleling previous findings that "poised genes" were acetylated. Northern analysis of the expression levels of PDGF-B, before and after differentiation of the cell line, indicated that a very low level of PDGF-B transcripts were present in undifferentiated cells, and that treatment of the cells with TPA resulted in a large increase in expression of the gene. On differentiation of the cells, no increase in enrichment of PDGF-B was seen in the antibody-bound fraction, indicating that acetylation was present at the gene locus prior to induction, and did not change once the gene was actively being transcribed.

A drawback of the technique used by Crane-Robinson and colleagues lies in that the antibody used by them recognises ϵ -acetyl lysine, and will therefore select for all acetylated core histones, and will not distinguish between histones, or between the different acetyltable isoforms of each histone. Yet both of these factors appear to be of some functional significance. It may be that active chromatin only contains acetylated histones H3 and H4, whereas "poised" chromatin contains acetylated histones H2A and H2B, for example, and the system will therefore not be able to distinguish between them.

Turner and colleagues used their isoform-specific antibodies to immunoprecipitate chromatin from a human cell line (O'Neill & Turner 1995), in a similar manner to that used by Crane-Robinson and colleagues, described above. O'Neill and Turner's experiments used either a pool of

antibodies to H4 acetylated at lys5, 8, and 12 (thus selecting out mono-acetylated histone H4) or each antibody individually. Their results confirmed immunofluorescence data showing H4 was underacetylated at centric and telomeric heterochromatin, but failed to detect an increased level of acetylation associated with any of the active genes studied, compared to bulk chromatin. Furthermore, when several gene loci, both constitutively or potentially active, and inactive, were examined, no increase in the level of acetylation was detected in actively transcribed or poised genes. For example, induction of c-fos transcription by treatment of cells with TPA showed no alteration in the level of acetylation at the locus. Thus, whereas Crane-Robinson found transcribed and poised genes enriched in acetylated chromatin fractions, Turner found no enrichment relative to bulk chromatin. Interestingly, while induction of the c-myc and c-fos genes with DMSO or TPA did not alter the level of acetylation within the genes, a transient increase in acetylation within the centric heterochromatin was noted.

1.5.3 Detection of histone acetylation by immunofluorescence

An alternative approach has been developed by Turner and colleagues, based on the use of antisera that can distinguish between histone H4 molecules acetylated at different lysine residues *in vivo*. Indirect immunofluorescence microscopy defines the distribution of H4 molecules acetylated at each lysine residue, and differentiate between possible functions of the different isoforms.

The antibodies against acetylated forms of histone H4 were produced in rabbits, using synthetic peptides corresponding to the N-terminal tail acetylated at each of lysines 5, 8, 12, and 16, and to tetra-acetylated histone H4 (Turner & Fellows 1989). The antibodies were subsequently used to show a definite association of acetylated histone H4 molecules with regions of transcriptional activity, in a variety of species. In the salivary glands of midge (*Chironomus*) larvae, for example, it was shown that defined regions of the interphase region were enriched in acetylated H4, although these did not correlate with bands of decondensed chromatin (known as interbands).

The transcriptionally active Balbiani rings, seen under the microscope as regions of decondensed (“puffed”) chromatin were also seen to be enriched in acetylated H4, in particular at the boundaries of the expanded chromatin, in non-transcribing flanking regions. This was speculated to facilitate efficient binding of the transcription machinery to regions flanking poised genes (Turner *et al* 1990). These results were expanded in the analysis of *Drosophila* polytene chromosomes, showing that H4 acetylated at each lysine residue gave a unique distribution pattern (Turner *et al* 1992). H4 acetylated at lys5 and lys8 were found in specific islands in all four chromosomes, whereas H4 acetylated at lys16 was found predominantly on the male X chromosome, playing a definite role in dosage compensation (see section 1.3.5). H4 acetylated at lys12 was found in heterochromatin. As there is no fixed order of site usage in *Drosophila*, contrary to most other species, all four acetyltable lysines are used in mono-acetylated H4, and the immunolabelling pattern consequently reflects the distribution of each isoform. It may be possible that *Drosophila* uses acetylating and deacetylating enzymes that are specific for each isoform, and that are situated in specific regions of the genome to give particular distribution patterns.

Lampbrush chromosomes from immature oocytes of the amphibian *Triturus cristatus* were labelled with the antisera against acetylated H4 at the bases of transcription loops, in particular of mono- and di-acetylated isoforms. The loops themselves contained foci of intense fluorescence. In contrast, chromosomes from mature oocytes were relatively underacetylated, in agreement with the low levels of transcription found in these chromosomes. Following treatment of the chromosomes with butyrate, however, levels of acetylation were shown to increase, giving similar patterns of fluorescence. In addition, the treatment appeared to induce the formation of vestigial transcription loops, indicating that perhaps hyperacetylation precedes loop formation (Somerville *et al* 1993).

The pattern of fluorescence obtained in human chromosomes has been discussed in section 1.3.5, but again there appears to be a distinct

correlation between histone H4 acetylation and R bands, where most genes are thought to reside (Craig & Bickmore 1994). Furthermore, both centric heterochromatin and the inactive X chromosome are shown to be underacetylated relative to the rest of the genome (Jeppesen & Turner 1993). Recent antibodies developed against acetylated isoforms of histones H2A and H3 have been used to label human chromosomes, and these histones too have been shown to be underacetylated in both the inactive X chromosome and centric heterochromatin (Belyaev *et al* 1996).

Lastly, by immunolabelling of metaphase chromosomes of ES cells with antibodies to acetylated histone H4, Turner and colleagues (Keohane *et al* 1996) showed that deacetylation of the inactive X chromosome follows both Xist expression and decrease in expression of genes on the inactive X chromosome. This suggests that deacetylation is not required for inactivation of the second X chromosome, but may be necessary for its maintenance. It was also shown to follow the appearance of the late-replicating (inactivated) X chromosome, suggesting that while underacetylation is a characteristic of late-replicating DNA, it is not a prerequisite for late replication.

1.5.4 Histone acetylation and heterochromatin

Braunstein and colleagues examined the relationship between histone acetylation and silencing in yeast (Braunstein *et al* 1993). They predicted that nucleosomes packaging the silent mating type loci, HML and HMR, would be underacetylated relative to the identical but active gene situated at the MAT locus. Furthermore, this acetylation pattern would be lost on disrupting silencing by mutation. To test these predictions, the group used an antibody raised against 20 amino acids of the N-terminal tail of histone H4 in *Tetrahymena*, where all acetylatable lysine residues are acetylated. This antibody was shown to cross-react with multiply acetylated histone H4 in yeast. Yeast chromatin was immunoprecipitated by a strategy similar to that used by Crane-Robinson and colleagues, and the antibody-bound fraction was tested for the enrichment of mating type genes. The results confirmed that the silent mating type genes, HML and HMR, were under-represented in

hyperacetylated chromatin, relative to the expressed MAT gene. The same experiment was then performed using chromatin from *sir2* and *sir3* strains, where silencing is repressed, and HML and HMR are expressed to the same level as MAT. HML and HMR sequences were found to be enriched in hyperacetylated histones, to the same extent as MAT. To determine whether this difference in acetylation was dependent on the different rates of transcription between the wild-type and mutant strains, rather than on a direct effect of silencing, the group constructed a silent mating type gene which could not be transcribed, even when introduced into a *sir3* strain. The mating type gene was underacetylated when present in the wild-type strain, but hyperacetylated to the level of the active MAT gene in the *sir3* strain. Thus acetylation of the genes correlated with their silenced status, even when the gene was incapable of being transcribed. Furthermore, telomere sequences, also silenced in yeast, were found packaged in hypoacetylated chromatin. Overexpression of the SIR2 protein, but not the SIR3 protein, was shown to decrease the level of acetylation associated with histones H2B, H3 and H4. Loss of the SIR2 protein led to increased histone acetylation of the silenced domains. Thus, SIR2, which is required for silencing *in vivo*, is responsible for promoting deacetylation at silenced loci. It may be that SIR2 encodes a yeast deacetylase.

CHAPTER TWO - MATERIALS AND METHODS

2.1 Cell Culture

2.1.1 Media and solutions

DMEM (Gibco BRL)

Dulbecco's Modified Eagle's Medium supplemented with 10-20% foetal calf serum (FCS) (Gibco BRL) and 30µg/ml L-proline.

MEM Alpha (Gibco BRL)

MEM Alpha medium supplemented with 10-20% FCS (Gibco BRL) and 1% chicken serum (ICM).

Trypsin/EDTA solution (T/E)

2.5% trypsin and 0.02% EDTA in buffered saline.

2.1.2 Cell lines

CHO-K1 is a Chinese hamster ovary fibroblast cell line. The cell line was available in the lab.

UT-1 is derived from the CHO-K1 cell line by growth in compactin, resulting in amplification of the HMG-R gene (Chin *et al* 1982). The cell line was obtained from the European Type Culture Collection.

DT40 is a chicken lymphoblastoid cell line. The pre-B cells have been transformed with the avian leukosis virus. The cell line was kindly donated by C Cooke (Swann Building, Institute of Cell and Molecular Biology, University of Edinburgh)

2.1.3 Thawing of cells stored in liquid nitrogen

All cell lines used in this project were stored in liquid nitrogen, in 1ml of culture medium and 10% glycerol. Cells were recovered from frozen by rapidly thawing them in a 37°C water bath, and resuspending them in 9ml of the appropriate medium in a sterile 9cm Petri dish, or in a T-25 flask. The culture medium was changed 24 hrs after plating out.

2.1.4 Maintenance of cell lines in culture

All cell culture work was carried out in a lamina flow hood.

CHO-K1 and UT-1 cells were cultured in DMEM, supplemented with 10% FCS and 30µg/ml L-proline. They were grown as a monolayer on sterile 9cm Petri dishes (Nunc) in a 37°C incubator, under 10% CO₂ atmosphere. The cells were passaged once a week, and were harvested by incubation with 4ml of T/E for 2-3 mins at 37°C.

DT40 cells were cultured in MEM Alpha medium, supplemented with 10% FCS and 1% chicken serum. They were grown in suspension, in sterile T-75 flasks in a 37°C incubator, under 5% CO₂ atmosphere. The cells were passaged twice a week.

2.1.5 Selection conditions

CHO-K1 and UT-1 cells were grown in the presence of 0.1 mg/ml 25-hydroxycholesterol (Sigma) dissolved in 95% EtOH in order to ensure full repression of the HMG-R gene.

UT-1 cells were grown in DMEM supplemented with 10% delipidised FCS, 30µg/ml L-proline, and 20µM simvastatin (kindly supplied by Merck, Sharpe & Dohme Research Laboratories) to ensure full expression of the HMG-R gene. CHO-K1 cells were grown in DMEM supplemented with 10% delipidised FCS and 30µg/ml to ensure expression of HMG-R.

2.1.6 Delipidisation of FCS

FCS was delipidised using Cabosil (BDH).

A 3% w/v Cabosil/serum mixture was prepared and stirred slowly o/n at 4°C. The mixture was subsequently centrifuged at 17,000 rpm for 60 min at 4°C. The supernatant was sterilised by filtering through a 0.45 micron filter and stored at -20°C till further use.

2.2 Bacterial Cell Culture

2.2.1 Media and solutions

All media were sterilised by autoclaving.

L-broth and agar

2.46g MgSO₄ , 10g Bacto-tryptone (Difco), 5g yeast extract (Difco) and 10g NaCl were added per litre of dH₂O. 15g agar (Oxoid Ltd) were added per litre broth for L-agar.

Terrific broth

12g Bacto-tryptone, 24g yeast-extract, 4g glycerol were added to 900ml of dH₂O. After autoclaving, 100ml of autoclaved phosphate solution (0.1M KH₂PO₄/0.72M K₂HPO₄) were added.

Ampicillin (Sigma)

A 50mg/ml stock solution was made in dH₂O, was filter sterilised and stored at -20°C. It was used at a final concentration of 50µg/ml.

Tetracycline (Sigma)

A 12mg/ml stock solution was made in 50% EtOH and stored at -20°C. The solution was used at a final concentration of 12µg/ml.

2.2.2 Bacterial strains

DH5α genotype - F⁻ endA1, hsdR17(r_k⁻,m_k⁻), supE44, thi-1λ, recA1, gyrA96, relA1, deoR, Δ(lacZYA-argF)-U169, φ80d|lacZΔM15

This strain was used as the host strain to transform several plasmids.

2.2.3 Preparation of competent cells for electroporation

DH5α bacterial cells from a frozen stock were streaked out onto a fresh L-agar plate and grown at 37°C o/n. A single colony was then used to inoculate 10 ml of L-broth, which was left to grow o/n at 37°C in a shaking incubator. The whole culture was then used to inoculate 1l of L-broth, which was grown at 37°C with

vigorous shaking to an Abs_{600} of 0.5 - 1.0, during which the cells are still in the log phase of growth. To harvest the cells, the flask containing the culture was chilled on ice for 15 - 30 min, and centrifuged for 15 min at 4000rpm at 4°C in a pre-cooled rotor. The pellets were resuspended in a total of 1l of sterile chilled dH₂O, and centrifuged as before. The pellets were resuspended in a total of 500ml of sterile dH₂O and re-centrifuged. This step was repeated using 100ml of sterile dH₂O. Pellets were then resuspended in 20ml of 10% glycerol, and centrifuged as before. The pellets were finally resuspended in 2-3ml of 10% glycerol, to a concentration of around 3.0×10^{10} cells/ml. This suspension was frozen on dry ice in aliquots, and stored at -70°C.

2.2.4 Transformation of competent cells by electroporation

An aliquot of competent cells (DH5 α) was thawed on ice. 1ng of the plasmid DNA was added to the cells and incubated on ice for 1 min. The mixture was then transferred to a chilled, sterile electroporation cuvette and subjected to a pulse of 2.5kV in a BioRad Gene Pulser. 1ml of L-broth was immediately added to the cells, they were transferred to a 15ml Falcon tube, and incubated at 37°C with constant shaking at 250 rpm for 1 hr. Aliquots of several different volumes were then spread onto L-agar plates containing the appropriate antibiotic selection and incubated o/n at 37°C.

2.3 Plasmid DNA Preparation

2.3.1 Solutions

STET

8% sucrose, 5% Triton X-100, 50mM EDTA pH8, 50mM Tris pH8

Solution I

50mM glucose, 10mM EDTA pH8, 25mM Tris pH8

Solution II

0.2M NaOH, 1% SDS

Solution III

for 100ml - 60ml 5M KAc, 11.5ml glacial acetic acid, 28.5ml dH₂O

2.3.2 Small scale plasmid DNA preparation - rapid boiling method

A single bacterial colony was used to inoculate 3ml of L-broth with appropriate antibiotic selection and was grown at 37°C o/n with continuous shaking. The culture was then centrifuged at 12,000rpm for 5 min. The pellet was then resuspended in 600µl STET and transferred to an eppendorff tube. 25µl of 10mg/ml lysozyme in STET was added to the suspension, and left on ice for 3 min. The tube was placed open-capped in a 95°C water-filled metal block for 3 min, and subsequently chilled on ice for 5 min. The tube was centrifuged at 12,000rpm for 15 min at 4°C, and the resulting pellet was removed using a pastette. An equal volume of isopropanol was added to the supernatant, was mixed and spun immediately at 12,000 rpm for 3 min. The pellet was rinsed with 95% EtOH and left to dry at RT. The pellet was resuspended in 100µl TE.

2.3.3 Large scale plasmid DNA preparation

A single bacterial colony was used to inoculate 100-200ml of L-broth with appropriate antibiotic selection and was grown o/n at 37°C with continuous shaking. The culture was then centrifuged at 5000rpm for 10 min in 50ml falcon

tubes, at 4°C. Each pellet was resuspended in 1.8ml (per 50ml of starting culture) of Solution I. To the suspension, 200µl of lysozyme at a concentration of 5mg/ml were added. The suspension was left at RT for 10 min. 4ml of Solution II were added, and the mixture was swirled and left on ice for 5 min. 2ml of Solution III were added to the mixture, vortexed until a fine white precipitate was formed, and left on ice for 15 min. The mixture was centrifuged at 5000rpm for 10 min. The supernatant was then filtered through fluted filter paper (Whatman) into a second falcon tube and 0.6 volumes of isopropanol were added to the mix. This was spun at 5000rpm for 10 min. The supernatant was discarded and the pellet was washed with a few drops of 70% EtOH, which were then removed with a fine-tipped pastette. The pellet was air-dried briefly before resuspending it in 400µl of TE. Next, 0.7g of CsCl and 67µl of EtBr were added to the mixture, and mixed well. A step gradient was prepared with a 65% w/v stock of CsCl in TE. Using a syringe with a medium-sized needle, 1.4ml of the 65% w/v CsCl stock were added to the 1.8ml tube. The more dense DNA/CsCl solution was then added to the bottom of the tube, again using a syringe and needle. The tubes were balanced and sealed, and spun at 100,000rpm for 2.5 hr in a Beckman table top ultra centrifuge. The plasmid band was then carefully extracted through the side of the tube with a needle and 1ml syringe, and placed in an eppendorff tube. The plasmid DNA was extracted three times with an equal volume of CsCl-saturated isopropanol. The pellet was precipitated with three volumes of 70% EtOH, left on ice for 30 min and spun at 12000rpm for 15 min, and lastly resuspended in 200µl of dH₂O.

2.4 Preparation of genomic DNA

2.4.1 Solutions

PBS

Phosphate-buffered saline

Lysis buffer

100mM Tris.HCl pH8.5, 5mM EDTA, 0.2%SDS, 200mM NaCl

NDS

0.5m EDTA, 10mM Tris pH 9.5, 1% N-laurylsarcosine

Proteinase K

A 10mg/ml stock solution was made in dH₂O.

2.4.2 Rapid isolation of DNA from mammalian cells

Medium was removed from the flasks containing the appropriate cells by suction, and the cells were washed briefly with PBS. 3mls of lysis buffer per 10cm³ tissue culture plate were added to the cells, and proteinase K was added to 100µg/ml. The cells were left for several hours or o/n at 37°C. An equal volume of phenol:chloroform was added to the lysed cells and gently mixed until the solution went milky ie. until precipitation was complete. The mixture was then spun for 10 min at 3000rpm and the top aqueous layer was transferred to a new tube. 0.6 volumes of isopropanol and 1/30 volume of 3M NaAc were added to the sample, and it was mixed gently to precipitate the DNA. The DNA was transferred with a yellow Gilson tip to an eppendorff tube filled with 70% EtOH and washed, and was finally left to air dry in a fresh eppendorff tube for 30 min. 500µl of dH₂O were added to the tube and the DNA was left to resuspend on a rotator o/n at 4°C.

2.4.3 Making plugs from mammalian tissue culture cells

Cells were harvested as described in section 2.1.4 and washed briefly in PBS. The cells were counted using a Coulter counter, pelleted by centrifuging at 1000rpm for 5 min at 4°C, and resuspended in PBS at a concentration of 2.0×10^7 cells/ml. An equal volume of 1% LMP agarose/PBS (pre-cooled to 50°C) was added to the cells and mixed. The cell/agarose suspension was then aliquoted into 100µl plug moulds and left to cool at 4°C. Once set, the plugs were gently pushed into 0.5ml NDS per plug, and were incubated at 50-55°C for 24 hr with 10mg proteinase K. After 24 hr, the NDS solution and proteinase K were replaced with fresh aliquots of NDS/proteinase K, and the plugs were incubated for a further 48 hr at 50-55°C. The plugs were then stored at 4°C in fresh NDS.

2.5 Purification and Concentration of DNA

2.5.1 Phenol : chloroform extraction

DNA was extracted twice by addition of an equal volume of phenol:chloroform and chloroform, and vortexing vigorously. The mixture was then centrifuged at 12,000rpm for 5 min. The upper, aqueous layer was carefully removed, avoiding precipitated protein found at the interface between the two layers. The DNA was then recovered by ethanol precipitation.

2.5.2 Ethanol precipitation

To concentrate DNA and remove salts, a 1/10 volume of 3M NaOAc was added to the DNA solution, followed by 2 volumes of 100% EtOH. This was mixed thoroughly and left at -20°C from 1hr to o/n. The tube was then centrifuged at 12,000rpm for 15 min at 4°C. The supernatant was removed, and the pellet was dried under vacuum. The pellet was then resuspended in the desired volume of dH₂O.

2.6 Enzymatic Manipulation of DNA

2.6.1 Restriction enzyme digestion of plasmid DNA

Digestion of DNA with restriction endonucleases was carried out in the appropriate buffer and at the temperature recommended by the manufacturer (Boehringer Mannheim).

2.6.2 Restriction enzyme digestion of genomic DNA

Digestion of DNA with restriction endonucleases was carried out in the appropriate buffer and at the temperature recommended by the manufacturer. Generally, 10µg of DNA were digested in a 50µl volume using 50 units of the appropriate enzyme. Digestion was carried out overnight at the appropriate temperature. Restriction digest reactions which were to be run on gels were stopped by addition of the loading dye (containing EDTA).

2.6.3 Restriction enzyme digestion of agarose plugs

Plugs were washed o/n in 4ml of TE per plug, at 4°C on a rotating wheel. They were washed 3-4 further times with TE for 30 min on the following day. The plugs were then pre-incubated o/n with 200µl of 1x restriction buffer per plug at 4°C. This was removed and replaced with 200µl of fresh 1x restriction buffer.

For the restriction enzyme digestion, the 1x restriction buffer was supplemented with 100µg/ml BSA, 1mM DTT, 1mM spermidine, and 20 units of enzyme. Digestion was carried out overnight at the appropriate temperature. Following digestion the tubes were cooled on ice for 15 min, and the liquid was removed from the tube with a pasteur pipette, prior to loading on a gel.

2.7 Amplification of DNA by Polymerase Chain Reaction (PCR)

2.7.1 Preparation of oligonucleotides

Oligonucleotides were synthesized, in the form of ammonium stocks, on an Applied Biosystems 381A oligonucleotide synthesizer, by A Gallagher. Oligonucleotides were precipitated from stocks by addition of 1/10 volume of 3M NaOAc and 2 volumes of 100% EtOH, and were incubated at -20°C for a minimum of 1 hr. They were pelleted by centrifugation at 12,000rpm for 15 min, washed twice with 75% EtOH, and dried under vacuum. The pellet was resuspended in 200µl TE and the concentration determined using a spectrophotometer, where $OD_{260} = 1$ for 25µg/ml of single-stranded DNA.

2.7.2 PCR materials

10x TAPS buffer

0.25M TAPS stock (Sigma), 0.5M KCl, 0.02M MgCl₂, 1% Tween 20, pH9.3

2.7.3 PCR conditions

Generally, 100ng of template DNA were amplified in 50µl in 0.5ml microcentrifuge tubes with 0.5µl of AmpliTaq polymerase (Perkin Elmer Cetus), 1x TAPS buffer, 1µM of each primer, and 200µM of each dNTP (Advanced Biotechnologies). The reaction was overlaid with 30µl of mineral oil.

PCR programs were run on a Hybaid Omnigene machine. The basic program was 30 cycles incorporating 3 different steps:

Denaturation - a short step at 94°C, usually 4 min in the first cycle, and 45 sec thereafter.

Annealing - an annealing temperature of around 5°C below the T_m of the primer was used, usually 45 sec long.

Extension - carried out at 72°C, usually for 1 min.

2.7.4 Primers and conditions for PCR

Mouse ribosomal protein S16

Oligonucleotide F740 - 5' GCT ACC AGG CCT TTG AGA TGG A 3'

Oligonucleotide F741 - 5' AGG AGC GAT TTG CTG GTG TGG A 3'

Reaction conditions

94°C 4 min	x1
94°C 45 sec ; 45°C 45 sec ; 72°C 1 min	x30
72°C 10 min	x1

Expected product size ~ 100bp

Chinese hamster HMG-R

Oligonucleotide P1 - 5' ATG TTG TCA CGA CTT TTC CGT ATG 3'

Oligonucleotide P10 - 5' GTG AAC AGG CCA GCA ATA CCT AAA 3'

Reaction conditions

94°C 4 min	x1
94°C 45 sec ; 50°C 45 sec ; 72°C 1 min	x30
72°C 10 min	x1

Expected product size ~ 300bp

pGEM primers for amplification of CpG island library (Cross *et al* 1994)

Oligonucleotide pGEMF - 5' CGG CCG CCT GCA GGT CGA CCT TAA 3'

Oligonucleotide pGEMR - 5' AAC GCG TTG GGA GCT CTC CCT TAA - 3'

Reaction conditions

94°C 7 min	x1
94°C 30 sec ; 50°C 45 sec ; 72°C 1 min	x35
72°C 10 min	x1

2.8 Isolation of RNA and Preparation of cDNA

2.8.1 Solutions

Solution D

Stock solution - 25g guanidinium thiocyanate, 29.3ml DEPC-treated H₂O, 1.32ml 1M Na citrate pH7, 2.64ml 10% sarcosyl.

The solution is allowed to dissolve at 65°C and can be stored for 3 months at RT. Just before use, 0.36ml of 2-mercaptoethanol were added per 50ml of the solution.

2.8.2 Isolation of RNA by Acid Guanidinium Thiocyanate Extraction

Total RNA used for Northern analysis was isolated from UT-1 and CHO-K1 cells by guanidinium thiocyanate extraction. Cells were directly lysed in complete Solution D using 2mls per 10cm³ cell culture dish. The mixture was transferred to a baked corex tube. 1/10 volume of 2M NaOAc pH4 was added to the solution, and was mixed by gentle inversion of the tube. 1 original volume of water-saturated phenol was subsequently added and mixed by inversion, followed by 1/5 of the original volume of CHCl₃ : isoamyl alcohol (49:1), again mixed by inversion. The mixture was shaken vigorously for 10 sec and cooled on ice for 15 min. The mixture was then centrifuged at 8000rpm for 20 min at 4°C. The upper aqueous layer was transferred to a fresh corex tube and mixed with 1 volume of isopropanol. This was left at -20°C for at least 1 hr. The solution was then centrifuged at 8000rpm for 20 min at 4°C. The supernatant was carefully removed without dislodging the pellet. The pellet was dissolved in 300µl of complete solution D and transferred to an eppendorff tube. RNA was then precipitated with 1 volume of isopropanol at -20°C for at least 1 hr. The solution was centrifuged at 12,000rpm for 10 min at 4°C. The supernatant was aspirated off and the pellet rinsed in 75% EtOH, and left to dry at RT. The pellet was resuspended in 50-200µl of DEPC-treated H₂O.

The concentration and quality of the isolated RNA was checked by running 1µl of the RNA on a 1% agarose gel.

2.8.3 RNA isolation for RT-PCR

RNA used for RT-PCR experiments was isolated using Total RNA Isolation Reagent (Advanced Biotechnologies Ltd). The reagent consists of a 14M solution of guanidine salts and urea which acts as a denaturing agent. During the extraction step, the RNA remains exclusively in the aqueous phase while DNA and proteins are extracted into an organic phase and interphase.

The RNA reagent was added directly to the cells, using 2.5ml of reagent per 10cm³ culture dish. The cell lysate was passed through a pipette several times and transferred to an eppendorff tube, and was incubated on ice for 5 min. 200µl of chloroform were added per 1ml of reagent and the mixture was shaken vigorously for 15 sec. The mixture was left on ice for 5 min and then centrifuged at 12,000rpm for 15 min at 4°C. The upper aqueous phase was subsequently transferred to a fresh eppendorff tube taking care not to disturb the interphase. 1 volume of isopropanol was added to the solution, which was left on ice for 10 min. The sample was centrifuged at 12,000rpm for 10 min at 4°C and the resulting supernatant was discarded. The RNA pellet was washed twice with 75% EtOH and allowed to air-dry at RT before resuspending it in 50-100µl of DEPC-treated H₂O.

The concentration and quality of the isolated RNA was checked by running 1µl of the RNA on a 1% agarose gel.

2.8.4 cDNA synthesis

Total RNA was converted into first strand cDNA using the Superscript™ kit (Gibco BRL) . 5µg of RNA was adjusted to a 12µl volume, including 1µl of the Oligo(dT) primer, with DEPC-treated H₂O. The sample was heated to 70°C for 10 min and cooled on ice for at least 1 min. To this was added 7µl of the reaction mixture, which consisted of 2µl of 10x PCR buffer, 2µl of

25mM MgCl₂, 1μl of 10mM dNTP mix, and 2μl 0.1M DTT per reaction. The sample was mixed gently, collected by brief centrifugation and incubated at 42°C for 5 min. 1μl (200 units) of the reverse transcriptase enzyme, SuperScript II RT, was added to the sample and the reaction was left to proceed at 42°C for 50 min. The reaction was terminated at 70°C for 15 min and chilled on ice. The cDNA was subsequently used directly in a PCR reaction (1μl per reaction).

2.9 Electrophoresis

2.9.1 Electrophoresis solutions

0.5x TBE

0.045M Tris-borate, 0.001M EDTA pH8

0.5x TAE

0.02M Tris-acetate, 0.0005M EDTA pH8

DNA Loading Buffer (10x)

0.25% bromophenol blue, 0.25% xylene cyanol FF, 30% glycerol in H₂O

10x MOPS

1M MOPS pH7, 3M NaAc pH7, 0.5M EDTA pH7.5, made up to 500mls with dH₂O

2.9.2 Size markers

500ng of the appropriate size marker were used per gel.

Size markers used were -

λ DNA digested with HindIII (Boehringer Mannheim)

φX174 digested with HaeIII (Boehringer Mannheim)

1kb ladder (Gibco BRL)

Table 2.1 lists the band sizes for λHindIII, φX HaeIII and the 1kb ladder.

2.9.3 DNA Agarose Gel Electrophoresis

DNA was separated according to its size on horizontal agarose (Flowgen) gels. The percentage of agarose used to make the gel depended on the size range of the DNA to be resolved. Digested plasmid or genomic DNA was generally run on 0.7 - 1% agarose gels, whereas smaller fragments, such as PCR products, were run on 1 - 2% agarose gels. All agarose gels were made with and run in 0.5x TAE. To stain the DNA, ethidium bromide was added to all agarose gels at a concentration of 1µg/ml. 1/10 of the sample volume of 10x loading buffer was added to the DNA prior to loading the sample on the gel. Gels were run at 30-150V depending on resolution and running time required.

λ Hind III (kb)	ϕ X Hae III (bp)	1kb ladder (bp)
23	1353	12216
9.5	1078	11198
6.5	872	10180
4	603	9162
2.3	310	8144
2.0	281	7126
0.5	271	6108
	234	5090
	194	4072
	118	3054
	72	2036
		1636
		1018
		517
		506
		396
		344
		295
		220
		201
		154
		134
		75

Table 2.1
Fragment sizes of DNA markers used in gel electrophoresis.

DNA fragments were visualised on a UV transilluminator and photographed using a video copy processor (Sony).

2.9.4 Purification of DNA from agarose

DNA fragments were run in 0.7% low melting point agarose (Ultrapure LMP agarose, Gibco BRL) in 0.5x TAE. Gels were viewed on a UV transilluminator and the required fragment was excised using a sterile blade and placed in an eppendorff tube, ensuring that a minimum of agarose was removed with the band.

DNA was recovered from gel slices by β agarase treatment. The gel slice was melted at 70°C for 5 min or until the agarose had melted completely. The tube was transferred to a 39°C waterbath and allowed to equilibrate for 5 min. 1/10 volume of β agarase buffer (BioLabs) was added to the tube, followed by 2 μ l (1-2 units) of β agarase per 100 μ l volume. The reaction was allowed to proceed for 30 min at 39°C, then 1/10 volume of 3M NaAc was added and the reaction was left on ice for 5 min. The tube was centrifuged at 12,000rpm for 5 min at 4°C and the supernatant was transferred to a new tube. 2 volumes of 100% EtOH were added, the tube was left on ice for 5 min, and centrifuged at 12,000rpm for 5 min at 4°C. The pellet was washed with 75% EtOH, dried, and resuspended in 10 μ l of dH₂O.

2.9.5 Pulsed field gel electrophoresis

Agarose plugs were washed in TE and equilibrated to the running buffer (0.5x TBE) over 3 hr. A 1% agarose gel was made up in 0.5x TBE, and the plugs were inserted into the wells. The wells were sealed with 1% LMP agarose / PBS. The gel was run in pre-cooled 0.5X TBE at 13°C, using Biorad equipment. Run times and conditions were varied depending on the size resolution required.

After electrophoresis the DNA was stained by gently agitating the gel in running buffer containing 250 μ g/ml EtBr for 20 min. The DNA was then visualised and photographed as described in section 2.9.3.

2.9.6 Electrophoresis of RNA

RNA was separated by electrophoresis on agarose gels containing 10% 10x MOPS and 17% formaldehyde. 1.2% agarose was dissolved in dH₂O, left to cool to 50°C, and the formaldehyde and 10x MOPS were added. The gel was poured immediately in a fume cupboard and left to set.

5µg of RNA, to be loaded onto the gel, were made up to the required volume in 50% formamide, 10% 10x MOPS and 16% formaldehyde. Prior to loading, the sample was heated to 65°C for 5 min, cooled on ice for 5 min, and the loading dye was added. Gels were run at 150V for 3 hr.

After electrophoresis, the RNA was stained if required by gently agitating the gel in dH₂O containing 250µg/ml EtBr for 20 min. RNA was visualised and photographed as for DNA.

2.10 Transfer of DNA and RNA onto membranes

2.10.1 Solutions

20x SSC

3M NaCl, 0.3M tri-sodium citrate pH7

Denaturing solution

0.5M NaOH, 1.5M NaCl

Neutralising solution

1M Tris.HCl, 2M NaCl pH 4.5-5.0

2.10.2 Southern transfer

DNA was transferred from agarose gels onto nylon membranes by capillary blotting.

DNA in the agarose gels was nicked by UV-irradiation in a Biorad Gene Linker (Biorad) at a setting of 60mJ.

The DNA was denatured by gently shaking the gel in denaturing solution for 30 min, followed by a quick wash in dH₂O. The gel was then neutralised by gentle shaking in neutralising solution for 30 min, and rinsed quickly in dH₂O. A large strip of 3MM blotting paper (Whatman) was soaked in 20x SSC and placed on a board. The ends of the paper were placed in a reservoir of 20x SSC, forming a wick. The gel was placed on top of the wet filter paper, and then a correctly sized piece of nylon membrane (Hybond-N+, Amersham), pre-wet in 2x SSC, was placed on top of the gel. Three pieces of correctly sized 3MM blotting paper, pre-wet in 2x SSC, were placed on top of the membrane. Air bubbles were carefully removed and any exposed wick was sealed off with Saran wrap (Dow Chemical Company). A weighted stack of paper towels was then placed on top.

Pulse field gels were blotted for two days, whereas conventional gels were blotted overnight. After blotting, DNA was fixed to the filter by gently shaking it in 0.5M NaOH for 15 min, followed by 15 min in neutralising solution. The filter was then left to air dry. Filters were stored wrapped in Saran wrap at RT.

2.10.3 Northern transfer

RNA was transferred from agarose gels to a nylon membrane (Hybond-N, Amersham) in the same way as DNA, except that both denaturing and neutralising steps were omitted. After blotting, RNA was bound to the membrane by exposing the filter to 1200 μ J of UV-irradiation in a Stratalinker. The filter was then left to air dry. Filters were stored wrapped in Saran wrap at RT.

2.11 Radiolabelling of DNA

2.11.1 Random priming of DNA probes

Probes were labelled with [α - 32 P]-dCTP by random priming from hexanucleotides using the Klenow fragment of *E coli* polymerase I.

50ng of DNA in a total volume of 11 μ l, made up with dH₂O if required, were initially denatured by heating to 95°C for 5 min on a PCR block. The DNA was then cooled rapidly on ice to prevent the strands from reannealing. The labelling reaction was carried out using a Random Prime kit (Boehringer Mannheim) according to the manufacturer's instructions. To the 11 μ l of denatured DNA were added 1 μ l each of dATP, dGTP, dTTP, 2 μ l of 10x reaction buffer, 1 μ l (2 units) of Klenow, and finally 30 μ Ci (10 μ Ci/ μ l) of [α - 32 P]-dCTP. The reaction was then incubated at RT for a minimum of 1 hr.

The percentage incorporation of the radiolabelled nucleotide was checked by TCA precipitation of 0.5 μ l of the reaction mix on a GF/B circular filter (Whatman). Unincorporated nucleotides were removed by running the reaction through a Sephadex G-50 Nick column (Pharmacia Biotech). The storage buffer was removed, and the column was washed by running through approximately 1ml of TE. The probe was then added to the top of the column, followed by 380 μ l of TE. The probe was then eluted with a further 400 μ l of TE, and collected in a tube. The probe was denatured by heating to 100°C for 5 min, and was cooled immediately on ice before adding it to the hybridisation mix.

2.11.2 End-labelling of DNA oligonucleotides

Oligonucleotides were labelled by the transfer of the radiolabelled phosphate group of [γ - 32 P]-ATP to the terminal 5'-OH group of the oligonucleotide, using polynucleotide kinase.

To 25-50ng of oligonucleotide DNA in a total of 7 μ l, made up with dH₂O if required, were added 2 μ l of PNK buffer (Boehringer Mannheim), 1 μ l (10 units) of polynucleotide kinase (Boehringer Mannheim), and 10 μ l of

(10 μ Ci/ μ l) [γ -³²P]-ATP. The reaction was incubated at 37°C for 40 min. It was added to the hybridisation mix without the need for removal of unincorporated nucleotides.

2.12 Hybridisation of membranes

2.12.1 Solutions

20x SSC

3M NaCl, 300mM Na₃citrate, pH7

Church and Gilbert

7% SDS, 0.5M NaPO₄, 1mM EDTA

Oligonucleotide hybridisation solution

5xSSC, 0.05% BSA, 0.05% ficoll, 0.1% SDS, 0.05% PVP, 0.1% NaPPi.

Filter before use.

2.12.2 Pre-hybridisation

The hybrid filter to be hybridised was rolled up and placed in a Hybaid hybridisation bottle. 25ml of hybridisation solution (Church and Gilbert) was added to the bottle, and the bottle was rotated in a hybridisation oven (Hybaid) for a minimum of 1 hr before adding the probe. Hybridisations were carried out at 65°C for random primed probes and at 5°C below the T_m of the oligonucleotide for end-labelled oligonucleotide probes.

2.12.3 Hybridisation

End-labelled oligonucleotides were added directly to the bottle after pre-hybridisation, avoiding direct contact with the filter. Hybridisation was carried out overnight at the same temperature as the pre-hybridisation. Random primed probes were added to the bottle after denaturation, avoiding direct contact with the filter, and the hybridisation was carried out overnight at 65°C.

2.12.4 Hybridisation washes

Following hybridisation, filters hybridised with random primed probes were washed directly in bottles, in the hybridisation oven. Filters were initially rinsed briefly in 2x SSC at RT, and then washed with 100ml of the following

solutions, each for 30 min, at 65°C : 2x SSC, 1x SSC/0.5% SDS, 0.5x SSC/0.5% SDS.

Filters hybridised with oligonucleotide probes were initially washed in 4x SSC for 15 min at RT, and then washed in 4x SSC/0.1% SDS for 30 min at 65°C.

The filters were then wrapped in Saran wrap, avoiding creases.

2.12.5 Detection of hybridisation signal

The filters were exposed to a phosphor screen (Molecular Dynamics) for hrs to several days. The screen was then scanned on a PhosphorImager (Molecular Dynamics). The image was displayed within a grey scale on a computer screen using Image Quant Molecular Dynamics software, which allowed adjustments to be made to improve visualisation of the signal prior to printing the image out on a laser printer.

2.12.6 Re-using filters

Radioactive probes were stripped from filters to enable them to be used again, by washing them very stringently. Filters were immersed in 500ml of 0.1% SDS, at 100°C for 5 min. The filters were checked by detection as described above.

2.13 Immunofluorescence

2.13.1 Media and solutions

DMEM

Dulbecco's Modified Eagle's Medium supplemented with 10-20% FCS and 30µg/ml L-proline.

MEM Alpha

MEM Alpha medium supplemented with 10% FCS and 1% chicken serum.

Trypsin/EDTA solution (T/E)

2.5% trypsin and 0.02% EDTA in buffered saline.

Colcemid

Stock solution (100x) is 10µg/ml colcemid in water, filter sterilized.

Hypotonic solution

75mM KCl

'Potassium chromosome medium' (KCM)

120mM KCl, 20mM NaCl, 10mM Tris-HCl pH8, 0.5mM EDTA and 0.1% Triton X-100

Formaldehyde solution

40%, diluted (1:10) just before use to 4% formaldehyde in KCM.

Vectashield (Vector)

Stored at 4°C

DAPI (Sigma)

4', 6-diamidino - 2 - phenylindole . Stock solution is 50µg/ml in water.

2.13.2 Antibodies and Sera

Primary antibodies

Autoimmune anti-centromere sera (CREST) were gifts from George Nuki at the Rheumatic Diseases Unit, Western General Hospital, Edinburgh, UK.

Rabbit sera R5/12 and R41/5, against histone H4 acetylated at Lys-12 and Lys-5 respectively, were gifts from Bryan Turner at the Department of Anatomy, University of Birmingham Medical School, UK.

For use, antibodies were diluted 1:100 in KCM containing 10% normal goat serum (NGS).

Secondary antibodies

Fluorescein isothiocyanate (FITC), tetramethylrhodamine isothiocyanate (TRITC) and 7-amino-4-methylcoumarin-3-acetic acid (AMCA) conjugated affinity-isolated goat anti-human and anti-rabbit immunoglobulins were obtained from Sigma, and used diluted 1:20 in KCM containing 10% NGS.

2.13.3 Cell culture

Confluent cultures were split at a ratio of 1:5. After 24 hrs, colcemid was added to a final concentration of 0.1µg/ml, and incubation was continued for 1 hr. This arrests the cells in metaphase. If required, sodium butyrate was also added to a final concentration of 4mM in order to inhibit the action of histone deacetylase in the cells.

CHO-K1 and UT-1 cell lines

The culture medium was removed from the plate and left on ice. The cells were trypsinized by incubation with 4 mls of T/E for 2-3 min at 37°C. The TE/cell suspension was diluted with an equal volume of cold culture medium set aside earlier, and the cells were harvested by centrifugation at 1000rpm for 10 min at 4°C. The supernatant was discarded and the pellet was gently resuspended and washed with the remaining saved culture medium to wash out any residual trypsin. The cells were centrifuged again at 1000rpm for 10 min at 4°C, and all but 100µl of the supernatant were removed. The pellet was gently resuspended in this and 5mls of cold KCl hypotonic solution were added, initially dropwise, maintaining a homogeneous suspension of cells. The suspension was incubated at 37°C for 10 min and then placed on ice.

DT40 cell line

The DT40 cells were harvested by centrifugation at 1200rpm for 3 min at 4°C. The supernatant was discarded and the pellet was gently resuspended. 4mls of KCl hypotonic solution were added, initially dropwise, maintaining a homogenous suspension of cells. The suspension was incubated at RT for 10 min and then placed on ice.

2.13.4 Preparation of metaphase spreads

The cell density of the hypotonic KCl/cell suspension was determined using a Coulter counter or a haemocytometer. If necessary, the suspension was diluted with further 75mM KCl to obtain $1-2 \times 10^5$ cells/ml (for CHO-K1 and UT-1 cells) or $2-4 \times 10^6$ cells/ml (for DT40 cells).

Cells were centrifuged onto slides using the Cyto-Tek centrifuge (Bayer Diagnostics UK Ltd) or Hereaus MegaFuge 'Cyto-system', fitted with 1ml disposable chambers. 500 μ l of the cell suspension were used per slide (containing approximately 1×10^5 CHO-K1 or UT-1 cells, or 1×10^6 DT40 cells), which were centrifuged for 10 min at 2000rpm (or 1200rpm with the Hereaus MegaFuge system) onto EtOH washed slides. After removing the slides from the centrifuge, any visible moisture was briefly allowed to dry, and the slides were then immersed in a Coplin jar containing KCM at RT for at least 10 min prior to carrying out the first antibody reaction.

2.13.5 Antibody Reactions

After permeabilizing the cells by immersion in KCM, they were not allowed to dry until finally fixed with formaldehyde.

Each slide was removed from KCM, and 40 μ l of the first antibody dilution was carefully applied to the sample area, which was then covered with a square of Parafilm (approximately 1.5cm²). The slide was then transferred to a humid chamber at RT for 1-2 hrs. The slide was removed from the humid chamber, and the antibody rinsed off with a few ml of KCM directed with a Pasteur pipette. The slide was then transferred to a Coplin jar containing KCM for 10 min. 40 μ l of the second antibody dilution was applied to the sample area after removing the slide from KCM, and the slide was transferred to a humid chamber. Following a 30 min incubation with the second antibody, the antibody was rinsed off as described above, and the slide was transferred to fresh KCM. Finally, the slides were fixed by

immersion in 4% formaldehyde in KCM at RT for 15 min, transferred to dH₂O for 10 min, and allowed to dry.

2.13.6 Fluorescence Microscopy

When required, slides were counterstained for DNA by applying 100µl of DAPI, at a concentration of 0.2µg/ml, for 10 min. Slides were mounted for microscopy with 40µl Vectashield (Vector) and the cover slip was sealed with rubber solution. Slides were stored in the dark until observed under the microscope.

All images were collected using a Zeiss Axioplan fluorescence microscope equipped with a 100W mercury source and a Photometrics CCD (charged coupled device) camera. Images were acquired and processed using software from Digital Scientific (Cambridge, UK).

2.13.7 Treatment of slides following immunofluorescence

Slides that had been through immunofluorescence were either fixed with 3:1 methanol:acetic acid or given an alkali treatment prior to undergoing FISH.

Slides were placed in 3:1 methanol:acetic acid for 15 min and immediately processed for FISH, or stored at -20°C until required. Alternatively, slides were washed for 30 sec at RT in the following solutions: 0.1M NaOH, dH₂O, 10mM Tris pH 7.5, dH₂O. The slides were then processed for FISH.

2.3 Plasmid DNA Preparation

2.3.1 Solutions

STET

8% sucrose, 5% Triton X-100, 50mM EDTA pH8, 50mM Tris pH8

Solution I

50mM glucose, 10mM EDTA pH8, 25mM Tris pH8

Solution II

0.2M NaOH, 1% SDS

Solution III

for 100ml - 60ml 5M KAc, 11.5ml glacial acetic acid, 28.5ml dH₂O

2.3.2 Small scale plasmid DNA preparation - rapid boiling method

A single bacterial colony was used to inoculate 3ml of L-broth with appropriate antibiotic selection and was grown at 37°C o/n with continuous shaking. The culture was then centrifuged at 12,000rpm for 5 min. The pellet was then resuspended in 600µl STET and transferred to an eppendorff tube. 25µl of 10mg/ml lysozyme in STET was added to the suspension, and left on ice for 3 min. The tube was placed open-capped in a 95°C water-filled metal block for 3 min, and subsequently chilled on ice for 5 min. The tube was centrifuged at 12,000rpm for 15 min at 4°C, and the resulting pellet was removed using a pastette. An equal volume of isopropanol was added to the supernatant, was mixed and spun immediately at 12,000 rpm for 3 min. The pellet was rinsed with 95% EtOH and left to dry at RT. The pellet was resuspended in 100µl TE.

2.3.3 Large scale plasmid DNA preparation

A single bacterial colony was used to inoculate 100-200ml of L-broth with appropriate antibiotic selection and was grown o/n at 37°C with continuous shaking. The culture was then centrifuged at 5000rpm for 10 min in 50ml falcon

2.14 Fluorescence *in situ* hybridisation (FISH)

2.14.1 Materials for FISH

Rnase A

Stock is 10mg/ml in 10mM Tris pH 7.5, 15mM NaCl. Heated to boiling for 5 min to destroy DNase, and stored frozen in aliquots. Used at 100µg/ml in 2xSSC.

Formamide

50mls of formamide are deionised with 5g of amberlite monobed resin (BDH) by stirring in a fume cupboard for 1 hr. Stored frozen in aliquots.

Salmon sperm DNA (Sigma)

Stock is 10mg/ml in dH₂O. Autoclaved to shear high molecular weight DNA and stored frozen in aliquots.

Human Cot-1 DNA for competitive hybridisation (Gibco BRL)

Stock is 1mg/ml and is already sonicated to 500bp. Stored frozen.

Chicken genomic DNA for competitive hybridisation

Genomic chicken DNA is sonicated to 500bp. Stored frozen.

Dextran sulphate

Stock is 50% in dH₂O and stored frozen in aliquots.

Skimmed milk (Marvel)

Working solution is 5% in 4xSSC.

Avidin-FITC/-TRITC (AvFITC/AvTRITC)(Vector)

Stock is 2mg/ml and is stored at 4°C. Working solution is 4µg/ml, diluted 1:500 in 4xSSC, 5% skimmed milk.

Biotinylated anti-avidin (BAA) (Vector)

Stock is 0.5mg/ml and is stored at 4°C. Working solution is 5µg/ml, diluted 1:100 in 4xSSC, 5% skimmed milk.

Anti-digoxygenin FITC (Boehringer Mannheim)

Stock is 200µg/ml and is stored at 4°C. Working solution is 15µg/ml, diluted 1:15 in 4xSSC, 5% skimmed milk.

Anti-sheep FITC (Vector)

Stock is 1.5mg/ml and is stored at 4°C. Working solution is 15µg/ml, diluted 1:100 in 4xSSC, 5% skimmed milk.

Vectashield (Vector)

Stored at 4°C.

DAPI (Sigma)

Stock is 50µg/ml in dH₂O and stored at 4°C. For counterstain use at a final concentration of 10µg/ml.

Hybridisation mix

50% deionised formamide, 10% dextran sulphate, 2xSSC, 1% Tween 20, volume made up with dH₂O. Made fresh when required.

2.14.2 Materials for labelling probes by nick translation

Dnase I (Boehringer Mannheim)

Stock is 1mg/ml in 0.15M NaCl, 50% glycerol and is stored frozen. Working dilution is 1:500 in dH₂O.

DNA Polymerase I (Gibco BRL)

Stock is 10U/µl and is stored frozen.

dNTPs (Pharmacia)

Stocks are 0.5mM, prepared by a 1:200 dilution in dH₂O of 100mM stocks. Stored frozen.

10x Nick translation salts

0.5M Tris pH 7.5, 0.1M MgSO₄, 1mM dithiothreitol, 500µg/ml BSA fraction V.

Biotin-16-dUTP (Boehringer Mannheim)

Stock is 1mM and is stored frozen.

Digoxigenin-11-dUTP (Boehringer Mannheim)

Stock is 1mM and is stored frozen.

Streptavidin alkaline phosphatase (Boehringer Mannheim)

Stored at 4°C. Working dilution is 1:1000 in 0.1M Tris, 0.15M NaCl pH7.5.

Anti-digoxigenin alkaline phosphatase (Boehringer Mannheim)

Stored at 4°C. Working dilution is 1:1000 in 0.1M Tris, 0.15M NaCl pH7.5.

Alkaline phosphatase substrate kit IV BCIP/NBT (Vector)

Stored at 4°C.

Biotinylated lambda standards (Gibco BRL)

Stock is 200pg/μl. Diluted to 10 and 1 pg/μl and stored frozen.

Digoxigenin-labelled DNA standards (Boehringer Mannheim)

Stock is 5μg/ml. Diluted to 10 and 1 pg/μl and stored frozen.

Buffer I

0.1M Tris pH7.5, 0.15M NaCl. Stored at RT.

Buffer II

0.1M Tris pH 7.5, 0.15M NaCl, 3% BSA fraction V. Stored at RT.

Buffer III

0.1M Tris pH 9.5. Stored at RT.

2.14.3 Probes

For localisation of the HMG-R locus on CHO-K1 and UT-1 metaphase chromosome spreads, the pRED227 plasmid was labelled with biotin and used in FISH experiments.

For hybridisation of CpG islands (CGIs) on DT40 metaphase chromosome spreads, the pooled CGI library was labelled with biotin by PCR, using pGEM primers and amplification conditions described in section 2.7. dTTP was substituted with biotin-16-dUTP in the amplification reaction.

All cosmids mapped to DT40 metaphase chromosome spreads were labelled with biotin or digoxigenin, and were used in single or two-colour FISH experiments.

2.14.4 Labelling of probes with biotin or digoxigenin by nick translation

500ng of probe were labelled per reaction, and if necessary the volume was adjusted with dH₂O to a total of 6μl. 2μl of 10x nick translation salts were added to the mixture, followed by 2.5μl each of 0.5mM dATP, dCTP, dGTP, and bio-16-dUTP (when labelling with biotin) or 2.5μl each of 0.5mM dATP, dCTP, dGTP, 1.5μl of dTTP and 1μl of dig-11-dUTP (when labelling with

digoxigenin). This was followed by 1µl of DNase I freshly diluted 1:500, and 1µl of DNA polymerase I. The reaction was incubated at 15°C for 90 min. The probe was then precipitated with 2 vols of EtOH and 1/10 vol 3M NaAc for a minimum of 1 hour at -20°C. The pellet was subsequently spun down and resuspended in 10 - 50 µl of TE.

2.14.5 Detection of biotin or digoxigenin

The labelling efficiency was tested for each probe to be used in FISH experiments. Serial ten-fold dilutions of the labelled probe, down to 10^{-5} , were spotted onto a nitrocellulose filter, which had been previously washed in 20x SSC for 20 min and air dried. A biotin- or dig-labelled DNA standard was also spotted onto the filter. The filter was UV-crosslinked and washed in Buffer I for 5 min. The filter was then transferred to Buffer II, and incubated at 60°C for 1 hr. The filter was incubated in Buffer I containing 10µl of streptavidin alkaline phosphatase, or anti-dig alkaline phosphatase, at RT for 10 min. The filter was then washed with Buffer I for 2 x 15 min, and was finally washed in Buffer III for 5 min. The filter was placed in a sealed plastic bag with 1 ml of the BCIP/NBT kit solution and incubated in the dark for several hours until the colour developed. The filter was then rinsed in Buffer I and allowed to dry prior to storage.

2.14.6 Cell culture

Cells were harvested as described in section 2.13.3.

2.14.7 Preparation of metaphase spreads

Following treatment with the hypotonic solution, a 1/10 vol of 3:1 methanol:acetic acid was added dropwise to the cell suspension. The cells were then centrifuged at 1000rpm for 10 min at 4°C. The supernatant was discarded and the pellet resuspended, and a further 5ml of 3:1 methanol:acetic acid were added to the cells, initially dropwise. The resulting mixture was centrifuged at 1000rpm for 10 min at 4°C. The supernatant

was discarded, the pellet was resuspended, and 5ml of 3:1 methanol:acetic acid were added, and the cell suspension was left overnight at -20°C. The cells were then centrifuged at 1000rpm for 10 min at 4°C, and the pellet was resuspended in 1-2ml of 3:1 methanol:acetic acid.

To make metaphase spreads on slides, 10µl of the cell suspension were dropped onto EtOH cleaned slides, and allowed to air dry prior to storage at -20°C. Slides were aged 3-4 days prior to *in situ* hybridisation. Tubes containing the cell suspensions were refilled with 3:1 methanol:acetic acid and stored at -20°C where they remained usable for up to two months.

2.14.8 *In situ* hybridisation with biotin labelled probes

The required amount of probe was precipitated with 2 volumes of EtOH using a spin vacuum. The pellet was then resuspended with 10µl of hybridisation mix per slide. The mix was allowed to resuspend for at least 1 hr at RT.

Slides were incubated with RNase in a Coplin jar (100µg/ml in 2xSSC) for 1 hr at 37°C. They were then dehydrated by washing in 70%, 90%, and 100% EtOH for 2 min each at RT, and then allowing them to air dry.

Target DNA was denatured by incubating the slides in 70% formamide / 2xSSC for 3 min at 70°C, and immediately dehydrating them in ice-cold 70%, 90%, and 100% EtOH for 2 min at RT. Probe DNA was denatured in a 70°C waterbath for 5 min and reannealed for 15 min at 37°C, along with competitor DNA and salmon sperm DNA if required.

10µl of probe/hybridisation mix were applied to the target area, and sealed under a 22x22mm coverslip using rubber solution (Tip-Top). The slides were then transferred to a metal tray and placed in a 37°C waterbath o/n.

Non-specifically bound probe was removed by washing the slides for 4 x 3 min in each of the following solutions: 50% formamide / 2xSSC at 45°C, 2xSSC at 45°C, and 0.1xSSC at 60°C. The slides were then transferred into a Coplin jar containing 4xSSC / 0.1% Tween 20.

40µl of blocking buffer (4xSSC / 5% skimmed milk) were applied to the target area under parafilm, and the slides were incubated for 5 min at RT. 40µl of avidin-FITC (diluted in the blocking buffer) were then applied to the target area under parafilm, and the slides were incubated for 30 min at 37°C. The slides were then washed for 3 x 2 min in 4xSSC / 0.1% Tween 20 at 45°C. 40µl of the second antibody layer, biotinylated anti-avidin, were applied to the target area as before, and incubated for 30 min at 37°C. The slides were washed as before, and the third antibody layer, avidin-FITC, was applied to the target area and the slides were incubated and washed as before.

Finally the slides were counterstained and mounted as described in section 2.13.6.

2.14.9 *In situ* hybridisation with digoxigenin labelled probes

The protocol used for *in situ* hybridisation with dig labelled probes was as described above, with the exception of the antibody layers. When using dig labelled probes only, the first antibody layer was anti-dig FITC, a polyclonal antibody raised in sheep, followed by the second layer of anti-sheep FITC. Washes between antibody layers were as for biotin labelled probes.

When using both biotin and dig labelled probes, four antibody layers were applied in the following order.

- I anti-dig FITC
- II anti-sheep FITC and avidin-TRITC
- III biotinylated anti-avidin
- IV avidin-TRITC

Anti-sheep FITC cross-reacts with biotinylated anti-avidin (raised in goat) and must therefore be used before the latter antibody.

2.14.10 Fluorescence microscopy

Images were collected as described in section 2.13.6.

2.15 Replication timing

2.15.1 Materials for replication timing

Bromodeoxyuridine (BrdU) (Boehringer Mannheim)

Stock is 10 μ M. Dilute 1:100 when adding to cells.

Methotrexate (MTX) (Sigma)

Stock is 0.1 μ M. Dilute 1:1000 when adding to cells.

Mimosine (MIM) (Sigma)

Stock is 10mM. Dilute 1:50 when adding to cells.

Nocodazole (NOC) (Sigma)

Stock is 3mM Dilute 1:10,000 when adding to cells.

Anti-BrdU FITC (Boehringer Mannheim)

Stock is 100 μ g/ml. Working dilution is 1:10 in 4xSSC, 5% skimmed milk.

Vectashield (Vector)

Stored at 4°C.

DAPI (Sigma)

Stock is 50 μ g/ml in dH₂O and stored at 4°C. For counterstain use at a final concentration of 10 μ g/ml

2.15.2 Replication timing experiments

The timing of the DT40 cell cycle is shown schematically in the figure below.

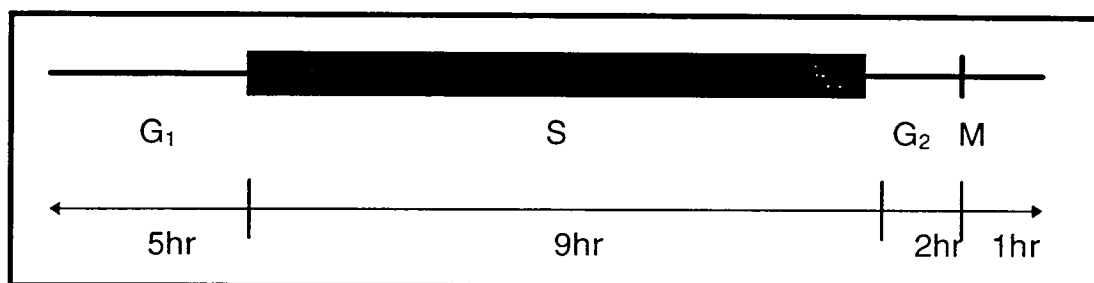


Figure 2.1

Timing of the DT40 cell cycle.

Continuous labelling

DT40 cells were synchronised in mid S-phase by addition of 0.1nM methotrexate for a full 17 hr cell cycle. To incorporate BrdU into late replicating DNA, cells were released from their methotrexate block by washing in fresh medium, and were grown a further 4.5 hrs in BrdU-containing medium. Cells were then arrested in mitosis by addition of colcemid to a final concentration of 0.1µg/ml for 1 hour. Cells were harvested and fixed in 3:1 Me:Ac, and metaphase chromosome spreads were prepared on slides, as described in section 2.14.7. To incorporate BrdU into early replicating DNA, cells were synchronised in mid S-phase by addition of 0.1nM methotrexate, in the presence of BrdU, for a full 17 hr cell cycle. Cells were then released from the methotrexate block by washing in fresh medium, and were grown a further 4.5 hrs in BrdU-free medium. Cells were then arrested in mitosis by addition of colcemid to a final concentration of 0.1µg.ml for 15 mins. Cells were harvested and fixed in 3:1 Me:Ac, and metaphase chromosome spreads were prepared on slides, as described in section 2.14.7.

Pulse labelling

To incorporate BrdU into early replicating DNA, cells were arrested in mitosis by addition of 300nM nocodazole for a full cell cycle. The cells were then released from the block by washing with fresh medium, and were grown to the G₁/S boundary by addition of 200µM mimosine for a full 17 hr cell cycle. The cells were subsequently released from the G₁/S block by washing in fresh medium and were grown in BrdU-containing medium for 30min to 3 hrs. BrdU was chased away with fresh medium and the cells were allowed to complete their cell cycle prior to arrest in mitosis with the addition of colcemid, as described earlier.

2.15.3 BrdU detection

Slides were dipped in 0.07M NaOH/EtOH for 3 min, and were then rinsed in PBS/1% skimmed milk for 10 min. 30µl of anti-BrdU FITC-conjugated

antibody were then applied to the target area, which was overlaid with parafilm. The slides were left in the dark at 37°C for 1 hr, in a moist chamber. The slides were rinsed 3 x 2 min in 4xSSC/0.1% Tween20 at 37°C. Finally the slides were counterstained and mounted as described in section 2.13.6.

2.15.4 Fluorescence microscopy

Images were collected as described in section 2.13.6.

CHAPTER THREE - RESULTS AND DISCUSSION

Histone H4 acetylation at the HMG-R locus

3.1 Introduction

3.1.1 Aim of the project

Immunofluorescence has clearly demonstrated that acetylation of histone H4 is confined to gene-rich, transcriptionally active regions. Silenced regions of chromatin, however, such as the facultative heterochromatin of the inactive X chromosome and constitutive centromeric heterochromatin, are underacetylated (section 1.5.3).

Data obtained by immunoprecipitation approaches, most significantly that obtained by Crane-Robinson and Turner (section 1.5.2), has generated dissimilar results. Crane-Robinson and coworkers have shown that both actively transcribed and potentially transcribable ("poised") genes (eg. the developmentally regulated β globin genes) are found in the acetylated chromatin fraction (Hebbes *et al* 1992, Clayton *et al* 1993). Silenced genes, such as tissue-specific genes (eg. ovalbumin), are underacetylated. Thus acetylation appears to be associated with the ability or potential for transcription, rather than transcription *per se*.

Turner and colleagues, however, do not distinguish between these two classes of genes - silenced or transcriptionally poised/active - and claim that the level of H4 acetylation of coding regions, whether actively transcribing or not, does not vary from that of bulk chromatin - ie. there is no difference in H4 acetylation between transcriptionally active and quiescent genes (O'Neill & Turner 1995). Constitutive heterochromatin, however, is found to be underacetylated.

Thus, whereas Crane-Robinson's results suggest that chromatin can be subdivided into 3 classes with reference to H4 acetylation - transcriptionally active/poised genes, quiescent genes, and constitutive heterochromatin - Turner's results subdivide chromatin into constitutive heterochromatin and the rest, referred to as bulk chromatin.

The reasons for the discrepancy between the two groups' results may be technical, a consequence of the different antibodies utilised in the two labs. Also, the properties of the immunoprecipitation technique are such that it is

unlikely to discriminate between different degrees of histone acetylation. Immunolabelling, on the other hand, has shown that different regions of the genome vary greatly in the degree to which they are acetylated, as shown by Jeppesen and Turner for histone H4 (Jeppesen *et al* 1992, Jeppesen & Turner 1993). Thus, while cytological resolution is insufficient to see histone acetylation associated with individual genes, the justification for the immunolabelling approach lies in the clear association between histone acetylation and coding regions of the genome. In a recent study of amplified arrays of dihydrofolate reductase genes found in a methotrexate-resistant cell line (Nicol & Jeppesen 1996), for example, it was shown by immunofluorescence that histone acetylation at the amplified arrays was located specifically at chromatin domains known to be transcriptionally active.

Given the inconsistency present within data obtained using an immunoprecipitation approach, the aim of this research project was to detect, using an *in situ* immunolabelling approach, changes in histone H4 acetylation that may accompany different expression states of an inducible gene. In addition, the use of a tandemly repeated gene would potentially allow histone acetylation to be observed with cytological resolution, the limit of resolution being in the range of 1-3Mb (Nicol & Jeppesen 1996). The system chosen for this study, therefore, was the Chinese hamster UT-1 cell line, in which drug resistance had been conferred by amplification of the inducible 3-hydroxy-3-methylglutaryl coenzyme A reductase (HMG-R) gene. Site-specific antisera, developed by Turner, were used to look for variation in the histone H4 acetylation pattern, in relation to the gene being actively transcribed or repressed.

3.1.2 3-hydroxy-3-methylglutaryl coenzyme A reductase (HMG-R)

HMG-R is a regulated membrane-bound enzyme that controls the synthesis of cholesterol and other polyisoprenoid compounds (Figure 3.1a). The activity of HMG-R can be suppressed in cultured cells by cholesterol entering via receptor-mediated endocytosis, in the form of plasma low-density-

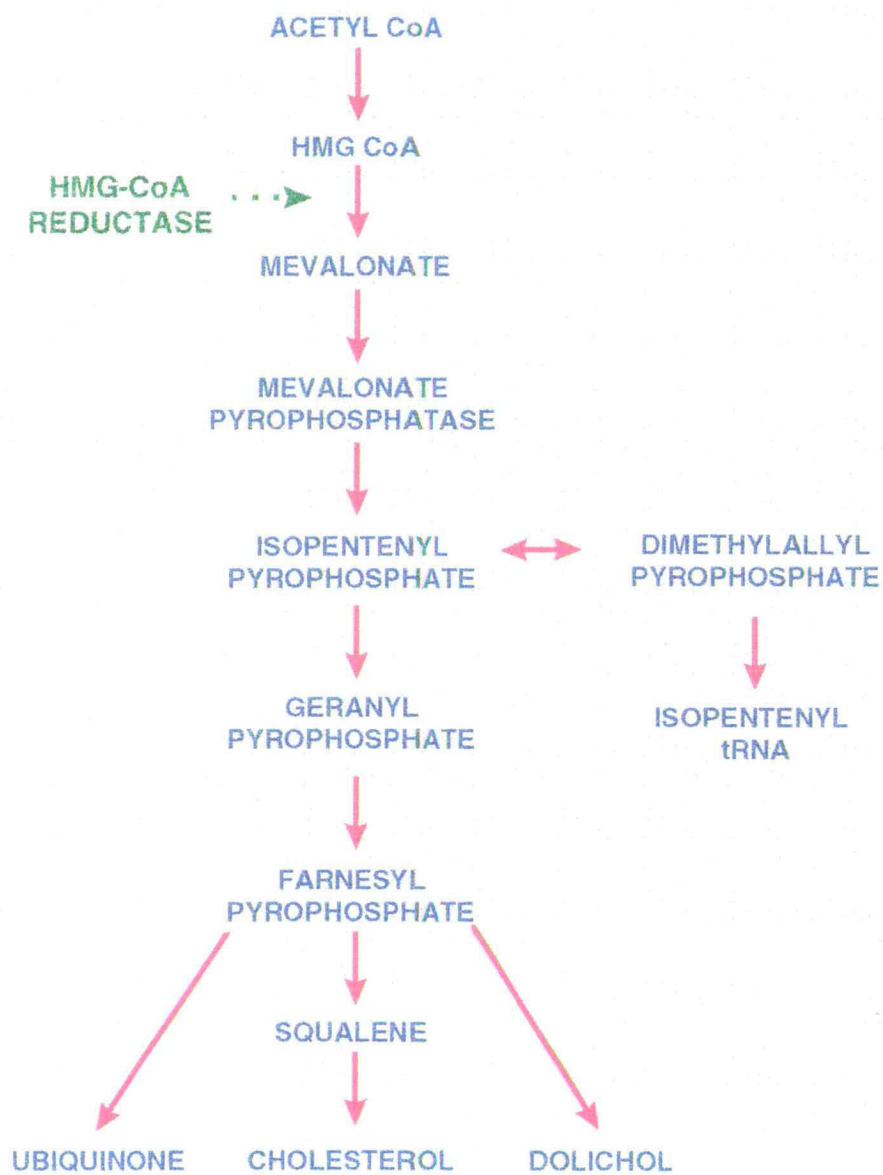


Figure 3.1a

Biochemical pathway for cholesterol synthesis.

lipoprotein (LDL) (Brown & Goldstein 1980). Enzyme activity can also be suppressed by addition of 25-hydroxycholesterol dissolved in organic solvents (Kandutsch & Chen 1975, von Gunten & Sinensky 1989). In the absence of plasma LDL, cells synthesize their own cholesterol by maintaining high levels of HMG-R activity. On addition of LDL (or 25-hydroxycholesterol) to the culture medium, the activity of HMG-R is reduced, thus turning off the cell's own synthesis of cholesterol which is no longer required. This reduction in HMG-R activity can be by as much as 98%, but never becomes 100%, as the low levels of HMG-R activity that persist in the presence of cholesterol appear to be important for cellular metabolism (Brown *et al* 1974, Brown *et al* 1978, Brown & Goldstein 1980). The activity of the enzyme is thus regulated by a feedback mechanism, as shown below.

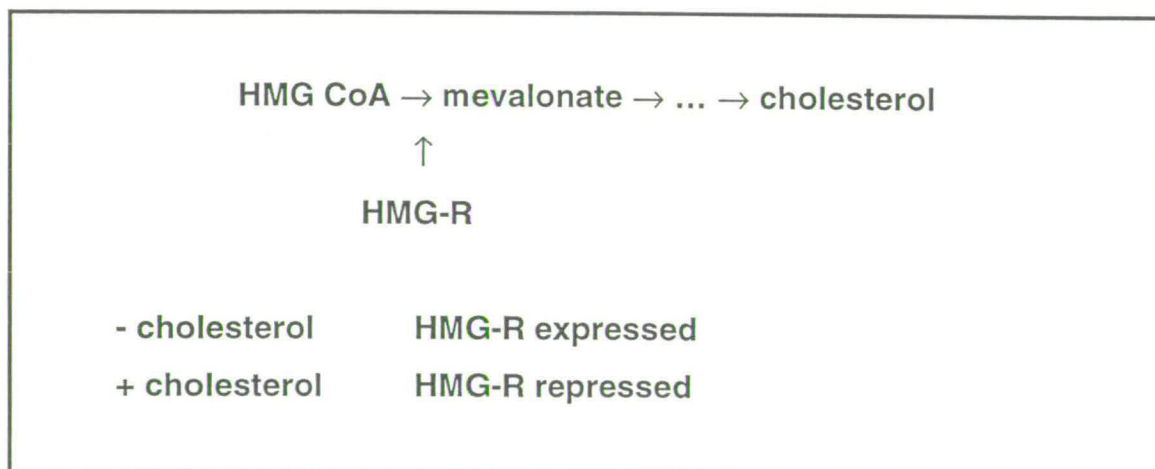


Figure 3.1b

Feedback mechanism of HMG-R regulation.

HMG-R is a 97kDa glycoprotein, that remains inserted in the endoplasmic reticulum (ER) membrane after its synthesis and glycosylation. The active site of the enzyme is present on the cytoplasmic side of the ER membrane, and it can be released by proteolytic digestion. It has an asparagine-linked high-mannose carbohydrate chain that remains associated with the membrane after proteolysis, but, in contrast with other transmembrane glycoproteins, it lacks a cleavable signal sequence for mediating membrane

insertion. It appears instead to possess an internal signal sequence that interacts with a signal recognition particle to direct insertion of the protein into the membrane, and that remains uncleaved following this event. It also appears to contain three potential sites for asparagine-linked glycosylation. The site chosen for glycosylation *in vivo* may depend on which site is exposed on the luminal side of the ER membrane.

The nucleotide sequence for HMG-R in Chinese hamster ovary (CHO) cells was determined by Chin and colleagues (Chin *et al* 1984) by screening cDNA libraries with a plasmid containing a 1.2kb cDNA of the gene (Luskey *et al* 1982). Five overlapping cDNAs were obtained, the longest of which (pRed227) spans the entire coding region as well as 163bp of 5'-untranslated region and 1650bp of 3'-untranslated region (Figure 3.5). One of these cDNA sequences was used to screen a bacteriophage λ library, to obtain recombinant clones spanning 25kb of genomic DNA, and encompassing both the coding sequence and 5' and 3' flanking sequences (Reynolds *et al* 1984). These genomic clones were used to define the intron-exon boundaries and to characterise the upstream promoter region of the gene. As shown in Figures 3.2 and 3.3, the gene spans 25kb and is divided into 20 exons. Figure 3.4 shows the cDNA sequence corresponding to the mRNA, and the predicted amino-acid sequence of the protein. The mRNA is heterogeneous, with multiple sites of transcription initiation at the 5' end and alternative sites of polyadenylation at the 3' end of the gene. These, in combination with multiple 5' splice donor sites for an intron found encoded in the 5'-untranslated region, give 16 different mRNAs with variable 5'-untranslated regions, which may be developmentally regulated. The mRNAs fall into two classes, I and II, based on two major clusters of initiation sites (Reynolds *et al* 1985). Although class I transcripts represent 70% of total mRNAs, both class I and class II transcripts are suppressed when cells are grown in presence of cholesterol. The promoter region lacks characteristic TATA and CCAAT boxes, is GC-rich, and contains repeat sequences homologous to 21bp repeats found in the SV40 promoter. The mouse homologue of HMG-R contains a CpG island so it is quite likely that the

Intron Number	Sequence of Exon-Intron Junctions		Intron Size
	5' Boundary	3' Boundary	
			kilobases
1	ACTTGTGAG gtaggag.....tggtgtttccttcag -24	GATCCAGGG -23	3.5
2	TTT GAG GAG gttagtg.....tctctctgccaatag 165 Glu (55)	GAT GTA TTG 166 Asp (56)	0.425
3	ATT TTA G gtaatac.....atcttgccattttag 277 Gly (93)	GT ATT GCT 278 Gly (93)	0.241
4	GGC TTA AA gtaagta.....ttttttttccccccag 365 Asn (122)	T GAA GCT 366 Asn (122)	1.7
5	AAC TCT CAG gtgagtc.....tggtttgtgcttcag 450 Gln (150)	GAT GAA GTA 451 Asp (151)	1.6
6	ATG TCA G gtttgta.....ttgctctctatccag 556 Gly (186)	GG GTG CGT 557 Gly (186)	3.2
7	GTC CTT GAG gtaagaa.....tgacttactttgtag 663 Glu (221)	CTT TCT CGG 664 Leu (222)	0.105
8	ATG ATT ATG gtaatga.....aatttggtttcttcag 780 Met (260)	TCT TTA GGT 781 Ser (261)	0.4
9	CTC TCC AA gtaagtt.....tttactctcacctag 941 Lys (314)	G ATG ATC 942 Lys (314)	0.107
10	AGA AAA C gtaacttt.....ttgcctctcacacag 1189 Val (397)	TT CAG GTT 1190 Val (397)	0.099
11	AGT GCC GAG gtgaggg.....ttctcattttcttcag 1365 Glu (455)	AAA GGT GCA 1366 Lys (456)	2.0
12	TAT TCC CTC gtatgtt.....acctgtgtttctag 1560 Leu (520)	GTG ATG GGA 1561 Val (521)	0.6
13	GCA ATA GGT gtaagt.....cattctctctgcttag 1719 Gly (573)	CTT GGT GGA 1720 Leu (574)	0.3
14	ACT AGC AG gtgtgga.....acctgtgttttacag 1877 Arg (626)	A TTT GCA 1878 Arg (626)	1.4
15	ATT TCC AAG gtaagtg.....tttactctctactag 1983 Lys (661)	GGC ACT GAG 1984 Gly (662)	1.8
16	GTG AGA GAA gtaagtg.....cacactgtgctctag 2154 Glu (718)	GTA TTA AAG 2155 Val (719)	0.6
17	TGT GGC CAG gtaagct.....cttttctacttccag 2295 Gln (765)	GAT GCA GCA 2296 Asp (766)	1.1
18	TGT CTG CAG gtatgtg.....ggtctccgattacag 2454 Gln (818)	ATG CTA GGT 2455 Met (819)	0.9
19	CAT AAC AG gtaagat.....cttttctgacatag 2609 Arg (870)	A TCG AAG 2610 Arg (870)	0.31

Figure 3.3

Exon-intron organisation of the HMG-R gene.

The nucleotide sequence of exon-intron junctions is shown. Exon sequences are in capital letters, intron sequences are in lowercase letters. The intron sizes are also indicated, and were taken in consideration when creating primers for PCR experiments.

This figure has been taken from Reynolds *et al* 1984.

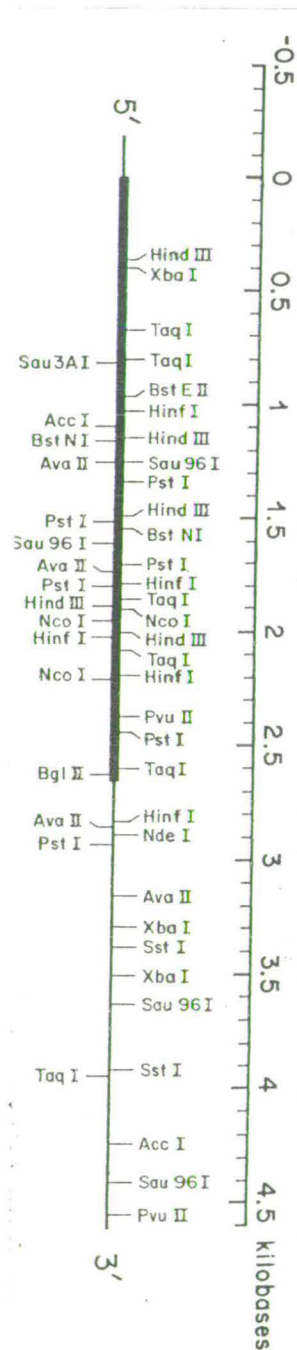


Figure 3.5

Restriction map of HMG-R cDNA sequence.

A complete restriction map for the indicated enzymes is shown for the region spanning the coding region and a large part of the 3' untranslated region. The cDNA region incorporated into the pRED227 plasmid is indicated.

This figure has been taken from Chin *et al* 1984.

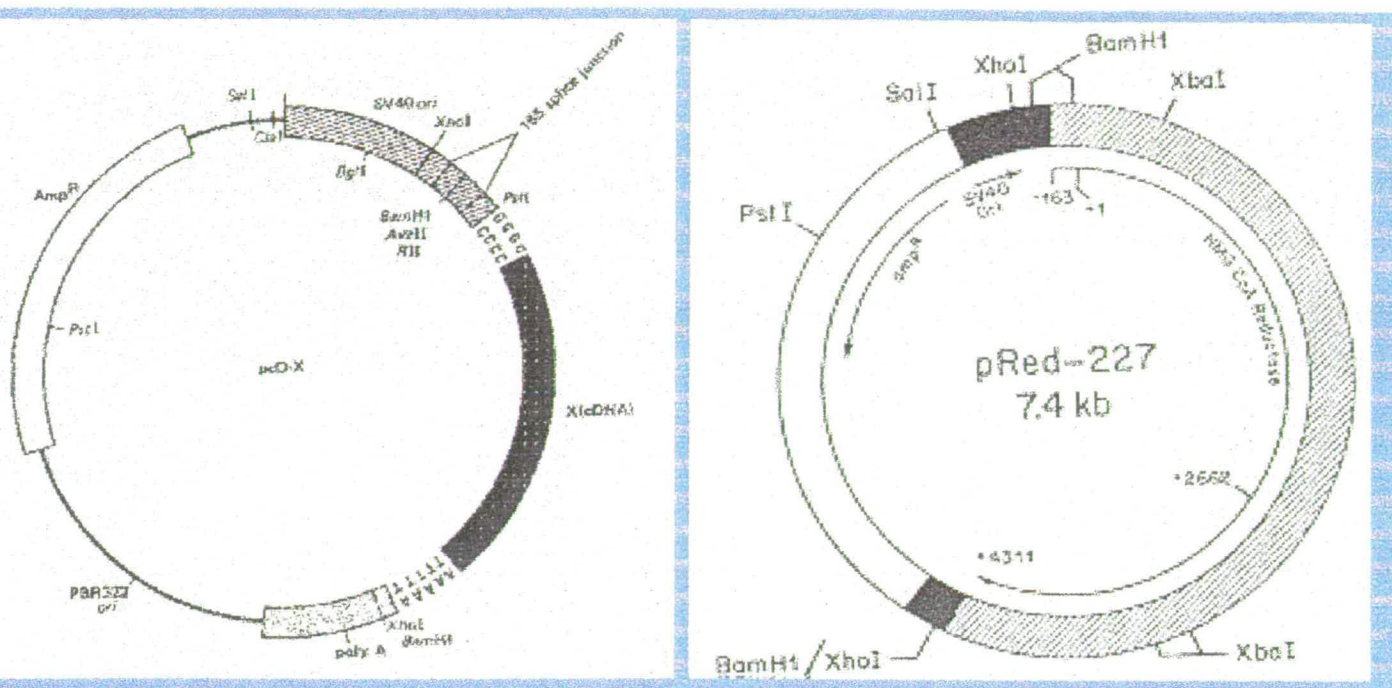


Figure 3.6

pRED227 plasmid.

The structure of the pCD vector into which 4.5kb of HMG-R cDNA sequence were inserted. This plasmid was used as a probe to detect HMG-R in all hybridisation experiments.

This figure was taken from Okayama & Berg 1983.

Chinese hamster gene also does. The 3'-untranslated region is unusually long, but does not appear to contain an open reading frame.

3.1.3 UT-1 cell line

The UT-1 cell line was developed by Brown, Goldstein and colleagues (Chin *et al* 1982). CHO cells were grown in the presence of the drug compactin, an inhibitor of cholesterol synthesis. This inhibitor is produced in several fungal strains, including *Penicillium brevicompactum*. The structure of compactin resembles that of mevalonate, the product of the HMG-R reaction (Goldstein *et al* 1979). Compactin therefore acts as a reversible competitive inhibitor of HMG-R. Low concentrations of the drug in culture medium blocks cholesterol synthesis in cells, causing them to rely on an exogenous source of cholesterol.

The underlying principle is that a cell line grown in the presence of a competitive inhibitor of an essential enzyme will select for those cells which have increased the amounts of enzyme produced. This is accomplished by gradually increasing the concentration of the inhibitor in the medium. After each increase, the large majority of cells are selected against and die. Those cells, however, which fortuitously have a higher copy number of the gene and thus can increase their enzyme production will survive and consequently be selected for.

By adapting CHO cells to increasing concentrations of compactin over an 8-month period, Chin and coworkers developed a clone of CHO cells, known as the UT-1 cell line, which reportedly had a 500-fold increase in HMG-R activity. UT-1 cells were able to grow for more than a year in the presence of 40 μ M compactin, whereas CHO cells did not survive in 0.3 μ M compactin.

To compare quantities of the HMG-R protein in the two cell lines, an antibody to rat liver HMG-R was prepared. By immunoblotting crude protein extracts electrophoresed on SDS-polyacrylamide gels, the relative amounts of HMG-R were estimated. While UT-1 cells gave a distinct band when 4 μ g of protein were loaded onto the gel, 400 μ g of the parental CHO protein gave a faint band. The authors thus concluded that UT-1 cells contained at least 100-fold

more HMG-R protein than CHO cells (Chin *et al* 1982). Both cell lines were then incubated with [³⁵S] methionine to visualise proteins immunoprecipitated with the rat anti-HMG-R antibody. In UT-1 cells, 2% of protein radioactivity was specifically precipitated by the antibody, in contrast with undetectable amounts in CHO cells. Reduction in enzyme activity, in the presence of cholesterol, was shown to be a consequence of a sharp decline in synthesis of the enzyme rather than in its degradation (Faust *et al* 1982), implying that regulation occurred at the transcriptional or translational level.

Levels of HMG-R RNA in UT-1 and CHO cells, grown in the absence or presence of cholesterol, were determined by Northern analysis (Chin *et al* 1982). In induced UT-1 cells, grown in the absence of cholesterol, two mRNA species of 4.2 and 4.7kb were detected. Neither of these were detected in UT-1 cells that had been incubated with cholesterol. No hybridisable RNA was detected in CHO cells grown in presence or absence of cholesterol, due to the level of sensitivity of the experiment. Both mRNA species detected in UT-1 cells were thought to be derived from the same gene, and the difference in size was claimed by the authors to be a result of post-translational processing. HMG-R RNA levels in response to cholesterol were also analysed by a cytoplasmic RNA filter hybridisation method (Luskey *et al* 1983). RNA in UT-1 cells was shown to decrease dramatically within 8 hours after addition of cholesterol, and by 90% within 12 hours. The reduction in HMG-R mRNA, in response to cholesterol, was correlated to the enzymatic activity. Parallel suppression of enzyme activity, enzyme synthesis, and levels of mRNA was observed (Luskey *et al* 1983).

The relative number of copies of HMG-R in UT-1 and CHO cells were estimated by Southern analysis (Luskey *et al* 1983). The authors proposed that, by densitometric scanning, there was a 15-fold increase in the amount of hybridisable HMG-R DNA in UT-1 cells relative to CHO cells, where the gene is believed to be single copy. Restriction enzyme digestion gave parallel patterns for both cell lines, indicating that there had been no gross structural rearrangement within the gene following its amplification. When UT-1 cells were grown in absence of compactin for a period of 3-4 months,

the level of HMG-R mRNA and enzymatic activity decreased, but the gene copy number remained the same. Subsequent addition of compactin produced a 30-fold increase in reductase activity over a 3-day period.

Based on the data described above, the advantages of the system used for this investigation are two-fold:

- HMG-R is a unique non-constitutively expressed gene whose transcriptional activity can be regulated by growth of UT-1 cells in presence or absence of cholesterol.
- The UT-1 cell line has a 15-fold amplification of the gene with no rearrangement, which may allow the gene and its associated chromatin to be resolvable at a cytological level.

3.1.4 Experimental approach

The experimental approach for the project consisted in identifying the amplified HMG-R gene locus by fluorescence *in situ* hybridisation, and resolving the acetylation profile at the locus by immunolabelling, using antisera raised against H4 acetylated at particular lysine residues. The acetylation profile of the gene was then monitored in relation to the gene's transcriptional status, in order to detect any difference in the degree of acetylation with changing gene expression.

3.2 Characterisation of the UT-1 cell line

The UT-1 cell line used throughout the duration of the project was originally placed in the European Type Culture Collection (ETCC) by Brown and Goldstein, who developed the cell line in 1982 (Chin *et al* 1982). Once obtained from the ETCC, the cells were passaged regularly in DMEM medium supplemented with foetal calf serum and L-proline.

The property of UT-1 cells of interest was the amplification of the HMG-R gene, and the accompanying resistance to the competitive inhibitor of the HMG-R gene, compactin. Throughout the project, an alternative competitor, simvastatin (a biochemical equivalent of compactin) was used, as a substitute for the latter drug, as it is more readily available.

The reported drug resistance of the cell line was tested, and the highest concentration of simvastatin at which the cells would survive was determined.

3.2.1 Drug titration test

To determine the extent to which the UT-1 cells were drug resistant, relative to the parental CHO-K1 cell line, cells were grown in the presence of varying concentrations of simvastatin (0.001-0.020mM) over a period of one week. The number of cells per plate were then counted with a Coulter Counter, and plotted on a graph with respect to simvastatin concentration.

Fig 3.7 shows the results obtained, in graph form.

CHO-K1 cells were able to survive moderately well in low concentrations (0.001-0.002mM) of simvastatin, but the growth rate deteriorated rapidly on increasing the concentration just over two-fold to 0.005mM.

UT-1 cells grew considerably better in the presence of all drug concentrations (0.001-0.010mM), confirming the cell line's resistance to the drug. At the highest concentration of 0.020mM simvastatin, the cells' growth rate slowed down considerably. The optimum concentration at which to grow the cells was thus determined to be 0.010mM simvastatin.

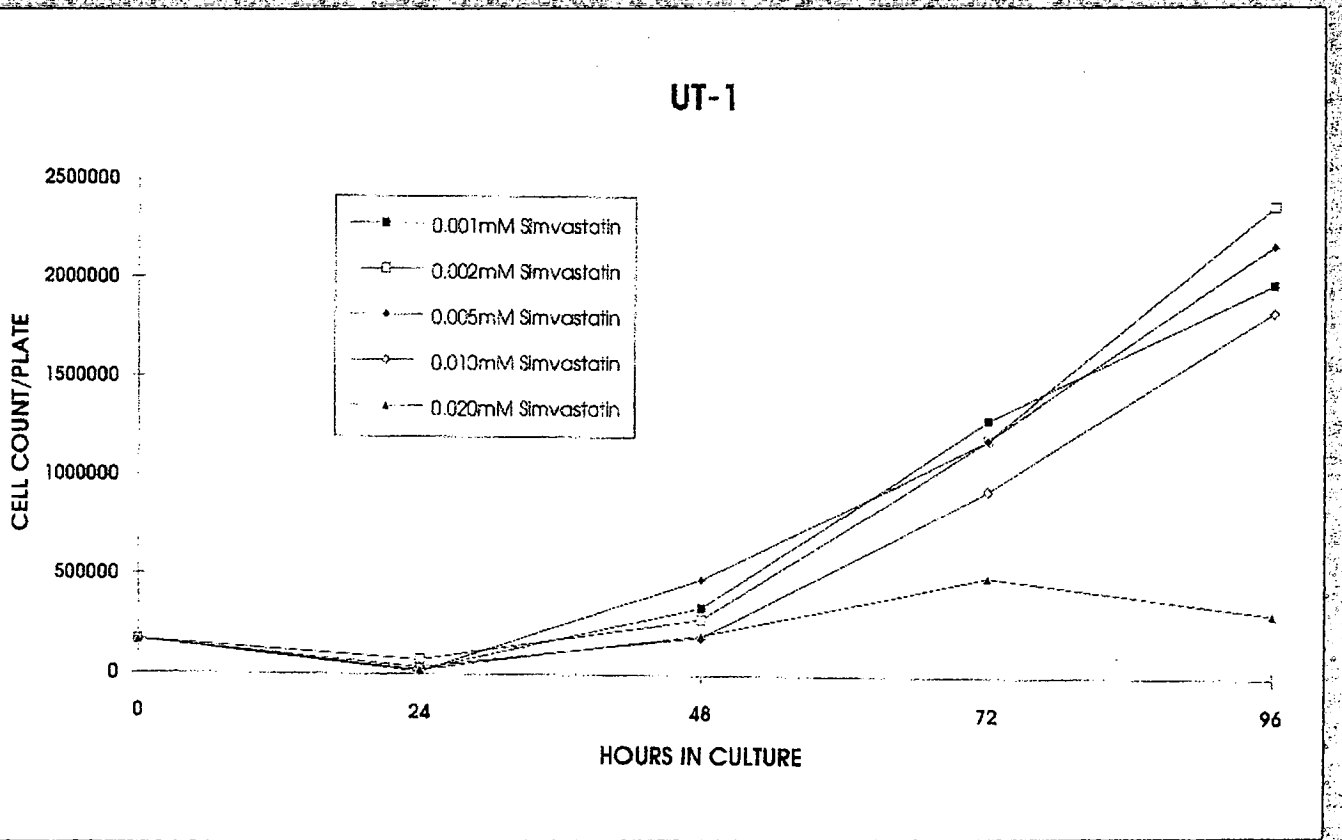
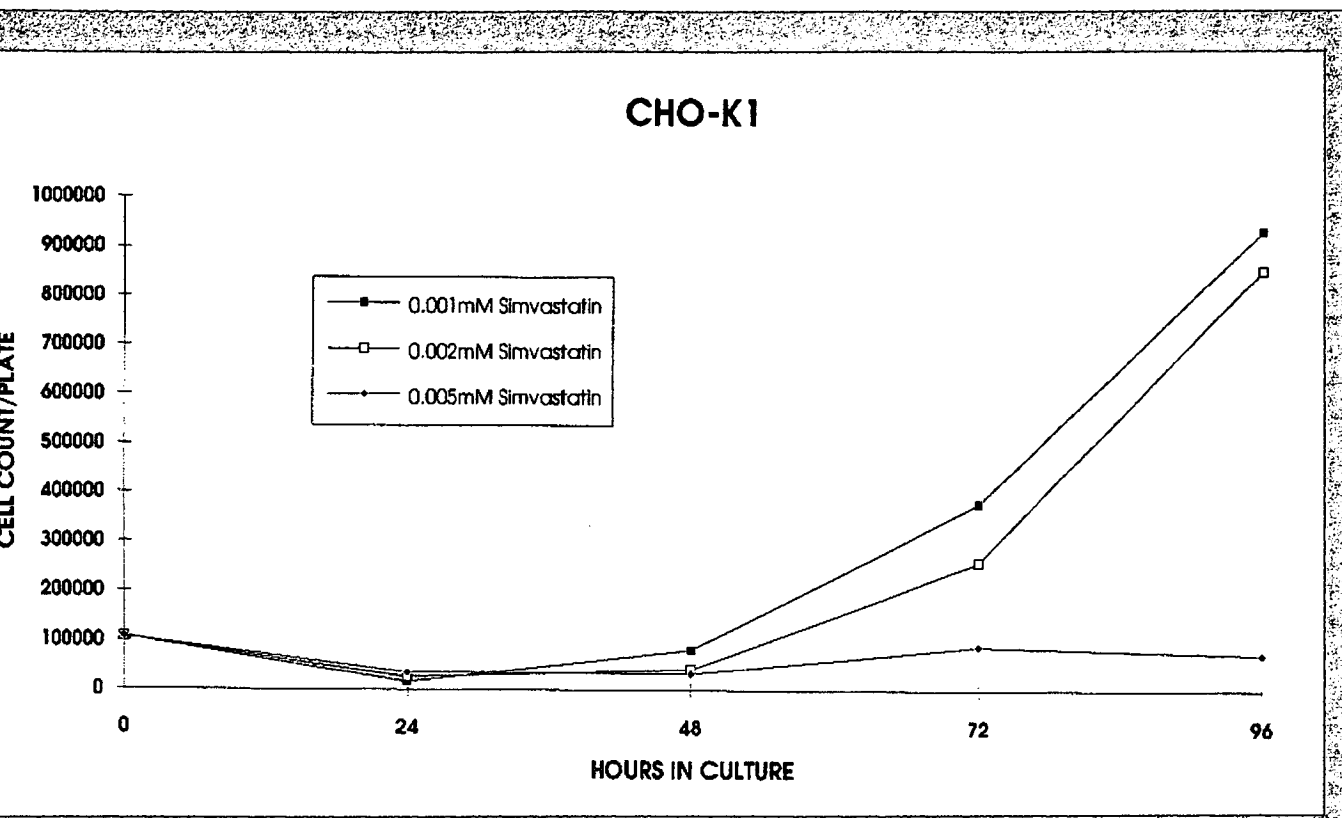


Figure 3.7

Resistance of CHO-K1 and UT-1 cells to simvastatin.

See text for details.

UT-1 cells thus showed a 4-fold increase in resistance to simvastatin. This was much lower than the reported 100-fold increase in resistance to compactin, but was deemed to be attributable to the use of a different inhibitor. Results discussed in later sections suggest however that the UT-1 cells may indeed have lost their drug resistance prior to arrival into the lab.

3.2.2 Regulation of HMG-R expression with cholesterol

In order to regulate expression of HMG-R, UT-1 cells were grown in the presence or absence of cholesterol, as shown in the table below.

Table 3.1

Growth conditions for UT-1 cells expressing/repressing HMG-R.

HMG-R expressed	HMG-R repressed
Lipid-free medium	Regular medium
Lipid-free medium + 10 μ M simvastatin	Regular medium + excess cholesterol

Regular medium (DMEM supplemented with foetal calf serum and L-proline) was used in conditions where repression of HMG-R was required, as any cholesterol present in the foetal calf serum would down-regulate expression of the gene. To ensure that enough cholesterol was present to repress the gene, the cells were also grown in presence of excess 25-hydroxycholesterol (1 μ g/ml).

Lipid-free medium was produced by delipidising the constituent foetal calf serum, utilising a silica (Cabosil) that binds to low-density-lipoproteins (LDLs). Growth of UT-1 cells in lipid-free medium initially turned out to be problematic, however, as the cells did not survive the first 24 hours post-plating. This appeared to be due to the lack of an attachment factor (vitronectin or fibronectin) required for adherence of the cells to the tissue culture dish. These attachment factors are adhesive glycoproteins found in the extracellular matrix deposited by cultured adherent cells. Vitronectin, in particular, has been shown to be the principle operative cell adhesion

molecule in medium containing serum at a concentration greater than 1%. It is known that these factors bind to glass, and thus it seemed likely that they were removed from the foetal calf serum by binding to the silica used in the delipidisation process (Keith Gooderham, Life Technologies™, personal communication). This was overcome by incubating the plates overnight in foetal calf serum diluted 1:10 in PBS, so that the adherant coated the bottom of the dish, and then washing the plates several times with PBS to remove all traces of the untreated foetal calf serum. The cells were then transferred to the dishes in lipid-free medium, and grew well.

3.3 Localisation of HMG-R by fluorescence *in situ* hybridisation

The cytological location of HMG-R in UT-1 and the parental CHO-K1 cells had not been previously determined. It was therefore necessary to map the gene in these cell lines, prior to carrying out the subsequent studies of cytological changes at these loci.

This was accomplished by fluorescence *in situ* hybridisation (FISH), using pRED227 (Figures 3.5 and 3.6) as a biotin-labelled probe, for detection of the HMG-R locus on metaphase chromosomes. The plasmid contains 4.5kb of HMG-R cDNA sequence, encompassing the entire coding region, and including 163bp of 5' untranslated region and 1650bp of 3' untranslated region.

3.3.1 Localisation of HMG-R

Localisation of HMG-R on UT-1 and CHO-K1 chromosomes was carried out using standard FISH protocols (section 2.14). Cells were arrested in metaphase by treatment with colcemid, and metaphase chromosome spreads were prepared by standard methods with methanol-acetic acid fixation. The HMG-R probe was labelled with biotin by a nick translation reaction. FISH experiments were carried out using 100ng of probe, and the hybridisation signal was detected using two layers of FITC-conjugated avidin, separated by a layer of biotinylated anti-avidin. Metaphase chromosome spreads were subsequently counterstained with DAPI.

Figure 3.8 shows the results obtained.

The FISH experiment confirmed that the gene locus was distinguishable at a cytological level in the UT-1 cell line. It confirmed that the gene had been amplified in the UT-1 cell line, as the hybridisation signal detected on UT-1 chromosomes was consistently stronger than that detected on the parental CHO-K1 cell line, containing a single copy of HMG-R. In addition, this was in agreement with Southern data obtained by Goldstein, Brown and colleagues, claiming there had been no rearrangement in the HMG-R gene as a result of its amplification in the UT-1 cell line. They had shown by Southern analysis,

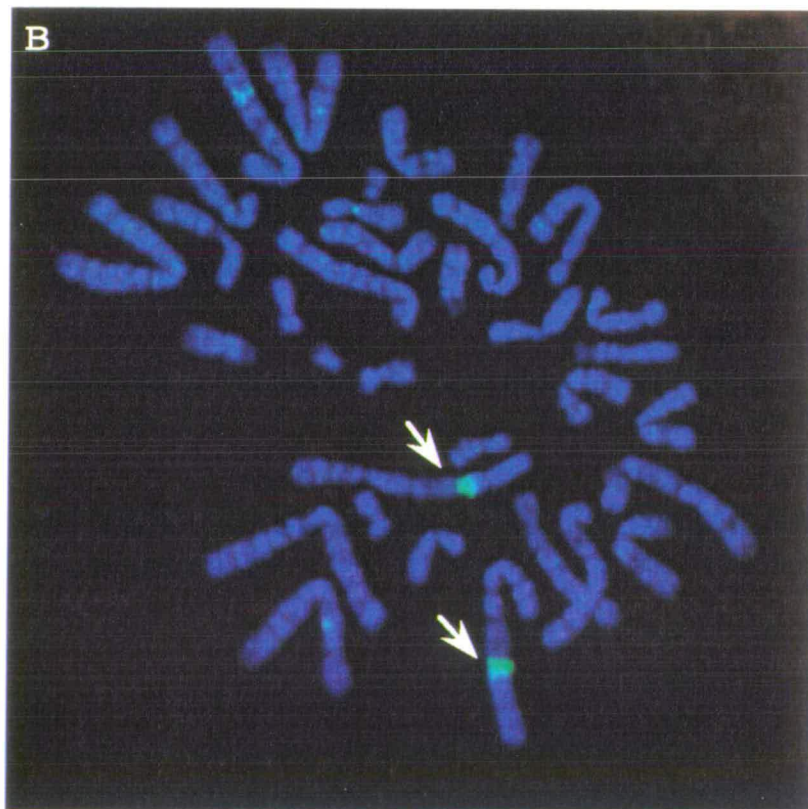
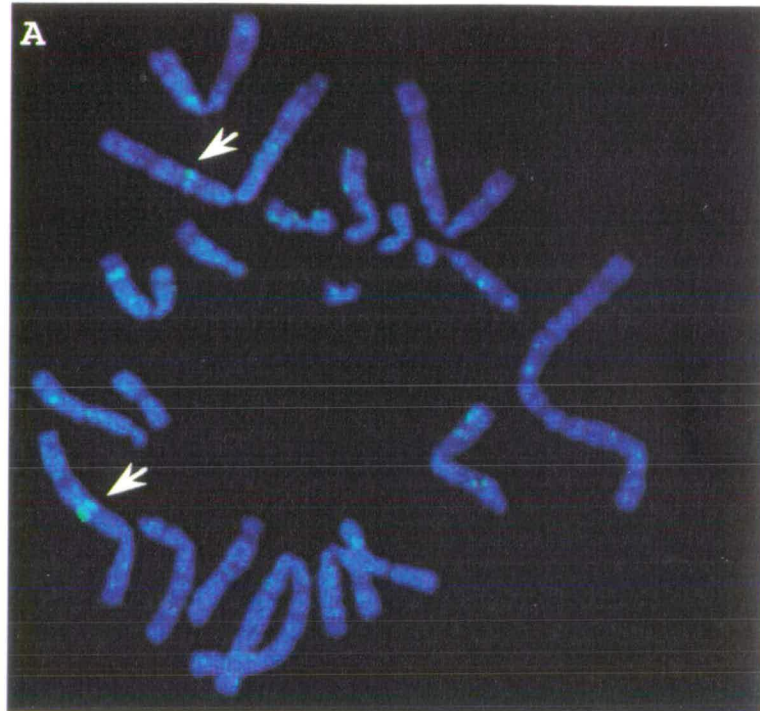


Figure 3.8

Localisation of HMG-R by FISH.

Metaphase chromosomes are counterstained with DAPI (blue), hybridised with biotin-labelled HMG-R cDNA. The HMG-R signal (indicated by arrow) is detected with avidin-FITC (green).

A. CHO-K1 metaphase chromosomes.

B. UT-1 metaphase chromosomes.

using a number of different restriction enzymes, that the genomic structure of the HMG-R gene was identical in both the parental (single-copy) and the amplified cell lines (Luskey *et al* 1983).

By FISH analysis, there was consistently a single hybridisation signal detected for HMG-R (one per allele), in both single copy and amplified cell lines, indicating that the gene had amplified in tandem arrays at a single locus rather than translocating onto different chromosomes. Thus no cytologically detectable rearrangement within the gene structure had occurred.

This did not allow me to determine, however, the size of the HMG-R amplicon, a factor of considerable importance when considering the resolution at which the gene locus would be visible. Previous work with genes amplified through selection regimes (Nicol & Jeppesen 1996) had set the limit of resolution to 1-3Mb.

3.4 Amplification of HMG-R in the UT-1 cell line

The UT-1 cell line reportedly has a 15-fold amplification of the HMG-R gene. In order to verify this, and to ensure that the amplification had been maintained in cells that had been passaged for some time, the genomic structure of the HMG-R gene was analysed by digestion with a selection of restriction enzymes.

3.4.1 Southern analysis

CHO-K1 and UT-1 genomic DNA was digested with a number of restriction enzymes: Bam HI, Bgl II, Eco RI, Hind III. The digested DNA was then electrophoresed on a 0.8% agarose gel, and blotted by standard Southern procedures. The resulting blot was hybridised with pRED227, a plasmid containing the entire cDNA sequence of HMG-R, to detect HMG-R-specific fragments.

The result is shown in figure 3.9, panel A. The pattern of restriction digests was identical in both the single-copy CHO-K1 and the amplified UT-1 cell lines, confirming that the HMG-R gene had not rearranged during the course of amplification in the UT-1 cell line, but had amplified in a tandem array.

The intensity of bands in the UT-1 restriction digests was considerably stronger than that of the single-copy CHO-K1 digests. This was indicative of the amplification of HMG-R in the UT-1 cell line. In order to quantify the extent of the amplification, the same blot was probed with Chinese hamster CENP-B cDNA (provided by L Bejarano, Bejarano & Valdivia 1996), as shown in figure 3.9, panel B. CENP-B is one of several centromeric proteins, and the gene should be single copy in all cell lines. This was confirmed by the single band seen in both CHO-K1 and UT-1 DNA when hybridising with CENP-B. CENP-B thus served as a loading control for the experiment, in order to standardise the amount of genomic DNA in each lane. With this in mind, signal intensities between corresponding CHO-K1 and UT-1 bands were quantified and compared by PhosphorImager analysis (Molecular Dynamics). The values obtained indicated that HMG-R was amplified 12-15

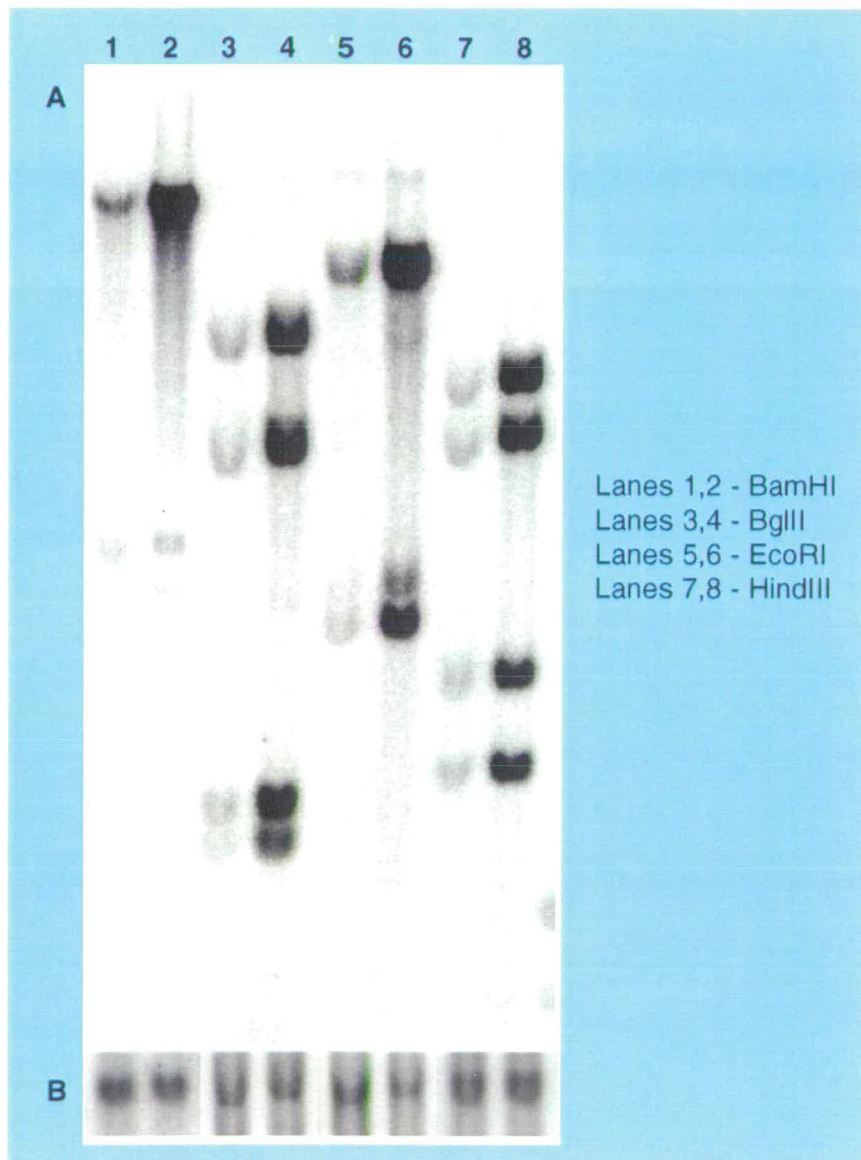


Figure 3.9

Southern analysis of HMG-R amplification in UT-1 cells.

Lanes 1, 3, 5, 7 - CHO-K1 genomic DNA

Lanes 2, 4, 6, 8 - UT-1 genomic DNA.

Genomic DNA from CHO-K1 and UT-1 cells was digested with the restriction enzymes specified above. The digested DNA was electrophoresed on an agarose gel, the gel was blotted and hybridised with radiolabelled HMG-R cDNA (panel A) and CENP-B cDNA (panel B) as an internal loading control. Quantification of the signal was determined by Phosphorimager analysis.

fold in the UT-1 cell line. This confirmed that, even after extended passaging, the cells had maintained their amplification.

3.4.2 PFG analysis

The HMG-R gene is 25kb in length. No information was available about the size of the amplicon in the UT-1 cell line, and thus whether the gene had amplified in tandem arrays of 25kb, or whether a larger region of DNA was contained within each amplicon. This information was relevant when considering if the amplified region was large enough to be resolved at a cytological level, in the immunolabelling experiments.

In order to determine the size of the amplicon, a series of pulse field gel experiments were set up. Partial digests were attempted using enzymes that cut on either side of the amplicon, such that complete digestion would allow the rough size of a single amplicon to be determined, whereas partial digestion would allow the size of the multimeric repeating unit within the amplified region to be determined. Fig 3.10 shows a schematic representation of the experimental approach.

Plugs containing CHO-K1 and UT-1 genomic DNA were digested with NdeI and Aval enzymes, that were known to cut once within the gene, and XhoI, known to cut outside the gene, based on the restriction map published in Reynolds *et al* 1984. This approach, using decreasing concentrations of enzyme in each reaction, gave inconclusive results. The restriction patterns of complete digests were too complex to allow resolution of the amplicon, and partial digests resulted in a smear of DNA rather than a clear ladder of bands.

Parallel experiments (discussed in section 3.7) suggested that regulation of gene expression, rather than gene amplification, was going to be the more significant factor to be taken into consideration when analysing the cytological data. Optimising of conditions for the PFG experiments was therefore not proceeded with.

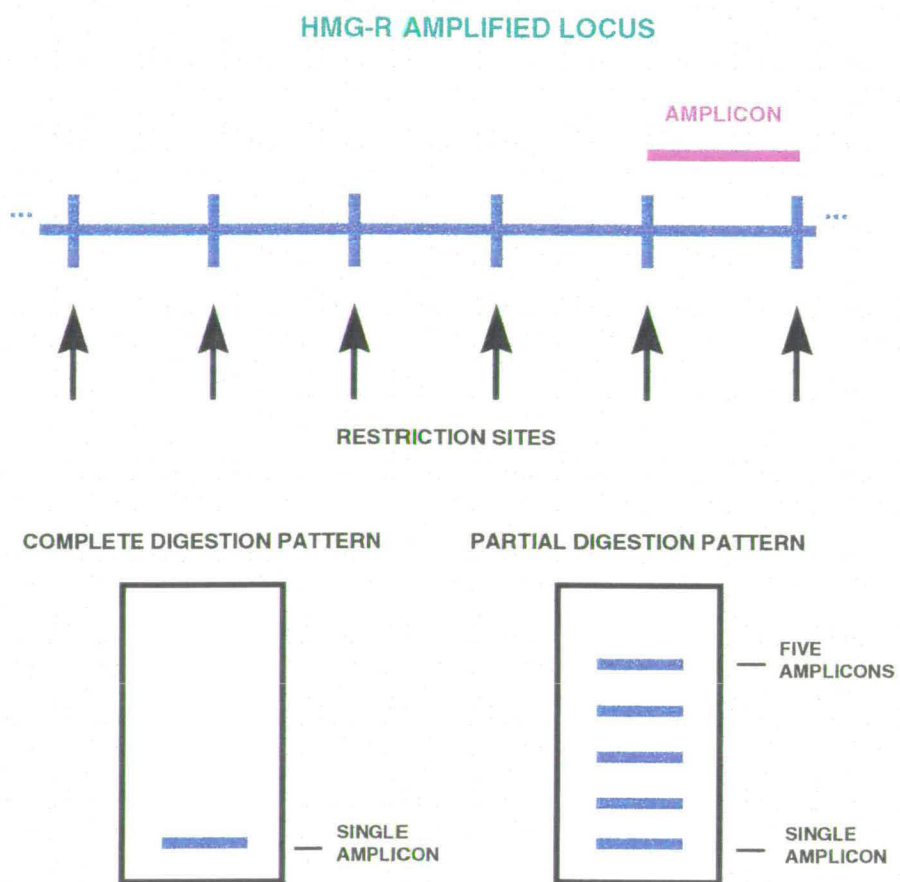


Figure 3.10

Experimental approach for pulse field gel analysis of HMG-R amplicon size.

See text for details.

3.5 Acetylation profile of UT-1 chromosomes

The acetylation profile of UT-1 chromosomes was determined by immunofluorescence, using an antibody specific for histone H4 acetylated at lysine 5 (R41, kindly donated by Brian Turner). The protocol for the immunofluorescence experiments is described in section 2.15.

3.5.1 Histone H4 acetylation profile

Metaphase chromosomes were labelled by immunofluorescence with the R41 antibody, to determine their acetylation profile. In addition to the R41 antibody, chromosomes were labelled with CREST sera to recognize the centromeres. Serum obtained from patients with scleroderma CREST contains antibodies to the centromeric proteins CENP-A, CENP-B, and CENP-C (Earnshaw & Rothfield 1985). The double labelling allowed the chromosomes to be identified with greater ease.

The acetylation profile of UT-1 chromosomes obtained with the R41 antibody is shown in figure 3.11, panel A. There is a banding pattern along the length of the chromosomes, reminiscent of R-banding. However, while most chromosomes were uniformly labelled by the antibody, one chromosome pair stood out, indicated by the arrows. The acetylation pattern of these chromosomes showed large regions of acetylation interrupted by large regions of underacetylation. This is reminiscent of the pattern observed by Jeppesen (Jeppesen & Turner 1993) in human metaphase chromosomes, where the inactive X is largely underacetylated. This distinctive pattern, specific to the chromosome pair, raised the possibility that the chromosomes may have rearranged on developing the UT-1 cell line, and that the large regions of underacetylated chromatin may have originated from the Chinese hamster inactive X.

In order to examine this hypothesis, CHO-K1 chromosomes were also immunolabelled with R41 and CREST sera, as shown in figure 3.11, panel B. Again, most chromosomes appeared to be uniformly acetylated, with the exception of one chromosome. This chromosome showed one arm to be

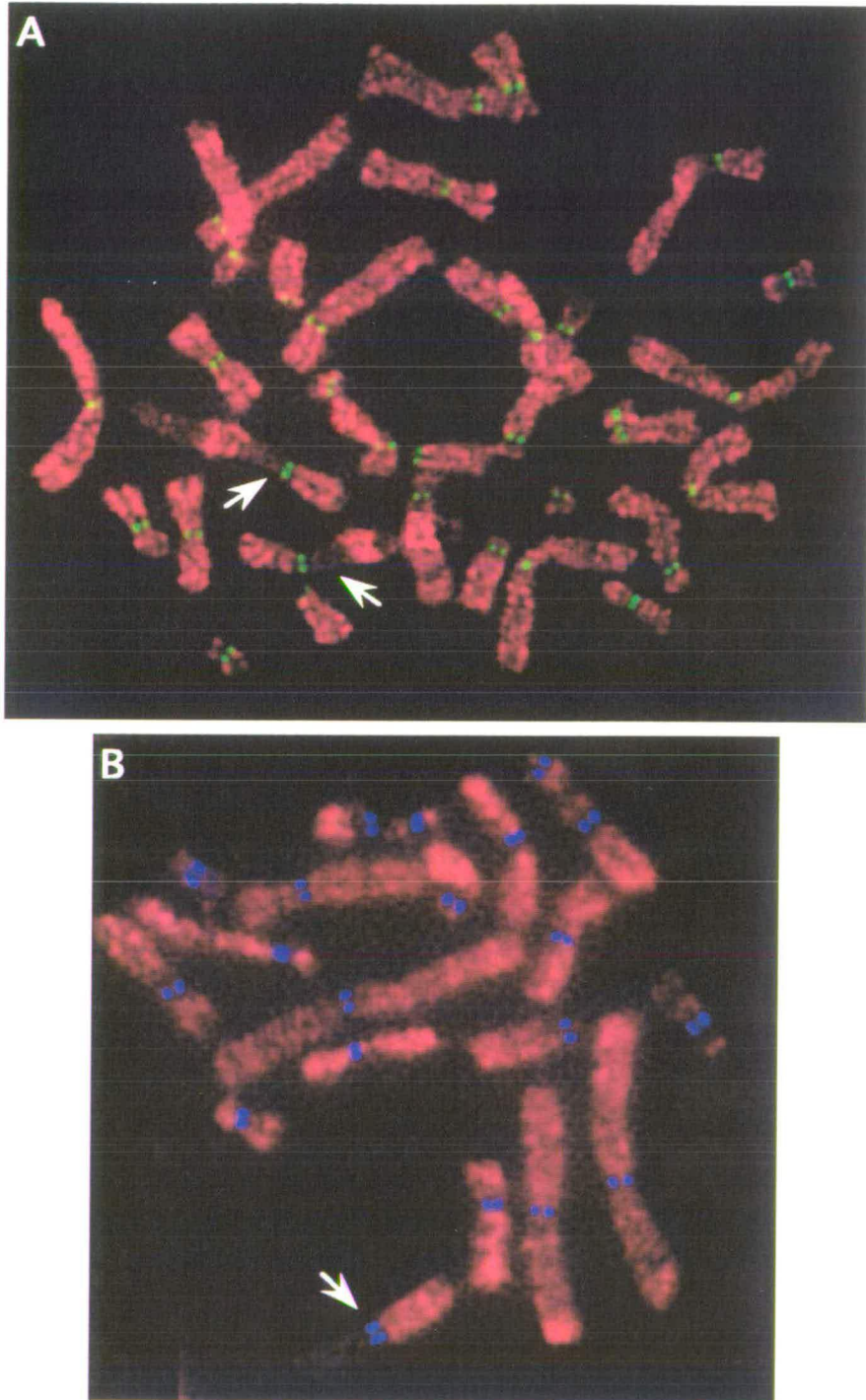


Figure 3.11

Acetylation profile of metaphase chromosomes determined by immunofluorescence.

A. Acetylation profile (red) and centromere localisation (green) of UT-1 chromosomes.
B. Acetylation profile (red) and centromere localisation (blue) of CHO-K1 chromosomes.
Arrows point to chromosomes containing large regions of underacetylated chromatin.

entirely underacetylated (indicated with an arrow). It is possible that the underacetylated X in the original Chinese hamster female rearranged to give rise to this chromosome in the CHO-K1 cell line, which in turn gave rise to the UT-1 chromosome with the unusual acetylation pattern. The Chinese hamster has an exceptionally large X chromosome, that has been produced as a result of duplication of the original X during the course of evolution (Ohno 1967). Thus, in addition to one entire X of the female being silenced, heterochromatinization spreads to the duplicated part of the 'active' X in both males and females. The large chromosomal regions of underacetylation seen in UT-1 and CHO-K1 chromosomes most likely derive from the original Chinese hamster inactive X, or the heterochromatinised portion of the active X. To test whether the underacetylated regions of the UT-1 and CHO-K1 chromosomes were derived from the original X chromosome, hybridisation with a Chinese hamster X paint was going to be carried out. Time did not allow completion of this experiment.

3.5.2 HMG-R locus relative to acetylation profile of UT-1 chromosomes

Localisation of the HMG-R locus, relative to the acetylation profile of the UT-1 chromosomes, was achieved in two steps. Metaphase chromosomes were initially immunolabelled with R41 (and CREST) to determine the acetylation profile. The HMG-R locus was subsequently identified by processing the slides through FISH, using biotin-labelled pRED227 to localise HMG-R.

The results are shown in figure 3.12, panel B. It was immediately noted that HMG-R was situated on the chromosome that had been previously noted for its unusual acetylation pattern. In addition, the gene appeared to lie close to the boundary between an underacetylated region and an acetylated region. The HMG-R locus was also mapped in the parental CHO-K1 chromosomes, to see whether it was situated on the CHO-K1 chromosome containing an underacetylated arm. Figure 3.12, panel A, shows that HMG-R is not located on this chromosome, but rather on chromosome 1. On creating the UT-1 cell line, it is possible that the CHO-K1 chromosome 1 rearranged with the

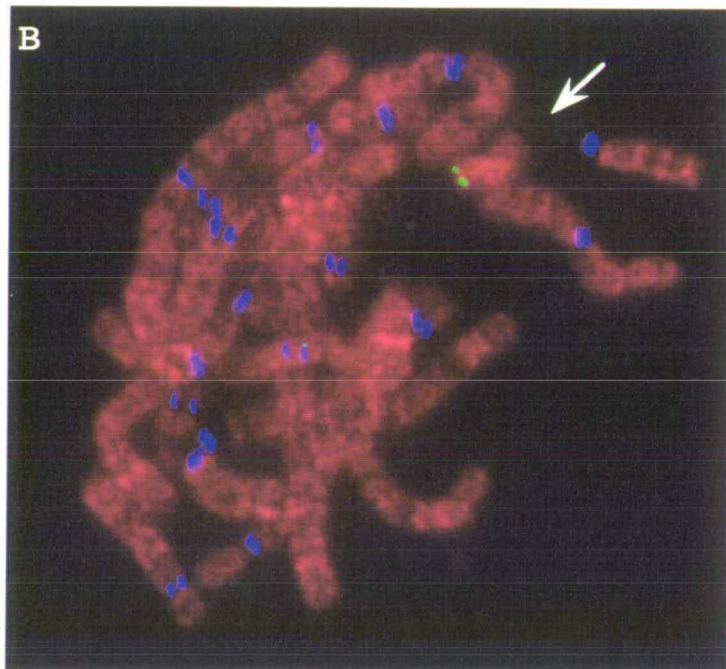
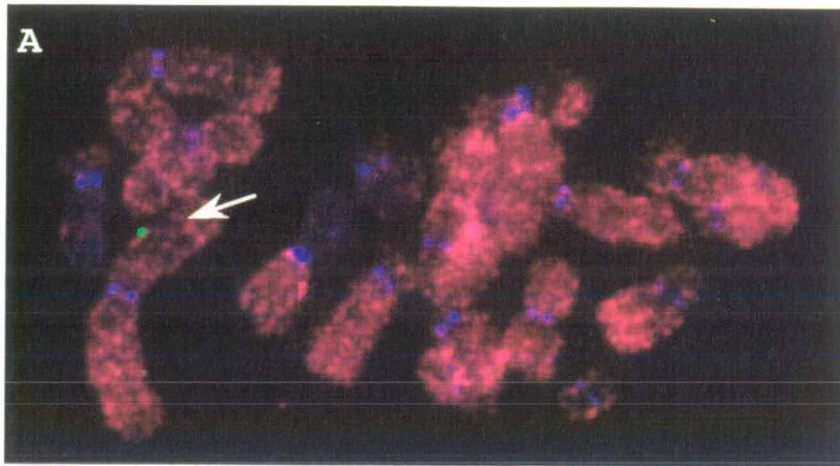


Figure 3.12
Localisation of HMG-R on metaphase chromosomes relative to their acetylation profile.
 Metaphase chromosomes have been labelled with anti-acetylated H4 (red) and CREST sera, showing the position of the centromere (blue), by immunofluorescence. HMG-R has been localised (indicated by arrow) with a biotin-labelled HMG-R cDNA probe (green) by FISH.
 A: CHO-K1 metaphase chromosomes
 B: UT-1 metaphase chromosomes

chromosome containing an underacetylated arm, thus bringing the HMG-R gene close to an underacetylated domain in UT-1 cells.

3.6 H4 acetylation at the HMG-R locus

The acetylation profile at the HMG-R locus was studied using a combination of immunofluorescence and FISH. The acetylation profile was initially determined by immunofluorescence, as described in the previous section, and the HMG-R locus was subsequently identified by FISH.

The aim of these experiments was to ascertain whether there was any variation in H4 acetylation at the HMG-R locus correlating with the gene's expression. Parallel experiments were therefore carried out using UT-1 cells grown in conditions where gene expression was induced or repressed, as detailed in Table 3.1 (section 3.2.3).

3.6.1 H4 acetylation profile - HMG-R induced

The acetylation profile was determined, with the R41 antibody, at the HMG-R locus for UT-1 cells grown in lipid-free medium and 0.010mM simvastatin. In these conditions the gene should be fully expressed.

Figure 3.13 shows the acetylation profile at the HMG-R locus, when the gene is expressed, in four different experiments. The gene locus, identified by the biotin-labelled pRED227 probe (and indicated by the arrows), was situated within acetylated chromatin, consistent with the gene's expressed state.

3.6.2 Acetylation profile - HMG-R repressed

The analysis was then carried out on metaphase chromosomes derived from UT-1 cells grown in regular medium, thus in presence of cholesterol, and in presence of excess cholesterol. In these conditions expression of HMG-R should be repressed.

Figure 3.15 shows the acetylation profile, obtained with the R41 antibody, at the HMG-R locus when the gene is repressed, in three different experiments. Again the gene locus appeared to lie within acetylated chromatin. At the resolution offered by the microscope, the acetylation pattern did not differ at the HMG-R locus when the gene was repressed and when gene expression was induced.

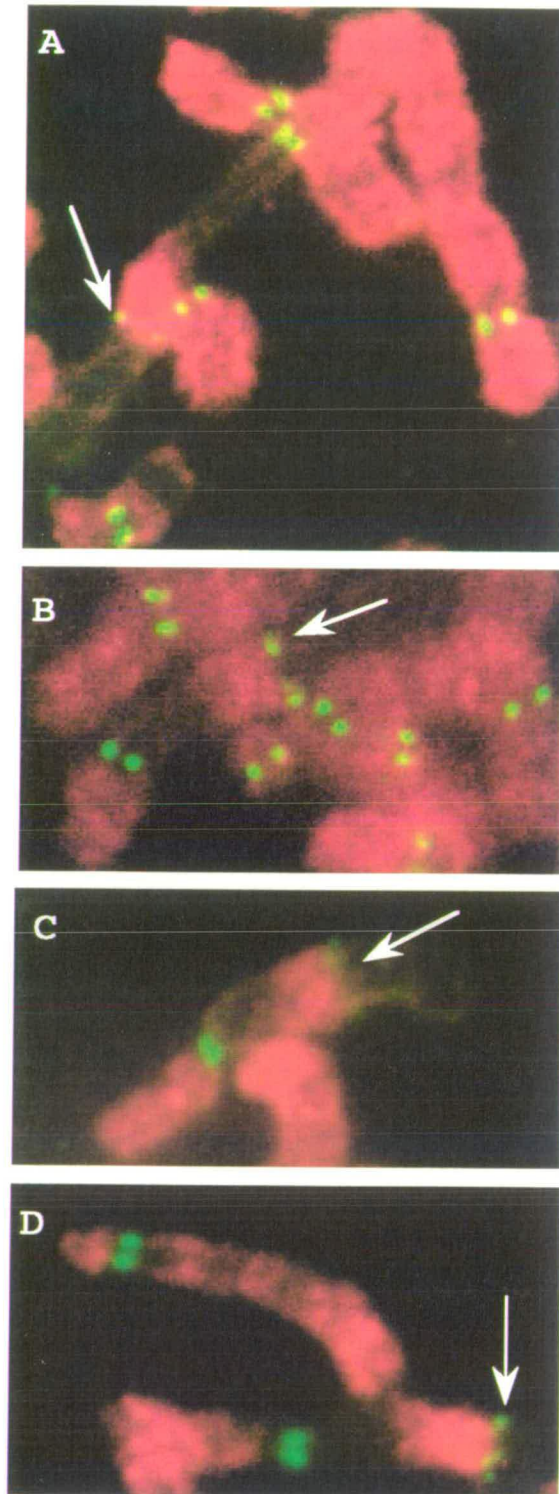


Figure 3.13

Acetylation profile at the HMG-R locus - HMG-R induced.

A, B, C, D. Metaphase chromosomes have been labelled with anti-acetylated H4 (red) and CREST sera, showing the position of the centromere (green), by immunofluorescence.

HMG-R has been localised (indicated by arrow) with a biotin-labelled HMG-R cDNA probe (green), by FISH.

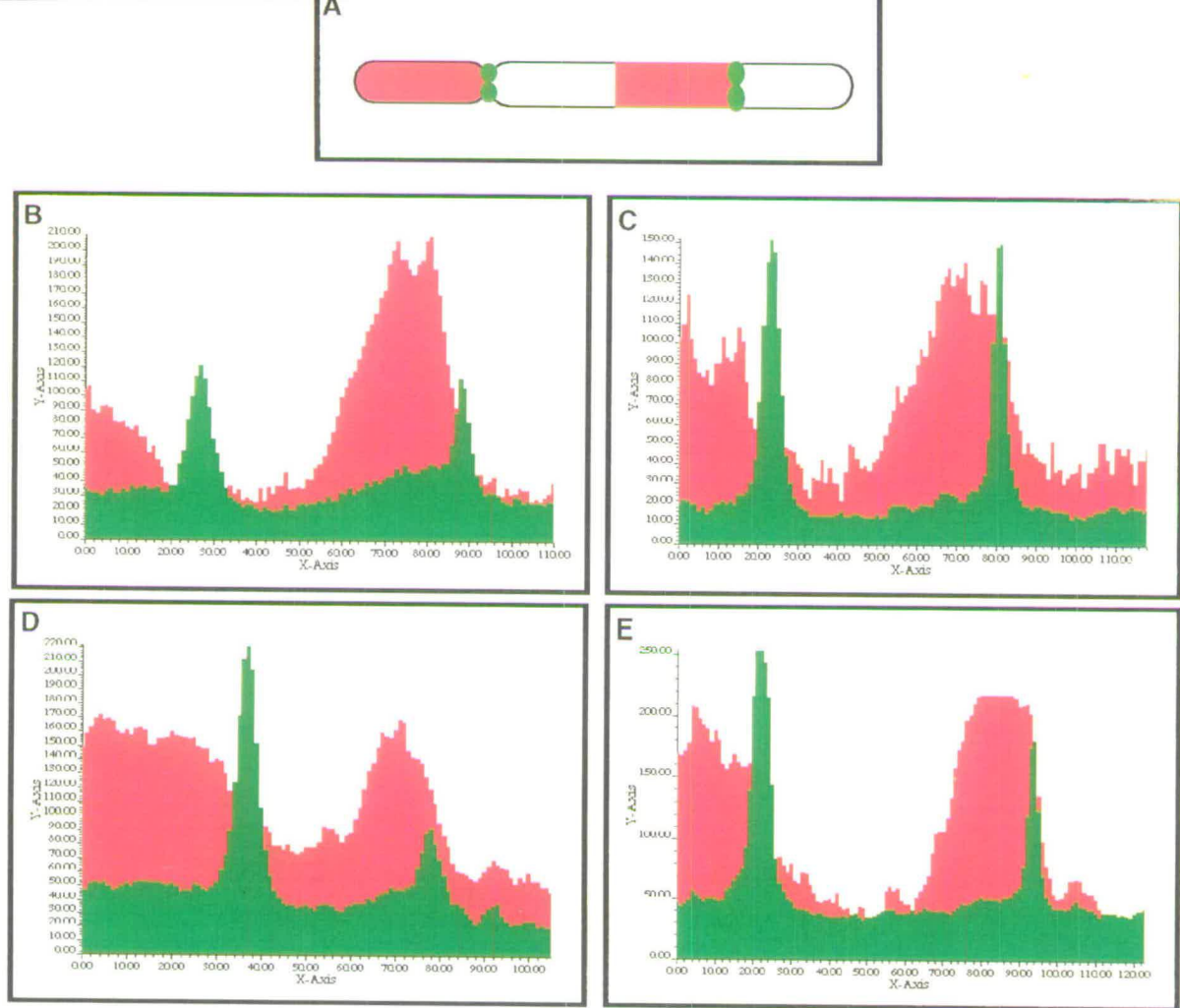


Figure 3.14

Quantification of fluorescence.

Quantification of fluorescence along chromosomes shown in figure 3.12.

A. Schematic representation of chromosome showing acetylation profile in red, and centromere and HMG-R locus in green.

Fluorescence graphs B, C, D, and E correspond to panels A, B, C, and D respectively in figure 3.12. Red peaks correspond to acetylated regions of the chromosome. Green peaks correspond to centromeric and HMG-R signals.

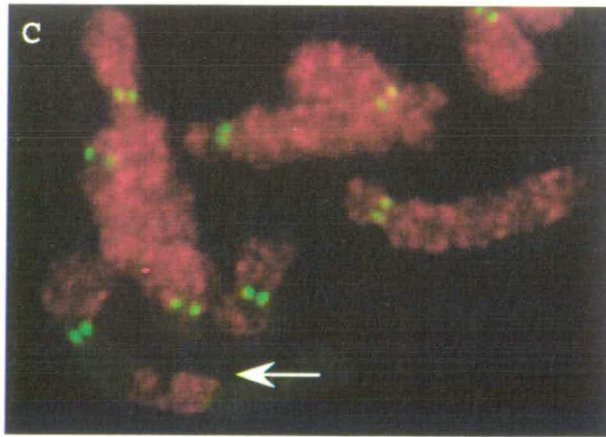
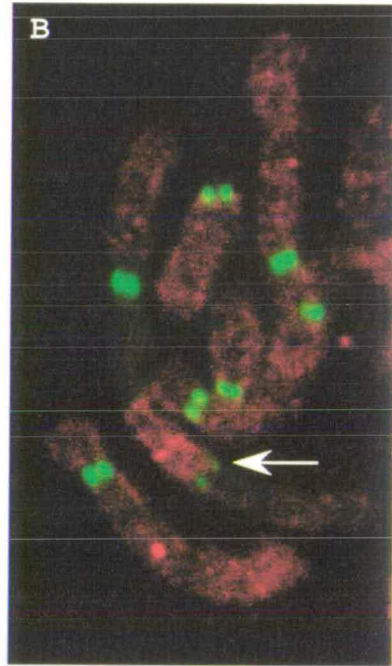
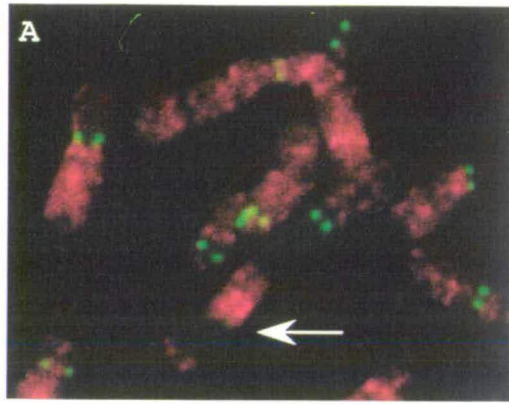


Figure 3.15

Acetylation profile at the HMG-R locus - HMG-R repressed.

A, B, C. Metaphase chromosomes have been labelled with anti-acetylated H4 (red) and CREST sera, showing the position of the centromere (green), by immunofluorescence.

HMG-R has been localised (indicated by arrow) with a biotin-labelled HMG-R cDNA probe (green), by FISH.

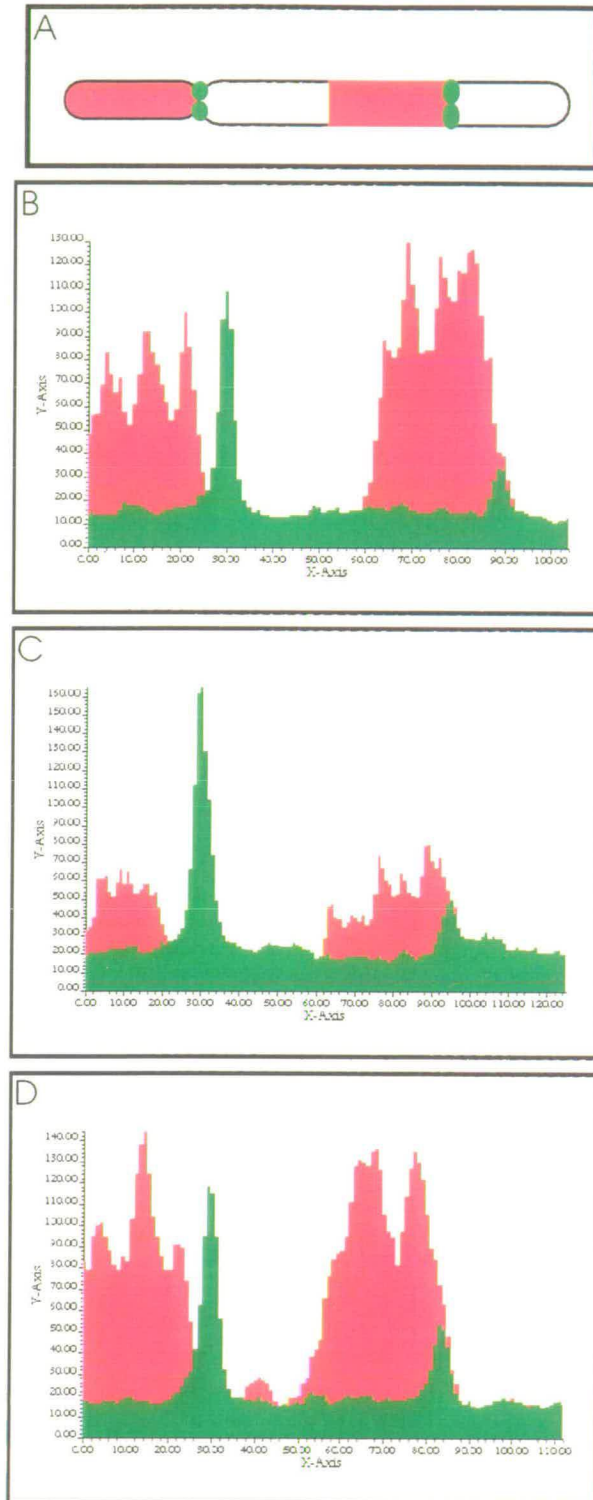


Figure 3.16

Quantification of fluorescence.

Quantification of fluorescence along chromosomes shown in figure 3.15.

A. Schematic representation of chromosome showing acetylation profile in red, and centromere and HMG-R locus in green.

Fluorescence graphs B, C, and D correspond to panels A, B, and C respectively in figure 3.15. Red peaks correspond to acetylated regions of the chromosome. Green peaks correspond to centromeric and HMG-R signals.

In order to evaluate this visual result, computer quantification of the level of acetylation at the HMG-R locus, relative to gene expression and repression, was carried out.

3.6.3 Quantification of fluorescence

The fluorescence profile obtained with the R41 antibody was quantified, using IPLab Spectrum software, by 'drawing' a line down the length of the relevant chromosome, and quantifying the fluorescence at each point along that line. The computer program obtained values for the fluorescence at each point along the imaginary line, and plotted these values on a graph.

The values obtained for each of the chromosomes shown in figures 3.13 and 3.15 are respectively shown in figures 3.14 and 3.16. The analysis confirmed that there was no significant difference between acetylation profiles at the HMG-R gene locus, when UT-1 cells were grown under inducing or repressing conditions for HMG-R expression.

3.6.4 Initial conclusions

The combined immunofluorescence and FISH data indicated that no distinction could be made between the acetylation profiles at the HMG-R locus, in relation to gene expression.

It was unclear, however, whether this result was a true reflection of the system that had been tested. Several points needed to be addressed before confirming the validity of the results obtained using the cytological approach. It is possible that no dramatic change in acetylation levels occurs at the HMG-R locus in association with changes in expression. This would correlate with Crane-Robinson's immunoprecipitation data, focusing on the acetylation status of the inducible PDGF-B gene in a human cell line (section 1.5.2). PDGF-B was shown to be enriched in acetylated histone H4 both before and after cell differentiation, which induces the gene's expression, indicating that acetylation was not associated with gene transcription *per se*, but rather with the potential for transcription (Clayton *et al* 1993).

It could also be that the resolution of this system is not sufficient to detect any change in the degree of acetylation, if it occurs. While it had been confirmed that HMG-R was amplified 12-15 fold in the UT-1 cells, the lack of information regarding the size of the amplicon left some doubt as to whether the system was resolvable at a cytological level.

In order to verify that no alteration in the UT-1 cells had occurred as a result of extensive passaging, the combined immunolabelling/FISH analysis of the acetylation profile at the HMG-R locus was repeated with earlier passages of UT-1 cells. These were freshly removed from liquid nitrogen, where they had been placed on arrival into the lab from the ETCC, and were therefore virtually the same cells that had been originally placed in the ETCC by Goldstein and colleagues.

The immunolabelling data obtained using these cells did not vary from that obtained from cells that had been passaged for longer. Figure 3.17 shows the acetylation profile at the HMG-R locus, when the gene is expressed (panel A) and repressed (panel B). Again, the acetylation profile at the HMG-R locus did not vary in relation to gene expression or repression. Quantification of the fluorescence confirmed this, as shown in figures 3.18 and 3.19.

Most importantly, it was necessary to address the possibility that regulation of HMG-R expression did not respond to the levels of cholesterol in the medium ie. that the gene was not induced in absence of cholesterol, or alternatively, not repressed in its presence. This was accomplished by the series of experiments described in the next section.

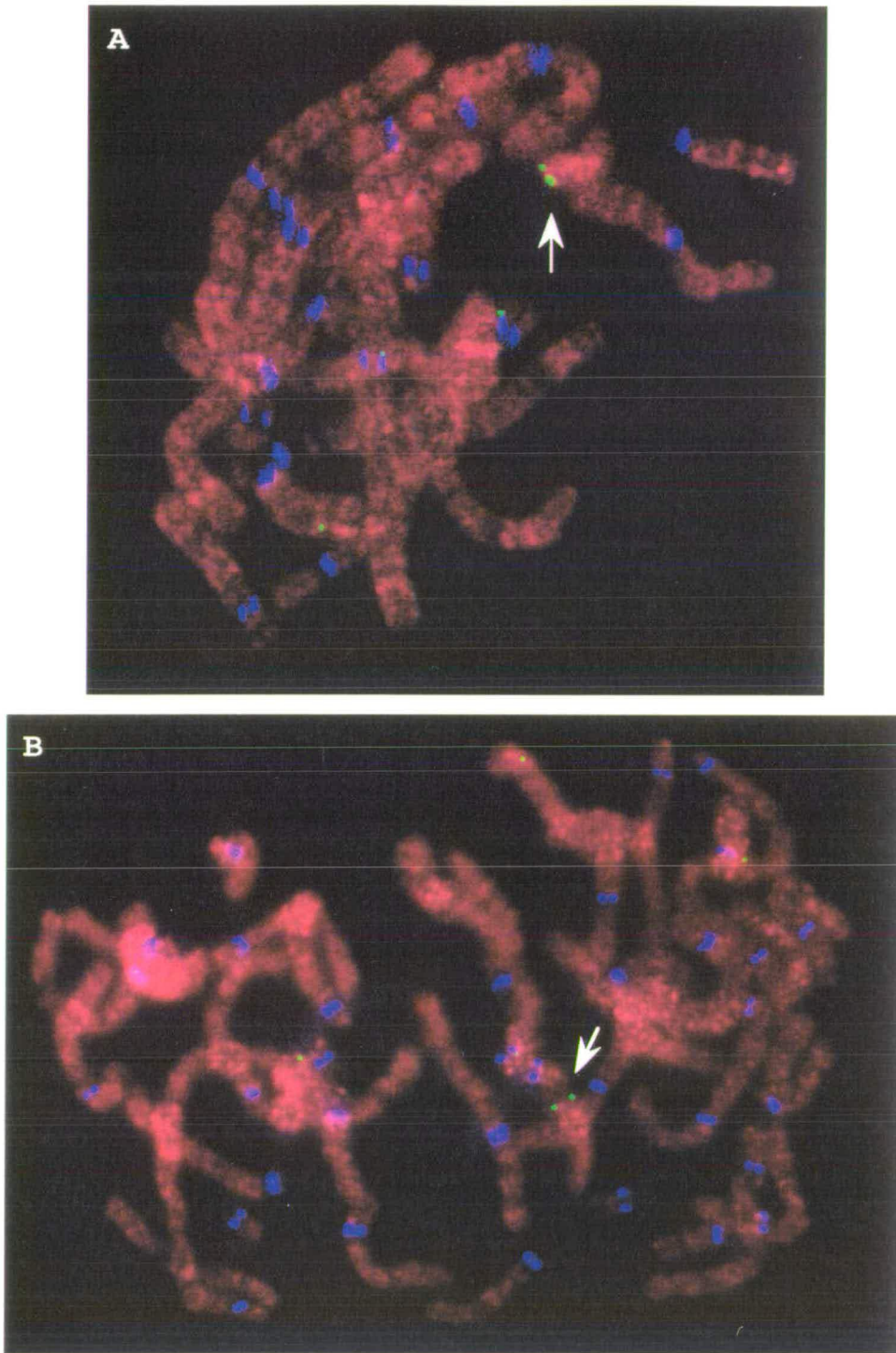


Figure 3.17

Acetylation profile at the HMG-R locus in early-passage UT-1 cells.

Metaphase chromosomes have been labelled with anti-acetylated H4 (red) and CREST sera, showing the position of the centromere (blue), by immunofluorescence.

HMG-R has been localised (indicated by arrow) with a biotin-labelled HMG-R cDNA probe (green), by FISH.

A. HMG-R expression is induced.

B. HMG-R expression is repressed.

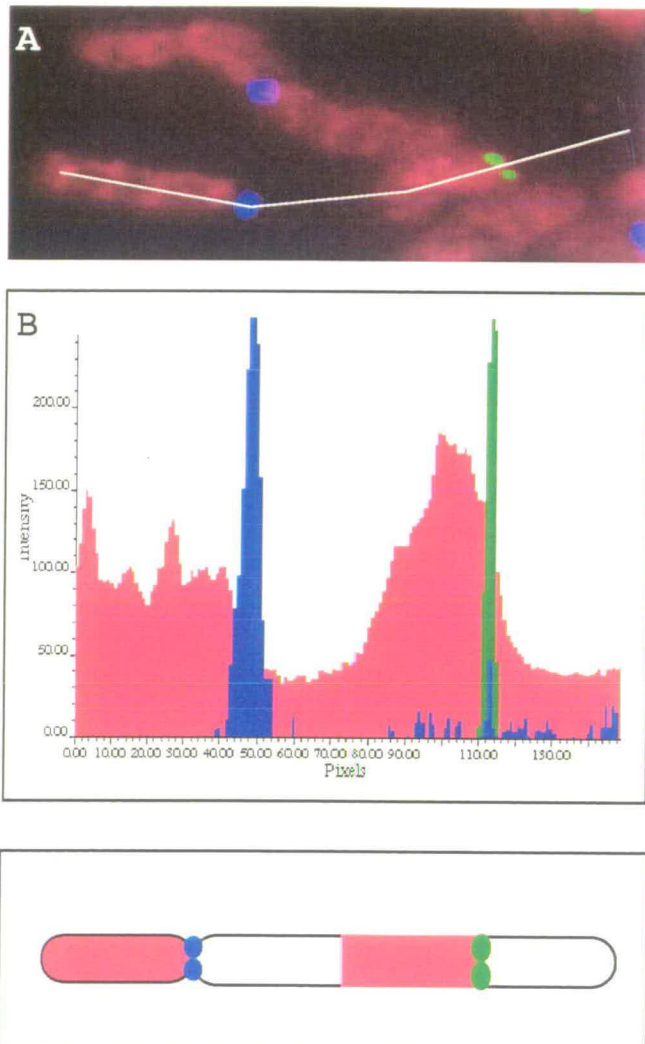


Figure 3.18

Quantification of fluorescence - HMG-R induced.

Quantification of fluorescence along chromosome shown in figure 3.17 (panel A) shown again here in panel A.

B. Red peaks correspond to acetylated regions of the chromosome. Blue peak corresponds to centromere and green peak corresponds to HMG-R signal.

C. Schematic representation of chromosome showing acetylation profile in red, centromere in blue, and HMG-R locus in green.

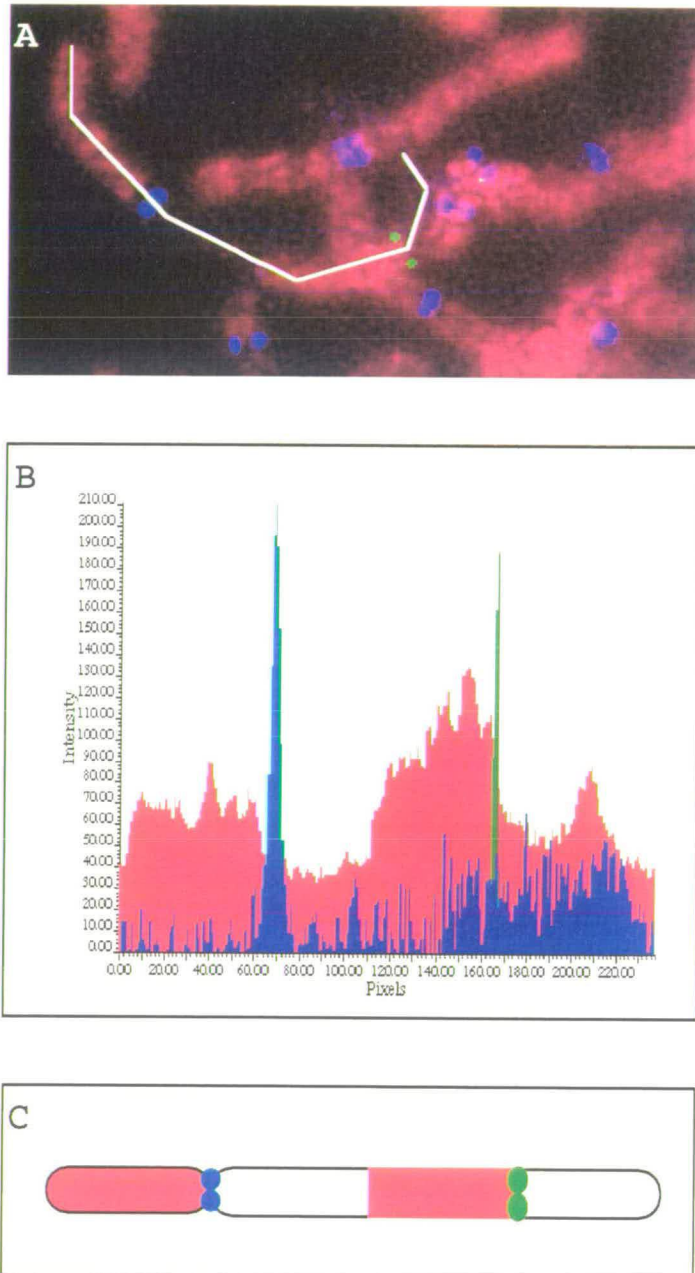


Figure 3.19

Quantification of fluorescence - HMG-R repressed.

Quantification of fluorescence along chromosome shown in figure 3.17 (panel B) shown again here in panel A.

B. Red peaks correspond to acetylated regions of the chromosome. Blue peak corresponds to centromere and green peak corresponds to HMG-R signal.

C. Schematic representation of chromosome showing acetylation profile in red, centromere in blue, and HMG-R locus in green.

3.7 Regulation of HMG-R expression

Given the unforeseen results obtained with the combined immunofluorescence and FISH analysis of H4 acetylation at the HMG-R locus, it was necessary to investigate the regulation of HMG-R expression in more detail in the UT-1 cells.

3.7.1 Northern analysis

The regulation of HMG-R expression in UT-1 cells was examined by Northern analysis. The level of HMG-R expression was determined in cells grown in conditions where expression of the gene was induced or repressed. RNA was isolated from cells using different protocols and electrophoresed on a formaldehyde/agarose gel. The gel was subsequently blotted, and the blot was hybridised with radiolabelled pRED227, containing the cDNA sequence for HMG-R. Figure 3.20, panel A, shows the result. To ensure equal amounts of RNA had been loaded in all lanes, the blot was also hybridised with Chinese hamster CENP-B, as shown in Fig 3.20, panel B.

Expression of HMG-R in UT-1 cells had been reported in the literature to be increased by 100-1000 fold on induction of the gene. The Northern results demonstrated that expression of HMG-R in the UT-1 cells did not increase to the same level following induction with lipid-free medium (lane 5). More importantly, it appeared that in conditions where the gene was supposed to be repressed, transcription was still taking place, even in the presence of excess cholesterol (lanes 3 and 4). Quantification of the bands by PhosphorImager analysis confirmed that the difference in expression between induced and repressed HMG-R was only 2-5 fold.

To confirm the validity of the result obtained by Northern analysis, expression levels of HMG-R were quantified by an alternative method for detection and analysis of gene expression, reverse transcription-polymerase chain reaction (RT-PCR).

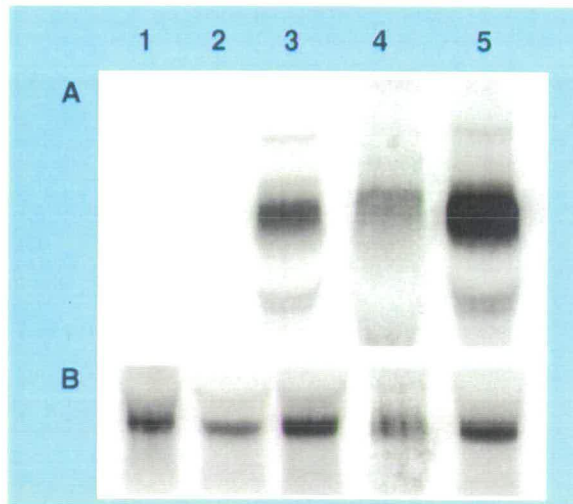


Figure 3.20

Northern analysis of HMG-R expression in CHO-K1 and UT-1 cells.

Lane 1 - CHO-K1 RNA - HMG-R OFF

Lane 2 - CHO-K1 RNA - HMG-R OFF - excess cholesterol

Lane 3 - UT-1 RNA - HMG-R OFF

Lane 4 - UT-1 RNA - HMG-R OFF - excess cholesterol

Lane 5 - UT-1 RNA - HMG-R ON - + simvastatin

Total RNA from CHO-K1 and UT-1 cells was electrophoresed on an agarose/formaldehyde gel. The gel was blotted, and hybridised with radiolabelled HMG-R cDNA (panel A) and CENP-B cDNA (panel B) as an internal loading control. quantification of the signal was determined by Phosphorimager analysis.

3.7.2 RT-PCR analysis

PCR is a highly sensitive system for the amplification of DNA. The reaction repeatedly synthesizes new strands of DNA by exponential amplification in the 5'→3' direction of a defined region of the starting template. The single-stranded template is obtained by denaturing double-stranded DNA. The reaction employs two primers, each complementary to opposite DNA strands of the region of interest. By repeated cycles of heating and cooling (to suit the annealing properties of the primer and the optimal temperature of the *Taq* DNA polymerase enzyme activity) the newly synthesized DNA accumulates in an exponential fashion until any one of the substrates or the enzyme is depleted. Figure 3.21 shows a typical curve of the kinetic progression of an amplification reaction.

The advantages of PCR can be exploited for the detection and quantification of gene expression, as RNA can be converted into cDNA by *in vitro* reverse transcription. The resulting cDNA can subsequently be subjected to PCR amplification. An endogenously expressed RNA, amplified alongside the RNA of interest, can be used as an internal control, thus allowing normalization of amounts of amplified product from the starting RNA. In this way, RT-PCR can be used to quantitatively assay gene expression, by measuring comparative values of gene expression relative to a constant internal standard.

Expression levels of the HMG-R gene were studied by RT-PCR, in UT-1 cells grown in conditions repressing and inducing HMG-R transcription. In these series of experiments, total RNA isolated from the cells was reverse-transcribed to produce cDNA. The cDNA served as the template for a PCR experiment using a set of primers designed to give rise to a 300bp product encoding the 5' end of the HMG-R cDNA. Figure 3.4 shows the position of the primers within the HMG-R cDNA sequence. Also included in the PCR experiments were a second set of primers, designed to give a 100bp product distinguishable from the HMG-R 300bp product on an agarose gel. This second product served as the internal loading control for the amount of template present in each reaction, so as to allow quantification of samples

across experiments. Different loading controls were used in the series of experiments, but conditions were optimised using primers specific for the mouse S16 ribosomal protein and the mouse synaptonemal complex SCP3 protein, which were able to amplify the Chinese hamster homologue. It was thought that both would be transcribed at equal levels across all cell types.

Figure 3.22 demonstrates the results obtained by RT-PCR.

The most striking observation was that in conditions repressing HMG-R expression, transcription was definitely taking place. In lanes 1 and 3, cells had been grown in regular medium, when cholesterol present in the foetal calf serum was thought to be sufficient to repress HMG-R transcription. On addition of excess cholesterol, transcription appeared to be reduced slightly (lanes 2 and 4), but was still significant. In addition, it was only approximately doubled in UT-1 cells grown in lipid-free medium, in the presence of simvastatin, when expression of the gene should be maximal. In the literature, the difference in transcription between induced and repressed states had been reported to be 100-1000 fold.

A possible explanation for this result lies in the kinetics of the PCR reaction. Quantitative analysis of RNA levels is based on an estimation of the starting amount of the RNA of interest, by measuring the corresponding amplified products. But this quantification is only valid if there is a direct correlation between the template and the amplification products. This estimation can thus only be performed during the exponential phase of the PCR amplification, before saturation of the reaction takes place (see figure 3.22). This was accomplished by modifying the RT-PCR reaction to allow quantification of HMG-R expression.

3.7.3 Quantitative RT-PCR analysis

In the following experiments, the kinetics of the amplification reaction was monitored by taking sample aliquots at regular intervals (every 5 cycles from cycle 5 to cycle 40) from the reaction. Detection and quantification of the amplification products was performed by agarose gel electrophoresis of the PCR samples, Southern blotting and hybridisation of the blot with

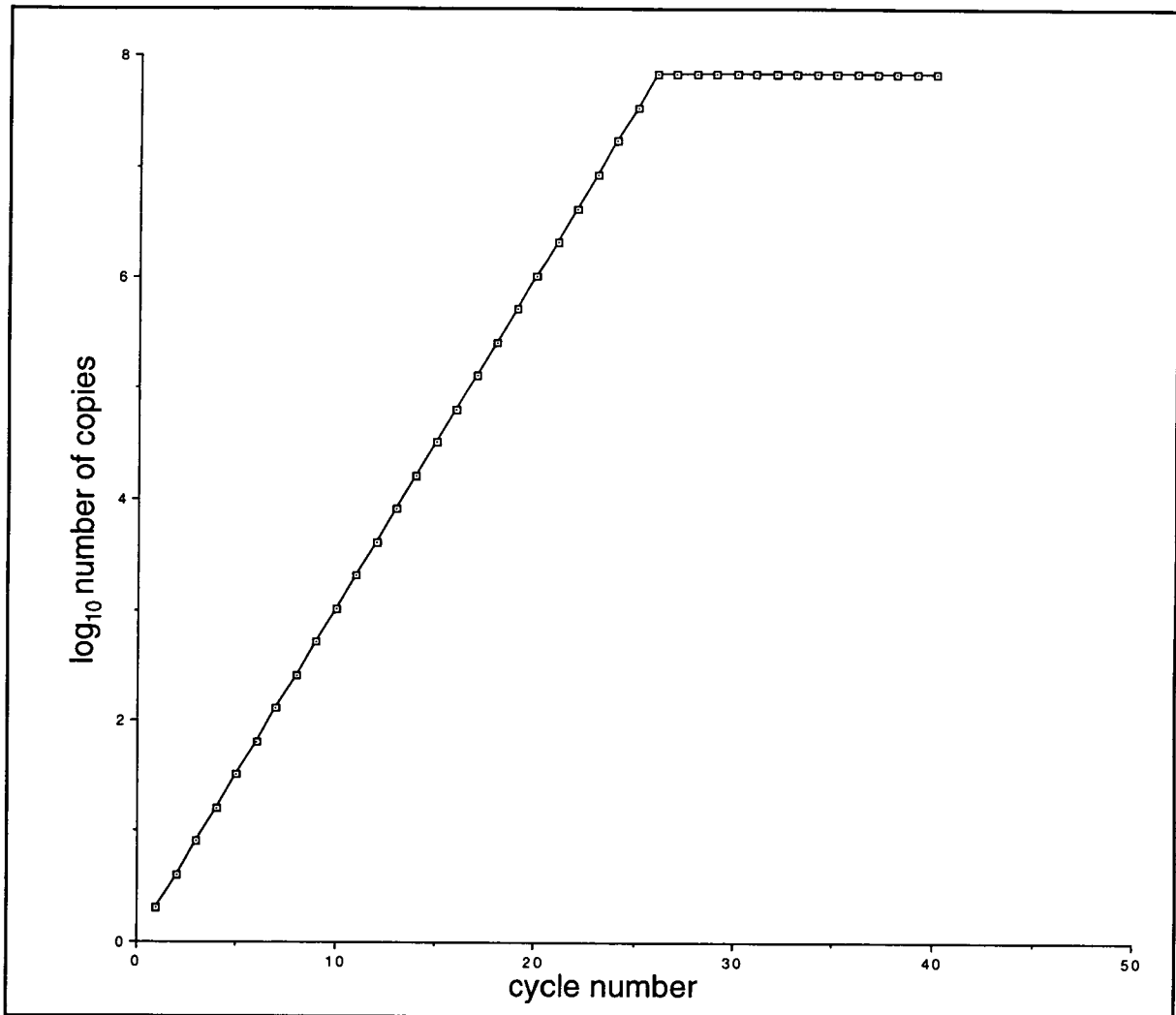


Figure 3.21

Theoretical kinetics of the amplification reaction.

Representation of the theoretical kinetics of an amplification reaction, assuming the amplification begins from one molecule of template. As the amount of template increases with each cycle of amplification, the reaction components (dNTPs and the Taq polymerase enzyme) become saturated. Once these components are completely saturated, no further amplification occurs.

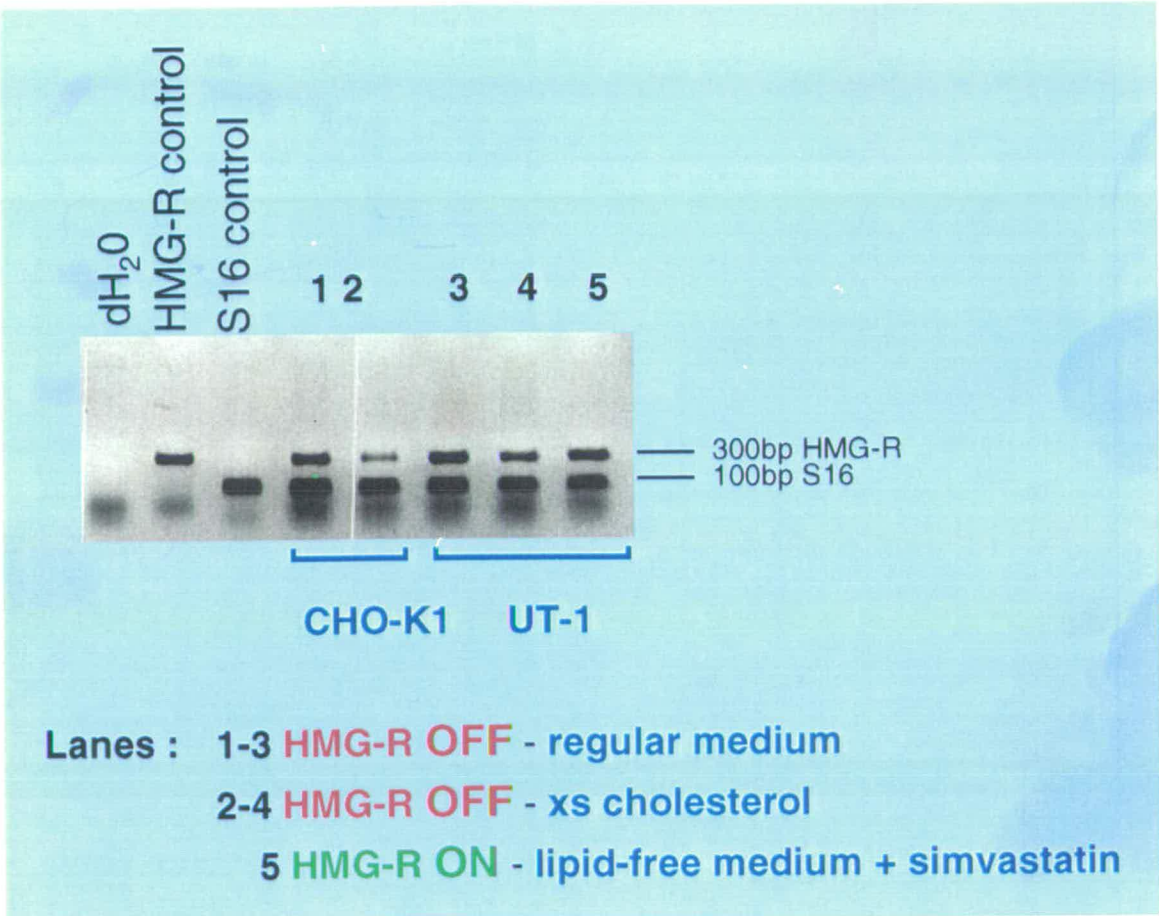


Figure 3.22

RT-PCR experiment.

RT-PCR was used to determine the expression levels of HMG-R in CHO and UT-1 cells grown in selective media. A 300bp HMG-R product was amplified from cDNA derived from the cells, and a 100bp S-16 product was amplified as an internal loading control.

See text for details.

radiolabelled oligonucleotide probes specific for the HMG-R and S16 PCR products. Analysis and quantification of the radioactive signal was performed by PhosphorImager analysis (Molecular Dynamics).

Figures 3.23 and 3.24 show the amplification kinetics of the RT-PCR assay performed on RNA obtained from CHO-K1 and UT-1 cell lines, grown in conditions where HMG-R expression was induced or repressed. HMG-R amplification was first seen at cycle 15 in the UT-1 cell line. In conditions where gene expression was induced (panel E), amplification was found to be 2-3 fold greater, by PhosphorImager analysis, than when expression was repressed (panels C and D). Figure 3.24 shows this result in graph form.

Thus, RT-PCR analysis of the regulation of gene expression confirmed the data obtained by Northern analysis. HMG-R transcription was taking place in repressing conditions, and, following induction, there was at most a 3-fold increase in gene expression over the basal non-induced level.

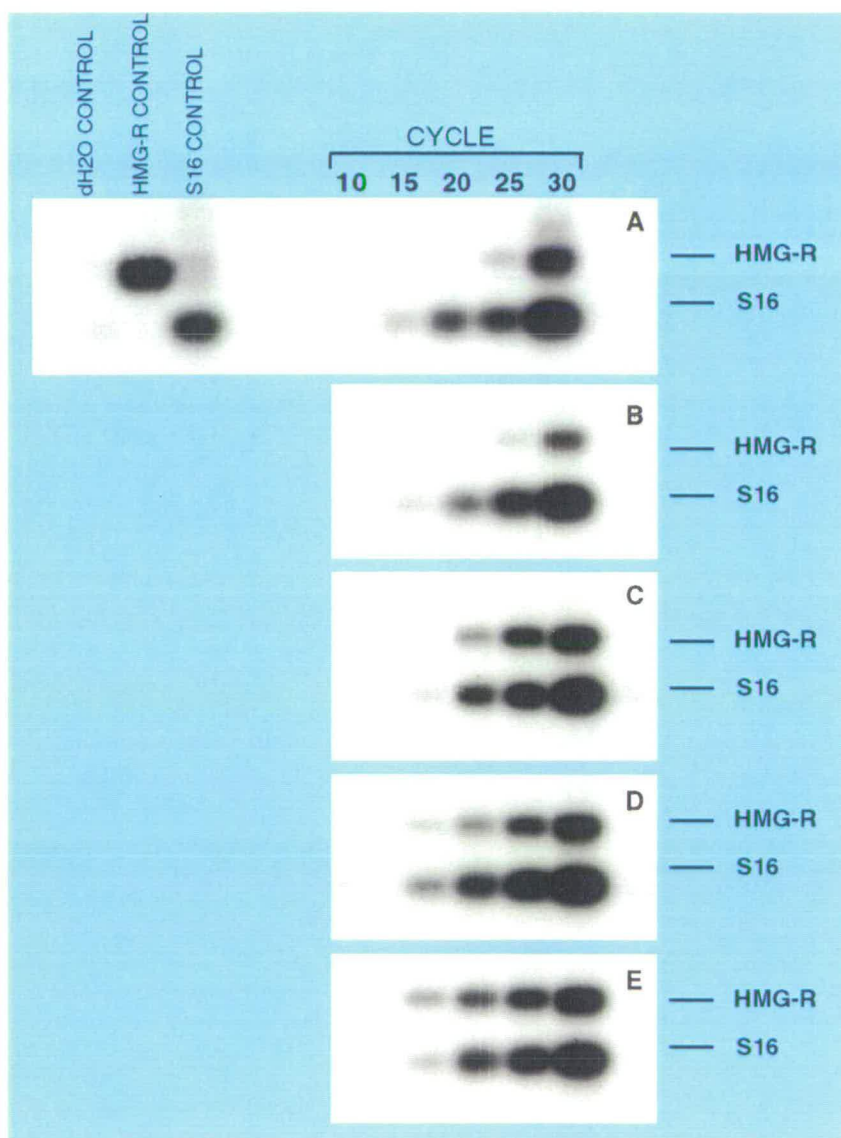


Figure 3.23

Quantitative RT-PCR experiment.

- A. CHO-K1 cDNA - HMG-R OFF
- B. CHO-K1 cDNA - HMG-R OFF - excess cholesterol
- C. UT-1 cDNA - HMG-R OFF
- D. UT-1 cDNA - HMG-R OFF - excess cholesterol
- E. UT-1 cDNA - HMG-R ON - + simvastatin

Amplification of 300bp HMG-R product and 100bp S16 product for internal control. Aliquots were taken every 5 cycles between cycles 10-30. Amplification products were electrophoresed on an agarose gel, southern blotted, and hybridised with radiolabelled oligonucleotide probes for HMG-R and S-16. Quantification of the signal was determined by PhosphorImager analysis.

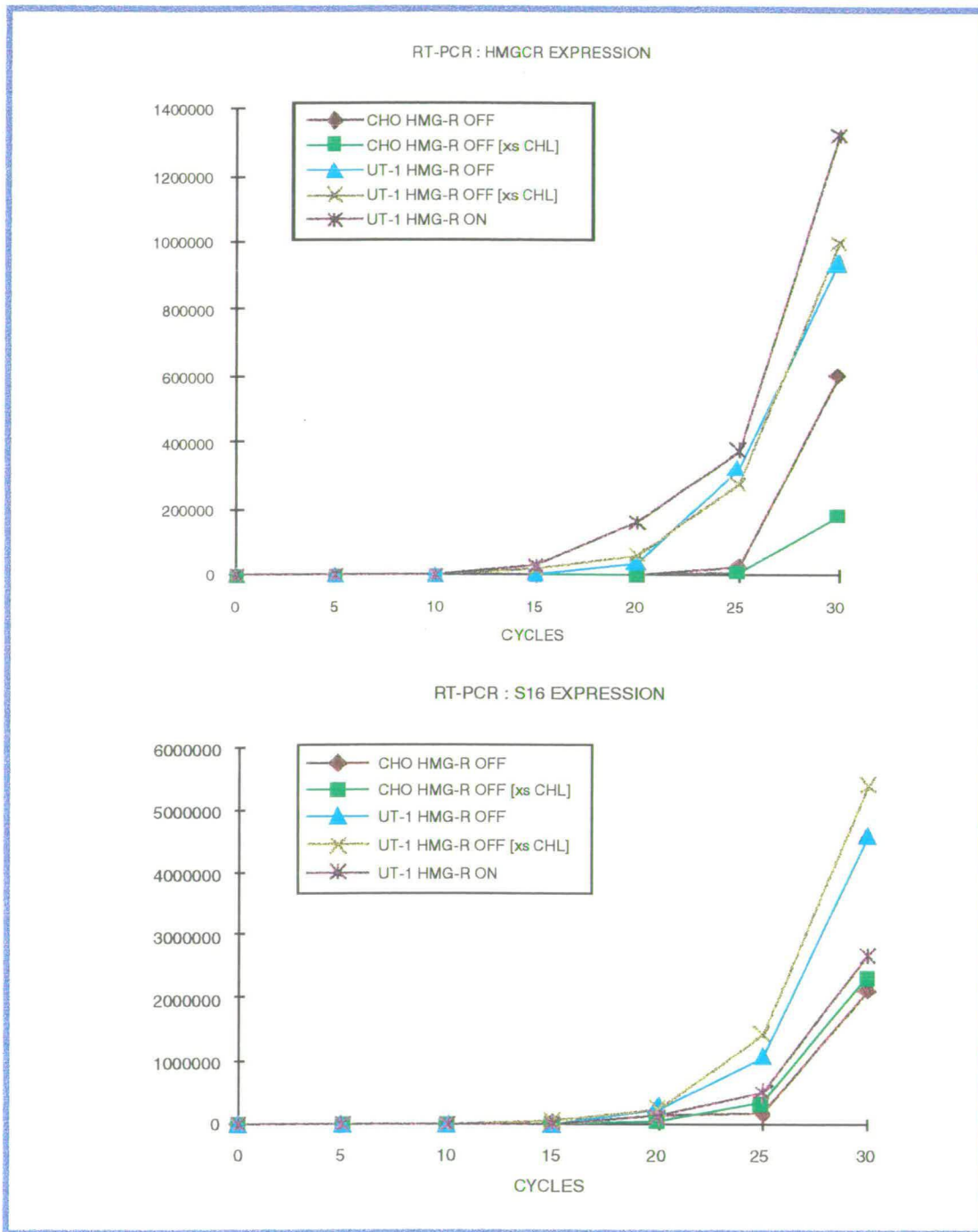


Figure 3.24

Kinetics of RT-PCR amplification shown in Figure 3.23.

Densitometric values for HMG-R and S-16 amplification for sample aliquots were determined by PhosphorImager analysis, and plotted on a graph.

3.8 Discussion

3.8.1 Analysis of results

This study was aimed at monitoring changes in histone H4 acetylation in response to different levels of transcriptional activity of an inducible gene. The distribution of histone acetylation was detected by an *in situ* immunolabelling approach, using an antibody which binds preferentially to histone H4 acetylated at lysine 5. The location of the amplified gene locus was identified by *in situ* hybridisation.

The initial data obtained by this approach suggested that no distinction could be made between the degree of histone H4 acetylation at the HMG-R locus when cells were grown under conditions inducing HMG-R expression, compared to cells in which HMG-R should be repressed. In both instances, the gene was contained within an acetylated H4 domain.

Subsequent examination of the regulation of HMG-R expression, by Northern blotting and quantitative RT-PCR analysis (section 3.7), indicated that transcriptional activity did not increase to a great extent in response to gene induction. On growing UT-1 cells in conditions where HMG-R expression should be repressed, transcription of the gene occurred at a basal, readily detectable level. In conditions where HMG-R expression should be induced, the increase in transcriptional activity, relative to the basal level, was 3-fold at the most.

The aim of the experiment was to study variation in histone acetylation that might accompany large changes in gene transcription. Thus, the subtle difference in transcriptional activity observed between the gene 'on' and the gene 'off' compromised the experimental approach. It was unlikely that a distinction in the degree of histone H4 acetylation could be made if the level of transcription varied to such a small degree as a result of gene induction.

On creating the UT-1 cell line, Brown and Goldstein's data showed that the enzymatic activity of the HMG-R gene was increased by 100-1000 fold following removal of lipids from cell culture medium (Chin *et al* 1982). This clearly did not occur during the course of this study. There are a number of

possible explanations for the observed discrepancy with Brown and Goldstein's data concerning regulation of HMG-R transcription.

The history of the UT-1 cell line prior to its deposition in the European Type Culture Collection is unclear. No information exists regarding the length of time the cells were passaged prior to their deposition, and thus whether they were passaged at any stage in absence of the competitive inhibitor of HMG-R. It is possible that loss of HMG-R amplification occurred prior to the cells' deposition, as a result of extended passaging. HMG-R amplification was reported by Brown and Goldstein to be 15-fold in UT-1 cells (Luskey *et al* 1983). Verification of this, by Southern analysis (section 3.6), concluded that the UT-1 cells I was passaging had a 12-15 fold amplification of the HMG-R gene, as determined by PhosphorImager analysis. Thus it is possible that one or two copies of the gene had been lost. With this in mind, it is not known whether the 100-1000 fold increase in transcription activity observed by Brown and Goldstein was the result of elevated transcription in all 15 copies of the gene, resulting in a sum total of a 100-1000 fold increase in expression, or whether some copies transcribed at highly increased levels whereas others transcribed at a basal level. In the latter case, it is possible that those copies of the gene transcribing at high levels had been lost during passaging, resulting in gene amplification but only a basal level of gene transcription. How this basal level of HMG-R transcription in UT-1 cells was still sufficient to confer increased resistance to simvastatin, relative to that of the parental CHO-K1 cells (section 3.2), is unclear. The increased resistance to simvastatin is only 4-fold, which, if a direct comparison between the two inhibitors can be made, is lower than the reported 100-fold increase to compactin (Chin *et al* 1982).

Given that HMG-R is a housekeeping gene, it is not surprising to find that a low level of transcription was maintained at all times. This is consistent with the transcription pattern of many house-keeping genes. The GC-rich promoter sequence of HMG-R, however, does differ from that of many house-keeping genes, in that it lacks a characteristic TATA and CCAAT box, required for accurate initiation of transcription. This is thought to be typical of

genes whose transcription is under the control of feedback regulation (Reynolds *et al* 1984). Thus it seems most likely that appropriate induction, rather than complete suppression, of HMG-R transcription was not occurring in the UT-1 cell line. In addition to loss of gene amplification, discussed earlier, this may have been due to inadequate delipidisation of the foetal calf serum used in the lipid-free medium required for growing the cells in HMG-R-inducing conditions. Any cholesterol still present in the medium might have been sufficient to repress gene induction. The presence of simvastatin should however have been sufficient to counter this effect. Unfortunately, the only way to test for quantities of cholesterol present in the medium was by means of a chromatographic assay, which was not undertaken.

Perhaps the most likely explanation for the loss of HMG-R regulation in the UT-1 cells can be found in the location the gene occupies. HMG-R was mapped by FISH to the boundary between an acetylated and an underacetylated domain. It is possible that the heterochromatic nature of the neighbouring underacetylated region may have affected the transcriptional activity of the gene, in a manner reminiscent of the position-effect variegation phenomenon found in *Drosophila*. In this case, the repressive characteristics of underacetylated chromatin may have spread to the HMG-R gene locus, inhibiting appropriate gene induction in the absence of cholesterol, and possibly decreasing the cells' resistance to simvastatin.

3.8.2 A role for histone acetylation?

Crane-Robinson's immunoprecipitation data showed that both active and 'poised' genes (genes with the potential to be transcribed in a particular cell) are found in acetylated chromatin. Thus, if genes are found within acetylated chromatin prior to the onset of their transcription, acetylation of histones can be considered to be a pre-condition for transcriptional activity.

Crane-Robinson's analysis of the acetylation status of the inducible gene, PDGF-B, by immunoprecipitation, showed that PDGF-B was contained within acetylated chromatin prior to induction, and the acetylation level did not change following induction (Clayton *et al* 1993). To a certain extent,

parallels can be drawn between the PDGF-B and HMG-R genes, suggesting that, had the change in transcriptional activity of the HMG-R gene following induction been significant, it is likely that the gene would have been found associated with acetylated H4 both before and after gene induction. Having said this, the aim of the project was to see if subtle differences in acetylation, not detectable by immunoprecipitation, could be observed by immunofluorescence.

Roles for histone acetylation may include that suggested by Jeppesen (Jeppesen 1997), whereby acetylation serves to propagate cell memory by 'marking' those chromosomal domains committed to gene expression, from generation to generation. Alternatively, it may serve to mark imprinted regions of the genome, distinguishing paternal and maternal homologues, and contributing towards their different replication times (Bickmore & Carothers 1995).

More importantly, the recent discovery of HAT activities in transcription factor complexes (Brownell & Allis 1995, Brownell *et al* 1996, Orgyzko *et al* 1996, Yang *et al* 1996, Mizzen *et al* 1996) lends weight to the view that histone acetylation is a prerequisite for transcription. Acetylation of nucleosomes found at promoters, by the HAT activity contained within transcription factors, may enhance the exposure of promoter elements to transcription factors. The manner in which the activating effect occurs - by acetylation-induced changes in nucleosomal conformation or direct unmasking of sites for transcription factor binding - is still unclear. Thus, normal chromatin may be thought to have a constitutive level of histone acetylation that allows basal transcription. Transcription may be repressed by targeting histone deacetylases to promoter regions (eg. Rpd3p), and conversely this repression may be relieved by the recruitment of transcription factors containing histone acetyltransferase activities (eg. p300/CBP). It is likely that these acetylating and deacetylating activities are not specific for individual genes, and therefore by complexing with subsets of transcriptional activator and repressor complexes they are directed to individual promoters. The presence of histone acetyltransferase and deacetylase activities in

transcriptional activating and repressing complexes has firmly established histone acetylation in the context of regulation of transcriptional activity.

CHAPTER FOUR - RESULTS AND DISCUSSION

Gene distribution in chicken chromosomes

4.1 Introduction

4.1.1 CpG islands

The vertebrate genome is characterised by a high degree of methylation at the cytosine of CpG dinucleotides, which occur on average every 50-100bp. However, in a small fraction of the genome (about 1%), CpG occurs approximately every 10bp, and is not methylated. This fraction of the genome was initially identified as short regions of genomic DNA which contained many sites for the methyl-sensitive restriction enzyme HpaII (Cooper *et al* 1983). It thus differs from bulk genomic DNA by being both unmethylated at CpG dinucleotides, and rich in G and C nucleotides (60-70%, compared with 40% in bulk genomic DNA). Sequences with these characteristics are found in short regions of 1-2kb, and are consequently referred to as CpG islands. In addition, whereas the CpG sequence is only represented at a quarter of the expected frequency in bulk genomic DNA, CpG island DNA does not show any suppression of CpG. This is thought to be a result of the high mutation rate specific to methylated CpGs. Cytosine is prone to deamination, and when methylated gives rise to thymine. As a consequence, methylated CpGs can sometimes be repaired to TpG. CpG dinucleotides found within CpG islands are not methylated, however, and thus do not succumb to mutation (for review see Bird 1987)

In humans, 60% of genes are associated with CpG islands. CpG islands have been found at the 5' end of all housekeeping genes analysed to date, and at the 5' end of a large proportion (40%) of genes with a tissue-restricted expression pattern. In most CpG island-associated genes analysed to date, the island has been found to include the promoter and to extend into the transcribed region of the gene, often including the first exon. This property of CpG islands allows their exploitation for the isolation of new genes.

At a chromosomal level, the distribution of CpG islands in the genome has been shown to coincide with R bands (Craig & Bickmore 1994). Craig and Bickmore isolated CpG islands by HpaII digestion, and hybridised these small biotinylated fragments to metaphase chromosomes by fluorescent *in*

situ suppression hybridisation. The hybridisation signal was shown to be unevenly distributed both within a single chromosome and between chromosomes. It localised to euchromatin corresponding to R bands - domains that are early-replicating, comparatively GC-rich, and less condensed than G bands. Colabelling of CpG islands and late replicating G bands elegantly showed that there was little overlap between the two subsets of chromatin. Thus CpG islands are predominantly found within early replicating DNA, which is generally thought to be gene-rich, whereas late-replicating DNA is sparsely populated with islands. This suggests that mammalian chromosomes are organised into domains with characteristic CpG island densities, that reflect gene density. More than 80% of CpG islands are found within R bands, which in turn represent 45% of the genome.

4.1.2 Purification of CpG islands

A novel method for isolating CpG islands was developed by Cross and colleagues (Cross *et al* 1994). They made use of the methyl-CpG binding domain (MBD) of the rat chromosomal protein MeCP2, an 85 amino acid polypeptide that binds to a single methylated CpG pair. This was attached to a nickel agarose matrix via a poly-histidine tag. The resulting matrix was packed into a column and was used to fractionate DNA according to its degree of CpG methylation, strongly retaining sequences that were highly methylated. The CpG island fractions of genomic DNA could thus be purified and cloned.

Figure 4.1 summarises the strategy used for the purification of CpG islands. In the first step, total genomic DNA is cut with MseI, an enzyme whose restriction site (TTAA) is found rarely in CpG islands, but frequently in bulk genomic DNA. Thus MseI is expected to produce predominantly intact CpG islands, and small fragments from the remaining bulk DNA. MseI fragments are passed over the MBD column and fragments that bind strongly are discarded. This step eliminates rare MseI fragments that contain clusters of methylated CpGs, which might otherwise contaminate the CpG island

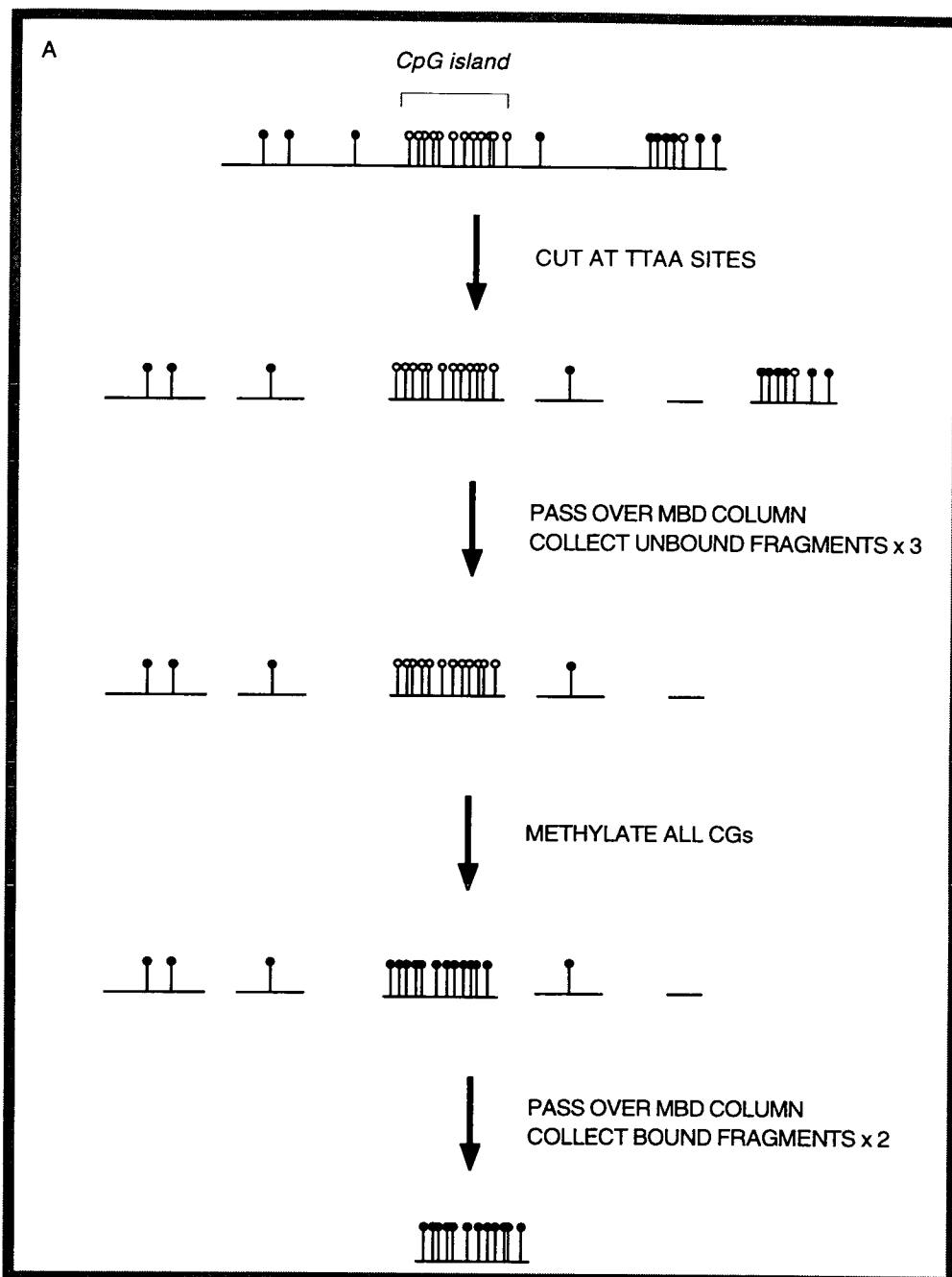


Figure 4.1

Construction of a CpG island library.

Flow diagram illustrating the strategy used for the purification of *Mse*I fragments containing CpG islands. The position of CpGs is indicated by vertical lines. Open circles denote unmethylated CpGs, and closed circles denote methylated CpGs. See text for details.

This figure has been adapted from Cross *et al* 1994.

fraction. The unbound fragments (containing unmethylated CpG islands) are subsequently methylated using the bacterial methyltransferase SssI (NEB). Pre-existing methylated CpGs which are not densely clustered show no change in their affinity for the binding column. Following *de novo* methylation, however, CpG islands are converted from being poor substrates for the binding column, to being very good substrates with a high affinity. Those fragments which are eluted at high salt, therefore, should be enriched for CpG islands.

4.1.3 Bias of CpG islands for microchromosomes in chicken.

The strategy described in the previous section was used by McQueen and colleagues (McQueen *et al* 1996) to prepare a CpG island library from chicken genomic DNA, to be used as a tool for the study of gene density in chicken chromosomes.

The chicken karyotype comprises 39 chromosome pairs, of which 29 are defined as 'microchromosomes' by virtue of their small size (see figures 4.2 and 4.3). While macrochromosomes are easily identified by morphology and individual banding patterns, microchromosomes are cytologically indistinguishable from each other. They account, however, for approximately 30% of the total 1200Mb of genomic DNA. Due to technical limitations, genes have been mainly mapped to specific macrochromosomal locations, whereas fewer have been mapped to the microchromosome group as a whole, and very few to individual microchromosomes (Burt *et al* 1995). Thus, to determine the overall chromosomal distribution of genes on chicken chromosomes, McQueen and coworkers isolated a CpG island library using the MBD binding column described above. A bulk library insert was then amplified from the pooled library, and labelled for hybridisation to chicken metaphase spreads by fluorescence *in situ* hybridisation. In the presence of competitor DNA, the CpG island library was found to colocalise mainly with the microchromosomes (see Figure 4.4). In the absence of competition, the probe hybridised to all chromosomes, implying that the bias of the CpG islands towards the microchromosomes is not due to repetitive sequences.

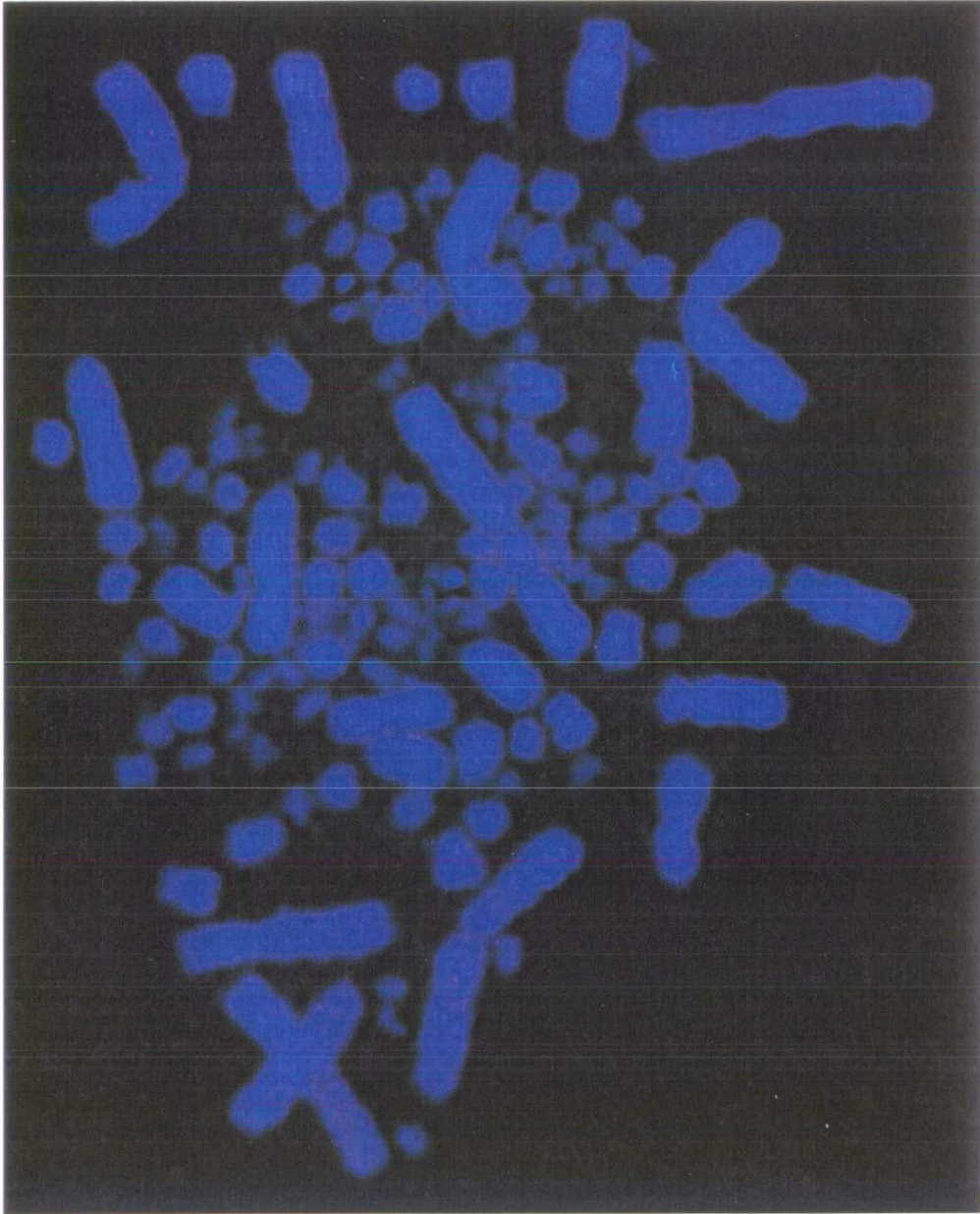


Figure 4.2
DT40 metaphase chromosomes counterstained with DAPI.

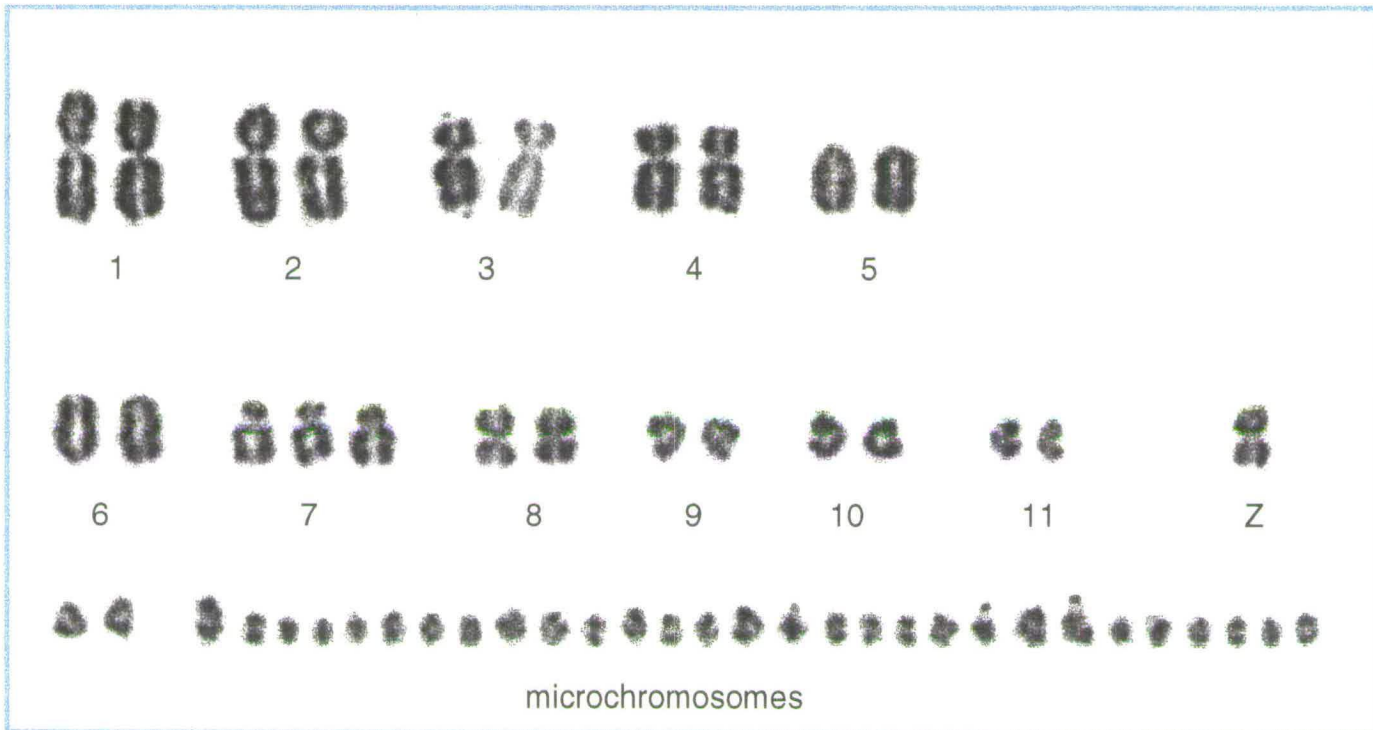


Figure 4.3

Karyotype of DT40 chromosomes.

Karyotype was determined using Quips™ Karyotyper software. Note trisomy of chromosome 7. Microchromosomes and the sex-determining W chromosome were unclassifiable.

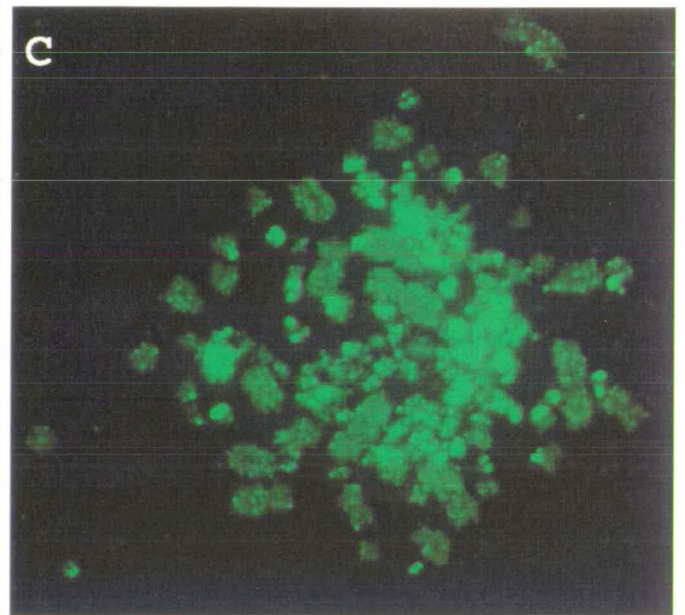
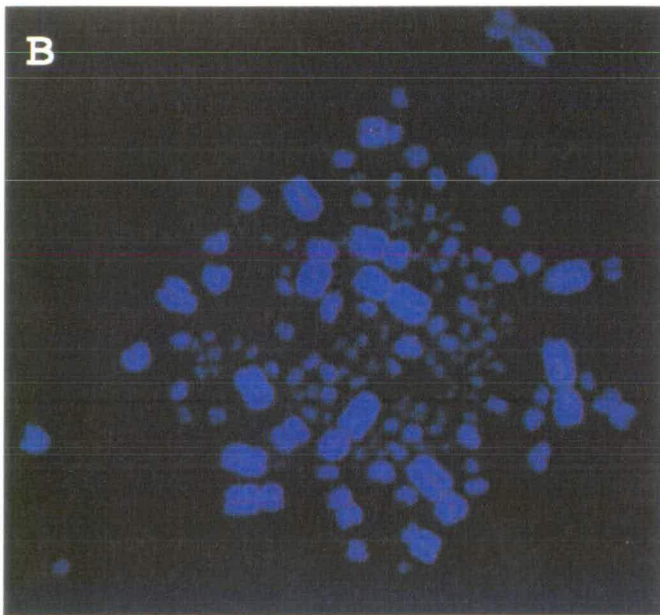
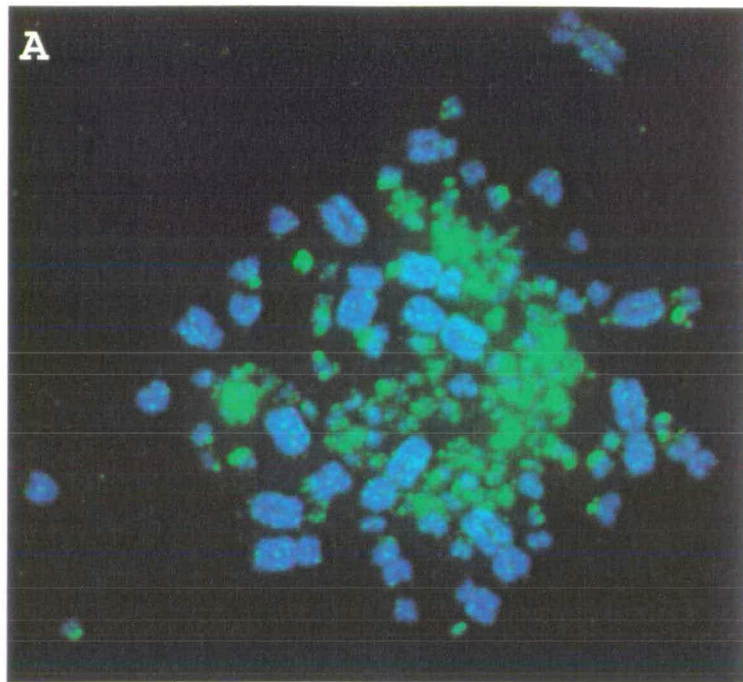


Figure 4.4

CpG island (CGI) distribution on DT40 chromosomes- CGI probe courtesy of H McQueen (McQueen *et al* 1996).

A. DT40 metaphase chromosomes counterstained with DAPI (blue) and hybridised with a biotinylated CGI probe and detected with avidin-FITC (green).

B. DAPI channel showing position of metaphase chromosomes.

C. FITC channel showing position of CGI hybridisation.

This result suggested that microchromosomes are particularly gene-rich. This is surprising when one considers firstly that few genes have been mapped to the microchromosomes (Burt *et al* 1995) and secondly that they represent only 30% (about 300Mb) of total genomic DNA, thus implying that the gene density on these microchromosomes is particularly high. Assuming that chicken has the same number of CpG islands as mammals, approximately 45,000, and that these are concentrated on the microchromosomes, one would expect to find one gene every 5-10kb of microchromosomal DNA.

4.2 Aim of the project

As a consequence of the data described above, a collaboration with H McQueen and colleagues was set up, aimed at gaining further insight into the chromosomal distribution of genes in chicken. The acetylation status of the chromosomes was examined, in order to determine whether histone H4 acetylation, generally thought to be indicative of gene transcriptional activity, reflected the bias of CpG islands for microchromosomes. In addition, I followed the replication of microchromosomes in order to determine whether these chromosomes were early-replicating, as might be expected if they are gene-rich. Lastly, in collaboration with H McQueen, I localised a set of cosmids on chicken metaphase chromosomes. The cosmids were characterised in parallel by her for the presence of CpG islands, thus allowing an estimate of CGI density for macrochromosomal versus microchromosomal DNA to be made.

4.3 Histone H4 acetylation of chicken chromosomes

The histone H4 acetylation profile of chicken chromosomes was determined by immunofluorescence, adapting the protocol described in section 3.4. Metaphase chromosome spreads made from DT40 cells (see section 2.13) were labelled with antisera raised against histone H4 acetylated at lysine 5. Figure 4.5 shows the acetylation profile of DT40 chromosomes, at several different exposures for the antibody fluorescence.

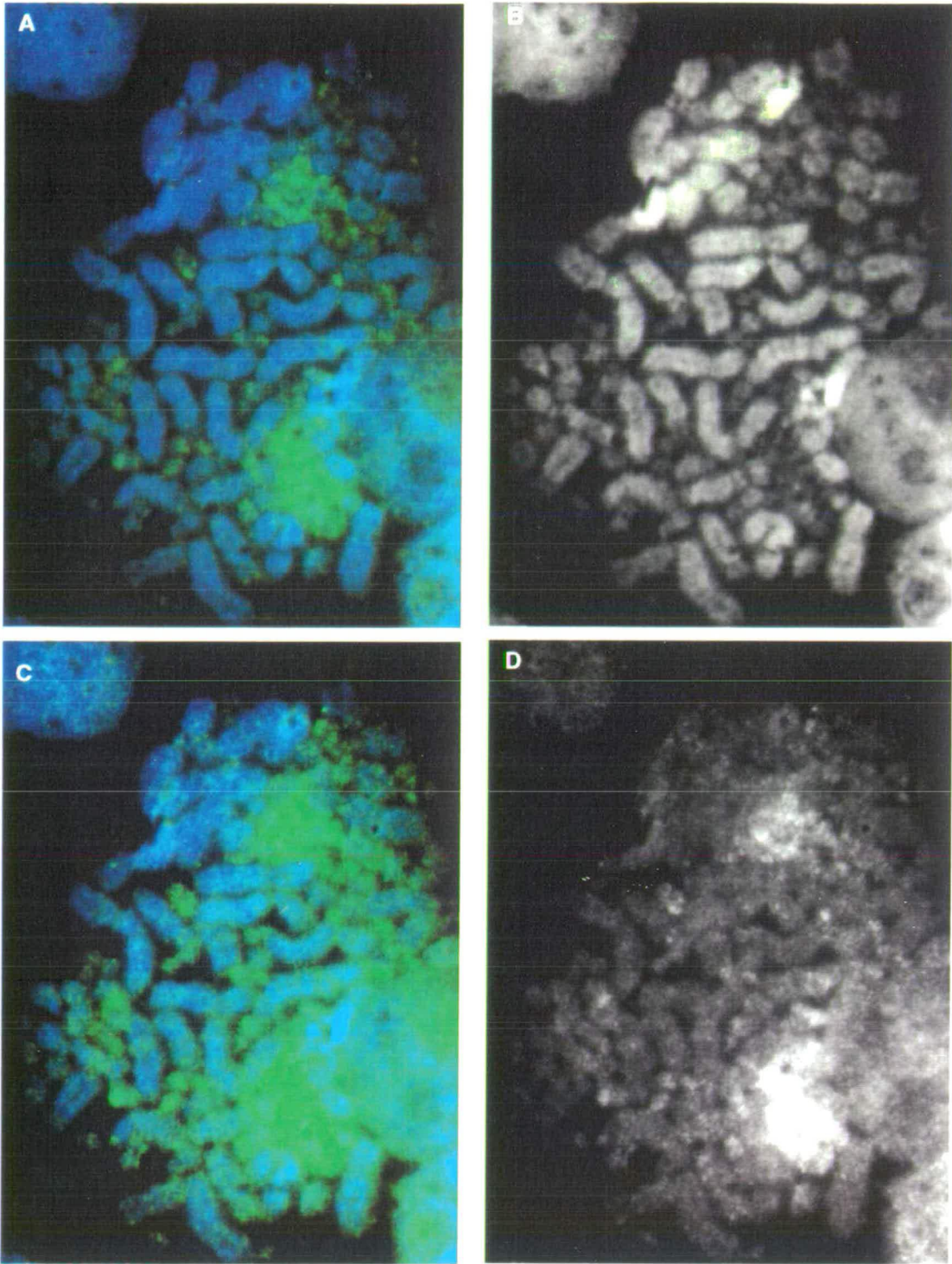


Figure 4.5

DT40 metaphase chromosomes labelled by immunofluorescence with anti-acetylated H4.

Chromosomes are counterstained with DAPI (blue) and antibody labelling is detected by FITC (green).

A. Acetylated H4 profile of DT40 metaphase chromosomes.

B. DAPI channel showing location of chromosomes.

C. Antibody labelling overexposed for microchromosome labelling to show banding on macrochromosomes.

D. FITC channel showing antibody labelling.

Acetylated histone H4 was found to be distributed throughout macro- and microchromosomes. This is not surprising given that genes are known to reside on both subsets of chromosomes, and thus transcription will take place on both micro- and macrochromosomes. However, the antibody appeared to show a strong preference for the microchromosomes, a result reminiscent of the bias of CpG islands for microchromosomes. The microchromosomes appeared to be strongly and uniformly labelled with the antibody, suggesting an enrichment in acetylated histone H4 in these chromosomes, and thus that they contain dense concentrations of transcriptionally active DNA. The macrochromosomes, on the other hand, were labelled unevenly with the antibody. Bands of acetylated chromatin and larger unacetylated domains, indicative of a dearth of active genes, were observed. This suggests that fewer genes might be found on the macrochromosomes than the microchromosomes. The sex-determining W chromosome, previously shown to be heterochromatic (Saitoh *et al* 1991), was also underacetylated. The observed acetylation profile of the chromosomes thus implies there is an enrichment in gene density, and transcriptional activity, on the microchromosomes, relative to the macrochromosomes.

4.4 Replication timing of chicken chromosomes

Given the correlation between early-replicating and gene-rich DNA in mammalian chromosomes (Craig 1994), the timing of DNA replication in the microchromosomes was analysed. While replication banding of chicken chromosomes has been carried out prior to this analysis (Schmid *et al* 1989, Ponce de Leon *et al* 1992, Ladjali *et al* 1995), there has been a lack of comment on the replication timing of microchromosomes, and no direct link has been established to date between their replication timing and gene density.

The kinetics of chromosome replication during S phase can be followed by detecting the incorporation of bromodeoxyuridine (BrdU), a thymidine analog, into replicating DNA. Thus, by labelling replicating DNA during particular

periods of S phase with BrdU, and detecting the label with an anti-BrdU antibody, the replication timing of macro- and microchromosomal DNA was investigated. A schematic outline of the experimental approaches can be found in Figures 4.6, 4.8, and 4.12, and the technical details are described in section 2.15.

4.4.1 Continuous labelling with BrdU

This approach was initially used to provide an estimate of the length of S phase in DT40 cells. Cells were grown in the presence of BrdU for increasing periods of time, ranging from 1 to 10hrs (see Figure 4.6 for a schematic representation of the experiment) and were then arrested in mitosis by addition of colcemid. In this manner, cells are synchronised at the end of the experiment, as all cells in mitosis at that time will have proceeded coordinately through the cell cycle. BrdU labelling during the final hours of culture is indicative of late replication, as any unlabelled DNA will have undergone replication early in S-phase, before addition of BrdU. Continuous labelling with BrdU for 10 hours, on the other hand, will label the entire length of the chromosome, as BrdU is present throughout the whole of S phase. Thus, during the hourly intervals between these two time points, the progression of DNA replication can be monitored. This approach visualised DNA replication along the length of each chromosome throughout the course of S phase, and allowed an estimate of the duration of S phase in DT40 cells to be made. Figure 4.7 shows DNA replication progression through S phase in DT40 metaphase chromosomes, by detection of BrdU incorporation with an FITC-conjugated anti-BrdU antibody. It was estimated that S phase lasted approximately 9 hours in DT40 cells.

Late replication

In order to investigate the replication events that occur in late S phase, cells were arrested in mid-S phase by addition of methotrexate for a full cell cycle (Craig & Bickmore 1994), and were subsequently released from the cell cycle block in BrdU-containing medium. Metaphase chromosomes were then prepared and BrdU incorporation was detected with an FITC-conjugated anti-

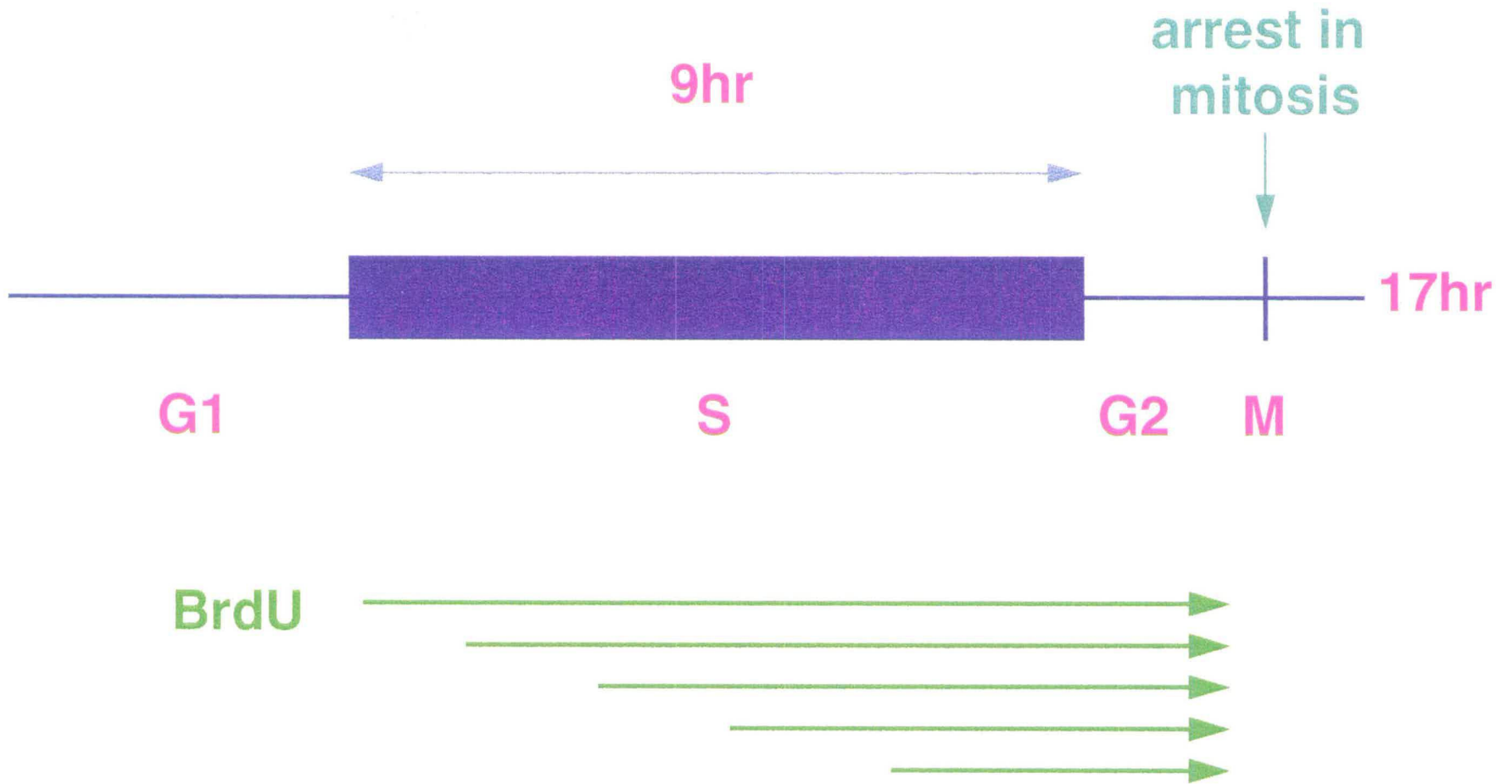


Figure 4.6

Schematic representation of progression of S phase monitored by BrdU incorporation.

Cells are grown in BrdU-containing medium for decreasing lengths of time prior to preparing metaphase chromosome spreads. Incorporation of BrdU is detected with an FITC-conjugated anti-BrdU antibody. See text for details. See Figure 4.7 for results.

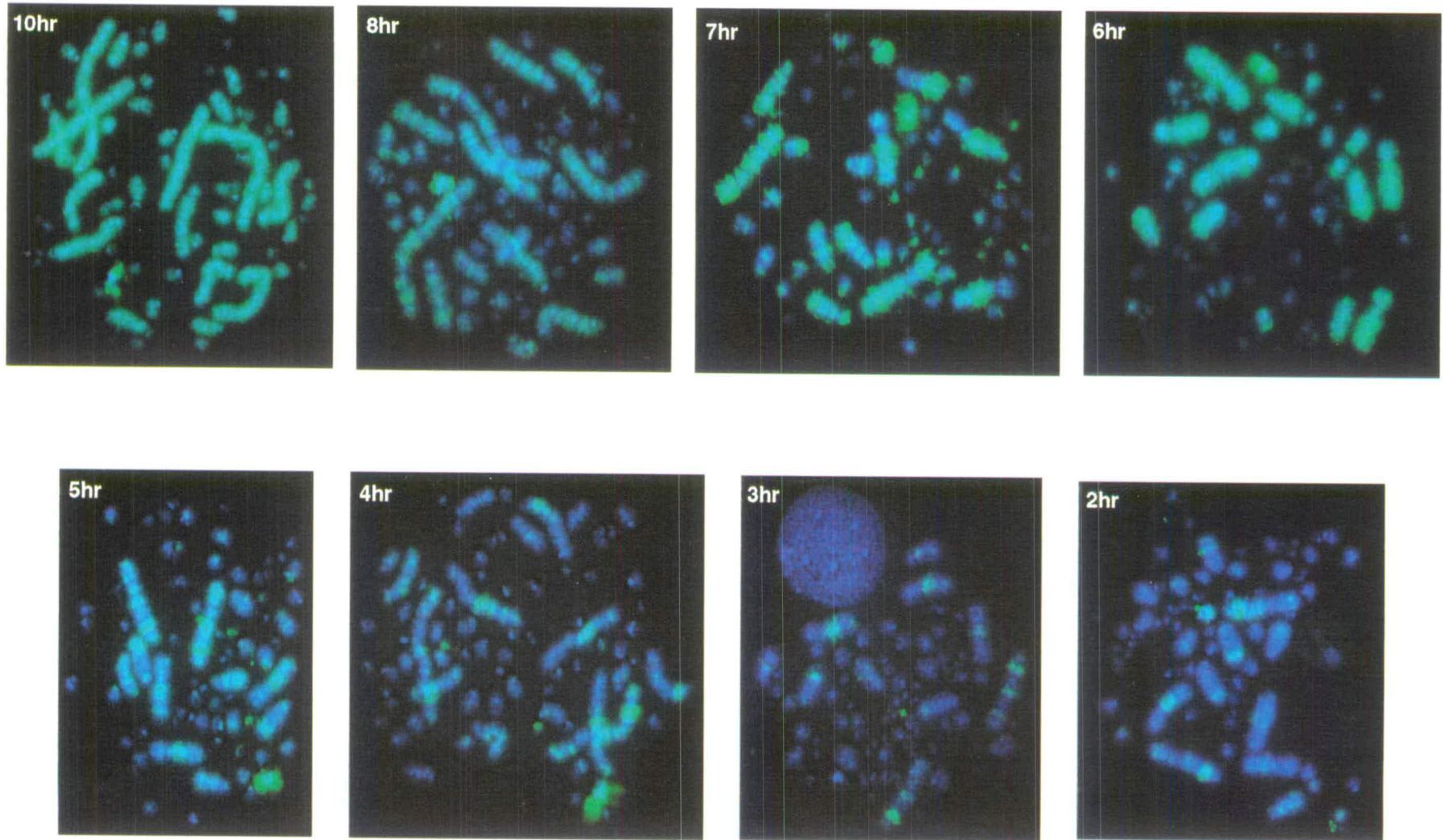


Figure 4.7

Incorporation of BrdU in replicating DNA of DT40 chromosomes.

Metaphase chromosomes are counterstained with DAPI (blue) and BrdU incorporation is detected with an FITC-conjugated anti-BrdU antibody (green). Replication is monitored throughout the course of S phase by addition of BrdU at hourly timepoints between 1 and 10 hours. See figure 4.6 for a schematic representation of the experimental approach.

BrdU antibody. Methotrexate arrests mammalian cells in the middle of S phase, when there is a marked reduction in the rate of DNA synthesis, known as the 3C pause (Holmquist *et al* 1982). Figure 4.8 shows a schematic representation of the approach used. Figure 4.9 shows the chromosomal regions found to replicate after release of the methotrexate block. BrdU incorporation, and hence replication, was only detected in macrochromosomal DNA, whereas microchromosomes were consistently unlabelled by the anti-BrdU antibody. This suggests they undergo replication prior to the methotrexate block. Given that large regions of the macrochromosomes were also unlabelled, it would seem that a large portion of the macrochromosomes also replicates prior to the methotrexate block. Methotrexate arrests mammalian cells in mid S phase, suggesting that both microchromosomes and some regions of the macrochromosomes replicate early, whereas the remainder of the macrochromosomes replicate in the second half of S phase. The alternative explanation is that methotrexate arrests the chicken cell cycle in late, rather than mid, S phase. In this case, the experiment has only observed incorporation of BrdU into very late replicating DNA. This explanation is supported by the first experiment, as the pattern of BrdU incorporation observed following methotrexate arrest is very similar to that observed in the last two panels (3hr and 2hr) of Figure 4.7.

Early replication

The methotrexate-induced arrest can also be applied to observe DNA replication prior to the cell cycle block. By growing the cells in medium containing both methotrexate and BrdU, BrdU is incorporated into DNA replicating prior to the methotrexate block (see Figure 4.8 for a schematic representation of the experiment). Any cells that are in late S phase at the time of methotrexate addition, will show metaphase chromosomes that are entirely labelled with BrdU. This allows those mitotic spreads to be excluded from the analysis. DT40 cells were grown in the presence of both BrdU and methotrexate for a full cell cycle. Cells were then released from the cell cycle block in BrdU-free medium, and were allowed to reach mitosis. Metaphase

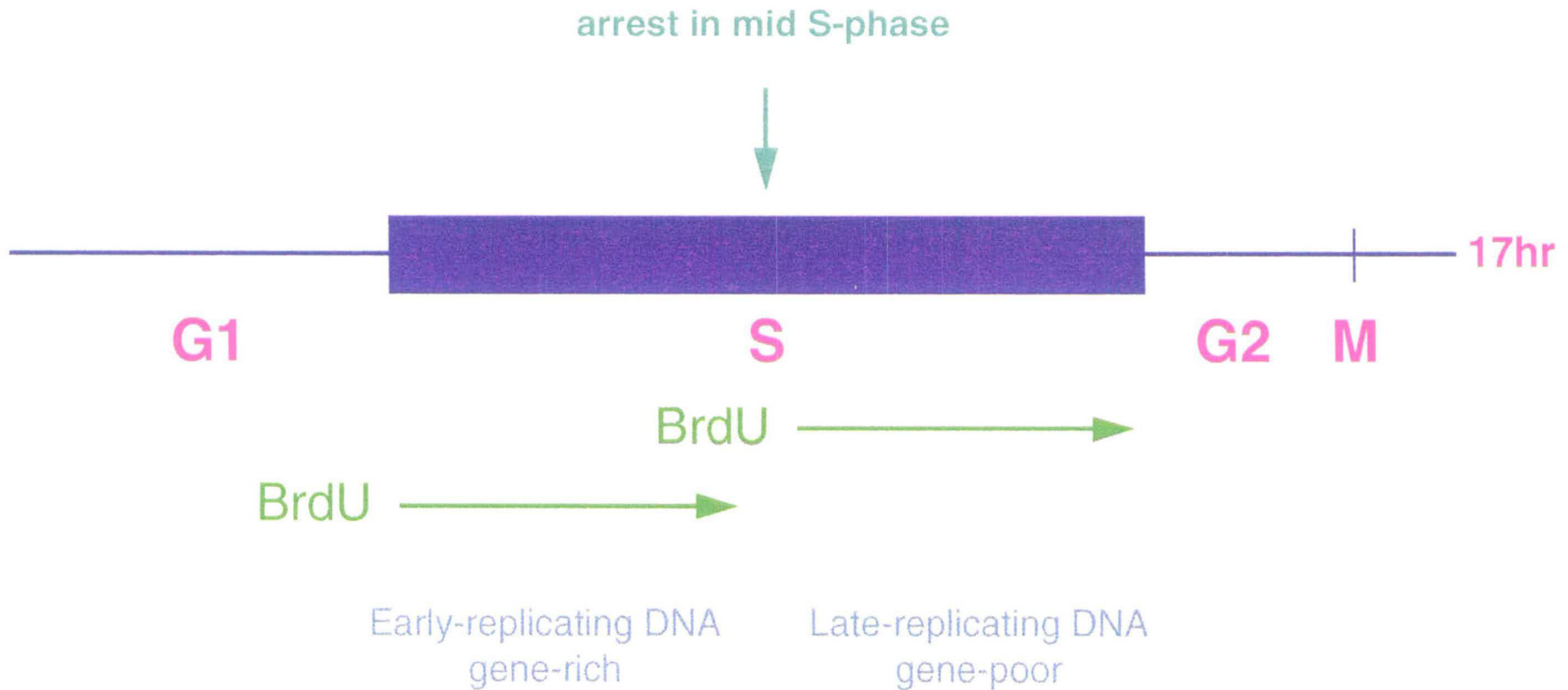


Figure 4.8

Schematic representation of BrdU incorporation in late or early replicating DNA.

To detect late-replicating DNA, cells are arrested in mid S phase with methotrexate, and released in BrdU-containing medium. Metaphase chromosome spreads are prepared and incorporation of BrdU is detected with an FITC-conjugated anti-BrdU antibody. To detect early-replicating DNA, cells are arrested in mid S-phase with methotrexate, in the presence of BrdU, and released into BrdU-free medium. See text for details. See Figures 4.9 and 4.10 for results.

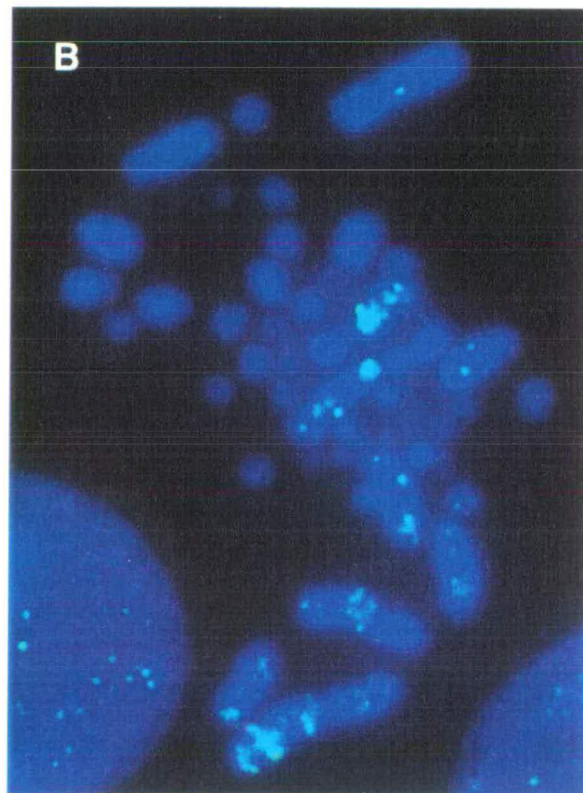
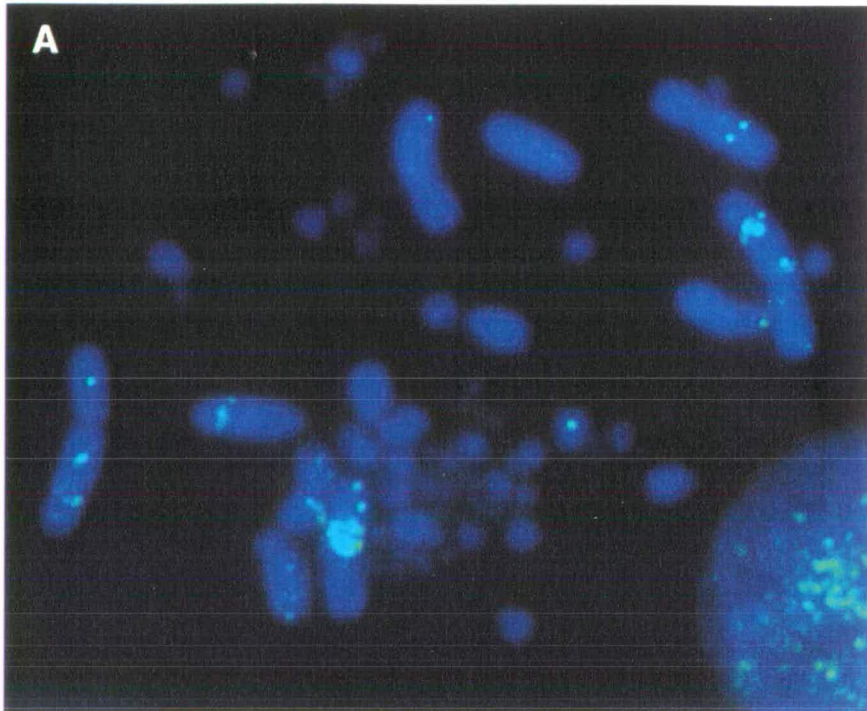


Figure 4.9

DNA replication following methotrexate block.

DT40 metaphase chromosomes counterstained with DAPI (blue) and showing incorporation of BrdU (green) in replicating DNA. Cells have been arrested with methotrexate and released in BrdU-containing medium, thus labelling late-replicating DNA.

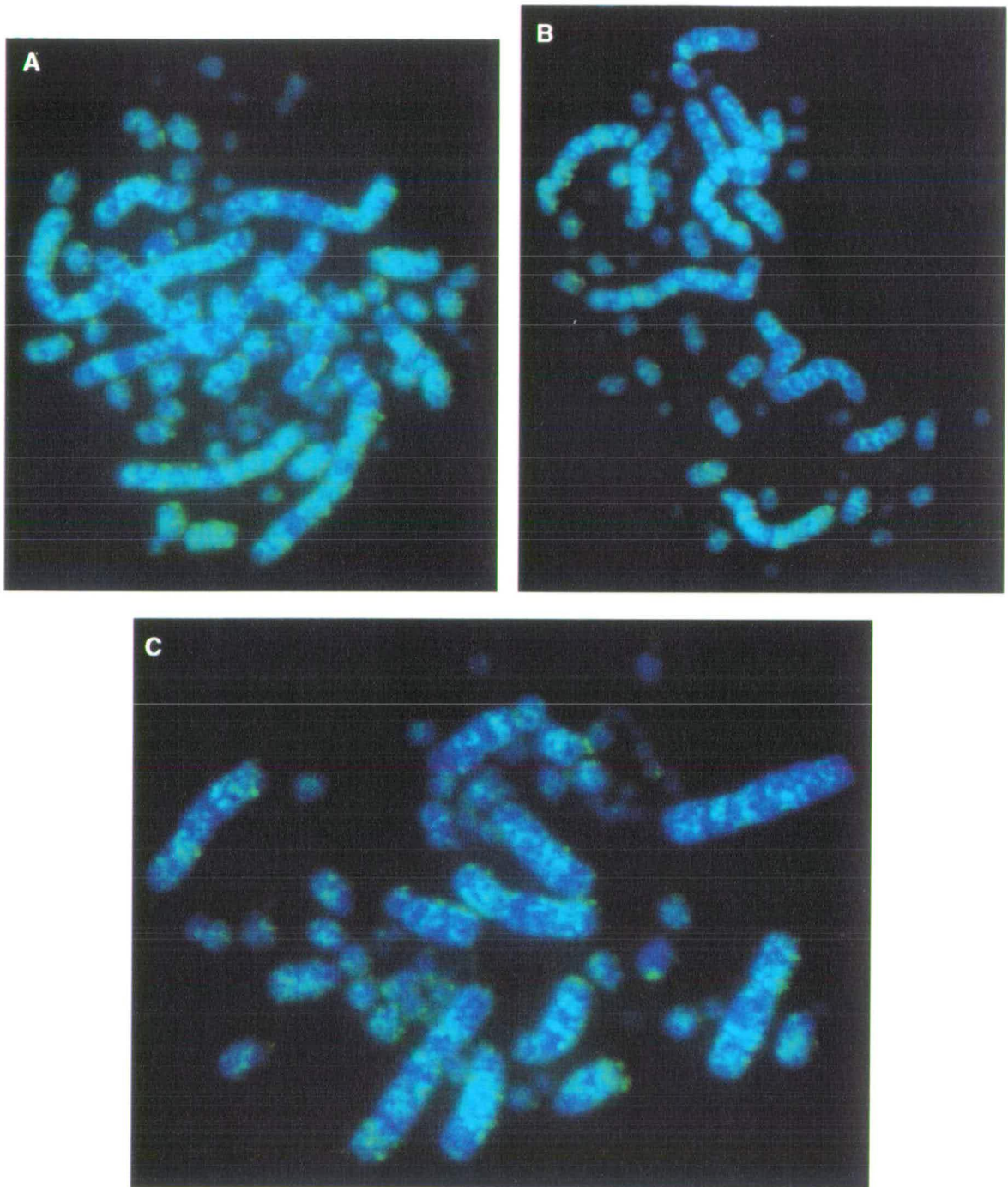


Figure 4.10

DNA replication prior to methotrexate block.

DT40 metaphase chromosomes counterstained with DAPI (blue) and showing incorporation of BrdU (green) in replicating DNA. Cells have been arrested with methotrexate in BrdU-containing medium, thus labelling early-replicating DNA.

chromosomes were then prepared and incorporation of BrdU was detected with an FITC-conjugated anti-BrdU antibody. Figure 4.10 shows the pattern of replication prior to the methotrexate block. Microchromosomes were found to replicate prior to the methotrexate block, as BrdU was incorporated into the chromosomes. The macrochromosomes were also labelled with the anti-BrdU antibody, implying that regions of these chromosomes replicate prior to the methotrexate block.

FACS scan analysis of DT40 cells arrested with methotrexate was undertaken with the help of W Bickmore. Figure 4.11 shows that addition of methotrexate to the medium results in an accumulation of DT40 cells in G₁ and S phase. Progression into G₂ was inhibited by methotrexate.

Figure 4.13 shows an alignment of chromosome 1 taken from DT40 metaphase chromosomes. The chromosome has been labelled for early or late replicating DNA (taken here as being before and after, respectively, the methotrexate block), and for the presence of acetylated histone H4. Due to the resolution of the images it is difficult to determine whether there is a colocalization of early replicating DNA and acetylated chromatin. However, DNA replicating before and after the methotrexate block is found in distinct regions of the chromosome, as might be expected.

4.4.2 Pulse labelling with BrdU

Pulse labelling is used to reveal chromosomal regions that undergo replication at specific intervals during S phase. In order to identify the timing of microchromosomal DNA replication, DT40 cells were arrested with nocodazole for a full cell cycle, thus synchronising cells in mitosis (Zieve *et al* 1980). The cells were subsequently allowed to progress to the G₁/S boundary by growth in the presence of the plant amino acid mimosine (Mosca *et al* 1992) for a full cell cycle. Mimosine inhibits initiation of DNA replication (Dijkwel & Hamlin 1992, Levenson & Hamlin 1993), and thus arrests synchronised cells at the G₁/S boundary. Release from the mimosine block allowed cells to commence replication synchronously. To observe DNA replication in early S phase, BrdU was pulsed for 1 hr periods at several time

points following entry into S phase. This approach is summarised in Figure 4.12. However, due to the shortage of time, these series of experiments have not been optimised and are yet to be completed. The results are therefore not included in the thesis.

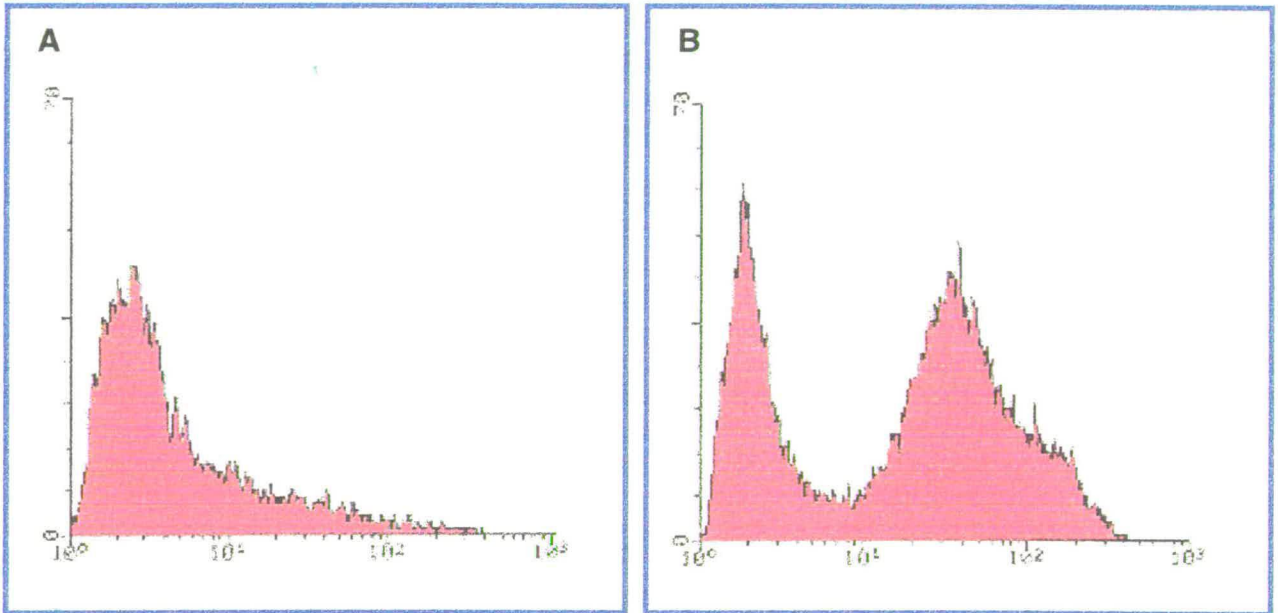


Figure 4.11

FACS scan analysis of DT40 cells grown in presence of methotrexate.

A. Cells grown in presence of methotrexate.

B. Control cells grown in absence of methotrexate - asynchronous culture.

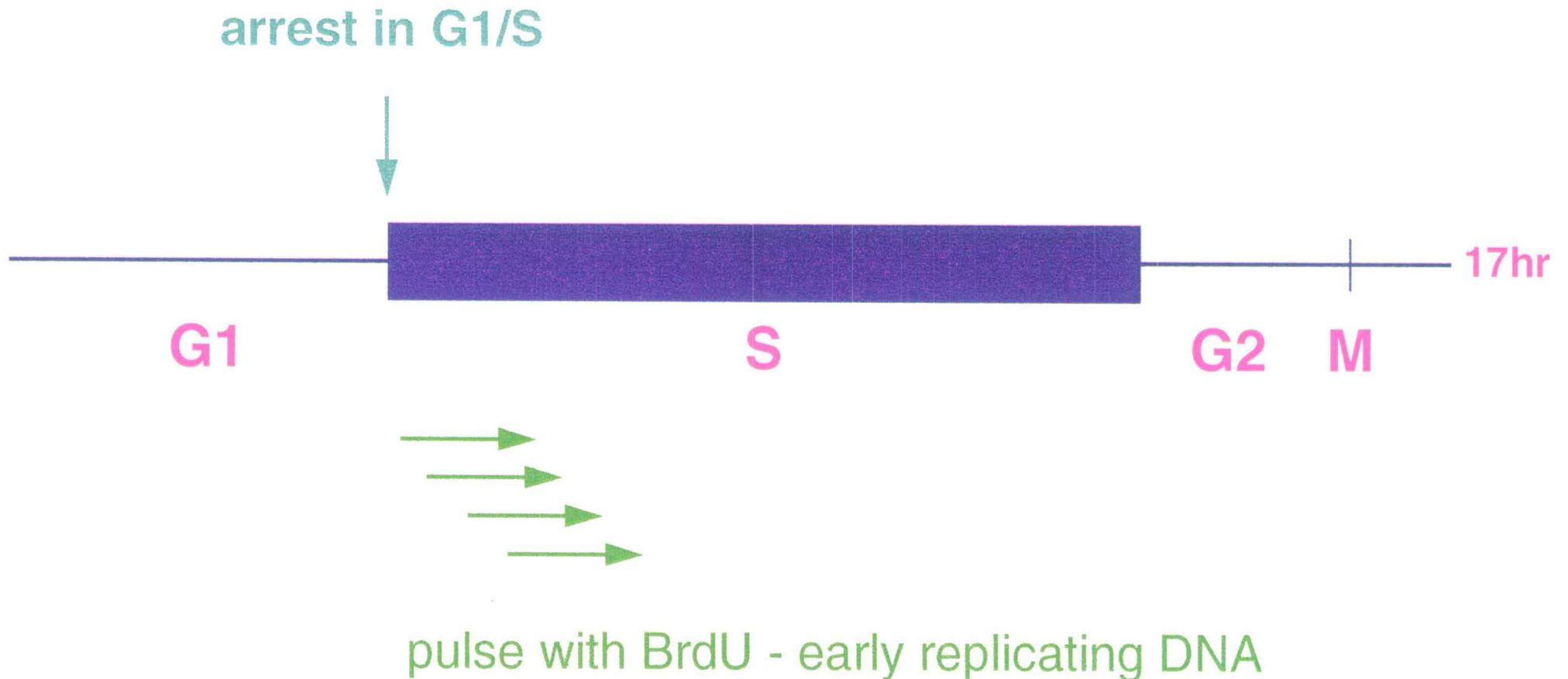


Figure 4.12

Schematic representation of BrdU incorporation in early replicating DNA.

Cells are arrested in G1/S with mimosine and released in BrdU-containing medium for 1-hour pulses. BrdU is subsequently washed out and cells are grown to M before preparing metaphase spreads. Incorporation of BrdU is detected with an FITC-conjugated anti-BrdU antibody.

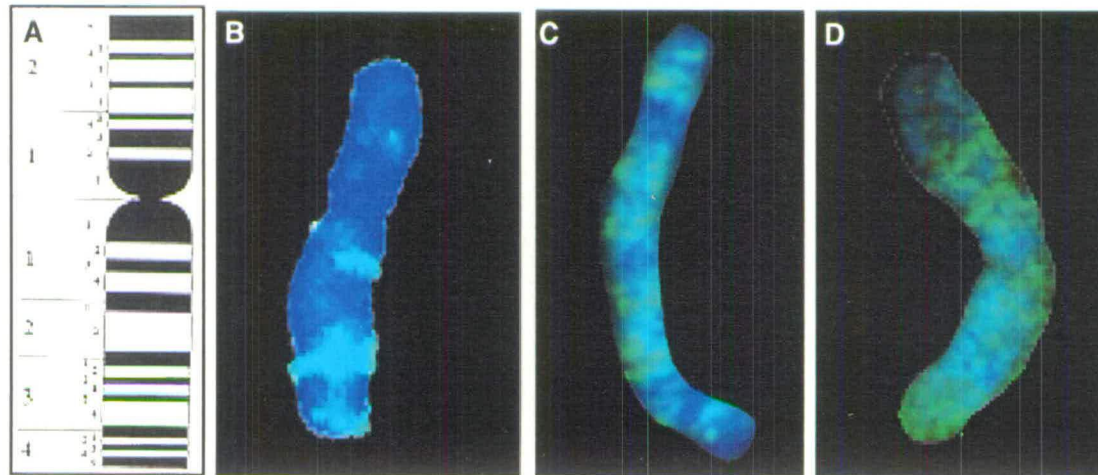


Figure 4.13

Alignment of chromosome 1.

A. Ideogram showing R- (white) and G- (black) bands.

B. DNA replicating after methotrexate block (green).

C. DNA replicating prior to methotrexate block (green).

D. Chromosome 1 labelled with anti-acetylated H4.

4.5 Cosmid mapping

In order to quantify the density and distribution of genes on the chicken chromosomes, the correlation between CpG island-rich cosmids and their chromosomal location was determined. 16 cosmids were selected at random by H McQueen from a chicken cosmid library (adult Leghorn male liver (Clontech)). A further two were selected for the presence of known CpG islands by PCR. These cosmids were mapped onto chromosomes by FISH, to determine their localisation on macro- or microchromosomes. They were independently analysed by H McQueen for the presence of CpG islands. In order to determine the number of CpG islands for each cosmid, the DNA was digested with MseI (restriction site TTAA), thus leaving most CGIs as large or intact fragments, and methylated to completion using SssI methylase. By end-labelling the fragments before passing them over the MBD column, it was possible to follow whether individual fragments were bound or unbound by the column. Cosmid DNA was thus passed over the MBD column at low salt and strongly binding CpG islands were eluted at high salt. The resulting fragments were visualised using radioactive sensitive film following size separation on an agarose gel. In this manner, CGIs were identified and quantified (0-5, see Table 4.1) for each cosmid analysed.

Figures 4.14 and 4.15 show the chromosomal location of several of the cosmids analysed. Each cosmid was labelled with biotin or digoxigenin, and hybridised to chicken metaphase chromosomes following standard FISH protocols (see section 2.14 for details).

Table 4.1 below summarises the chromosomal location and CpG island content of each cosmid analysed to date for both sets of criteria. The cosmids are numbered, and their location is either macrochromosomal (M) or microchromosomal (μ).

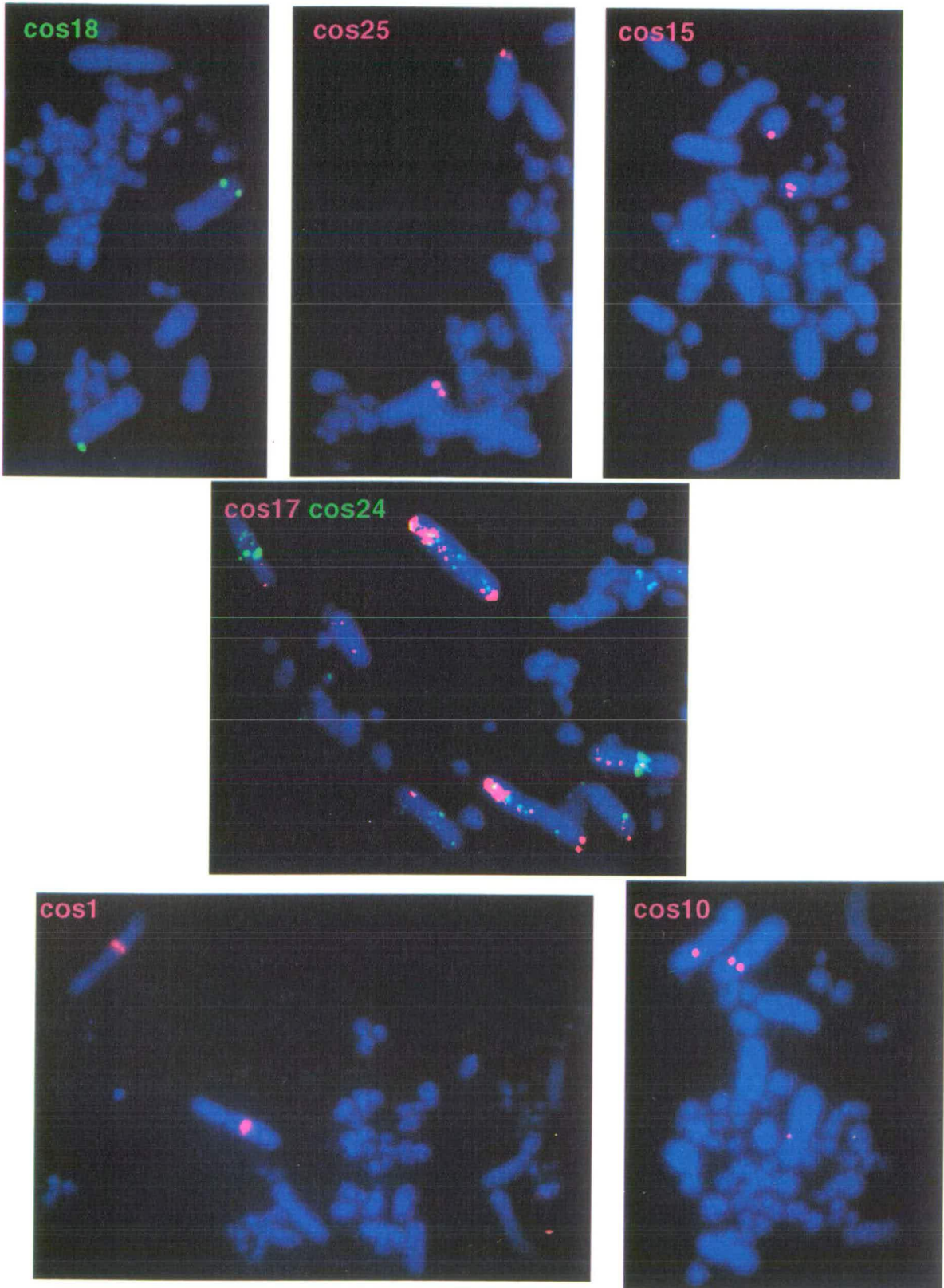


Figure 4.14
A selection of cosmids mapping to DT40 metaphase macrochromosomes by FISH.
 Cosmids were labelled with biotin or digoxigenin and hybridised to chromosomes following standard FISH techniques.

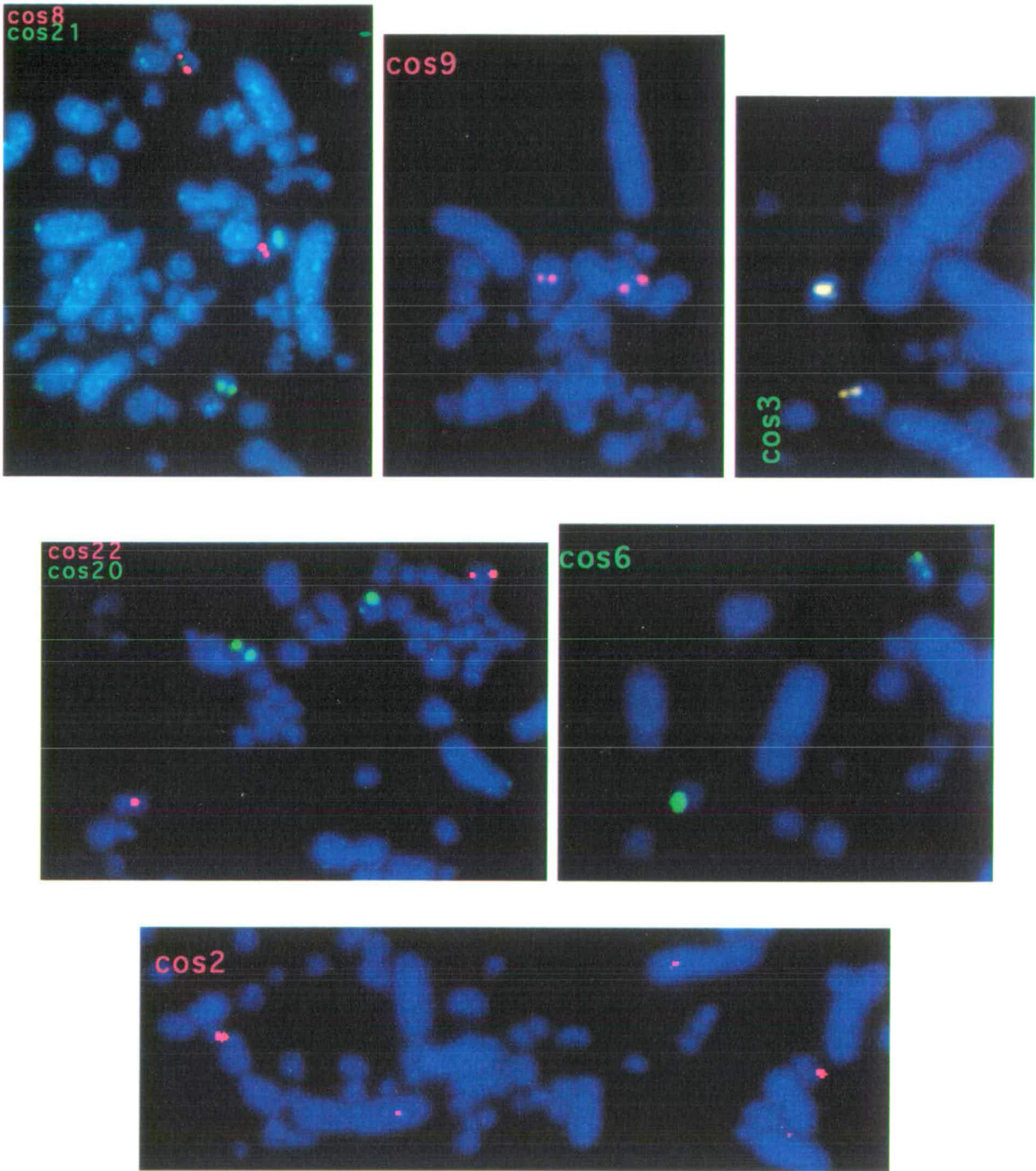


Figure 4.15

A selection of cosmids mapped to chicken metaphase microchromosomes by FISH.

All cosmids were labelled with biotin or digoxigenin and were hybridised to metaphase chromosomes following standard FISH protocols.

Table 4.1
Cosmid chromosomal location and CGI content

COSMID	CGI FRAGMENTS PER COSMID	LOCATION	COSMID	CGI FRAGMENTS PER COSMID	LOCATION
1	0	M	2	1	μ
5	1	M	3	3	μ
10	0	M	6	2	μ
15	0	M	7	4	μ
17	0	M	8	1	μ
18	0	M	9	5	μ
19	1	M	16	1	μ
25	0	M	20	3	μ

All cosmids mapping to the macrochromosomes were found to be poor in CpG islands, whereas those mapping to microchromosomes were enriched in CpG islands. This supported the bias for CpG islands on microchromosomal DNA shown previously by FISH using the CGI probe (McQueen *et al* 1996). In order to relate the above results with respect to gene number, rather than CpG islands, the cosmids are currently being sequenced and analysed for the presence of genes.

4.6 Discussion

The above analysis of chicken microchromosomes has generated some surprising data. Originally considered to be genetically inert reserves of DNA, where few genes had been mapped, the microchromosomes appear to be playing an unexpectedly active role. McQueen and colleagues have shown a bias for CpG islands on the microchromosomes (McQueen *et al* 1996), suggesting that a large proportion of genes are found there. This initial result

has been supported by the strong correlation between CGI-rich cosmids and their localisation on the microchromosomes (section 4.5).

The acetylation profile of the microchromosomes also indicates there is an enrichment of genetically active chromatin in these chromosomes. There is a strong preference in their labelling by an antibody that recognises acetylated histone H4, relative to that of the macrochromosomes. This suggests that microchromosomes are enriched in hyperacetylated histones, and thus in transcriptionally active chromatin, implying, as a consequence, that they are gene-rich. The replication timing experiments, using methotrexate to block in S phase, have shown that regions of the macrochromosomes replicate both before and after the methotrexate arrest in S phase. The microchromosomes are only seen to replicate before the methotrexate block. It is uncertain whether methotrexate arrests DT40 cells in mid S phase, as it does mammalian cells. The results imply it arrests later in S phase. The pulse labelling experiments, however, using nocodazole and mimosine to block the cell cycle as described in section 4.4.2, will provide a more detailed analysis of replication timing at the beginning of S phase. Taken together, these series of experiments imply that microchromosomes do not consist of genetically inert DNA, and support the original assertion that these chromosomes are gene-rich rather than being simply GC-rich.

While a bias for the presence of both acetylated histone and early-replicating DNA has been shown on the microchromosomes, the features are not confined solely to these chromosomes. Regions containing acetylated histones and early-replicating chromatin were also seen in the macrochromosomes. This is not surprising given the known residence of genes there. The results seem to imply, however, that there are large regions in the macrochromosomes that are relatively gene-poor, whereas the microchromosomes appear to be densely populated with genes.

The advantage in maintaining so many gene-rich microchromosomes is unclear. However, the chromosomal organization within the avian species is highly conserved - most birds have 39-40 chromosome pairs, of which 6-8 are macrochromosomes and the rest microchromosomes. It has been

suggested that the microchromosomes are conserved in birds in order to maintain archaic linkage groups found there (Tegelstrom & Rytman 1981). This idea is constructed on the assumption that the chromosomes are too small for multiple recombinations to take place. Rodionov and colleagues have suggested instead (Rodionov *et al* 1992) that microchromosomes contain sites of recombinational hot spots, required to ensure correct disjunction of homologues in meiosis. It has also been proposed that the macrochromosomes are a the product of tandem fusion events involving several smaller chromosomes (Nanda & Schmid 1994). The presence of a number of interstitial telomeric sequence motifs, identified by FISH, on chromosome 1 favours this explanation. Alternatively, the same group argues that the occurrence of prominent telomeric signals on some of the microchromosomes support the argument for a breakdown of part of the original telomeric region to smaller microchromosomes. In either case, the high density of active genes found on the microchromosomes is an unexpected finding, with interesting implications both for chicken genome mapping and for our understanding of evolution of the avian karyotype.

Concluding remarks

This PhD project was embarked on in the hope of clarifying some of the existing controversies regarding the role of histone acetylation in gene regulation. The initial project aimed at correlating changes in histone H4 acetylation in response to varying levels of transcriptional activity of an inducible gene, using a cytological approach. Unfortunately, the cell line obtained for this study did not allow much headway to be made. While the techniques were successfully set up, little additional information was acquired that might have contributed to the growing understanding of histone acetylation. The second project extended initial observations made by McQueen *et al* (1996), which indicated that, contrary to general belief, microchromosomes in the chicken were CpG island- and gene-rich. The analysis of acetylation patterns of histone H4 throughout the chicken genome substantiated this observation, as acetylated H4 was found to be strongly biased towards the microchromosomes. Genetic activity in the chicken thus appears to be concentrated in the microchromosomes, which constitute a minority of the genome. Given that there is an association of increased levels of histone acetylation with transcriptionally active DNA, this approach provided an ideal alternative method for visualising gene distribution in the chicken genome, thus eliminating any inherent sequence bias towards GC-rich DNA which might have occurred using the CGI approach.

LIST OF REFERENCES

Ajiro K, Nishimoto T (1985) : Specific site of histone H3 phosphorylation related to the maintenance of premature chromosome condensation. Evidence for catalytically induced interchange of the subunits. **J Biol Chem** 260 : 15379-15381.

Alfageme CR, Zweidler A, Marowald A, Cohen LH (1974) : Histones of *Drosophila* embryos. Electrophoretic isolation and structural studies. **J Biol Chem** 248 : 3729-3736.

Allan J, Harborne N, Rau DC, Gould H (1982) : Participation of core histone "tails" in the stabilization of the chromatin solenoid. **J Cell Biol** 93 : 285-297.

Allegra P, Sterner R, Clayton DF, Allfrey VG (1987) : Affinity chromatographic purification of nucleosomes containing transcriptionally active DNA sequences. **J Mol Biol** 196 : 379-388.

Allfrey VG, Faulkner R, Mirsky AE (1964) : Acetylation and methylation of histones and their possible role in the regulation of RNA synthesis. **J Mol Biol** 196 : 397-388.

Allis CD, Gorovsky MA (1989) : Histone phosphorylation in macro- and micronuclei of *Tetrahymena thermophila*. **Biochemistry** 20 : 3828-3833.

Almouzni G, Khochbin S, Dimitrov S, Wolffe AP (1994) : Histone acetylation influences both gene expression and development of *Xenopus laevis*. **Dev Biol** 165 : 654-664.

Annunziato AT, Eason MB, Perry CA (1995) : Relationship between methylation and acetylation of arginine-rich histones in cycling and arrested HeLa cells. **Biochemistry** 34 : 2916-2924.

Attisano L, Lewis PN (1990) : Purification and characterization of two porcine liver nuclear histone acetyltransferases. **J Biol Chem** 265 : 3949-3955.

Ausio J, Van Holde KE (1986) : Histone hyperacetylation: its effects on nucleosome conformation and stability. **Biochemistry** 25(6) : 1421-1428.

Bejarano LA, Valdivia MM (1996) : Molecular cloning of an intronless gene for the hamster centromere antigen CENP-B. **Biochem Biophys Acta** 1307 : 21-26.

Belyaev ND, Keohane AM, Turner BM (1996) : Differential underacetylation of histones H2A, H3 and H4 in the inactive X chromosome in human female cells. **Hum Genet** 97 : 573-578.

Berezney R (1991) : The nuclear matrix: a heuristic model for investigating genomic organization and function in the cell nucleus. **J Cell Biochem** 47 : 109-123.

Bird AP (1987) : CpG islands as gene markers in the vertebrate nucleus. **Trends Genet** 3(12) : 342-347.

Boffa LC, Walker J, Chen TA, Sterner R, Mariani MR, Allfrey VG (1990) : Factors affecting nucleosome structure in transcriptionally active chromatin - histone acetylation, nascent RNA and inhibitors of RNA synthesis. **Eur J Biochem** 194 : 811-823.

Bode J, Henco K, Wingender E (1980) : Modulation of the nucleosome structure by histone acetylation. **Eur J Biochem** 110 : 143-152.

Bode J, Gomez-Lira MM, Scroter H (1983) : Nucleosomal particles open as the histone core becomes hyperacetylated. **Eur J Biochem** 130 : 437-445.

Bone JR, Lavender JS, Richman R, Palmer MJ, Turner BM, Kuroda MI (1994) : Acetylated histone H4 on the male X chromosome is associated with dosage compensation in *Drosophila*. **Genes & Dev** 8 : 96-104.

Boulikas T, Wiseman JM, Garrad WT (1980) : Points of contact between histone H1 and the histone octamer. **Proc Natl Acad Sci (USA)** 77 : 121-131.

Boulikas T (1988) : At least 60 ADP-ribosylated variant histones are present in nuclei from dimethylsulfate-treated and untreated cells. **EMBO J** 7 : 57-67.

Bowdish KS, Mitchell AP (1993) : Bipartite structure of an early meiotic upstream sequence from *Saccharomyse cerevisiae*. **Mol Cell Biol** 13 (4) : 2172-2181.

Bradbury EM (1992) : Reversible histone modifications and the chromosome cell cycle. **Bioessays** 14 : 9-16.

Braunstein M, Rose AB, Holmes SG, Allis CD, Broach JR (1993) : Transcriptional silencing in yeast is associated with reduced nucleosome acetylation. **Genes & Dev** 7 : 592-604.

Bresnick EH, John S, Hager GL (1990) : Glucocorticoid receptor-dependent disruption of a specific nucleosome on the mouse mammary tumor virus promoter is prevented by sodium butyrate. **Proc Natl Acad Sci (USA)** 87: 3977-3981.

Breneman JW, Yau PM, Swiger RR, Teplitz R, Smith HA, Tucker JD, Bradbury EM (1996) : Activity banding of human chromosomes as shown by histone acetylation. **Chromosoma** 105 : 41-49.

Brown MS, Dana SE, Goldstein JL (1974) : Regulation of 3-hydroxy-3-methylglutaryl coenzyme A reductase activity in cultured human fibroblasts: comparison of cells from a normal patient and from a patient with homozygous familial hypercholesterolemia. **J Biol Chem** 249 (3) : 789-796.

Brown MS, Faust JR, Goldstein JL, Kaneko I, Endo A (1978) : Induction of 3-hydroxy-3-methylglutaryl coenzyme A reductase activity in human fibroblasts incubated with compactin (ML-236B), a competitive inhibitor of the reductase. **J Biol Chem** 253 : 1121-1128.

Brown MS, Goldstein JL (1980) : Multivalent feedback regulation of HMG CoA reductase, a control mechanism coordinating isoprenoid synthesis and cell growth. **J Lipid Res** 21 : 505-517.

Brownell JE, Allis CD (1995) : An activity gel assay detects a single, catalytically active histone acetyltransferase subunit in *Tetrahymena* macronuclei. **Proc Natl Acad Sci (USA)** 92 : 6364-6368.

Brownell JE, Zhou J, Ranalli T, Kobayashi R, Edmondson DG, Roth SY, Allis CD (1996) : *Tetrahymena* histone acetyltransferase A: a homolog to yeast Gcn5p linking histone acetylation to gene activation. **Cell** 84 : 843-851.

Burt DW, Bumstead N, Bitgood JJ, Ponce de Leon FA, Crittenden LB (1995) : Chicken genome mapping: a new era in avian genetics. **Trends Genet** 11(5) : 190- 194.

Chicoine LG, Allis CD (1986) : Regulation of histone acetylation during macronuclear differentiation in *Tetrahymena*: evidence for control at the level of acetylation and deacetylation. **Dev Biol** 116: 477-485.

Chin DJ, Luskey KL, Anderson RGW, Faust JR, Goldstein JL, Brown MS (1982) : Appearance of crystalloid endoplasmic reticulum in compactin-resistant Chinese hamster cells with a 500-fold increase in 3-hydroxy-3-methylglutaryl-coenzyme A reductase. **Proc Natl Acad Sci (USA)** 79 : 1185-1189.

Chin DJ, Luskey KL, Faust JR, MacDonald RJ, Brown MS, Goldstein JL (1982) : Molecular cloning of 3-hydroxy-3-methylglutaryl coenzyme A reductase and evidence for regulation of its mRNA. **Proc Natl Acad Sci (USA)** 79 : 7704-7708.

Chin DJ, Gil G, Russell DW, Liscum L, Luskey KL, Basu SK, Okayama H, Berg P, Goldstein JL, Brown MS (1984) : Nucleotide sequence of 3-hydroxy-

3-methylglutaryl coenzyme A reductase, a glycoprotein of endoplasmic reticulum. **Nature** 308 : 613-617.

Clarke DJ, O'Neill LP, Turner BM (1993) : Selective use of H4 acetylation sites in the yeast *S. cerevisiae*. **Biochem** 294 : 557-561.

Clayton AL, Hebbes TR, Thorne AW, Crane-Robinson C (1993) : Histone acetylation and gene induction in human cells. **FEBS** 336 : (1) : 23-26.

Cook PR (1994) : RNA polymerase: structural determinant of the chromatin loop and the chromosome. **Bioessays** 16(6) : 425-430.

Cooper DN, Taggart MH, Bird AP (1983) : Unmethylated domains in vertebrate DNA. **Nucl Acids Res** 3 : 647-658.

Cote J, Quinn J, Workman JL, Peterson CL (1994) : Stimulation of GAL4 derivative binding to nucleosome DNA by the yeast SWI/SNF complex. **Science** 265 : 53-60.

Covault J, Chalkley R (1980) : The identification of distinct populations of acetylated histone. **J Biol Chem** 255 : 9110-9116.

Craig JM, Bickmore WA (1994) : The distribution of CpG islands in mammalian chromosomes. **Nature genetics** 7 : 376-381.

Cross SH, Charlton JA, Nan X, Bird A (1994) : Purification of CpG islands using a methylated DNA binding column. **Nature genetics** 6 : 236-244.

Cross SH, Bird AP (1995) : CpG islands and genes. **Curr Op Genet Dev** 5 : 309-314.

Csordas A (1990) : On the biological role of histone acetylation. **Biochem J** 265 : 23-38.

Cusick ME, DePamphilis ML, Wasserman PM (1984) : Dispersive segregation of nucleosomes during replication of simian virus 40 chromosomes. **J Mol Biol** 178 : 249-271.

d'Anna JA, Gurley LR, Tobey RA (1983) : Extent of histone modifications and H1⁰ content during cell cycle progression in the presence of butyrate. **Exp Cell Res** 147 : 407-417.

Davie JR (1995) : The nuclear matrix and the regulation of chromatin organization and function. **Int Rev Cytol** 162A : 191-250.

Davie JR, Murphy LC (1990) : Level of ubiquitinated histone H2B in chromatin is coupled to ongoing transcription. **Biochemistry** 29 : 4752-4757.

Davie JR, Murphy LC (1994) : Inhibition of transcription selectively reduces the level of ubiquitinated histone H2B in chromatin. **Biochem Biophys Res Commun** 203 : 344-350.

Davie JR, Hendzel MJ (1994) : Multiple functions of dynamic acetylation. **J Cell Biochem** 55 : 98-105.

de Murcia G, Huletsky A, Poirier GG (1988) : Modulation of chromatin structure by poly(ADP-ribosyl)ation. **Biochem Cell Biol** 66 : 626-635.

Dijkwel PA, Hamlin JL (1992) : Initiation of DNA replication in the dihydrofolate reductase locus is confined to the early S period in CHO cells synchronized with the plant amino acid mimosine. **Mol Cell Biol** 12 (9) : 3715-3722.

Dimitrov S, Almouzni G, Dasso M, Wolffe AP (1993) : Chromatin transitions during early *Xenopus* embryogenesis: changes in histone H4 acetylation and linker histone type. **Dev Biol** 160 : 214-227.

Earnshaw WC, Rothfield N (1985) : Identification of a family of human centromere proteins using autoimmune sera from patients with scleroderma. **Chromosoma** 91(3-4) : 313-321.

Faust JR, Luskey KL, Chin DJ, Goldstein JL, Brown MS (1982) : Regulation of synthesis and degradation of 3-hydroxy-3-methylglutaryl-coenzyme A reductase by low density lipoprotein and 25-hydroxycholesterol in UT-1 cells. **Proc Natl Acad Sci (USA)** 79 : 5205-5209.

Felsenfeld G (1978) : Chromatin. **Nature** 271 : 115-122.

Felsenfeld G (1996) : Chromatin unfolds. **Cell** 86 : 13-19.

Fisher-Adams G, Grunstein M (1995) : Yeast histone H4 and H3 N-termini have different effects on the chromatin structure of the GAL1 promoter. **EMBO J** 14(7) : 1468-1477.

Garcia-Ramirez M, Dong F, Ausio J (1992) : Role of the histone "tails" in the folding of oligonucleosomes depleted of histone H1. **J Biol Chem** 267 : 19587-19595.

Garcia-Ramirez M, Rocchini C, Ausio J (1995) : Modulation of chromatin folding by histone acetylation. **J Biol Chem** 270 (30) : 17923-17928.

Goldstein JL, Helgeson JAS, Brown MS (1979) : Inhibition of cholesterol synthesis with compactin renders growth of cultured cells dependent on the low density lipoprotein receptor. **J Biol Chem** 254 (12) : 5403-5409.

Grunstein M (1990) : Histone function in transcription. **Ann Rev Cell Biol** 6 : 643-678.

Hartman PG, Chapman GE, Moss T, Bradbury EM (1977) : Studies on the role and mode of operation of the very-lysine-rich histone H1 in eukaryotic chromatin: the three structural regions of the histone H1 molecule. **Eur J Biochem** 77 : 45-51.

Hassan AB, Cook PR (1994) : Does transcription by RNA polymerase play a direct role in the initiation of replication? **J Cell Sci** 107 : 1381-1387.

Hayes JJ, Wolffe AP (1993) : Preferential and asymmetric interaction of linker histones with 5S DNA in the nucleosome. **Proc Natl Acad Sci (USA)** 90 : 6415-6419.

Haynes SR, Dollard C, Winston F, Beck S, Trowsdale J, Dawid IB (1992) : The bromodomain: a conserved sequence found in human, *Drosophila*, and yeast proteins. **Nucl Acids Res** 80 : 2603.

He DC, Nickerson JA, Penman S (1990) : Core filaments of the nuclear matrix. **J Cell Biol** 110 : 569-580.

Hebbes TR, Thorne AW, Crane-Robinson C (1988) : A direct link between core histone acetylation and transcriptionally active chromatin. **EMBO J** 7 (5) : 1395-1402.

Hebbes TR, Thorne AW, Clayton AL, Crane-Robinson C (1992): Histone acetylation and globin gene switching. **Nuc Acids Res** 20 (5) : 1017-1022.

Hebbes TR, Clayton AL, Thorne AW, Crane-Robinson C (1994) : Core histone hyperacetylation co-maps with generalized DNaseI sensitivity in the chicken b-globin chromosomal domain. **EMBO J** 13 : 1823-1830.

Hecht A, Laroche T, Strahl-Bolsinger S, Gasser SM, Grunstein M (1995) : Histone H3 and H4 N-termini interact with SIR3 and SIR4 proteins: a molecular model for the formation of heterochromatin in yeast. **Cell** 80 : 583-592.

Hendzel MJ, Davie JR (1989) : Distribution of methylated histones and histone methyltransferases in chicken erythrocyte chromatin. **J Biol Chem** 264 : 19208-19214.

Hendzel MJ, Davie JR (1991) : Dynamically acetylated histones of chicken erythrocytes are selectively methylated. **Biochem J** 273 : 753-758.

Hendzel MJ, Deleuve GP, Davie JR (1991) : Histone deacetylase is a component of the internal nuclear matrix. **J Biol Chem** 266: 21936-21942.

Hendzel MJ, Davie JR (1992) : Acetylation and methylation of histones H3 and H4 in chicken immature erythrocytes are not directly coupled. **Biochem Biophys Res Commun** 185 : 414-419.

Hershko A (1988) : Ubiquitin-mediated protein degradation. **J Biol Chem** 263: 15237-15240.

Holmquist G (1989) : Evolution of chromosome bands: molecular ecology of noncoding DNA. **J Mol Evol** 28 : 469-486.

Holmquist G, Gray M, Porter T, Jordan J (1982) : Characterisation of Giemsa dark- and light-band DNA. **Cell** 31 : 121-128.

Hoshikawa Y, Kwon HJ, Yoshida M, Horinouchi S, Beppu T (1994) : Trichostatin A induced morphological changes and gelsolin expression by inhibiting histone deacetylase in human carcinoma cell lines. **Exp Cell Res** 214 : 189-197.

Ikegami S, Ooe Y, Shimizu T, Kasahara T, Tsurata T, Kijima M, Yoshida M, Beppu T (1993) : Accumulation of multiacetylated forms of histones by trichostatin A and its developmental consequences in early starfish embryos. **Roux's Arch Dev Biol** 202 : 144-151.

Imai BS, Yau P, Baldwin JP, Ibel K, May RP, Bradbury EM (1986) : Hyperacetylation of core histones does not cause unfolding of nucleosomes. Neutron scatter data accords with disc shape of the nucleosome. **J Biol Chem** 261 : 8784-8792.

Ip YT, Jackson V, Meier J, Chalkley R (1988) : The separation of transcriptionally engaged genes. **J Biol Chem** 263 (28) : 14044-14052.

Jackson V, Shires A, Tanphaichitr N, Chalkley R (1976) : Modifications of histones immediately after synthesis. **J Mol Biol** 104 : 471-483.

Jackson DA, Dickinson P, Cook PR (1990) : The size of chromatin loops in HeLa cells. **EMBO J** 9 : 567-571.

Jentsch S, Seufert W, Sommer T, Reins HA (1990) : Ubiquitin-conjugating enzymes: Novel regulators of eukaryotic cells. **Trends Biochem Sci** 15 : 195-198.

Jeppesen P, Mitchell A, Turner B, Perry P (1992) : Antibodies to defined histone epitopes reveal variations in chromatin conformation and

- underacetylation of centric heterochromatin in human metaphase chromosomes. **Chromosoma** 101 : 322-332.
- Jeppesen P, Turner BM (1993) : The inactive X chromosome in female mammals is distinguished by a lack of histone H4 acetylation, a cytogenetic marker for gene expression. **Cell** 74 : 281-289.
- Jeppesen P (1997) : Histone acetylation: a possible mechanism for the inheritance of cell memory at mitosis. **Bioessays** 19(1) 67-74.
- Johnson LA, Tapscott SJ, Eisen H (1992) : Sodium butyrate inhibits myogenesis by interfering with the transcriptional activation function of MyoD and myogenin. **Mol Cell Biol** 12 : 5123-5130.
- Johnson LM, Jayne PS, Kahn ES, Grunstein M (1990) : Genetic evidence for the interaction between SIR3 and histone H4 in the repression of the silent mating type loci in *Saccharomyces cerevisiae*. **Proc Natl Acad Sci USA** 87 : 6286-6290.
- Johnson LM, Fisher-Adams G, Grunstein M (1992) : Identification of a non-basic domain in the histone H4 N-terminus required for repression of the yeast silent mating loci. **EMBO J** 11 : 2201-2209.
- Kandutsch AA, Chen HW (1975) : Regulation of sterol synthesis in cultured cells by oxygenated derivatives of cholesterol. **J Cell Physiol** 85: 415-424.
- Kaplan LJ, Bauer R, Morrison E, Langan TA, Fasman GD (1984) : The structure of chromatin reconstituted with phosphorylated H1. Circular dichroism and thermal denaturation studies. **J Biol Chem** 259 : 8777-8785.
- Kaufmann SH, Gibson W, Shaper GH (1983) : Characterisation of the major polypeptides of the rat liver nuclear envelope. **J Biol Chem** 258 : 2710-2719.
- Kayne PS, Kim U-J, Han M, Mullen JR, Yoshizaki F, Grunstein M (1988) : Extremely conserved histone H4 N terminus is dispensable for growth but essential for repressing the silent mating loci in yeast. **Cell** 55 : 27-39.
- Kelly TJ, Jallepalli PV, Clyne RK (1994) : Silence of the ORCs. **Current Biology** 4 (3) : 238-241.
- Keohane AM, O'Neill LP, Belyaev ND, Lavender JS, Turner BM (1996) : X-inactivation and histone H4 acetylation in embryonic stem cells. **Dev Biol** 180 : 618-630.
- Khochbin S, Wolffe AP (1993) : Developmental regulation and butyrate-inducible transcription of the *Xenopus* histone H10 promoter. **Gene** 128 : 173-180.

Kijima M, Yoshida M, Sugita K, Horinouchi S, Beppu T (1993) : Trapoxin, an antitumor cyclic tetrapeptide, is an irreversible inhibitor of mammalian histone deacetylase. **J Biol Chem** 268 : 22429-22435.

Kornberg RD, Lorch Y (1995) : Interplay between chromatin structure and transcription. **Curr Op Cell Biol** 7 : 371-375.

Krajewski WA, Luchnik AN (1991) : Relationship of histone acetylation to DNA topology and transcription. **Mol Gen Genet** 230 : 442-448.

Kress H, Tonjes R, Doenecke D (1986) : Butyrate induced accumulation of a 2.3kb polyadenylated H1⁰ histone mRNA in HeLa cells. **Nuc Acids Res** 14 : 7189-7197.

Kruh J (1982) : Effects of sodium butyrate, a new pharmacological agent, on cells in culture. **Mol Cell Biochem** 42 : 65-82.

Kuo M-H, Brownell JE, Sobel RE, Ranalli TA, Cook RG, Edmondson DG, Roth SY, Allis CD (1996) : Transcription-linked acetylation by Gcn5p of histones H3 and H4 at specific lysines. **Nature** 383 : 269-272.

Ladjali K, Tixier-Bolchard M, Crihiu EP (1995) : High resolution chromosome preparations for G- and R-banding in *Gallus domesticus*. **J Hered** 86 : 136-139.

Lee DY, Hayes JJ, Pruss D, Wolffe AP (1993) : A positive role for histone acetylation in transcription factor access to nucleosomal DNA. **Cell** 72 : 73-84.

Levenson V, Hamlin JL (1993) : A general protocol for evaluating the specific effects of DNA replication inhibitors. **Nuc Acids Res** 21 (17) : 3997-4004.

Lewin B (1994) : Chromatin and gene expression: constant questions, but changing answers. **Cell** 79 : 397-406.

Li W, Nagaraja S, Delcuve GP, Hendzel MJ, Davie JR (1993) : Effects of histone acetylation, ubiquitination and variants on nucleosome stability. **Biochem J** 296 : 737-744.

Lin R, Leone JW, Cook RG, Allis CD (1989) : Antibodies specific to acetylated histones document the existence of deposition- and transcription-related histone acetylation in *Tetrahymena*. **J Cell Biol** 108 : 1577-1588.

Ling X, Harkness TAA, Schultz MC, Fisher-Adams G, Grunstein M (1996) : Yeast histone H3 and H4 amino termini are important for nucleosome

assembly in vivo and in vitro: redundant and position-independent functions in assembly but not in gene regulation. **Genes Dev** 10 : 686-699.

Loidl P (1988) : Towards an understanding of the biological function of histone acetylation. **FEBS Lett** 227 (2) : 91-95.

Loidl P (1994) : Histone acetylation : facts and questions. **Chromosoma** 103 : 441-449.

Lopez-Rodas G, Brosch G, Georgieva EI, Sendra R, Franco L, Loidl P (1993) : Histone deacetylase - a key enzyme for the binding of regulatory proteins to chromatin. **FEBS** 317 (3) : 175-180.

Lorch Y, LaPointe JW, Kornberg RD (1987) : Nucleosomes inhibit the initiation of transcription but allow chain elongation with the displacement of histones. **Cell** 49 : 203-210.

Lu MJ, Dadd CA, Mizzen CA, Perry CA, McLachlan DR, Annunziato AT, Allis CD (1994) : Generation and characterization of novel antibodies highly selective for phosphorylated linker histone H1 in *Tetrahymena* and HeLa cells. **Chromosoma** 103 : 111-121.

Lu MJ, Mpoke SS, Dadd CA, Allis CD (1995) : Phosphorylated and dephosphorylated linker histone H1 reside in distinct chromatin domains in *Tetrahymena* macronuclei. **Mol Cell Biol** 6 : 1077-1087.

Lucchesi JC, Manning JE (1987) : Gene dosage compensation in *Drosophila melanogaster*. **Adv Genet** 24 : 371-429.

Luskey KL, Chin DJ, MacDonald RJ, Liscum L, Goldstein JL, Brown MS (1982) : Identification of a cholesterol-regulated 53000-dalton cytosolic protein in UT-1 cells and cloning of its cDNA. **Proc Natl Acad Sci (USA)** 79 : 6210-6214.

Luskey KL, Faust JR, Chin DJ, Brown MS, Goldstein JL (1983) : Amplification of the gene for 3-hydroxy-3-methylglutaryl coenzyme A reductase, but not for the 53-kDa protein, in UT-1 cells. **J Biol Chem** 258 (13) : 8462-8469.

Lutter LC, Judis L, Paretti RF (1992) : Effects of histone acetylation on chromatin topology in vivo. **Mol Cell Biol** 12 (11) : 5004-5014.

McArthur M, Thomas JO (1996) : A preference of histone H1 for methylated DNA. **EMBO J** 15 (7) : 1705-1714.

Mahadevan LC, Willis AC, Barratt MJ (1991) : Rapid histone H3 phosphorylation in response to growth factors, phorbol esters, okadaic acid, and protein synthesis inhibitors. **Cell** (Cambridge, Mass) 65 : 775-783.

McKenzie EA, Kent NA, Dowell SJ, Moreno F, Bird LE, Mellor J (1993) : The centromere and promoter factor, 1, CPF1, of *Saccharomyces cerevisiae* modulates gene activity through a family of factors including SPT21, RPD1 (SIN3, RPD3 and CCR4). **Mol Gen Genet** 240 (3) : 374-386.

McQueen HA, Fantes J, Cross SH, Clark VC, Archibald A, Bird A (1996) : CpG islands of chicken are concentrated on microchromosomes. **Nature genetics** 12 : 321-324.

Meersseman G, Pennings S, Bradbury EM (1992) : Mobile nucleosomes - a general behavior. **EMBO J** 11 : 2951-2959.

Megee PC, Morgan BA, Smith MM (1995) : Histone H4 and the maintenance of histone integrity. **Genes & Dev** 9 : 1716-1727.

Mingarro I, Sendra R, Salvador ML, Franco L (1993) : Site specificity of pea histone acetyltransferase B in vitro. **J Biol Chem** 268 : 13248-13255.

Mizzen CG, Yang X-J, Kokubo T, Brownell JE, Bannister AJ, Owen-Hughes T, Workman J, Wang L, Berger SL, Kouzarides T, Nakatani Y, Allis CD (1996) : The TAF_{II}250 Subunit of TFIID has histone acetyltransferase activity. **Cell** 87 : 1261-1270.

Mosca PJ, Dijkwel PA, Hamlin JL (1992) : The plant amino acid mimosine may inhibit initiation of origins of replication in Chinese hamster cells. **Mol Cell Biol** 12 : 4375-4383.

Munks RJL, Moore J, O'Neill LP, Turner BM (1991) : Histone H4 acetylation in *Drosophila*: frequency of acetylation at different sites defined by immunolabelling with site-specific antibodies. **FEBS Lett** 284 : 245-248.

Nacheva GA, Guschin DY, Preobrazhenskaya OV, Karpov VL, Ebralidse KK, Mirzabekov AD (1989) : Change in the pattern of histone binding to DNA upon transcriptional activation. **Cell** 58 : 27-36.

Nakayasu H, Berezney R (1991) : Nuclear matrices: identification of the major nuclear matrix proteins. **Proc Natl Acad Sci (USA)** 88 : 10312-10316.

Nanda I, Schmid M (1994) : Localisation of the telomeric (TTAGGG)_n sequence in chicken (*Gallus domesticus*) chromosomes. **Cytogenet Cell Genet** 65 : 190-193.

Nasmyth K, Stillman D, Kipling D (1987) : Both positive and negative regulators of HO transcription are required for mother-cell-specific mating-type switching in yeast. **Cell** 48 (4) 579-587.

Nelson DA (1982) : Histone acetylation in baker's yeast. Maintenance of the hyperacetylated configuration in log phase protoplasts. **J Biol Chem** 257 : 1565-1568.

Newton C (1993) : Two jobs for the origin recognition complex. **Science** 262 : 1830-1831.

Nickel BE, Davie JR (1989) : Structure of polyubiquitinated histone H2A. **Biochemistry** 28 : 964-968.

Nicol L, Jeppesen P (1996) : Chromatin organization in the homogeneously staining regions of a methotrexate-resistant mouse cell line: interspersed of inactive and active chromatin domains distinguished by acetylation of histone H4. **J Cell Sci** 109 : 2221-2228.

Norton VG, Imai BS, Yau P, Bradbury EM (1989) : Histone acetylation reduces nucleosome core particle linking number change. **Cell** 57 : 449-457.

Norton VG, Marvin KW, Yau P, Bradbury EM (1990) : Nucleosome linking number change controlled by acetylation of histones H3 and H4. **J Biol Chem** 265 : 19848-19852.

Ogryzko VV, Schiltz RL, Russanova V, Howard BH, Natakani Y (1996) : The transcriptional coactivators p300 and CBP are histone acetyltransferases. **Cell** 87 : 953-959.

Ohno S (1967) : Monographs on endocrinology, vol 1 "Sex chromosomes and sex-linked genes". Springer-Verlag, Berlin.

Ohsumi K, Katagiri C, Kishimoto T (1993) : Chromosome condensation in *Xenopus* mitotic extracts without histone H1. **Science** 262 : 2033-2035.

O'Neill LP, Turner BM (1995) : Histone H4 acetylation distinguishes coding regions of the human genome from heterochromatin in a differentiation-dependent but transcription-independent manner. **EMBO J** 14 (16) : 3946-3957.

O'Neill TE, Meersseman G, Pennings S, Bradbury EM (1995) : Deposition of histone H1 onto reconstituted nucleosome arrays inhibits both initiation and elongation of transcripts by T7 RNA polymerase. **Nuc Acids Res** 23 (6) : 1075-1082.

Ormandy CJ, de Fazio A, Kelly PA, Sutherland RL (1992) : Transcriptional regulation of prolactin receptor gene expression by sodium butyrate in MCF-7 human breast cancer cells. **Endocrinology** 131 : 982-984.

Parseghian MH, Henschen AH, Kriegstein KG, Hamkalo BA (1994) : A proposal for a coherent mammalian histone H1 nomenclature correlated with amino acid sequences. **Protein Sci** 3 : 575-587.

Parthun MR, Widom J, Gottschling DE (1996) : The major cytoplasmic histone acetyltransferase in yeast: links to chromatin replication and histone metabolism. **Cell** 87 : 85-94.

Pennings S, Meersseman G, Bradbury EM (1991) : Mobility of positioned nucleosomes on 5S rDNA. **J Mol Biol** 220 : 101-110.

Pennings S, Meersseman G, Bradbury MM (1994) : Linker histones H1 and H5 prevent the mobility of positioned nucleosomes. **Proc Natl Acad Sci (USA)** 91 : 10275-10279.

Pennisi E (1997) : Opening the way to gene activity. **Science** 275 : 155-157.

Perry M, Chalkley R (1982) : Histone acetylation increases the solubility of chromatin and occurs sequentially over most of the chromatin. **J Biol Chem** 257 (13) : 7336-7347.

Perry CA, Annunziato AT (1991) : Histone acetylation reduces H1-mediated nucleosome interactions during chromosome assembly. **Exp Cell Res** 196 : 337-345.

Perry CA, Dadd CA, Allis CD, Annunziato AT (1993) : Analysis of nucleosome assembly and histone exchange using antibodies specific for acetylated H4. **Biochemistry** 32 : 13605-13615.

Perry CA, Allis CD, Annunziato AT (1993) : Parental nucleosomes segregated to newly replicated chromatin are underacetylated relative to those assembled *de novo*. **Biochemistry** 32 : 13615-13623.

Peterson CL & Hersowitz I (1992) : Characterisation of the yeast SWI1, SWI2, and SWI3 genes, which encode a global activator of transcription. **Cell** 68 : 573-583.

Pfeffer U, Ferrari N, Tosetti F, Vidali G (1988) : Histone hyperacetylation is induced in chick erythrocyte nuclei during reactivation in heterokaryons. **Expt Cell Res** 178 : 25-30.

Pfeffer U, Vidali G (1991) : Histone acetylation : recent approaches to a basic mechanism of genome organization. **Int J Biochem** 23 (3) : 277-285.

Pienta KJ, Getzenberg RH, Coffey DS (1991) : Cell structure and DNA organization. **CRC Crit Rev Eukaryotic Gene Express** 1 : 355 - 385.

Ponce de Leon FA, Li Y, Weng Z (1992) : Early and late replicative chromosomal banding patterns of *Gallus domesticus*. **J Hered** 83 : 36-42.

Realini CA, Althaus FR (1992) : Histone shuttling by poly(ADP-ribosylation). **J Biol Chem** 267 : 18858-18865.

Reneker J, Brotherton TW (1991) : Postsynthetic methylation of core histones in K562 cells is associated with bulk acetylation but not with transcriptional activity. **Biochemistry** 30 : 8402-8407.

Reynolds GA, Basu SK, Osborne TF, Chin DJ, Gil G, Brown MS, Goldstein JL, Luskey KL (1984) : HMG CoA reductase: a negatively regulated gene with unusual promoter and 5' untranslated regions. **Cell** 38: 275-285.

Reynolds GA, Goldstein JL, Brown MS (1985) : Multiple mRNAs for 3-hydroxy-3-methylglutaryl coenzyme A reductase determined by multiple transcription initiation sites and intron splicing sites in the 5'-untranslated region. **J Biol Chem** 260 (18) : 10369-10377.

Richmond TJ, Finch JT, Rushton B, Rhodes D, Klug A (1984) : Structure of the nucleosome particle at 7 resolution. **Nature (London)** 311 : 532-537.

Ridsdale JA, Davie JR (1987) : Chicken erythrocyte polynucleosomes which are soluble at physiological ionic strength and contain linker histones are highly enriched in -globin gene sequences. **Nuc Acids Res** 15: 1081-1096.

Riggs AD, Pfeifer GP (1992) : X chromosome inactivation and cell memory. **Trends Genet** 8 : 169-174.

Roberge M, O'Neill TE, Bradbury EM (1991) : Inhibition of 5S RNA transcription in vitro by nucleosome cores with low or high levels of histone acetylation. **FEBS Lett** 288 : 215-218.

Rodionov AV, Chelysheva LA, Solovei IV, Myakoshina YA (1992) : Chiasmata distribution in lambrush chromosomes of the chicken *Gallus gallus domesticus*: recombination hot spots and their possible significance for correct disjunction of homologous chromosomes in the first meiotic division. **Genetika** 28(7) : 151-160.

Roth SY, Collini MP, Draetta G, Beach D, Allis CD (1991) : A cdc2-like kinase phosphorylates histone H1 in the amitotic macronucleus of *Tetrahymena*. **EMBO J** 10 : 2069-2075.

Roth SY, Allis CD (1996) : Histone acetylation and chromatin assembly: a single escort, multiple dances? **Cell** 87 : 5-8.

Roth SY (1996) : Something about silencing. **Nature genetics** 14 : 3-4.

Roufa DJ (1978) : Replication of a mammalian genome: the role of *de novo* protein biosynthesis during S phase. **Cell** 13 : 129-138.

Saitoh Y, Saitoh H, Ohtomo K, Mizuno S (1991) : Occupancy of the majority of DNA in the chicken W chromosome by bent-repetitive sequences. **Chromosoma** 101 : 32-40.

Schwartz AL, Trausch JS, Ciechanover A, Slot JW, Geuze H (1992) : Immunoelectron microscopic localization of the ubiquitin-activating enzyme E1 in HepG2 cells. **Proc Natl Acad Sci (USA)** 89 : 5542-5546.

Schmid M, Enderle E, Schindler D, Schempp W (1989) : Chromosome banding and DNA replication patterns in bird karyotypes. **Cytogenet Cell Genet** 52 : 139-146.

Seale RL (1978) : Nucleosomes associated with newly replicated DNA have an altered conformation. **Proc Natl Acad Sci (USA)** 75 : 2717-2721.

Shen X, Yu L, Weir JW, Gorovsky MA (1995) : Linker histones are not essential and affect chromatin condensation in vivo. **Cell** 82 : 47-56.

Shen X, Gorovsky MA (1996) : Linker histone H1 regulates specific gene expression but not global transcription in vivo. **Cell** 86 : 475-483.

Shibata K, Inagaki M, Ajiro K (1990) : Mitosis-specific histone H3 phosphorylation in vitro in nucleosome structures. **Eur J Biochem** 192 : 87-93.

Simpson RT, Thoma F, Brubaker JM (1985) : Chromatin reconstituted from tandemly repeated cloned DNA fragments and core histones: a model system for study of higher order structure. **Cell** 42 : 799-808.

Smith MM (1991) : Histone structure and function. **Curr Op Cell Biol** 3 : 429-437.

Sobel RE, Cook RG, Perry CA, Annunziato AT, Allis CD (1995) : Conservation of deposition-related acetylation sites in newly synthesized histones H3 and H4. **Proc Natl Acad Sci (USA)** 92 : 1237-1241.

Sommerville J, Baird J, Turner BM (1993) : Histone H4 acetylation and transcription in amphibian chromatin. **J Cell Biol** 120 (2) : 277-290.

Stillman DJ, Dorland S, Yu Y (1994) : Epistasis analysis of suppressor mutations that allow HO expression in the absence of the yeast SWI5 transcriptional activator. **Genetics** 136 : 781-788.

Studitsky VM, Clark DJ, Felsenfeld G (1994) : A histone octamer can step around a transcribing polymerase without leaving the template. **Cell** 76 : 371-382.

Studitsky VM, Clark DJ, Felsenfeld G (1995) : Overcoming a nucleosomal barrier to transcription. **Cell** 83 : 19-27.

Swerdlow PS, Schuster T, Finley D (1990) : A conserved sequence in histone H2A which is a ubiquitination site in higher eukaryotes is not required for growth in *Saccharomyces cerevisiae*. **Mol Cell Biol** 10 : 4905-4911.

Taunton J, Hassig CA, Schreiber SL (1996) : A mammalian histone deacetylase related to the yeast transcriptional regulator Rpd3p. **Science** 272 : 408-411.

Tazi J, Bird A (1990) : Alternative chromatin structure at CpG islands. **Cell** 60 : 909-920.

Tegelstrom H, Rytman H (1981) : Chromosomes in birds (*Aves*): evolutionary implications of macro- and microchromosome numbers and length. **Hereditas** 94 : 225-233.

Thompson JS, Ling, X, Grunstein M (1994) : Histone H3 amino terminus is required for telomeric and silent mating locus repression in yeast. **Nature** 369 : 245-247.

Thomsen B, Bendixen C, Westergaard O (1991) : Histone hyperacetylation is accompanied by changes in DNA topology in vivo. **Eur J Biochem** 201 : 107-111.

Thorne AW, Kmiciek D, Mitchelson K, Sautiere P, Crane-Robinson C (1990) : Patterns of histone acetylation. **Eur J Biochem** 193 : 701-713.

Triolo T, Sternglanz R (1996) : Role of interactions between the origin recognition complex and SIR1 in transcriptional silencing. **Nature** 381 : 251-253.

Turner BM (1989) : Acetylation and deacetylation of histone H4 continue through metaphase with depletion of more-acetylated isoforms and altered site usage. **Exp Cell Res** 182 : 206-214.

Turner BM (1991) : Histone acetylation and control of gene expression. **J Cell Sci** 99 : 13-20.

Turner BM (1993) : Decoding the nucleosome. **Cell** 75 : 5-8.

Turner BM, Fellows G (1989) : Specific antibodies reveal ordered and cell-cycle-related use of histone H4 acetylation sites in mammalian cells. **Eur J Biochem** 179 : 131-139.

Turner BM, O'Neill LP, Allan IM (1989) : Histone H4 acetylation in human cells. Frequency of acetylation at different sites defined by immunolabelling with site-specific antibodies. **FEBS Lett** 253 : 141-145.

Turner BM, Franchi L, Wallace H (1990) : Islands of acetylated histone H4 in polytene chromosomes and their relationship to chromatin packaging and transcriptional activity. **J Cell Sci** 96 : 335-346.

Turner BM, Birley AJ, Lavender J (1992) : Histone H4 isoforms acetylated at specific lysine residues define individual chromosomes and chromatin domains in *Drosophila* polytene nuclei. **Cell** 69 : 375-384.

Ura K, Wolffe AP, Hayes JJ (1994) : Core histone acetylation does not block linker histone binding to a nucleosome including a *Xenopus borealis* 5S rRNA gene. **J Biol Chem** 269 (44) : 27171-27174.

Ura K, Hayes JJ, Wolffe AP (1995) : A positive role for the nucleosome mobility in the transcriptional activity of chromatin templates: restriction by linker histones. **EMBO J** 14 (15) : 3752-3765.

Van Holde KE (1988) : "Chromatin", Springer-Verlag, New York.

Van Holde KE, Lohr DE, Robert C (1992) : What happens to nucleosomes during transcription? **J Biol Chem** 267 : 2837-2840.

Van Holde KE, Zlatanova J (1994) : Unusual DNA structures, chromatin and transcription. **Bioessays** 16 : 59-68.

Vavra KJ, Allis CD, Gorovsky MA (1982) : Regulation of histone acetylation in *Tetrahymena* macro- and micronuclei. **J Biol Chem** 257 : 2591-2598.

Verreault A, Kaufman PD, Kobayashi R, Stillman B (1996) : Nucleosome assembly by a complex of CAF-1 and acetylated histone H3/H4. **Cell** 87 : 95-104.

Vettese-Dadey M, Grant PA, Hebbes TR, Crane-Robinson C, Allis CD, Workman JL (1996) : Acetylation of histone H4 plays a primary role in enhancing transcription factor binding to nucleosomal DNA in vitro. **EMBO J** 15 (10) : 2508-2518.

Vidal M, Strich R, Esposito RE, Gaber RF (1991) : RPD1 (SIN3/UME4) is required for maximal activation and repression of diverse yeast genes. **Mol Cell Biol** 11 : 6306-6316.

Vidali G, Ferrari N, Pfeffer U (1988) : Histone acetylation: A step in gene activation. **Adv Exp Med Biol** 231 : 583-596.

von Gunten CF, Sinensky M (1989) : Treatment of CHO-K1 cells with 25-hydroxycholesterol produces a more rapid loss of 3-hydroxy-3-methylglutaryl-coenzyme A reductase activity than can be accounted for by enzyme turnover. **Biochem Biophys Acta** 1001 : 218-224.

Wansink DG, Manders EEM, van der Kraan I, Aten JA, van Driel R, de Jong L (1994) : RNA polymerase II transcription is concentrated outside replication domains throughout S-phase. **J Cell Sci** 107 : 1449-1456.

Wolffe AP (1991) : Developmental regulation of chromatin structure and function. **Trends Cell Biol** 1 : 61-66.

Wolffe AP (1996) : Histone deacetylase: a regulator of transcription. **Science** 272 : 371-372.

Worrad DM, Turner BM, Schultz RM (1995) : Temporally restricted spatial localization of acetylated isoforms of histone H4 and RNA polymerase II in the 2-cell mouse embryo. **Development** 121 : 2949-2959.

Wu RS, Panusz HT, Hatch CL, Bonner WM (1986) : Histones and their modifications. **CRC Crit Rev Biochem** 20 : 201-263.

Yang X-J, Ogryzko VV, Nishikawa J, Howard BH, Nakatani Y (1996) : A p300/CBP-associated factor that competes with the adenoviral oncoprotein E1A. **Nature** 382 : 319-324.

Yoshida M, Kijima M, Akita M, Beppu T (1990) : Potent and specific inhibition of mammalian histone deacetylase both in vivo and in vitro by trichostatin A. **J Biol Chem** 265 : 17174-17179.

Yoshida M, Hoshikawa Y, Koseki K, Mori K, Beppu T (1990) : Structural specificity for biological activity of trichostatin A, a specific inhibitor of mammalian cell cycle with potent differentiation-inducing activity in Friend leukemia cells. **J Antibiot** 43:1101-1106.

Zieve GW, Turnbull D, Mullins JM, McIntosh JR (1980) : Production of large numbers of mitotic mammalian cells by use of the reversible microtubule inhibitor nocodazole. Nocodazole accumulated mitotic cells. **Exp Cell Res** 126 : 397-405.

Zini N, Mazzotti G, Santi P, Rizzoli R, Gallanzi A, Rana R, Maraldi NM (1989)
: Cytochemical localization of DNA loop attachment sites to the nuclear
lamina and to the inner nuclear matrix. **Histochemistry** 91 : 199-204